2020

Obese Zucker Rats as a Reverse Translational Model of Human Left Ventricular Hypertrophy

Mackenzie Shelby Newman
msnewman@mix.wvu.edu

2020

Obese Zucker Rats as a Reverse Translational Model of Human Left Ventricular Hypertrophy

Mackenzie Shelby Newman

Obese Zucker Rats as a Reverse Translational Model of Human Left Ventricular Hypertrophy

Mackenzie Shelby Newman

Dissertation submitted to the School of Medicine at West Virginia University

in partial fulfillment of the requirements for the degree of

Doctor of Philosophy in

Cellular & Integrative Physiology

Stan Hileman, Ph.D., Chair

Han-Gang Yu, Ph.D.

Timothy Nurkiewicz, Ph.D.

Karen Martin, Ph.D.

Kathleen Brundage, Ph.D.

Department of Physiology & Pharmacology

Morgantown, West Virginia

2020

Keywords: left ventricular hypertrophy, transcriptome, obese Zucker rat, obesity, heart failure

ABSTRACT

Obese Zucker Rats as a Reverse Translational Model of Human Left Ventricular Hypertrophy

Mackenzie Shelby Newman

Heart failure is a lifelong disability that is a comorbidity in nearly one out of eight deaths and leads to mortality within five years for over half of those affected. Left ventricular hypertrophy (LVH) is one of the most reliable independent predictors of heart failure. It has been observed to occur in nearly 20% of individuals in a large, representative US population study with sex-specific disparities. Obesity, cardiovascular diseases, and increased age are common comorbidities. Pathological LVH is irreversible in humans and early diagnosis is often missed due to lack of symptoms. Obese Zucker rats (OZR) are a rat strain that naturally develop phenotypical LVH without surgical intervention or a high fat diet. OZR develop obesity due to dysfunctional leptin signaling, which mimics the situation most often seen in obese humans. These animals also develop many conditions, such as hypertension and glucose intolerance, that mimic the human population at risk for LVH. These animal models are necessary for research as live human donor tissue is scarce. The central hypothesis is that genes and proteins that are differentially expressed during development of LVH, with regard to sex and obesity status, may serve as clinical biomarkers or therapeutic targets for detection and prevention of heart failure. No previous studies have addressed these comparisons on an exome-wide basis. In the present research, I address these knowledge gaps with transcriptome analysis of rat and human left ventricle (LV) tissue in a sex- and obesity-specific manner. Specific genes that were identified and which are involved in cardiac development and function were then validated at the protein level to form a gene signature (NPPA, NPPB, HBB, MYL7, PDK4) that may be targetable as a future diagnostic or represent targets for intervention. Finally, I provide a novel method to reduce the expression of NPPA, the gene with the highest upregulation in both male and female obese humans and rats using targeted siRNA. In conclusion, this work defines novel genome-wide transcriptomes of LVH in male and female humans with or without regard to obesity, and male and female obese Zucker rats. Comparison of these datasets coupled to cross-species protein expression allows for confirmation of whether an individual gene or geneset is translationally-relevant for further investigation in LVH. Future work should address transcriptomic and proteomic changes throughout the course of LVH development and whether intervention of specific gene targets can ameliorate onset of LVH. The work presented here provides a framework for the discovery of future LVH-related genes and proteins in order to improve the quality of life and burden on the healthcare system from LVH and, ultimately, heart failure.

ACKNOWLEDGEMENTS

There's neither enough space nor time here to tell you all what you mean to me, so I'll try to make it brief.

To my committee—

Dr. Yu, thank you for these opportunities and everything else. You're one of the most intelligent people I've ever been lucky enough to learn from.

Drs. Hileman and Nurkiewicz, thanks for keeping this going.

Drs. Brundage and Martin, thank you for challenging my science at every corner.

To my friends here—

Emily, Brian, Timur, Drew, Quincy, Brad, Sion, Joe, Evan, Henry, Jesse, and everyone else, please don't ever lose touch.

To my family—

Brenda, Marc, Alex, Carrie, Daisy, Megan, et al, you've always been there and I don't tell you often enough what that means to me.

There are too many names to mention everyone here, but know that you're always on my mind.

"As we get close to the river, we see that everybody is already there, and I mean everyone."

This is dedicated to Franklin and Helen.

TABLE OF CONTENTS

ABBREVIATIONS

ANP	atrial natriuretic peptide
BMI	body mass index
BMI25	BMI less than 25 (lean)
BMI30	BMI greater than 30 (obese)
BNP	brain natriuretic peptide
DCM	dilated cardiomyopathy
DE	differential expression
DEG	differentially-expressed genes
ECG	electrocardiography
ECHO	echocardiography
FPKM	fragments per kilobase of transcript per million mapped reads
GSTT1	glutathione S-transferase theta 1
HBA1	hemoglobin subunit alpha
HBB	hemoglobin subunit beta
HF	heart failure
HIST1H2AC	histone H2A type 1C
ISCH	ischemic
LEPR	leptin receptor (gene)
LV	left ventricle
LVH	left ventricular hypertrophy
LZR	lean Zucker rat
MAPK	mitogen-associated protein kinase
MYL7	myosin light chain 7
NF	non-failed heart
NPPA	natriuretic peptide A (gene)
NPPB	natriuretic peptide B (gene)
NPRA	natriuretic peptide type A receptor
NPRB	natriuretic peptide type B receptor
OZR	obese Zucker rat
p_adj	adjusted p-value
PDK4	pyruvate dehydrogenase kinase 4
PLA2G2A	phospholipase A2 group IIA
TAC	trans-aortic constriction

CHAPTER 1

General Introduction

Heart Failure (HF)

HF occurs when the heart cannot sufficiently supply blood to the body. A lack of blood means a lack of oxygen and other nutrient delivery to tissues and organs, resulting in fatigue, peripheral edema, organ dysfunction, and fainting, among many other symptoms. It is an extremely detrimental disease because by the time it is diagnosed, significant irreversible damage is already present, thus explaining the high mortality rates. The most common comorbidities of HF, namely obesity, chronic kidney disease, hypertension, diabetes, and smoking, are present in 52% of HF patients (13, 38, 52). HF can present acutely or chronically. In acute situations, frequently caused by underlying conditions such as arrhythmias or myocardial infarction, immediate treatment is pivotal because the heart has not had the same adaptive changes that accompany chronic HF. Although adaptive changes in chronic HF may be beneficial initially, they may ultimately lead to worse damage over time.

In HF, the Frank-Starling mechanism fails. In a healthy heart, this mechanism describes the positive correlation between simultaneous increases in cardiac output and right atrial pressure (reflective of blood returning to the heart from circulation). The hallmark of HF is decreased cardiac output, yet right atrial pressure is still increased. Cardiac output is defined as the product of stroke volume and heart rate. In HF, decreases in stroke volume are the result of diastolic and/or systolic dysfunction. In the former, ventricular filling is reduced (often due to stiffness or reduced lumen volume; ejection fraction is preserved), leading to less blood being pumped into circulation. In the latter, loss of myocyte contractility reduces the heart's capacity to pump. Changes in heart rate are most frequently the result of compensatory measures.

Multiple systems facilitate adaptive changes for HF. Sympathetic input, endothelin, and angiotensin II are elevated in order to increase systemic vascular resistance and therefore both arterial and venous pressure. This causes vasoconstriction to compensate for reduced cardiac output. Sympathetic input, endothelin, and angiotensin II also increase contractility and heart rate to raise cardiac output in light of reduced stroke volume, but these can also promote arrythmias. Vasopressin and aldosterone are also elevated, in order to increase blood volume, but these can also cause peripheral edema. Atrial and brain natriuretic peptides (ANP and BNP, respectively) are released in HF to counterbalance the effects of these extremely elevated neurohumoral adaptations. Increases in blood volume (preload) and arterial vasoconstriction (afterload) can exacerbate HF by increasing the amount of total work output from the heart, as it is pumping a larger volume against a higher pressure gradient.

Treatment of HF

There is no treatment that can reverse HF, as cardiac tissue damage is irreparable (65). Despite this, numerous treatments have been shown to aid in patient survival, and survival rates have been increasing over the last few decades. Many medications have been shown to be effective post-HF; these have varying effects on the cardiovascular system that are principally related to hypertension and heart rate. Some of these classes of drugs include angiotensin-converting enzyme (ACE) inhibitors, angiotensin receptor blockers (ARBs), and angiotensin receptor neprilsyin inhibitors (ARNIs) (to reduce afterload and therefore reduce work required per stroke), I_f blockers and beta-blockers (to reduce heart rate/risk of arrhythmias in individuals with tachycardia), aldosterone antagonists and diuretics (to reduce blood volume), and digoxin (to increase contractility) (90). Heart transplant has been shown to be effective, but this is extremely costly and not recommended for elderly patients (72). The survival median is

approximately 9.5 years after transplant, but the average is only five years. Transplantable hearts are in extreme demand, too, with less than 50% of patients desiring them actually receiving them from 1987-2012 (10). Heart transplant requires frequent post-operative attention because reduced parasympathetic cardiac innervation result in increased resting heart rate, reduced stroke volume, and increases in systolic and diastolic blood pressures (3, 104). Implantable devices, such as cardioverter-defibrillators, have been shown to be effective in patients with reduced ejection fraction. Left ventricular assist devices (LVAD), which are mechanical pumps that aid the LV to pump blood to the body, have been shown to be effective as well: from 2006-2014, the survival rate at one year was 80% and at two years was 70% in those who received implanted devices (58). Similarly, the in-hospital mortality rate dropped from 47% to 13% from 2005-2011 (58). Though still costly, these devices are not as expensive as a transplant and are much more widely available. However, they are extremely invasive, too: the 30-day readmission rate after implantation was 44% in one meta-study (57). The most common complications were infection, stroke, and gastrointestinal bleeding, as well arrhythmias and device malfunction. Like pacemakers, LVAD require new batteries over time, and therefore another invasive surgery (72).

HF Impact and Detection

HF is a devastating condition that affects over 2% of the global population (48) and is a comorbidity in one out of eight deaths (22). Nearly $40 billion USD in annual healthcare costs are attributed to HF (124), yet these are expected to rise to $69.8 billion USD by 2030 (48). From 2013-2016, HF affected 6.2 million Americans aged 20 or greater, with projections of a 46% increase leading into 2030 and an overall 0.5% greater occurrence in the global population (48). Individuals aged 40 or greater are at a 20% risk of developing HF regardless of sex, but sex, race, age, and BMI are all factors in the development of HF (52). Males develop HF at rates

that are 6-14% greater than females. In the 60-79 age demographic, males and females develop HF at rates of 6.9% and 4.8%, respectively, while above age 80, these rates rise to 12.8% and 12%, respectively (10). Lifetime risks are 30-42% in white males, 20-29% in black males, 32-39% in white females, and 24-46% in black females (52). From 2005-2015, there was a 27% increase in HF incidence (10, 48). The one-year mortality rate after HF for those aged less than 55 years was 17% in males and 14% in females, but for those aged 85 or greater, the rates sharply increased to 58% in men and 49% in women (10). The five-year mortality rate for all HF patients in a 1,282-patient study was 42%, with no significant difference between sexes (68). Obesity (BMI > 30kg/m^2) doubles the risk of HF over lean individuals (BMI < 25kg/m^2) (52) with or without hypertension, a 100% increase in males and a 90% increase in females, according to the Framingham study (56, 63).

Common markers of cardiovascular damage, such as elevated circulating BNP, urinary albumin to creatine ratio, serum γ-glutamyl transferase, and hematocrit (28, 34, 122), typically precede HF, but these may not be assessed in patients with no outward symptoms of cardiovascular damage. Left ventricular (LV) dysfunction is a hallmark feature of pending HF. Systolic LV dysfunction is present in 5% of patients, while diastolic dysfunction is present in 36% (60). In data from 2005-2010, lowered ejection fraction, a marker of LV function, was present in 50% of individuals (113) with HF.

Left Ventricle (LV)

Proper function of the LV is critical to whole-body homeostasis as this chamber is responsible for pumping blood from the heart back into circulation. The LV is nearly 60% of overall heart volume (66) and is made up primarily of cardiomyocytes, a specialized type of muscle cell that contains a high density of mitochondria compared to skeletal muscle cells, and

which carries cardiac action potentials that allow for rapid cycles of polarization and depolarization resulting in heart contraction. These cells have a low turnover rate with age; fewer than 50% are considered to be replaced under normal growth over a lifetime (11, 134). Fetal cardiomyocytes, instead of dividing, increase in size as the organism ages (134). There is a growing body of evidence for resident cardiac stem/progenitor cells, but their capacity to replace lost cells has not been fully elucidated (11, 134). The remaining minor cell populations in the LV are primarily fibroblasts, smooth muscle cells, and endothelial cells, which provide support and help maintain cardiomyocyte function (111).

Left Ventricular Hypertrophy (LVH)

The hallmark of LVH, as the name implies, is an enlargement and thickening of the LV. There are two focal types: inward hypertrophic remodeling, wherein the chamber lumen volume is reduced, and outward hypertrophic remodeling, wherein the lumen volume increases. The former is associated with pathological cardiac hypertrophy and the latter is necessary in physiological hypertrophy. Numerous structural and functional changes underlie LVH, and although many have been investigated, none are completely understood. The most common feature of LVH is increased cardiomyocyte size (61). Electrical restructuring of the ventricle is secondary to cellular reorganization, as thickening of the ventricle wall leads to decreased conduction (18), which is usually accompanied by alterations in extracellular matrix composition and fibrosis (12). Compensatory mechanisms lead typically to increases in voltage within the QRS complex, as recorded by ECG (116), but changes have been witnessed in LVH such as increased R wave peak time, ST depression or elevation, and T wave inversion (14, 116). The QRS complex represents the period of ventricular depolarization (i.e. isovolumetric contraction) and the ST segment represents the period of ventricular repolarization (ejection). Changes in

these parameters, such as lengthened time period or increased voltage, reflect thickened ventricle tissue, resulting in greater resistance to the propagation of electrical signal. However, these electrical changes do not occur in all cases (4, 5).

Physiological LVH

Importantly, not all LVH is detrimental. Physiological LVH occurs in normal circumstances: growth from childhood to adulthood, pregnancy, and exercise, i.e. situations where there is an increased tissue demand for oxygen and other nutrition in circulation (and therefore increased bloodflow) (61, 71, 74). The focal biochemical pathways involved are often growth factor-based, such as the insulin-like growth factor-1 (IGF1) pathway, which leads to activation of phosphoinositol-3 kinase, Akt, and downstream mTOR (75, 85, 99). Although increased activity of this pathway is seen in some cancers (128), it is considered to have only necessary, transient effects with regard to physiological LVH (74). Cardiac fetal gene expression (e.g. calcineurin, nuclear factor of activated T cells (NFAT), atrial natriuretic peptide (ANP), BNP, skeletal α-actin, and myosin heavy chain 7) is not significantly upregulated (70, 129). Proteins involved in the sarcomere, such sarco/endoplasmic reticulum Ca2+-ATPase, actin, and alpha- and beta-myosin heavy chains are increased in physiological LVH to facilitate contraction. The activation and increased production of these cellular components are considered to be reversible, even in cases of chronic exercise training. Cardiac function remains normal or increases over the period of exercise acclimation (74).

Pathological LVH

Pathological LVH develops due to a chronic insult such as increased pressure load (e.g. hypertension), volume load (valvular disease), or an underlying cardiomyopathy. Similar to physiological LVH, sarcomere counts and myocyte volume are increased, but in contrast,

fibrosis and cellular necrosis/apoptosis are common. Changes in cardiac function are essentially the same as those seen in chronic HF: cardiac output decreases without a decrease in right atrial pressure. Hypertension in particular causes increased peripheral resistance and therefore increased right atrial pressure. Typically, diastolic dysfunction precedes systolic dysfunction, i.e. decreased passive compliance (filling) precedes decreased contractility.

Adaptive changes are similar as well. As previously discussed, increases in sympathetic input and angiotensin II (which are associated with and promote hypertension), and endothelin increase heart rate and contractility in order to compensate for reduced stroke volume and therefore raise cardiac output. These hormones all act through G protein-coupled receptor pathways that are mediated by Gαq, which have been directly implicated in the development of cardiac hypertrophy. Gαq activates phospholipase C (PLC), which causes protein kinase C to activate numerous mitogen-activated protein kinases (MAPKs) associated with cellular stress. Activation of these pathways is also known to cause pro-fibrotic signaling, therefore further decreasing cardiac compliance. These hormones also activate phospholipase C, which causes downstream changes in calcium homeostasis and activation/nuclear translocation of NFAT, a transcription factor that causes expression of many cardiac-specific genes (31, 49, 74, 77). Expression of fetal genes such as NPPA and NPPB, which encode for ANP and BNP, respectively, is increased (32, 35, 44, 50, 86), in order to counterbalance elevations in aldosterone seen in hypertensive situations. Chronic elevations in these hormones ultimately contribute to irreversible damage of the myocardium and raise the risk of HF without early intervention.

Atrial and Brain Natriuretic Peptides

The primary function of ANP and BNP is to decrease fluid volume by acting on distal portions of the nephron through binding to their cognate receptors, NPRA (gene NPR1) and NPRB (gene NPR2), respectively. Receptor activation in the heart and vasculature counteracts angiotensin: ANP and BNP are anti-hypertrophic, anti-fibroproliferative, and anti-hypertensive at physiological concentrations. ANP preferentially binds NPR1 and BNP preferentially binds NPR2, likely due to sequence homology. A third receptor, NPRC (gene NPR3), internalizes circulating natriuretic peptides, leading to their degradation. All three receptors are widely expressed, but with some tissue-specific enrichment: NPR1 in breast, lung, adipose tissue, and kidney, with NPR2 in brain, muscle, and female tissues (endometrium, cervix, uterus), and NPR3 in lung, kidney and urinary bladder, muscle, and adipose and soft tissue (121). NPRA and NPRB are GTPases upon activation; ligand binding causes receptor dimerization and initiates the conversion of intracellular GTP to cGMP. Elevated cGMP then may activate protein kinase G (PKG) to cause downstream effects such as ion channel modulation via phosphorylation (98, 115).

N-terminal pro B-type natriuretic peptide (pro-NT BNP) is currently used as a clinical marker for LVH and HF (88, 91, 92). NPPA/ANP (measured as NT-pro-ANP) has been shown to be associated with cardiovascular dysfunction and death (110). However, these findings have not resulted in approval for use of ANP as a biomarker of HF. Pro-NT BNP is preferred to ANP due to its longer circulating half-life (40). ANP and ANP mimetics have been explored pharmaceutically for kidney injury due to expression of NPRA in distal nephron to regulate sodium clearance (84) and have been shown to have benefits in HF patients (83, 130), with one being approved in Japan. However, none have made it to market in the United States.

Elevated ANP and BNP are generally considered to be beneficial in LVH. Despite this, extreme, persistent increases may be detrimental. Elevated levels of ANP have been shown to modulate heart rate (HR), effective refractory period (ERP), and action potential duration (APD) in cardiac tissue and cell preparations in mice, rats, dogs, rabbits, guinea pigs, and humans with mixed effects across species (8, 9, 55, 80, 112). ANP was shown to have no effect or decrease HR in dogs (8, 9), decrease HR in rats (80), and have no effect or an increase on HR in humans (80). ERP was shown to be increased in dogs and decreased in humans (80). ANP decreased APD in human, dog, rabbit, and guinea pig cardiac preparations (80), but had no effect on guinea pigs or dogs in another set of studies (55, 112). Natriuretic peptide receptor activation in cardiomyocytes is a likely cause of cardiac disturbances due to the dependence of hyperpolarization-activated cyclic nucleotide-gated (HCN) channels on intracellular cGMP; these channels are pivotal in maintaining the "funny" current in pacemaker cells that regulates and maintains heart rate. One human NPPA mutation, a single base deletion which causes a frameshift resulting in an extra 12 amino acids at the C-terminus, has been identified in humans that causes elevated, persistent ANP levels in the blood. Both humans and mice expressing this mutant NPPA exhibit atrial fibrillation (41). Overall, these data suggest that chronically elevated ANP signaling may contribute to the presentation of abnormal cardiac functions. Conversely, there is evidence in mice that NPPA or NPRA ablation results in pronounced cardiac hypertrophy and hypertension, leading to early mortality (81, 93).

Diagnosis of LVH

LVH is frequently asymptomatic, particularly early in its progression or in those with no obvious comorbidities. Initial diagnosis is derived from echocardiography (the same measurements can be derived by using an implanted catheter, computer tomography, or magnetic

resonance imaging). These data can be analyzed as a pressure-volume loop, in order to determine basic cardiac parameters such as stroke volume, cardiac output, and ejection fraction. These parameters can then be used to gauge the presence of LVH. A basic representation of the changes in a pressure-volume loop due to LVH is shown in Figure 1. In line with this analysis, direct measurements of the LV can be taken directly from imaging and interpreted. These are often used in the Devereux formula to calculate LV mass:

$$\text{LV mass} = 0.8\ (1.04[\ ([\text{LVEDd} + \text{IVSd} + \text{PWd}]^3 - \text{LVEDd}^3)]) + 0.6$$

LVEDd: LV end diastolic diameter

IVSd: intraventricular septal diameter at end diastole

PWd: posterior wall thickness at end diastole

(all units are centimeters)

The resultant value is then normalized to body weight (39). LVH is initially suspected in males with LV mass >115g/m^2 and in females with LV mass >95g/m^2 in females (47).

However, LVH diagnosis is not based on a single test and, beyond echocardiography, 12-lead electrocardiography is required in order to confirm electrical disturbances in the heart. Changes in electrical conduction manifest inconsistently in LVH, so clinical criteria seek to address multiple parameters at once. QRS complex alterations are most commonly seen in LVH (116) as this mechanism is active at the end of diastole and initiates systole, therefore reflecting the beginning of the period when the ventricle is contracting. Using Sokolow-Lyon criteria, the sum of the S wave in the V1 lead is added to the larger R wave in leads V5 or V6. Values greater

than or equal to 35mm and an R wave greater than or equal to 11mm in the aVL lead are indicative of LVH (47, 109). Using Cornell and Cornell Product criteria, where the sum of the S wave in V3 and the R wave in aVL leads is used, a value greater than 28mm in men or 20mm in females indicates LVH (21). Differences in accuracy between the criteria have been shown to be dependent on BMI status (101), age (108), underlying condition such as myocardial infarction (102) or hypertension (132) and the population studied (94, 114).

Cardiac MRI may also be used to diagnose LVH. This technique allows for higher accuracy and precision versus echocardiography, as well as the identification of subtypes of LVH. This technique is expensive, however, and not necessary for patients who have met LVH diagnostic criteria using other methods (89, 107).

Treatment of LVH

There is no cure for LVH, given that it is considered to be irreversible, yet many treatments have been implicated. Lifestyle changes, such as diet, exercise, and cessation of smoking, may have the largest impact on overall cardiovascular health. Like with HF, pharmaceuticals that reduce blood pressure have been shown to be effective at alleviating comorbidities of LVH, particularly hypertension or other conditions that increase the mechanical load put on the heart. Some of these drug classes include angiotensin converting enzyme inhibitors, angiotensin receptors blockers, calcium channel blockers, beta-blockers, and diuretics (133).

Models of LVH

LVH is nearly impossible to study in primary human cardiac tissue due to the scarcity of live donor tissue. Despite this, there are currently no laboratory models of cardiac hypertrophy that faithfully mimic the human disease. LVH is a progressive pathological adaptation which

develops over an extended period of time. Surgical methods of LVH induction are extremely rapid and thus may not follow the same transcriptional changes seen in humans. Genetic animal models of LVH have phenotypical changes that are seen in human LVH but are not directly translatable due to the overexpression or deletion of a gene not being relevant to the vast majority of the population.

Transverse aortic constriction (TAC), the most common model used in rodents and larger mammals, requires invasive surgery to place a tie around the aorta and a follow-up procedure to remove it. Due to invasiveness and human variability with tightness of the tie, there is a mortality risk and experimental inconsistency with aortic banding (62, 118, 119). Improvements to the model have been made, such as applying the band during closed-chest surgery, but many of the previous issues with variability remain (36, 51). A recent study used o-rings rather than nylon sutures around the aorta in order to allow for more reproducibility between animals and found a markedly decreased mortality rate and greater reproducibility in results (76).

Transgenic models have also been investigated, but often lack direct translational applicability in humans because humans seldom have only a single gene entirely knocked out or overexpressed in isolation. In a rat model overexpressing Ren2 (the gene encoding for renin, an enzyme that helps regulate angiotensin levels and therefore blood pressure), LV weights were increased in tandem with blood pressure and markers of fibrosis (123). These rats do not develop obesity. Overexpression of α_1 adrenergic receptors leads to LVH by a proposed mechanism involving Gαq, as described above (74, 78, 78). Overexpression of Gαq itself, a G-protein linked to alpha-1 adrenergic receptors, angiotensin II receptors, and endostatin type A receptors, has been shown to have a role in general cardiac hypertrophic development (31, 74, 77). Overexpression of PKC-β2, a further downstream mediator of these same receptors, led to LVH

and expression of pro-fibrotic genes, purportedly via phospholipase C activation (74, 125). In a study comparing mice overexpressing RAS versus wild-type mice exposed to TAC treatment, the degree of LVH was equal between the two and this was associated with significant increases in collagen deposition (a marker of fibrosis) as well as in ANP and BNP levels (43, 74).

The MAPK signaling pathway has been widely accepted to play an important role in cardiac hypertrophy and HF in both humans and rodents, but the specific mechanisms involved are debated (74, 136). Neonatal rat cardiomyocytes *in vitro* have been shown to exhibit hypertrophy when expressing lentiviral-mediated, constituently-active MAP2K3 (126) or via pharmacological activation of the direct downstream effector p38α (27). In contrast, transgenic mice overexpressing constituently-active MAP2K3 do not produce cardiac hypertrophy (64), and mice possessing dominant-negative p38α *in vivo* have exhibited significant increases in hypertrophy versus controls according to one group of investigators (17) and demonstrated no changes in LV thickness compared to wild-type mice from another group (135). These inconsistent results from rodents do not clarify the role of MAP2K3 in myocyte hypertrophy. MAP2K3 transcript levels have been shown to increase 4.7-fold in human HF (15) and increased MAP2K3 activity has been associated with hypertrophy in human embryonic stem cell-derived cardiomyocytes (37). In our preliminary dataset of 18 human hearts, we found increased protein expression of MAP2K3 and phosphorylation of p38 in LVH that was positively associated with BMI in male, but not female, hearts (87).

The Role of Obesity in LVH

Obesity is the most powerful independent predictor of LVH and it nearly doubles the risk of HF in both males and females. It is one of the simplest diagnostics to measure due to lack of cost and invasiveness and therefore is extremely viable in initial determination of LVH

susceptibility. Generally speaking, body mass increases in obesity require increased cardiac output due to more tissue needing to be perfused compared to lean individuals. This leads to an increase in blood volume, thus increasing venous pressure and thus right atrial pressure. Under the Frank-Starling mechanism, this causes an increase in overall cardiac output, and therefore work done by the heart. Obesity is also frequently accompanied by hypertension (over 50% of cases (2)), further perpetuating workload on the heart by increasing afterload (96, 105). Chronically, this leads to diastolic dysfunction and systolic dysfunction via the mechanisms described for LVH and HF.

Models of Obesity

As previously stated, obesity is one of the most common risk factors associated with both LVH and HF. Many rodent models of obesity have been developed, but the majority of them fall under two categories: diet-induced obesity (DIO) or transgenically-induced obesity. Whereas most models under either category are hyperphagic, sedentary, and develop insulin resistance, the transgenic models tend to develop more pronounced hyperglycemia, another risk factor for HF, as compared to DIO animals (69). DIO animals do not develop HF (16, 73). The most common type of DIO, using a 45% or 60% high-fat diet, does not produce the degree of obesity observed in many transgenic models (69). While transgenic animals allow for focused research into the mechanisms induced by discrete genetic changes with regard to obesity, these specific genetic changes may not be relevant to the wider human population. By contrast, obesity in humans is nearly always diet-induced. Although the polygenic nature of outbred animals in these studies may better mimic the wider human population, the underlying mechanisms may not be as easily determinable as compared with inbred strains. In addition, in transgenic models, it can be

difficult to discern whether the physiological differences are the result of genetic alteration per se or versus the obesity itself.

Leptin Signaling

The most well-known transgenic models of rodent obesity share one common feature: disruptions in leptin input. Leptin is a hormone principally produced and secreted by adipose tissue in levels positively associated with fat mass. It was originally discovered by genome sequencing in the *ob/ob* mouse, a mouse that exhibits extreme obesity due to the fact that it lacks leptin. There are multiple isoforms of the leptin receptor (all encoded from a single LEPR gene that undergoes exon shuffling), denoted as Ob-Ra, Ob-Rb, Ob-Rc, Ob-Rd, Ob-Re, and Ob-Rf. All six isoforms contain an N-terminal domain that binds leptin and contains fibronectin III binding domains. The short (Ob-Ra, Ob-Rc, Ob-Rd, and Ob-Rf) and long (Ob-Rb) isoforms have a single transmembrane spanning domain, then a box 1 motif and a janus kinase (JAK) binding domain, but the short isoforms do little to any intracellular signaling. The long isoform, Ob-Rb, also has a suppressor of cytokine signaling (SOCS) domain, a box 2 domain, and a box 3 domain; these are necessary for full JAK-STAT pathway signaling. Ob-Re is a circulating, soluble receptor that serves to bind and transport leptin, though its role, if any, in obesity is unclear. The short isoforms are thought to perhaps play a role in leptin transport in areas such as the blood-brain barrier, but they do not contain all domains necessary for full JAK-STAT activation, and thus only Ob-Rb is considered to be a fully active receptor (42). Not surprisingly, loss of Ob-Rb, such as occurs in the *db/db* mouse, also leads to excessive obesity.

Leptin receptors on the cell surface (10-20% of the overall receptors per cell) typically exist as dimers (127). Upon a dimerized receptor binding one leptin molecule, the dimers form a tetramer (103) and a conformational change initiates signaling. JAK2 is recruited to the box 1

and box 2 domains and phosphorylates the receptor at Tyr985 and Tyr1138. Next, members of the STAT protein family (notably STAT3) bind Tyr1138, are phosphorylated, then dimerize and translocate to the nucleus to act as transcription factors. PI3K, the major intracellular signaling molecule activated by insulin, is also activated by leptin binding Ob-Rb. This leads to downstream Akt/mTOR, MAPK/ERK/JNK, and p38MAPK induction (33, 42). One notable gene that is upregulated by STAT3 activation is SOCS3, which serves to negatively regulate leptin receptor activation by feeding back in a manner that inhibits intracellular signaling induced by leptin (33, 42). Downstream of STAT3 activation, protein tyrosine phosphatase 1B (PTP1B) is also activated and reduces leptin signaling.

Leptin receptors are widely distributed throughout the body and serve to regulate many physiological processes, including cell growth and energy expenditure, and possess the ability to communicate with other cytokines and hormones. The central effect of leptin on body weight comes from its actions in the arcuate nucleus (ARC) of the hypothalamus, where it binds functional leptin receptors on two distinct populations of neurons. Pro-opiomelanocortin (POMC) neurons are activated by leptin and secrete alpha-melanocyte stimulating hormone (αMSH) amongst other POMC-derived peptides whereas leptin inhibits neurons coexpressing Agouti-related peptide and neuropeptide Y (AgRP/NPY). These first-order neurons then project to other areas of the hypothalamus, such as the paraventricular nucleus and lateral hypothalamus, as well as to areas of the brain stem to regulate food intake and energy expenditure. αMSH and AgRP neurons, along with melanocortin 3 receptor (MC3R) and melanocortin 4 receptors (MC4R), form what is referred to as the melanocortin system. αMSH and AgRP compete for binding at these receptors and deletion of MC4R leads to an obese phenotype, suggesting that αMSH input typically dominates in this system. Reciprocal innervations also exist between

POMC and AgRP/NPY neurons, suggesting a highly coordinated response to changes in leptin that occurs with starvation or obesity. Overall, the actions of leptin in the hypothalamus lead to increased satiety, anorexia, and energy expenditure. By contrast, these central actions of leptin are directly opposed by that of ghrelin, a hormone released from the stomach that stimulates hunger (1, 42, 69, 120). Importantly, a lack of leptin is only rarely an explanation for human obesity and, typically, obese individuals have very high circulating levels of leptin. These individuals are considered to be resistant to the anorexigenic effects of leptin, and the sites of this resistance may include decreased transport at the blood-brain barrier as well as deficits in neural responses to leptin.

Transgenic Models of Obesity

The more commonly used rodent models of obesity are those with mutations in LEP or LEPR. There are notable examples of rodents with mutations or deletions in downstream effectors, such as POMC knockout mice (23, 131), POMC and AgRP double knockout mice (30), MC3R knockout mice (19), MC4R knockout mice and rats (53, 82), MC3R and MC4R double knockout mice (25), and AgRP overexpressing mice (45). In a mouse model with designer receptors exclusively activated by designer drugs (DREADDs), activation of AgRP neurons led to feeding and eventual increased adiposity, while inhibition of these populations reduced feeding (59). Lesser-used models that have direct leptin or leptin receptor mutations or deletions include s/s mice (mutated Tyr1138 in Ob-Rb, which is critical for STAT3 binding) (6, 7) and Koletsky rats (LEPR mutation resulting in undetectable Ob-Rb mRNA levels) (117). Nonetheless, the most common rodent models of obesity are the *ob/ob* mouse, *db/db* mouse, and OZR. *ob/ob* mice contain an early stop codon in the mRNA for leptin, leading to the ablation of leptin protein production and circulating hormone levels (137). The effects of leptin deficiency

on food intake, metabolism, and neuroendocrine dysfunction in this mouse model are entirely ameliorated by leptin injection (79). As mentioned above, obese humans are rarely obese due to a lack of leptin, so while the *ob/ob* mouse has been invaluable as a tool to examine how leptin influences body weight regulation, they may not be a good translational model. *db/db* mice and OZR have separate missense mutations in the LEPR gene that result in either an absence of receptor (*db/db* mice) or a significantly reduced ability of Ob-Rb to signal (OZR). Both models have elevated circulating concentrations of leptin (46, 69, 95). A hallmark of *db/db* mice is their development of diabetes type II-like symptoms, thus they are frequently used as a model of diabetes in addition to obesity (46, 69). A parallel model of diabetes and obesity has been outbred into OZR, and is known as the Zucker diabetic fatty rat (106).

Zucker Rats and Human Relevance

OZR are used as a model for a variety of human diseases, e.g. hypertension, metabolic syndrome, chronic kidney disease, hyperlipidemia, and mild diabetes, depending on the age of the animal. They were initially inbred from rats that spontaneously developed obesity when given free access to food, developing up to 50% of their body mass as fat (compared to around 20% in lean controls). They are hyperphagic at a young age (fewer than three weeks) and can become over twice the body weight of lean controls as early as six weeks of age (24). In research, they have been historically favored, as compared to *ob/ob* and *db/db* mice, because Zuckers do not develop hyperglycemia to an extreme extent, therefore making this model more suitable for studying the effect of obesity alone (54, 74).

Despite a persistent increase in body weight starting early in life, no changes in mean arterial pressure of OZR were noted at 8 weeks of age in one study (97) and at both 9 and 13 months in another (29). Regardless, LVH has been established to be present by week 12 (100).

Cardiomyocyte hypertrophy has been seen in OZR that exhibited increased QT interval as young as 16 weeks of age (67). A study of young rats (aged 9-13 weeks) looking at mRNA levels for NPPA and NPPB, both of which are elevated in human LVH and HF, only found a significant increase in NPPB, and this was unexpectedly in the lean animals (20). Another study in 5-6 month old Zucker rats found increases in both ANP and BNP, the peptide products of NPPA and NPPB (26). The longer amount of time required for LVH development in these animals is more comparable to human LVH than other TAC models, and their shared cardiac hormone profile, make them a viable model for obesity-related LVH.

Conclusions

Pathological LVH is a poorly-understood disease with many negative prognostic outcomes, most notably HF. As a comorbidity with obesity and rising obesity rates throughout the world, research into the development of LVH is implicit for future diagnoses and treatment. Investigating LVH in humans directly is hindered by the lack of availability of live donor tissue, therefore the development of new animal models is critical for the future of LVH research. The purpose of this research is to validate genes and proteins known to play a role in human HF that are also present in LVH as potential biomarkers of heart damage, then develop a novel model of LVH to further study the roles of these genes and proteins. The central hypothesis is that genes and proteins that are differentially expressed in HF and LVH, with regard to sex and obesity status, may serve as clinical biomarkers or therapeutic targets for detection and prevention of HF. This will be explored via two specifics aims:

1. To identify differentially expressed genes that are common between human HF and LVH compared to non-failed hearts

2. To develop novel models to characterize the differentially expressed genes in human LVH

Figures

Figure 1. Representative pressure-volume loop of LVH and normal heart

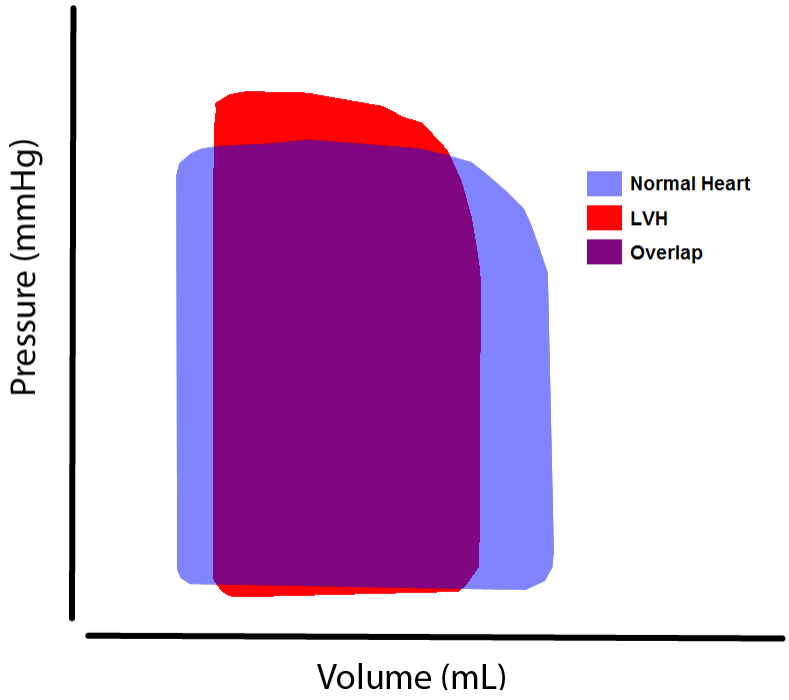

Figure 1. A basic representation of changes in a pressure-volume loop for a normal heart (blue) and an LVH heart (red). The narrowing of the LVH heart loop shows decreased total filling volume, reflecting reduced left ventricular lumen. The increased height of the loop represents increased pressure necessary for ejection, as seen in hypertension.

References

(1) Andermann ML, Lowell BB. Toward a Wiring Diagram Understanding of Appetite Control. Neuron 2017 Aug 16;95(4):757-78.

(2) Aronow WS. Association of obesity with hypertension. Ann Transl Med 2017 Sep;5(17):350.

(3) Arrowood JA, Minisi AJ, Goudreau E, Davis AB, King AL. Absence of parasympathetic control of heart rate after human orthotopic cardiac transplantation. Circulation 1997 Nov 18;96(10):3492-8.

(4) Bacharova L. Left ventricular hypertrophy: disagreements between increased left ventricular mass and ECG-LVH criteria: the effect of impaired electrical properties of myocardium. J Electrocardiol 2014 Sep;47(5):625-9.

(5) Bacharova L, Estes EH. Left Ventricular Hypertrophy by the Surface ECG. J Electrocardiol 2017 Nov;50(6):906-8.

(6) Bates SH, Kulkarni RN, Seifert M, Myers MG, Jr. Roles for leptin receptor/STAT3-dependent and -independent signals in the regulation of glucose homeostasis. Cell Metab 2005 Mar;1(3):169-78.

(7) Bates SH, Stearns WH, Dundon TA, Schubert M, Tso AW, Wang Y, et al. STAT3 signalling is required for leptin regulation of energy balance but not reproduction. Nature 2003 Feb 20;421(6925):856-9.

(8) Beaulieu P, Cardinal R, De LA, Lambert C. Direct chronotropic effects of atrial and C-type natriuretic peptides in anaesthetized dogs. Br J Pharmacol 1996 Aug;118(7):1790-6.

(9) Beaulieu P, Cardinal R, Page P, Francoeur F, Tremblay J, Lambert C. Positive chronotropic and inotropic effects of C-type natriuretic peptide in dogs. Am J Physiol 1997 Oct;273(4):H1933-H1940.

(10) Benjamin EJ, Muntner P, Alonso A, Bittencourt MS, Callaway CW, Carson AP, et al. Heart Disease and Stroke Statistics-2019 Update: A Report From the American Heart Association. Circulation 2019 Mar 5;139(10):e56-e528.

(11) Bergmann O, Bhardwaj RD, Bernard S, Zdunek S, Barnabe-Heider F, Walsh S, et al. Evidence for cardiomyocyte renewal in humans. Science 2009 Apr 3;324(5923):98-102.

(12) Berk BC, Fujiwara K, Lehoux S. ECM remodeling in hypertensive heart disease. J Clin Invest 2007 Mar;117(3):568-75.

(13) Bibbins-Domingo K, Pletcher MJ, Lin F, Vittinghoff E, Gardin JM, Arynchyn A, et al. Racial differences in incident heart failure among young adults. N Engl J Med 2009 Mar 19;360(12):1179-90.

(14) Birnbaum Y, Alam M. LVH and the diagnosis of ST. J Electrocardiol 2014 Sep;47(5):655-60.

(15) Boheler KR, Volkova M, Morrell C, Garg R, Zhu Y, Margulies K, et al. Sex- and age-dependent human transcriptome variability: implications for chronic heart failure. Proc Natl Acad Sci U S A 2003 Mar 4;100(5):2754-9.

(16) Brainard RE, Watson LJ, Demartino AM, Brittian KR, Readnower RD, Boakye AA, et al. High fat feeding in mice is insufficient to induce cardiac dysfunction and does not exacerbate heart failure. PLoS One 2013;8(12):e83174.

(17) Braz JC, Bueno OF, Liang Q, Wilkins BJ, Dai YS, Parsons S, et al. Targeted inhibition of p38 MAPK promotes hypertrophic cardiomyopathy through upregulation of calcineurin-NFAT signaling. J Clin Invest 2003 May;111(10):1475-86.

(18) Burchfield JS, Xie M, Hill JA. Pathological ventricular remodeling: mechanisms: part 1 of 2. Circulation 2013 Jul 23;128(4):388-400.

(19) Butler AA, Kesterson RA, Khong K, Cullen MJ, Pelleymounter MA, Dekoning J, et al. A unique metabolic syndrome causes obesity in the melanocortin-3 receptor-deficient mouse. Endocrinology 2000 Sep;141(9):3518-21.

(20) Cabiati M, Raucci S, Liistro T, Belcastro E, Prescimone T, Caselli C, et al. Impact of obesity on the expression profile of natriuretic peptide system in a rat experimental model. PLoS One 2013;8(8):e72959.

(21) Casale PN, Devereux RB, Alonso DR, Campo E, Kligfield P. Improved sex-specific criteria of left ventricular hypertrophy for clinical and computer interpretation of electrocardiograms: validation with autopsy findings. Circulation 1987 Mar;75(3):565-72.

(22) Centers for Disease Control and Prevention. Underlying Causes of Death, 1999-2017. 2020. National Center for Health Statistics.

(23) Challis BG, Coll AP, Yeo GS, Pinnock SB, Dickson SL, Thresher RR, et al. Mice lacking pro-opiomelanocortin are sensitive to high-fat feeding but respond normally to the acute anorectic effects of peptide-YY(3-36). Proc Natl Acad Sci U S A 2004 Mar 30;101(13):4695-700.

(24) Charles River Laboratories. Zucker Rat Growth Chart. 2-1-2020. Charles River Laboratories.

(25) Chen AS, Marsh DJ, Trumbauer ME, Frazier EG, Guan XM, Yu H, et al. Inactivation of the mouse melanocortin-3 receptor results in increased fat mass and reduced lean body mass. Nat Genet 2000 Sep;26(1):97-102.

(26) Chen WK, Yeh YL, Lin YM, Lin JY, Tzang BS, Lin JA, et al. Cardiac hypertrophy-related pathways in obesity. Chin J Physiol 2014 Jun 30;57(3):111-20.

(27) Clerk A, Michael A, Sugden PH. Stimulation of the p38 mitogen-activated protein kinase pathway in neonatal rat ventricular myocytes by the G protein-coupled receptor agonists, endothelin-1 and phenylephrine: a role in cardiac myocyte hypertrophy? J Cell Biol 1998 Jul 27;142(2):523-35.

(28) Coglianese EE, Qureshi MM, Vasan RS, Wang TJ, Moore LL. Usefulness of the blood hematocrit level to predict development of heart failure in a community. Am J Cardiol 2012 Jan 15;109(2):241-5.

(29) Conti M, Renaud IM, Poirier B, Michel O, Belair MF, Mandet C, et al. High levels of myocardial antioxidant defense in aging nondiabetic normotensive Zucker obese rats. Am J Physiol Regul Integr Comp Physiol 2004 Apr;286(4):R793-R800.

(30) Corander MP, Rimmington D, Challis BG, O'Rahilly S, Coll AP. Loss of agouti-related peptide does not significantly impact the phenotype of murine POMC deficiency. Endocrinology 2011 May;152(5):1819-28.

(31) D'Angelo DD, Sakata Y, Lorenz JN, Boivin GP, Walsh RA, Liggett SB, et al. Transgenic Galphaq overexpression induces cardiac contractile failure in mice. Proc Natl Acad Sci U S A 1997 Jul 22;94(15):8121-6.

(32) Deschepper CF, Masciotra S, Zahabi A, Boutin-Ganache I, Picard S, Reudelhuber TL. Functional alterations of the Nppa promoter are linked to cardiac ventricular hypertrophy in WKY/WKHA rat crosses. Circ Res 2001 Feb 2;88(2):223-8.

(33) Devos R, Guisez Y, Van der Heyden J, White DW, Kalai M, Fountoulakis M, et al. Ligand-independent dimerization of the extracellular domain of the leptin receptor and determination of the stoichiometry of leptin binding. J Biol Chem 1997 Jul 18;272(29):18304-10.

(34) Dhingra R, Gona P, Wang TJ, Fox CS, D'Agostino RB, Sr., Vasan RS. Serum gamma-glutamyl transferase and risk of heart failure in the community. Arterioscler Thromb Vasc Biol 2010 Sep;30(9):1855-60.

(35) Dries DL. Natriuretic peptides and the genomics of left-ventricular hypertrophy. Heart Fail Clin 2010 Jan;6(1):55-64.

(36) Eichhorn L, Weisheit CK, Gestrich C, Peukert K, Duerr GD, Ayub MA, et al. A Closed-chest Model to Induce Transverse Aortic Constriction in Mice. J Vis Exp 2018 Apr 5;(134).

(37) Foldes G, Mioulane M, Wright JS, Liu AQ, Novak P, Merkely B, et al. Modulation of human embryonic stem cell-derived cardiomyocyte growth: a testbed for studying human cardiac hypertrophy? J Mol Cell Cardiol 2011 Feb;50(2):367-76.

(38) Folsom AR, Shah AM, Lutsey PL, Roetker NS, Alonso A, Avery CL, et al. American Heart Association's Life's Simple 7: Avoiding Heart Failure and Preserving Cardiac Structure and Function. Am J Med 2015 Sep;128(9):970-6.

(39) Foppa M, Duncan BB, Rohde LE. Echocardiography-based left ventricular mass estimation. How should we define hypertrophy? Cardiovasc Ultrasound 2005 Jun 17;3:17.

(40) Fu S, Ping P, Wang F, Luo L. Synthesis, secretion, function, metabolism and application of natriuretic peptides in heart failure. J Biol Eng 2018;12:2.

(41) Galimberti ES, Kannankeril P, Kor K, Muhammad R, Blair M, Darbar D. Abstract 19074: NPPA Overexpression in Mice Increases Susceptibility to Atrial Fibrillation. Circulation 2012 Nov 20;126(Suppl 21):A19074.

(42) Gorska E, Popko K, Stelmaszczyk-Emmel A, Ciepiela O, Kucharska A, Wasik M. Leptin receptors. Eur J Med Res 2010 Nov 4;15 Suppl 2:50-4.

(43) Gottshall KR, Hunter JJ, Tanaka N, Dalton N, Becker KD, Ross J, Jr., et al. Ras-dependent pathways induce obstructive hypertrophy in echo-selected transgenic mice. Proc Natl Acad Sci U S A 1997 Apr 29;94(9):4710-5.

(44) Grabowski K, Riemenschneider M, Schulte L, Witten A, Schulz A, Stoll M, et al. Fetal-adult cardiac transcriptome analysis in rats with contrasting left ventricular mass reveals new candidates for cardiac hypertrophy. PLoS One 2015;10(2):e0116807.

(45) Graham M, Shutter JR, Sarmiento U, Sarosi I, Stark KL. Overexpression of Agrt leads to obesity in transgenic mice. Nat Genet 1997 Nov;17(3):273-4.

(46) Halaas JL, Gajiwala KS, Maffei M, Cohen SL, Chait BT, Rabinowitz D, et al. Weight-reducing effects of the plasma protein encoded by the obese gene. Science 1995 Jul 28;269(5223):543-6.

(47) Hashem MS, Kalashyan H, Choy J, Chiew SK, Shawki AH, Dawood AH, et al. Left ventricular relative wall thickness versus left ventricular mass index in non-cardioembolic stroke patients. Medicine (Baltimore) 2015 May;94(20):e872.

(48) Heidenreich PA, Albert NM, Allen LA, Bluemke DA, Butler J, Fonarow GC, et al. Forecasting the impact of heart failure in the United States: a policy statement from the American Heart Association. Circ Heart Fail 2013 May;6(3):606-19.

(49) Hein L, Stevens ME, Barsh GS, Pratt RE, Kobilka BK, Dzau VJ. Overexpression of angiotensin AT1 receptor transgene in the mouse myocardium produces a lethal phenotype associated with myocyte hyperplasia and heart block. Proc Natl Acad Sci U S A 1997 Jun 10;94(12):6391-6.

(50) Houweling AC, van Borren MM, Moorman AF, Christoffels VM. Expression and regulation of the atrial natriuretic factor encoding gene Nppa during development and disease. Cardiovasc Res 2005 Sep 1;67(4):583-93.

(51) Hu P, Zhang D, Swenson L, Chakrabarti G, Abel ED, Litwin SE. Minimally invasive aortic banding in mice: effects of altered cardiomyocyte insulin signaling during pressure overload. Am J Physiol Heart Circ Physiol 2003 Sep;285(3):H1261-H1269.

(52) Huffman MD, Berry JD, Ning H, Dyer AR, Garside DB, Cai X, et al. Lifetime risk for heart failure among white and black Americans: cardiovascular lifetime risk pooling project. J Am Coll Cardiol 2013 Apr 9;61(14):1510-7.

(53) Huszar D, Lynch CA, Fairchild-Huntress V, Dunmore JH, Fang Q, Berkemeier LR, et al. Targeted disruption of the melanocortin-4 receptor results in obesity in mice. Cell 1997 Jan 10;88(1):131-41.

(54) Kava R, Greenwood MRC, Johnson PR. Zucker (fa/fa) Rat. ILAR Journal 32[3], 4-8. 1990.

(55) Kecskemeti V, Pacher P, Pankucsi C, Nanasi P. Comparative study of cardiac electrophysiological effects of atrial natriuretic peptide. Mol Cell Biochem 1996 Jul;160-161:53-9.

(56) Kenchaiah S, Evans JC, Levy D, Wilson PW, Benjamin EJ, Larson MG, et al. Obesity and the risk of heart failure. N Engl J Med 2002 Aug 1;347(5):305-13.

(57) Khazanie P, Hammill BG, Patel CB, Eapen ZJ, Peterson ED, Rogers JG, et al. Trends in the use and outcomes of ventricular assist devices among medicare beneficiaries, 2006 through 2011. J Am Coll Cardiol 2014 Apr 15;63(14):1395-404.

(58) Kirklin JK, Naftel DC, Pagani FD, Kormos RL, Stevenson LW, Blume ED, et al. Seventh INTERMACS annual report: 15,000 patients and counting. J Heart Lung Transplant 2015 Dec;34(12):1495-504.

(59) Krashes MJ, Koda S, Ye C, Rogan SC, Adams AC, Cusher DS, et al. Rapid, reversible activation of AgRP neurons drives feeding behavior in mice. J Clin Invest 2011 Apr;121(4):1424-8.

(60) Lam CS, Lyass A, Kraigher-Krainer E, Massaro JM, Lee DS, Ho JE, et al. Cardiac dysfunction and noncardiac dysfunction as precursors of heart failure with reduced and preserved ejection fraction in the community. Circulation 2011 Jul 5;124(1):24-30.

(61) Lazzeroni D, Rimoldi O, Camici PG. From Left Ventricular Hypertrophy to Dysfunction and Failure. Circ J 2016;80(3):555-64.

(62) Lei B, Chess DJ, Keung W, O'Shea KM, Lopaschuk GD, Stanley WC. Transient activation of p38 MAP kinase and up-regulation of Pim-1 kinase in cardiac hypertrophy despite no activation of AMPK. J Mol Cell Cardiol 2008 Sep;45(3):404-10.

(63) Levy D, Kenchaiah S, Larson MG, Benjamin EJ, Kupka MJ, Ho KK, et al. Long-term trends in the incidence of and survival with heart failure. N Engl J Med 2002 Oct 31;347(18):1397-402.

(64) Liao P, Georgakopoulos D, Kovacs A, Zheng M, Lerner D, Pu H, et al. The in vivo role of p38 MAP kinases in cardiac remodeling and restrictive cardiomyopathy. Proc Natl Acad Sci U S A 2001 Oct 9;98(21):12283-8.

(65) Lien CL, Harrison MR, Tuan TL, Starnes VA. Heart repair and regeneration: recent insights from zebrafish studies. Wound Repair Regen 2012 Sep;20(5):638-46.

(66) Lin FY, Devereux RB, Roman MJ, Meng J, Jow VM, Jacobs A, et al. Cardiac chamber volumes, function, and mass as determined by 64-multidetector row computed tomography: mean values among healthy adults free of hypertension and obesity. JACC Cardiovasc Imaging 2008 Nov;1(6):782-6.

(67) Lin YC, Huang J, Kan H, Castranova V, Frisbee JC, Yu HG. Defective calcium inactivation causes long QT in obese insulin-resistant rat. Am J Physiol Heart Circ Physiol 2012 Feb 15;302(4):H1013-H1022.

(68) Loehr LR, Rosamond WD, Chang PP, Folsom AR, Chambless LE. Heart failure incidence and survival (from the Atherosclerosis Risk in Communities study). Am J Cardiol 2008 Apr 1;101(7):1016-22.

(69) Lutz TA, Woods SC. Overview of animal models of obesity. Curr Protoc Pharmacol 2012 Sep;Chapter 5:Unit5.

(70) Maillet M, van Berlo JH, Molkentin JD. Molecular basis of physiological heart growth: fundamental concepts and new players. Nat Rev Mol Cell Biol 2013 Jan;14(1):38-48.

(71) Malhotra A, Sharma S. Hypertrophic Cardiomyopathy in Athletes. Eur Cardiol 2017 Dec;12(2):80-2.

(72) Marasco SF, Summerhayes R, Quayle M, McGiffin D, Luthe M. Cost comparison of heart transplant vs. left ventricular assist device therapy at one year. Clin Transplant 2016 May;30(5):598-605.

(73) Martins MA, Murucci CP, Bermond M, V, Dos SL, Monteiro de Assis ALE, Valentim NB, et al. Hypercaloric diet models do not develop heart failure, but the excess sucrose promotes contractility dysfunction. PLoS One 2020;15(2):e0228860.

(74) McMullen JR, Jennings GL. Differences between pathological and physiological cardiac hypertrophy: novel therapeutic strategies to treat heart failure. Clin Exp Pharmacol Physiol 2007 Apr;34(4):255-62.

(75) McMullen JR, Shioi T, Huang WY, Zhang L, Tarnavski O, Bisping E, et al. The insulin-like growth factor 1 receptor induces physiological heart growth via the phosphoinositide 3-kinase(p110alpha) pathway. J Biol Chem 2004 Feb 6;279(6):4782-93.

(76) Melleby AO, Romaine A, Aronsen JM, Veras I, Zhang L, Sjaastad I, et al. A novel method for high precision aortic constriction that allows for generation of specific cardiac phenotypes in mice. Cardiovasc Res 2018 Oct 1;114(12):1680-90.

(77) Mende U, Kagen A, Cohen A, Aramburu J, Schoen FJ, Neer EJ. Transient cardiac expression of constitutively active Galphaq leads to hypertrophy and dilated cardiomyopathy by

calcineurin-dependent and independent pathways. Proc Natl Acad Sci U S A 1998 Nov 10;95(23):13893-8.

(78) Milano CA, Dolber PC, Rockman HA, Bond RA, Venable ME, Allen LF, et al. Myocardial expression of a constitutively active alpha 1B-adrenergic receptor in transgenic mice induces cardiac hypertrophy. Proc Natl Acad Sci U S A 1994 Oct 11;91(21):10109-13.

(79) Mistry AM, Swick AG, Romsos DR. Leptin rapidly lowers food intake and elevates metabolic rates in lean and ob/ob mice. J Nutr 1997 Oct;127(10):2065-72.

(80) Moghtadaei M, Polina I, Rose RA. Electrophysiological effects of natriuretic peptides in the heart are mediated by multiple receptor subtypes. Prog Biophys Mol Biol 2016 Jan;120(1-3):37-49.

(81) Mori T, Chen YF, Feng JA, Hayashi T, Oparil S, Perry GJ. Volume overload results in exaggerated cardiac hypertrophy in the atrial natriuretic peptide knockout mouse. Cardiovasc Res 2004 Mar 1;61(4):771-9.

(82) Mul JD, van BR, Bergen DJ, Brans MA, Brakkee JH, Toonen PW, et al. Melanocortin receptor 4 deficiency affects body weight regulation, grooming behavior, and substrate preference in the rat. Obesity (Silver Spring) 2012 Mar;20(3):612-21.

(83) Nagai T, Honda Y, Nakano H, Honda S, Iwakami N, Mizuno A, et al. Rationale and Design of Low-dose Administration of Carperitide for Acute Heart Failure (LASCAR-AHF). Cardiovasc Drugs Ther 2017 Dec;31(5-6):551-7.

(84) Naranjo V, Contreras A, Merino B, Plaza A, Lorenzo MP, Garcia-Caceres C, et al. Specific Deletion of the Astrocyte Leptin Receptor Induces Changes in Hippocampus Glutamate Metabolism, Synaptic Transmission and Plasticity. Neuroscience 2019 Nov 6.

(85) Neri Serneri GG, Boddi M, Modesti PA, Cecioni I, Coppo M, Padeletti L, et al. Increased cardiac sympathetic activity and insulin-like growth factor-I formation are associated with physiological hypertrophy in athletes. Circ Res 2001 Nov 23;89(11):977-82.

(86) Newman MS, Nguyen T, Watson MJ, Hull RW, Yu HG. Transcriptome profiling reveals novel BMI- and sex-specific gene expression signatures for human cardiac hypertrophy. Physiol Genomics 2017 Jul 1;49(7):355-67.

(87) Newman M, Infanto AM, Watson MJ, Hull RW, Yu HG. Abstract 140: BMI- and Gender-specific Increase of MAP2K3/p38 Activity in Human Cardiac Hypertrophy. Circulation Research 2017 Feb 23;119(Suppl 1):A140.

(88) Ojji DB, Opie LH, Lecour S, Lacerda L, Adeyemi OM, Sliwa K. The proposed role of plasma NT pro-brain natriuretic peptide in assessing cardiac remodelling in hypertensive African subjects. Cardiovasc J Afr 2014 Sep;25(5):233-8.

(89) Oseni AO, Qureshi WT, Almahmoud MF, Bertoni AG, Bluemke DA, Hundley WG, et al. Left ventricular hypertrophy by ECG versus cardiac MRI as a predictor for heart failure. Heart 2017 Jan 1;103(1):49-54.

(90) Owens AT, Brozena SC, Jessup M. New Management Strategies in Heart Failure. Circ Res 2016 Feb 5;118(3):480-95.

(91) Paget V, Legedz L, Gaudebout N, Girerd N, Bricca G, Milon H, et al. N-terminal pro-brain natriuretic peptide: a powerful predictor of mortality in hypertension. Hypertension 2011 Apr;57(4):702-9.

(92) Palazzuoli A, Gallotta M, Quatrini I, Nuti R. Natriuretic peptides (BNP and NT-proBNP): measurement and relevance in heart failure. Vasc Health Risk Manag 2010 Jun 1;6:411-8.

(93) Pandey KN. Genetic Ablation and Guanylyl Cyclase/Natriuretic Peptide Receptor-A: Impact on the Pathophysiology of Cardiovascular Dysfunction. Int J Mol Sci 2019 Aug 14;20(16).

(94) Park JK, Shin JH, Kim SH, Lim YH, Kim KS, Kim SG, et al. A comparison of cornell and sokolow-lyon electrocardiographic criteria for left ventricular hypertrophy in korean patients. Korean Circ J 2012 Sep;42(9):606-13.

(95) Phillips MS, Liu Q, Hammond HA, Dugan V, Hey PJ, Caskey CJ, et al. Leptin receptor missense mutation in the fatty Zucker rat. Nat Genet 1996 May;13(1):18-9.

(96) Poirier P, Giles TD, Bray GA, Hong Y, Stern JS, Pi-Sunyer FX, et al. Obesity and cardiovascular disease: pathophysiology, evaluation, and effect of weight loss. Arterioscler Thromb Vasc Biol 2006 May;26(5):968-76.

(97) Porsti I, Kahonen M, Wu X, Arvola P, Ruskoaho H. Long-term physical exercise and atrial natriuretic peptide in obese Zucker rats. Pharmacol Toxicol 2002 Jul;91(1):8-12.

(98) Potter LR, Yoder AR, Flora DR, Antos LK, Dickey DM. Natriuretic peptides: their structures, receptors, physiologic functions and therapeutic applications. Handb Exp Pharmacol 2009;(191):341-66.

(99) Reiss K, Cheng W, Ferber A, Kajstura J, Li P, Li B, et al. Overexpression of insulin-like growth factor-1 in the heart is coupled with myocyte proliferation in transgenic mice. Proc Natl Acad Sci U S A 1996 Aug 6;93(16):8630-5.

(100) Ren J, Walsh MF, Jefferson L, Natavio M, Ilg KJ, Sowers JR, et al. Basal and ethanol-induced cardiac contractile response in lean and obese Zucker rat hearts. J Biomed Sci 2000 Sep;7(5):390-400.

(101) Rider OJ, Ntusi N, Bull SC, Nethononda R, Ferreira V, Holloway CJ, et al. Improvements in ECG accuracy for diagnosis of left ventricular hypertrophy in obesity. Heart 2016 Oct 1;102(19):1566-72.

(102) Rodriguez-Padial L, Akerstrom F, Robles-Gamboa C, Andres J, Ruiz-Baena J. Diagnostic accuracy of left ventricular hypertrophy in patients with myocardial infarction by computer-assisted electrocardiography (ELECTROPRES). Ann Noninvasive Electrocardiol 2013 Mar;18(2):170-80.

(103) Roujeau C, Jockers R, Dam J. New pharmacological perspectives for the leptin receptor in the treatment of obesity. Front Endocrinol (Lausanne) 2014;5:167.

(104) Sadowsk HS. Cardiac Translplantation: A Review. Physical Therapy 1996 May 1;76(5):498-515.

(105) Sardu C, De LC, Wallner M, Santulli G. Diabetes Mellitus and Its Cardiovascular Complications: New Insights into an Old Disease. J Diabetes Res 2019;2019:1905194.

(106) Shiota M, Printz RL. Diabetes in Zucker diabetic fatty rat. Methods Mol Biol 2012;933:103-23.

(107) Sipola P, Magga J, Husso M, Jaaskelainen P, Peuhkurinen K, Kuusisto J. Cardiac MRI assessed left ventricular hypertrophy in differentiating hypertensive heart disease from hypertrophic cardiomyopathy attributable to a sarcomeric gene mutation. Eur Radiol 2011 Jul;21(7):1383-9.

(108) Sohaib SM, Payne JR, Shukla R, World M, Pennell DJ, Montgomery HE. Electrocardiographic (ECG) criteria for determining left ventricular mass in young healthy men; data from the LARGE Heart study. J Cardiovasc Magn Reson 2009 Jan 16;11:2.

(109) Sokolow M, Lyon TP. The ventricular complex in left ventricular hypertrophy as obtained by unipolar precordial and limb leads. 1949. Ann Noninvasive Electrocardiol 2001 Oct;6(4):343-68.

(110) Song W, Wang H, Wu Q. Atrial natriuretic peptide in cardiovascular biology and disease (NPPA). Gene 2015 Sep 10;569(1):1-6.

(111) Souders CA, Bowers SL, Baudino TA. Cardiac fibroblast: the renaissance cell. Circ Res 2009 Dec 4;105(12):1164-76.

(112) Stambler BS, Guo GB. Atrial natriuretic peptide has dose-dependent, autonomically mediated effects on atrial refractoriness and repolarization in anesthetized dogs. J Cardiovasc Electrophysiol 2005 Dec;16(12):1341-7.

(113) Steinberg BA, Zhao X, Heidenreich PA, Peterson ED, Bhatt DL, Cannon CP, et al. Trends in patients hospitalized with heart failure and preserved left ventricular ejection fraction: prevalence, therapies, and outcomes. Circulation 2012 Jul 3;126(1):65-75.

(114) Su FY, Li YH, Lin YP, Lee CJ, Wang CH, Meng FC, et al. A comparison of Cornell and Sokolow-Lyon electrocardiographic criteria for left ventricular hypertrophy in a military male population in Taiwan: the Cardiorespiratory fitness and HospItalization Events in armed Forces study. Cardiovasc Diagn Ther 2017 Jun;7(3):244-51.

(115) Suga S, Nakao K, Hosoda K, Mukoyama M, Ogawa Y, Shirakami G, et al. Receptor selectivity of natriuretic peptide family, atrial natriuretic peptide, brain natriuretic peptide, and C-type natriuretic peptide. Endocrinology 1992 Jan;130(1):229-39.

(116) Szewieczek J, Gasior Z, Dulawa J, Francuz T, Legierska K, Batko-Szwaczka A, et al. ECG low QRS voltage and wide QRS complex predictive of centenarian 360-day mortality. Age (Dordr) 2016 Apr;38(2):44.

(117) Takaya K, Ogawa Y, Hiraoka J, Hosoda K, Yamori Y, Nakao K, et al. Nonsense mutation of leptin receptor in the obese spontaneously hypertensive Koletsky rat. Nat Genet 1996 Oct;14(2):130-1.

(118) Takimoto E, Champion HC, Li M, Belardi D, Ren S, Rodriguez ER, et al. Chronic inhibition of cyclic GMP phosphodiesterase 5A prevents and reverses cardiac hypertrophy. Nat Med 2005 Feb;11(2):214-22.

(119) Tarnavski O, McMullen JR, Schinke M, Nie Q, Kong S, Izumo S. Mouse cardiac surgery: comprehensive techniques for the generation of mouse models of human diseases and their application for genomic studies. Physiol Genomics 2004 Feb 13;16(3):349-60.

(120) Toda C, Santoro A, Kim JD, Diano S. POMC Neurons: From Birth to Death. Annu Rev Physiol 2017 Feb 10;79:209-36.

(121) Uhlen M, Fagerberg L, Hallstrom BM, Lindskog C, Oksvold P, Mardinoglu A, et al. Proteomics. Tissue-based map of the human proteome. Science 2015 Jan 23;347(6220):1260419.

(122) Velagaleti RS, Gona P, Larson MG, Wang TJ, Levy D, Benjamin EJ, et al. Multimarker approach for the prediction of heart failure incidence in the community. Circulation 2010 Oct 26;122(17):1700-6.

(123) Villarreal FJ, MacKenna DA, Omens JH, Dillmann WH. Myocardial remodeling in hypertensive Ren-2 transgenic rats. Hypertension 1995 Jan;25(1):98-104.

(124) Voigt J, Sasha JM, Taylor A, Krucoff M, Reynolds MR, Michael GC. A reevaluation of the costs of heart failure and its implications for allocation of health resources in the United States. Clin Cardiol 2014 May;37(5):312-21.

(125) Wakasaki H, Koya D, Schoen FJ, Jirousek MR, Ways DK, Hoit BD, et al. Targeted overexpression of protein kinase C beta2 isoform in myocardium causes cardiomyopathy. Proc Natl Acad Sci U S A 1997 Aug 19;94(17):9320-5.

(126) Wang Y, Huang S, Sah VP, Ross J, Jr., Brown JH, Han J, et al. Cardiac muscle cell hypertrophy and apoptosis induced by distinct members of the p38 mitogen-activated protein kinase family. J Biol Chem 1998 Jan 23;273(4):2161-8.

(127) Wauman J, Zabeau L, Tavernier J. The Leptin Receptor Complex: Heavier Than Expected? Front Endocrinol (Lausanne) 2017;8:30.

(128) Weroha SJ, Haluska P. The insulin-like growth factor system in cancer. Endocrinol Metab Clin North Am 2012 Jun;41(2):335-50, vi.

(129) Wilkins BJ, Dai YS, Bueno OF, Parsons SA, Xu J, Plank DM, et al. Calcineurin/NFAT coupling participates in pathological, but not physiological, cardiac hypertrophy. Circ Res 2004 Jan 9;94(1):110-8.

(130) Yandrapalli S, Jolly G, Biswas M, Rochlani Y, Harikrishnan P, Aronow WS, et al. Newer hormonal pharmacotherapies for heart failure. Expert Rev Endocrinol Metab 2018 Jan;13(1):35-49.

(131) Yaswen L, Diehl N, Brennan MB, Hochgeschwender U. Obesity in the mouse model of pro-opiomelanocortin deficiency responds to peripheral melanocortin. Nat Med 1999 Sep;5(9):1066-70.

(132) Yi S, Wang F, Wan M, Yi X, Zhang Y, Sun S. Prediction of stroke with electrocardiographic left ventricular hypertrophy in hypertensive patients: A meta-analysis. J Electrocardiol 2020 Apr 28;61:27-31.

(133) Yildiz M, Oktay AA, Stewart MH, Milani RV, Ventura HO, Lavie CJ. Left ventricular hypertrophy and hypertension. Prog Cardiovasc Dis 2019 Nov 21.

(134) Yutzey KE. Cardiomyocyte Proliferation: Teaching an Old Dogma New Tricks. Circ Res 2017 Feb 17;120(4):627-9.

(135) Zhang S, Weinheimer C, Courtois M, Kovacs A, Zhang CE, Cheng AM, et al. The role of the Grb2-p38 MAPK signaling pathway in cardiac hypertrophy and fibrosis. J Clin Invest 2003 Mar;111(6):833-41.

(136) Zhang W, Elimban V, Nijjar MS, Gupta SK, Dhalla NS. Role of mitogen-activated protein kinase in cardiac hypertrophy and heart failure. Exp Clin Cardiol 2003;8(4):173-83.

(137) Zhang Y, Proenca R, Maffei M, Barone M, Leopold L, Friedman JM. Positional cloning of the mouse obese gene and its human homologue. Nature 1994 Dec 1;372(6505):425-32.

CHAPTER 2

Transcriptome profiling reveals novel BMI- and sex-specific gene expression signatures for human cardiac hypertrophy

Mackenzie S. Newman[1], Tina Nguyen[1], Michael J. Watson[2], Robert W. Hull[3], and Han-Gang Yu[1]

[1]Physiology and Pharmacology, West Virginia University, Morgantown, West Virginia;

[2]Department of Surgery, Duke University, Durham, North Carolina; and

[3]Department of Cardiology, West Virginia University, Morgantown, West Virginia

Original publication: Physiol Genomics. 2017 Jul 1;49(7):355-367. doi: 10.1152/physiolgenomics.00122.2016. Epub 2017 May 12.

Abstract

How obesity or sex may affect the gene expression profiles of human cardiac hypertrophy is unknown. We hypothesized that body-mass index (BMI) and sex can affect gene expression profiles of cardiac hypertrophy. Human heart tissues were grouped according to sex (male, female), BMI (lean<25 kg/m^2, obese>30 kg/m^2), or LVH and non-LVH nonfailed controls (NF). We identified 24 differentially expressed (DE) genes comparing female with male samples. In obese subgroup, there were 236 DE genes comparing LVH with NF; in lean subgroup, there were seven DE genes comparing LVH with NF. In female subgroup, we identified 1,320 significant genes comparing LVH with NF; in male subgroup, there were 1,383 significant genes comparing LVH with NF. There were seven significant genes comparing obese LVH with lean NF; comparing male obese LVH with male lean NF samples we found 106 significant genes; comparing female obese LVH with male lean NF, we found no significant genes. Using absolute value of $\log_2$ fold-change > 2 or extremely small *P* value (10^{-20}) as a criterion, we identified nine significant genes (HBA1, HBB, HIST1H2AC, GSTT1, MYL7, NPPA, NPPB, PDK4, PLA2G2A) in LVH, also found in published data set for ischemic and dilated cardiomyopathy in HF. We identified a potential gene expression signature that distinguishes between patients with high BMI or between men and women with cardiac hypertrophy. Expression of established biomarkers natriuretic peptide A (NPPA) and B (NPPB) were already significantly increased in hypertrophy compared with controls.

Introduction

In a recent global body mass index (BMI) mortality collaboration study from data collected from 3.9 million adults, the risk of dying before 70 yr of age was 19% for men and 11% for women of normal weight (12). For obese men and women, that risk increased to 30%

for men and 15% for women; thus, obesity caused an absolute increased risk of 11% for men and 4% for women (12). While this large-scale study confirmed the obesity-mortality causal link, it did not address the question, "why does obesity cause nearly three times more premature death in men than in women?"

While HF is frequently the final state of cardiovascular disease, cardiac hypertrophy is a major independent predictor of progressive heart disease and increased mortality (11). Cardiac hypertrophy is also one of the most common independent features in obesity, even in the absence of hypertension or diabetes mellitus (1, 3, 20, 34, 45, 48). Cardiomyocyte hypertrophy has been found to be the most common cause of sudden cardiac death in morbid obese patients (14). Advances in studies of signaling pathways in both physiological and pathological hypertrophies have led to a recent proposal that aims to treat cardiac hypertrophy as a new therapeutic target (6, 17).

Numerous studies from animal models, mostly rodents, have yielded at least 26 "key signaling molecules or processes" critical in hypertrophy and HF and thus are potential targets for new treatment of HF (38). However, clinical trials for new drugs have seldom been successful (22, 38). While finding new therapeutic targets in HF remains important, understanding genetic and molecular mechanisms of cardiac hypertrophy has recently gained increasing interest due to early-stage presentation during the time course of HF development (6, 17).

Studies in molecular signaling pathways have revealed different responses of several key signaling proteins to physiological and pathological hypertrophic stimuli (4). Notably, the expression levels of ANP and beta-myosin heavy chain (β-MHC) protein increased only by

receiving aortic banding compared with sham in an experimental mouse cardiac hypertrophy model (4).

Adding to the complexity of understanding the underlying mechanisms of cardiac hypertrophy is the potential contribution of obesity and sex. Obesity caused higher rates of cardiac hypertrophy, reduced quality of life, and shorter life expectancies compared with age-matched lean individuals (29, 35). A recent study in 2.3 million adolescents from 1967 to 2010 found that overweight and obese individuals (measured by BMI) were strongly associated with increased cardiovascular mortality in adults (43). A high rate of sudden cardiac death in individuals with morbid obesity has been recognized for centuries (9). A high prevalence of sudden cardiac death has also been found in young obese people (5). For every 1 kg/m2 increase in BMI, HF risk increases by 5% in men and 7% in women (23). In ventricular biopsy samples from obese patients, the number of adipocytes increases as the ejection fraction decreases (30). Comparatively, sex differences in cardiovascular physiology are well known, but sex-specific manifestations in human cardiovascular disease have only been recently recognized (19, 21, 32). In the meantime, most mechanistic studies of cardiac hypertrophy have only been conducted in male animal models.

Methodologically, previous studies used Northern blotting, real-time PCR, and microarray cDNA for cardiac gene expression profiling under various hypertrophic conditions (26). Recent advances in next-generation sequencing (NGS) such as RNA-Seq (or transcriptome analysis) offer a unique opportunity to provide an overall snapshot of mRNA expression of all cardiac genes with high accuracy. Advantages of RNA-Seq over other sequencing methods such as cDNA microarrays are a combination of high-throughput sequencing, single-base resolution,

low background noise, and a wide dynamic range for quantification of gene expression levels (46).

In this work, we used RNA-Seq to investigate the potential effects of BMI and sex on gene expression profiles of human heart with LVH.

Methods

Human Heart Samples

Acquisition of human heart samples was approved by the Institutional Review Board (IRB) for the protection of human subjects at both West Virginia University and Duke University. Deidentified frozen human heart samples with pathological characterization were provided by the Department of Surgery at Duke University School of Medicine. Whole heart tissue was snap-frozen in liquid nitrogen immediately after collection from surgical procedures. LV were dissected and stored in −80°C freezer until use. Patient characterizations of the samples are provided in Table 1. Average age of patients is 47.21 ± 2.65 yr (ranging from 19 to 67 yr). The control group, in which hearts had no hypertrophy or failure, is designated the nonfailed (NF) group, with a mean age of 46.00 ± 3.69 yr (n = 12). In the hypertrophy group, the mean age is 48.42 ± 2.65 yr (n = 12). LVH (n = 12, 6 women, 6 men) samples were verified by echocardiograph (echo) measurement and interpreted by a cardiologist. NF hearts (n = 12, 6 female, 6 male) with echo data showing the absence of LVH were used as controls. Information of patients' age, sex, and BMI was obtained from pathological reports. BMI <25 was considered "lean" and BMI >30 was considered "obese."

Ethics Approval and Consent to Participate

Use of human heart samples in this research was approved by the West Virginia University IRB and the Duke University IRB.

Total RNA Isolation, NGS (RNA-Seq), and Bioinformatics Analysis

Total RNA was isolated using an RNA Fibrous Tissue Miniprep Kit (Qiagen). Quality of RNA was verified with an Agilent 2100 Bioanalyzer and RNA 6000 Pico Kit. Only samples that had RNA integrity number >7.0 were submitted for sequencing. The samples were then subjected to polyA enrichment followed by fragmentation, first- and second-strand synthesis, adenylation of 3′-ends, adapter ligation, DNA fragment enrichment, and real-time PCR quantification.

Sequencing was performed using NextSeq 500 (Illumina). Bcl sequencing data were converted to FastQ using onboard instrument software. Reads were mapped to human reference genome (hg38) using Spliced Transcripts Alignment to a Reference (STAR) (13).

Differential expression analysis was performed with NOISeq (v.2.14.1) (41) using RStudio version 0.99.879 (37). NOISeq is a newly developed tool for differential expression analysis. Compared with the commonly used DeSeq (2), NOISeq offered a set of tools for better quality control to avoid false positive discoveries (41). Gene annotation information was obtained from the Ensembl Biomart database, release 85 (50). Gene expression levels are indicated by FPKM (fragments per kilobase of transcript per million mapped reads) (42). FPKM was then normalized for batch effect using the ARSyNseq module included with the NOISeq package. Data were analyzed by the noiseqbio method under default conditions. The CPM filtering method was used for differential analyses where at least one group contained five or fewer replicates; otherwise, the Wilcoxon test was used for filtering.

The HF data set was extracted from a recent publication by Liu et al. (28). We used this HF data set against our LVH data set to explore the potential significance of newly identified

differentially expressed (DE) genes as “a gene expression signature” for prediction during the course of HF.

Gene Ontology Enrichment and Pathway Analysis

Gene Ontology (GO) enrichment analysis was carried out by using a comprehensive gene set enrichment tool, Enrichr (10, 25). This web-based tool contains 180,184 annotated gene sets from 102 gene set libraries (25). It calculates four parameters: P value, q value or adjusted P value, z score, and a combinational score; higher indicates larger significance. Interaction Network Analysis of Differentially Expressed Genes (GeneMANIA) (47) was used for coexpression and association of significant DE genes.

Immunoblotting

Tissues sections were submerged in minimal lysis buffer [fresh protease and phosphatase inhibitors (Sigma), 20 mM Tris, 150 mM NaCl, 10 mM EGTA, and 10 mM EDTA at pH 7.4] on ice and homogenized briefly at high speed. Samples were then centrifuged for 15 min increments at 10,000 g to pellet debris. Supernatants were placed into new tubes, and protein concentration was recorded with Bradford’s method on an Eppendorf Biophotometer.

For Western blotting procedures, protein concentrations were normalized between samples to 10–30 μg and mixed with Non-Reducing Lane Marker (Thermo Scientific) with 5% β-mercaptoethanol. After being heated in a water bath to 95°C for 5 min, samples were cooled to 4°C and then loaded into a 4–12% bis-Tris gel (Invitrogen). Electrophoresis was carried out at 80 V for 30 min and then 140 V for the remainder.

Proteins were transferred to 0.45 micron nitrocellulose membranes (Thermo Fisher) at 30 V for 1 h. Blots were blocked with 3% BSA-V in Tris-buffered saline plus Tween 20 (TBS-T) for 1 h before primary antibody (1:1,000 dilution; Cell Signaling) was added on a shaker at 4°C

overnight. Primary antibody solution was replaced with fresh 3% BSA-V in TBS-T containing secondary antibodies at 1:10,000 dilution for 1 h at room temperature on a shaker. After five washes with TBS-T, blots were developed with a standard ECL kit (Life Technologies) or ECL Prime (Amersham) on X-ray film or using a G:BOX digital imaging system (Syngene).

Statistics

For Western blots, data are shown as means ± SE; Student's t-test was used for statistical analysis with $P < 0.05$ being considered as statistically significant, marked with the symbol *. For gene expression, gene size adjusted P value (false discovery rate) < 0.05 was used ($p\_adj < 0.05$) to identify significant genes.

We used DE gene data (FPKM) and statistics in ischemic cardiomyopathy (ISCH) and dilated cardiomyopathy from a recent publication (28). It is possible to obtain the test statistic based on a single pair of objects (one disease, one nondisease control) due to the availability of multiple reads per subject in RNA-Seq methodology.

Results

Human Heart Sample Characteristics

Table 1 summarizes the characteristics of human hearts used in the study. The average age of the patients is 47.21 ± 2.65 yr (ranging from 19 to 67 yr, n = 24), 48.42 ± 3.93 yr for the LVH group (n = 12), and 46.00 ± 3.69 yr for the NF group (n = 12). LVH (n = 12, 6 women, 6 men) samples were diagnosed by echo measurement and interpreted by a cardiologist. Nonfailed without LVH (NF) hearts (n = 12, 6 female, 6 male) confirmed with echo were used as controls for LVH. Information on patients' age, sex, and BMI was obtained from pathological reports.

Sex-Specific LVH Gene Expression Profiles

Comparing LVH with NF samples (n = 9 for each group), we found only one significant gene, NPPA (Fig. 1A). NPPA was increased by 11.6-fold in LVH ($p\_adj = 0.004$). This result contradicts previous gene expression reports on human cardiac hypertrophy, which have identified at least 76 significant genes by using conventional techniques such as PCR, Southern blotting, and Northern blotting (26). We wondered whether sex might play a role in this unexpected result.

When we compared gene expression profiles of women vs. men, independent of LVH and BMI, we found 24 significantly DE genes (Fig. 1B, Supplemental Table S1 in Appendix A). A heat map generated from these 24 DE genes shows different patterns of cardiac gene expression between women and men (Fig. 1C). Furthermore, female and male samples can be clearly separated using the 24 DE genes, illustrated by principal component analysis (Fig. 1D).

Informed by the sex influence on gene expression, we next examined the effect of LVH on gene expression profiles in female and male groups separately. When comparing female LVH (n = 4) with female NF (n = 3) samples, we found 1,320 DE genes (Fig. 1E, Supplemental Table S2 in Appendix A). In the male LVH over NF comparison, we identified 1,383 DE genes (Fig. 1F, Supplemental Table S3 in Appendix A).

BMI- and Sex-Specific LVH Gene Expression Profiles

To investigate potential effects of obesity on cardiac gene expression, we compared obese (BMI30) with lean (BMI25) groups (n = 9 for each group) and found no significant DE genes. However, in the obese group, we found 236 significant genes in LVH compared with NF samples (n = 4 for each group) (Fig. 2A, Supplemental Table S4 in Appendix A). In the lean

group, we found seven significant genes in LVH compared with NF samples (n = 3 for each group) (Fig. 2B, Supplemental Table S5 in Appendix A).

Next, when we compared obese LVH with lean NF samples (n = 4 for each group), we found seven significant genes (Fig. 2C, also see Supplemental Table S6 in Appendix A). Considering the factor of sex, we compared male obese LVH with male lean NF samples (n = 3 for each group) and found 106 significant genes (Fig. 2D, Supplemental Table S7 in Appendix A). However, comparing female obese LVH with female lean NF samples (n = 3 for each group) yielded no significant DE genes. One possibility is that LVH and obesity can independently alter the expression levels of DE genes but in opposite directions.

Distribution of Sex- and BMI-Specific Significant Cardiac Gene Expression

Figure 3 summarizes the distribution of DE genes under different conditions. We identified a total of 23,521 genes in human hearts. No significant DE genes were found in obesity over lean samples and in female lean NF compared with female obese LVH. One gene was found to be upregulated in LVH compared with NF. Seven DE genes were identified in lean LVH (six upregulated and one downregulated). Seven DE genes were found in lean NF vs. obese LVH (five upregulated and two downregulated). Among the 24 DE genes found in women vs. men, five were upregulated, and 19 downregulated. Among 106 DE genes found in male lean NF compared with male obese LVH, 61 were upregulated, and 45 were downregulated. Among the 236 DE genes found in the obese group, 38 were upregulated, and 198 were downregulated. Among 1,320 DE genes found in female LVH, 330 were upregulated and 990 downregulated. Among 1,383 DE genes found in male LVH, 137 were upregulated, and 1,246 were downregulated.

Sex- and BMI-Specific Significant Gene Expression Signature

To identify sex-specific LVH DE genes, we compared male LVH and female LVH DE genes. Figure 4A shows a scatterplot of DE genes shared by LVH-M and LVH-F. Quadrant I displays 80 genes that are upregulated in female LVH but downregulated in male LVH; quadrant II displays six genes that are upregulated in both female and male LVH; quadrant III displays 141 genes that are downregulated in both female and male LVH; quadrant IV displays 15 genes that are downregulated in female LVH but upregulated in male LVH. Figure 4B shows a heat map generated from the 80 DE genes from quadrant I of Fig. 4A, demonstrating the sex-specific modulation of gene expression in LVH.

Using abs(log2FC) > 1 as a criterion, we identified 213 sex- and BMI-specific significant genes (Supplemental Table S8 in Appendix A). Using abs(log2FC) > 2 as a criterion, we identified 27 sex- and BMI-specific significant genes (Supplemental Table S9 in Appendix A).

Significance of LVH DE Genes: Implication in Ischemic and/or Dilated Cardiomyopathy in HF Patients

To explore the potential significance of these findings, we compared LVH DE genes with those recently identified in ischemic cardiomyopathy (ISCH) and dilated cardiomyopathy (DCM) (28). Supplemental Figure S1A shows a scatterplot of DE genes found in obese LVH and in the previously published ISCH data set (28). There are 37 LVH DE genes found in ISCH (Supplemental Table S10 in Appendix A). Quadrant I displays 16 genes that are upregulated in obese LVH but downregulated in ISCH; quadrant II displays four gene that is upregulated in both obese LVH and ISCH; quadrant III displays 14 genes that are downregulated in both obese LVH and ISCH; quadrant IV displays three genes that are downregulated in obese LVH and upregulated in ISCH. Supplemental Figure S1B shows a scatterplot of DE genes found in obese

LVH and in the published DCM data set (28). There are 58 LVH DE genes found in DCM (see Supplemental Table S11 in Appendix A). Quadrant I displays 27 genes that are upregulated in obese LVH but downregulated in DCM; quadrant II displays three genes that are upregulated in both obese LVH and DCM; quadrant III displays 17 genes that are downregulated in both obese LVH and DCM; quadrant IV displays 11 genes that are downregulated in obese LVH and upregulated in DCM. Supplemental Figure S1C shows a scatterplot of DE genes found in obese LVH and in the published ISCH/DCM data set (28). There are 31 LVH DE genes found in ISCH/DCM data set (see Supplemental Table S12 in Appendix A). Quadrant I displays 16 genes that are upregulated in obese LVH but downregulated in ISCH/DCM; quadrant II displays three genes that are upregulated in both obese LVH and ISCH/DCM; quadrant III displays eight genes that are downregulated in both obese LVH and ISCH/DCM; quadrant IV displays four genes that are downregulated in obese LVH and upregulated in ISCH/DCM.

Supplemental Fig. S2A shows a scatterplot of DE genes found in female LVH and in the published ISCH data set (28). There are 111 female LVH DE genes found in ISCH (Supplemental Table S13 in Appendix A). Quadrant I displays 41 genes that are upregulated in obese LVH but downregulated in ISCH; quadrant II displays 14 genes that are upregulated in both obese LVH and ISCH; quadrant III displays 46 genes that are downregulated in both obese LVH and ISCH; quadrant IV displays 10 genes that are downregulated in obese LVH and upregulated in ISCH. Supplemental Fig. S2B shows a scatterplot of DE genes found in female LVH and in the published DCM data set (28). There are 181 female LVH DE genes found in DCM (Supplemental Table S14 in Appendix A). Quadrant I displays 63 genes that are upregulated in obese LVH but downregulated in DCM; quadrant II displays 20 genes that are upregulated in both obese LVH and DCM; quadrant III displays 76 genes that are downregulated

in both obese LVH and DCM; quadrant IV displays 22 genes that are downregulated in obese LVH and upregulated in DCM.

Supplemental Figure S2C shows a scatterplot of DE genes found in female LVH and in the published ISCH/DCM data set (28). There are 98 LVH DE genes found in ISCH/DCM (Supplemental Table S15 in Appendix A). Quadrant I displays 56 genes that are upregulated in obese LVH but downregulated in ISCH/DCM; quadrant II displays six genes that are upregulated in both obese LVH and ISCH/DCM; quadrant III displays 26 genes that are downregulated in both obese LVH and ISCH/DCM; quadrant IV displays 10 genes that are downregulated in obese LVH and upregulated in ISCH/DCM. Supplemental Figure S2D shows a scatterplot of DE genes found in male LVH and in published ISCH data set (28). There are 121 LVH DE genes found in ISCH (Supplemental Table S16 in Appendix A). Quadrant I displays 46 genes that are upregulated in obese LVH but downregulated in ISCH; quadrant II displays 16 genes that are upregulated in both obese LVH and ISCH; quadrant III displays 44 genes that are downregulated in both obese LVH and ISCH; quadrant IV displays 15 genes that are downregulated in obese LVH and upregulated in ISCH. Supplemental Figure S2E shows a scatterplot of DE genes found in male LVH and in the published DCM data set (28). There are 196 LVH DE genes found in DCM (Supplemental Table S17 in Appendix A). Quadrant I displays 98 genes that are upregulated in obese LVH but downregulated in DCM; quadrant II displays 17 genes that are upregulated in both obese LVH and DCM; quadrant III displays 46 genes that are downregulated in both obese LVH and DCM; quadrant IV displays 35 genes that are downregulated in obese LVH and upregulated in DCM. Supplemental Figure S2F shows a scatterplot of DE genes found in male LVH and in the published ISCH/DCM data set (28). There are 80 LVH DE genes found in ISCH/DCM (see Supplemental Table S18 in Appendix A).

Quadrant I displays 33 genes that are upregulated in obese LVH but downregulated in ISCH/DCM; quadrant II displays 15 genes that are upregulated in both obese LVH and ISCH/DCM; quadrant III displays 21 genes that are downregulated in both obese LVH and ISCH/DCM; quadrant IV displays 11 genes that are downregulated in obese LVH and upregulated in ISCH/DCM.

Gene Expression Signatures

To explore potential implications of LVH DE genes for future development of HF, we selected 10 DE genes according to three criteria: abs(log2FC)>2, extremely small p_adj value (10−20), and whether they have been found in the published ISCH and DCM HF data set (28) (Table 2). Figure 5A shows the heat map of male LVH (LVH-M) and female LVH (LVH-F) compared with their respective NF controls. In male LVH, among expression levels of 10 DE genes, four (HBB, PLA2G2A, HBA1, PLXDC2) are changed by less than one standard deviation, five (NPPA, NPPB, PDK4, HIST1H2AC, GSTT1) are increased, and one (MYL7) is decreased. In female LVH, among expression levels of 10 DE genes, eight (HBB, NPPA, NPPB, PDK4, PLA2G2A, HBA1, HIST1H2AC, PLXDC2) are increased, and two (MYL7, GSTT1) are decreased. Figure 5B shows the heat map of ISCH and DCM compared with NF using the published data (28). Among the expression levels of these 10 genes, seven (HBB, NPPA, NPPB, MYL7, PDK4, HIST1H2AC, PLXDC2) are increased in ISCH, seven (HBA1, HBB, NPPA, NPPB, MYL7, PDK4, HIST1H2AC) are increased in DCM, and two (PLA2G2A, GSTT1) are decreased, compared with controls.

Validation of 10 DE Genes

Expression of NPPA (ANP) and NPPB (BNP) in LVH, ISCH, and DCM.

ANP and brain-type natriuretic peptide (BNP) are biomarkers for HF with left ventricular dysfunction (8, 16). We found that the transcripts of NPPA (gene that encodes ANP) were increased in LVH by 24-fold in men (LVH_M, 697 FPKM; NF_M, 29 FPKM; p_adj = 0.01825), 7.4-fold in women (LVH_F, 148 FPKM; NF_F, 20 FPKM; p_adj = 0.0324), 13.3-fold in BMI25 (LVH_BMI25, 601 FPKM; NF_BMI25, 45 FPKM; p_adj = 7×10−15), and 16.4-fold in the BMI30 (LVH_BMI30, 327 FPKM, NF_BMI30, 23 FPKM; p_adj = 1.4×10−14) subgroup, respectively (Fig. 6A, top). Its expression was also increased by 19-fold in ISCH (ISCH 234, 876 FPKM; NF-ISCH, 46 FPKM; p_adj = 0) and 5.4-fold in DCM (DCM 333, 251 FPKM; NF-DCM, 46 FPKM; p_adj = 4.4×10−7) (Fig. 6A, top) (28). Immunoblotting experiments confirmed that ANP protein expression was increased by 90% in LVH compared with NF after being normalized to α-actin (LVH: 1.10 ± 0.15, n = 8; NF: 0.58 ± 0.05, n = 5) (Fig. 6A, middle and bottom).

Similarly, we found that the transcripts of NPPB (gene that encodes BNP) were increased in LVH by 7.5-fold in male (LVH_M, 121 FPKM; NF_M, 16 FPKM; p_adj = 0.0136), fivefold in female (LVH_F, 130 FPKM; NF_F, 28 FPKM; p_adj = 0.0146), and 3.4-fold in BMI30 (LVH_BMI30, 121 FPKM; NF_BMI30, 36 FPKM; p_adj = 0.04) subgroups, respectively (Fig. 6B, top). Its expression was also increased by 11-fold in ISCH (ISCH 234, 1,772 FPKM; NF-ISCH, 159 FPKM; p_adj = 1.79×10−13) and fourfold in DCM (DCM 333, 617 FPKM; NF-DCM, 159 FPKM; p_adj = 8.96×10−7) (28) (Fig. 6B, top). BNP protein expression was increased by 151% in LVH compared with NF control (NF) after being normalized to α-actin (LVH: 1.31 ± 0.52, n = 9; NF: 0.52 ± 0.11, n = 9) (Fig. 6B, middle and bottom).

Expression of HBA1 and HBB in LVH, ISCH, and DCM.

Figure 7 shows the protein expression of HBA1 (Fig. 7A) and HBB (Fig. 7D). Both were increased in female LVH over NF (HBA1: LVH_F = 0.46 ± 0.029, NF_F = 0.26 ± 0.04, n = 3, $P < 0.05$; HBB: LVH_F = 0.36 ± 0.42, NF_F = 0.23 ± 0.02, n = 3, $P < 0.05$) but were not changed in male LVH compared with NF (HBA1: LVH_M = 0.17 ± 0.07, NF_M = 0.17 ± 0.06, n = 6, $P > 0.05$; HBB: LVH_M = 0.98 ± 0.14, NF_M = 0.94 ± 0.13, n = 6, $P > 0.05$) (Fig. 7, B and E). These female LVH-specific increases in protein expression of HBA1 and HBB are consistent with the corresponding increase in transcripts in female LVH (~11-fold increase of HBA1, Fig. 7C; ~44-fold increase of HBB, Fig. 7F). HBA1 transcripts were reported to increase by 3.8-fold in ischemic and 6.9-fold in dilated cardiomyopathy, respectively (Fig. 7C) (28); similarly, HBB transcripts were reported to increase by sixfold in ISCH and 11.6-fold in DCM, respectively (Fig. 7F) (28).

Expression of GSTT1 and PLA2G2A in LVH, ISCH, and DCM.

Figure 8 shows the protein expression of GSTT1 and PLA2G2A (Fig. 8A, men; Fig. 8B, women). GSTT1 levels were increased by 10-fold in male LVH (LVH_M = 0.70 ± 0.22, NF_M = 0.07 ± 0.06, n = 3, $P < 0.05$) but no significant changes were detected in female LVH (LVH_F = 0.94 ± 0.57, NF_F = 0.97 ± 0.61, n = 3, $P > 0.05$) (Fig. 8C). PLA2G2A levels were increased in female LVH by fivefold (LVH_F = 0.25 ± 0.20, NF_F = 0.05 ± 0.01, n = 3, $P < 0.05$) and in male LVH by sevenfold (LVH_M = 0.07 ± 0.02, NF_M = 0.01 ± 0.005, n = 3, $P < 0.05$) (Fig. 8D). PLA2G2A levels are noticeably lower in male (Fig. 10A, middle lane) than in female (Fig. 8B, middle lane) LV.

Changes in protein expression levels of GSTT1 are consistent with those in transcripts, a 13.7-fold increase in male LVH for GSTT1 (Fig. 8E). However, for PLA2G2A, there is a higher

increase in transcripts in female LVH (6.4-fold) than in male LVH (1.8-fold) (Fig. 8F). In ISCH and DCM, GSTT1 transcripts were reported to increase by 40 and 260%, respectively (28), whereas PLA2G2A transcripts were increased by 4.2-fold and 5.6-fold, respectively (28).

Expression of PDK4 and MYL7 in LVH, ISCH, and DCM.

Figure 9 shows the protein expression of PDK4 and MYL7 (Fig. 9A, women; Fig. 9B, men). PDK4 levels were increased by 2.2-fold in male LVH over NF (LVH_M = 1.335 ± 0.307, NF_M = 0.514 ± 0.107, n = 3, $P < 0.05$) but not significantly altered in female LVH compared with NF (LVH_M = 1.282 ± 0.3594, NF_M = 0.5801 ± 0.08030, n = 3, $P > 0.05$) (Fig. 9C). On the other hand, MYL7 levels were decreased by 27% in female LVH over NF (LVH_F = 0.8958 ± 0.1007, NF_F = 1.225 ± 0.04868, n = 3, $P < 0.05$) but not significantly changed in male LVH compared with NF (LVH_M = 1.687 ± 0.2885, NF_M = 1.646 ± 0.2225, n = 3, $P > 0.05$) (Fig. 9D).

PDK4 transcript levels were increased in male LVH by 2.3-fold and in female LVH by 1.4-fold (Fig. 9E). PDK4 transcripts levels were reported to increase (by 2.2-fold) only in ischemic HF (28) (Fig. 9E).

MYL7 transcript levels were increased in male LVH by 74% and in female LVH by 60% (Fig. 9F). MYL7 transcripts levels were reported to increase by 3.2-fold in both ISCH and DCM (28) (Fig. 9F).

Expression of HIST1H2AC in LVH, ISCH, and DCM.

Figure 10 shows the protein expression of HISTH2AC (Fig. 10A). The expression levels were increased by 154% in female LVH over NF (LVH_F = 1.55 ± 0.29, NF_F = 0.61 ± 0.09, n = 3, $P < 0.05$) and by 254% in male LVH over NF (LVH_M = 2.49 ± 0.41, NF_M = 0.98 ± 0.37, n = 6, $P < 0.05$), respectively (Fig. 10B), consistently with the increased transcripts in female

LVH (~5-fold) and male-LVH (~2-fold) (Fig. 10C). HIST1H2AC transcripts were reported to increase by 2.9-fold in ISCH and 5.4-fold in DCM, respectively (Fig. 10C) (28).

Finally, protein expression and re-examination of gene expression for PLXDC2 showed insignificant changes in LVH over NF. Thus, it was removed from DE genes for further data analysis.

GO Enrichment and Pathway Analysis

We performed GO enrichment analysis for nine DE genes (NPPA, NPPB, HBB, HBA1, PDK4, MYL7, HIST1H2AC, GSTT1, PLA2G2A). In "biological process," the top two most significant processes are receptor guanylyl cyclase signaling pathway (q value = 0.0004) (involving NPPA, NPPB) and oxygen transport (q value = 0.0005) (involving HBB, HBA1) (Supplemental Table 19). In "cellular component," the top two most significant components are endocytic vesicle lumen and hemoglobin complex (q value = 0.0004), both involving HBB and HBA1 (Supplemental Table 20). In "molecular function," HBB and HBA1 are involved in the top five most significant functions, including oxygen transporter activity (q value = 0.0003), oxygen binding (q value = 0.0008), peroxidase activity (q value = 0.0008), oxidoreductase activity (q value = 0.0008), and antioxidant activity (q value = 0.002) (Supplemental Table 21).

DE Gene Interaction Network Analysis

To further explore potential interactions among nine DE genes, we performed gene interaction network analysis using GeneMANIA (47). Network interaction in terms of predicted physical interaction and coexpression was analyzed. Among our nine DE genes, we found three clusters: NPPA, NPPB, HBB, HBA1, HIST1H2AC, and MYL7 form the largest cluster; PDK4 and PLA2G2A are coexpressed together; and GSTT1 is not associated with other eight DE genes (Supplemental Fig. S3). Within the largest cluster, NPPA, NPPB, and MYL7 are coexpressed.

HBB is coexpressed and associated with HBA1 and HIST1H2AC. NPPB also is associated with HBB and HIST1H2AC.

Discussion

In the present work, we used transcriptome sequencing to explore the potential effects of BMI and sex on gene expression profiles of human hearts with and without LVH. We found both BMI and sex can unmask a large set of genes whose expression levels are significantly affected by LVH.

We explored the implications of BMI- and sex-specific LVH DE genes in HF. Previously, sex-specific differences in gene expression profiles of HF were investigated using cDNA microarray. In new-onset HF, 35 upregulated and 16 downregulated transcripts were identified in men vs. women (21). At end-stage DCM, there were 55 and 31 differentially regulated genes in female and male, respectively (19). Nineteen DE genes were shared by both males and females (19). Most recently, RNA-Seq was used on six patients to identify 983 DE genes in ISCH vs. NF [union of three pairs, see Table 1 in (28)], 1,109 DE genes in DCM vs. NF [union of six pairs, Table 1 in (28)], and 825 DE genes [union of two pairs, Table 1 in (28)] in which 476 genes were overexpressed in ISCH and 349 genes were overexpressed in DCM. Sex and obesity status were not specified in the article. We performed correlation studies of our LVH data and the published data in both types of HF, ISCH and DCM (28). Our scatterplots display numerous downregulated (quadrant II) and upregulated (quadrant III) DE genes in obese LVH, women, and male LVH, which are also found in ISCH and DCM.

We selected nine DE genes that were significantly changed in multiple LVH vs. NF analyses within our data set and were shared by LVH, ISCH, and DCM, to provide a gene expression signature. There were five overexpressed genes (HBB, NPPA, NPPB, PDK4,

HIST1H2AC); one downregulated gene, GSTT1; and three regulated in opposite directions (MYL7 decreased in LVH, increased in cardiomyopathy; PLA2G2A increased in female LVH, but decreased in cardiomyopathy; HBA1 increased in female LVH and DCM, but decreased in ISCH). For male LVH, the expression levels of three genes (HBB, PLA2G2A, HBA1) were not changed by more than one standard deviation.

Roles of Nine DE Genes in Human Cardiac Hypertrophy and Failure

Using GeneChip and TaqMan PCR, the first gene expression fingerprint of HF revealed 103 genes in 10 functional groups between NF and HF samples (40). ANP and BNP were two upregulated genes in HF. Using quantitative PCR, we found NPPA transcripts to be increased in dilated HF patients of both sexes (7). "Expression profiling-based biomarkers" was proposed in a transcriptome analysis of endomyocardial biopsies from 48 HF patients, which used 96 DE genes to predict cardiomyopathy etiology accurately (ischemic vs. nonischemic) (24). A clinical study in 2008 on 3,580 patients found that women had new-onset acute HF more frequently and less DCM compared with men (33).

In both male and female samples from end-stage DCM, microarrays identified upregulated NPPA and downregulated PLA2G2A expression, respectively (19). NPPA and NPPB overexpression was also detected, by microarrays, in new-onset HF patients (both male and female) with DCM (21). Most recently, RNA-Seq was used to show overexpressed NPPA and NPPB as well as decreased expression of PLA2G2A in both DCM and ischemic cardiomyopathy (Fig. 7) using a much smaller sample size (one disease vs. one control) (28).

ANP is mainly produced in the atria, whereas BNP is primarily produced in the ventricles, in response to myocardial stress. Both peptides have been reported as valuable diagnostic markers in HF (16). NH2-terminal pro-BNP (NT-proBNP) and midregional pro-ANP

(MR-proANP) are inactive precursors of BNP and ANP, respectively, with long half-lives. These peptides are both current standards of care for patients with acute or chronic HF (31, 49). Increased NT-proBNP has also been found to be closely associated with HF patients with cachexia (BMI <20) (18). NT-proBNP has recently been confirmed as a reliable risk biomarker for fatal cardiovascular events in Type 2 diabetes patients (44).

Increased transcripts and protein expression of ANP and BNP were readily detected in LVH compared with NF in our study (Fig. 6). However, we found much higher NPPA expression than NPPB in male LVH (NPPA, 697 FPKM; NPPB, 121 FPKM) but not in female LVH (NPPA, 148 FPKM; NPPB, 130 FPKM). NPPA expression was increased more in male (24-fold) than in female (7.4-fold) LVH. In addition, the strongest association of LVH with increased NPPA expression was found between lean and obese groups, and such an association was not found for NPPA. In previously published HF gene expression data (28) we found both NPPA and NPPB expression levels are higher in ISCH (NPPA, 876 FPKM; NPPB, 1,772) than in DCM (NPPA, 251 FPKM; NPPB, 617).

In a 2014 report that examined mRNA expression of LV with sudden cardiac death, the expression of HBA1 and HBB mRNA was found to be increased, while PDK4 levels were downregulated (39). PDK4 is one of the key regulators of metabolism (36). Its expression levels in human hearts are decreased during development and tend to be reduced in HF (36). We found the gene expression levels for HBA1 and HBB were upregulated only in female LVH, while PDK4 levels were increased only in male LVH.

MYL7, one of the myosin light chains that plays a key role in cardiogenesis (15), is increased in human hypertrophic cardiomyopathy (26). We found its gene expression levels were increased only in female LVH.

The roles of GSTT1, PLA2G2A, and HIST1H2AC in human cardiac hypertrophy or failure are unknown. We found that GSTT1 gene expression levels were upregulated in male, but not in female, LVH. Gene expression levels for PLA2G2A and HIST1H2AC were upregulated in LVH of both sexes with a greater increase in female LVH.

Limitations of the Study

Small sample size

We used a total of 18 samples. For subgroups such as obese female LVH, there were three samples for each group. Although it fulfills the minimal requirement for statistical analysis, it may lead to underestimates of the amount of significant genes in each subgroup, as well as large variations in expression levels. However, small samples sizes have demonstrated impact of the identified significant genes, particularly with very small p_adj values, such as PDK4 (p_adj < 10−6). In a recent study, the gene signatures identified by RNA-Seq from only six HF patients were used to accurately classify a large set of 313 patients with microarray data (28). It illustrated the use of RNA-Seq as an effective approach to discover novel gene expression signature based on an extremely small sample size.

Sample variations.

Intrinsic individual differences exist at genetic levels. Clinical diagnoses of LVH were based on echo. As shown in patient sample characteristics (Table 1), there are some samples with borderline LVH that were deemed as NF in pathological reports.

Despite these limitations our data provide an argument for using BMI- and sex-specific gene expression signatures containing multiple significant genes, rather than a single gene, to offer a more accurate prediction for future progression to HF.

Conclusions

We identified nine differentially expressed genes in LVH that are BMI- and sex-sensitive. Validation of these nine genes (forming a "gene expression signature") in a large cardiac hypertrophy population may have the potential to help in the early diagnosis of HF, which occurs at a significantly high rate in the obese population.

Figures

Figure 1: Sex-specific left ventricle hypertrophy (LVH) differential expression profiles (volcano)

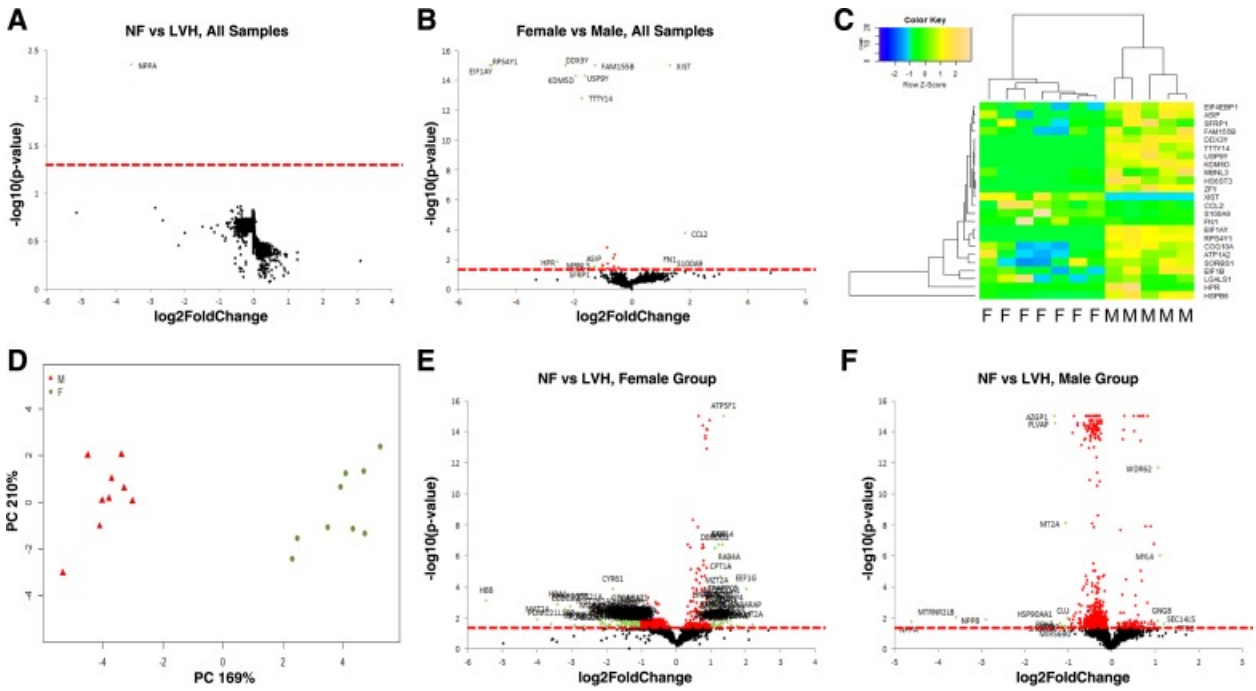

Figure 1. A: NF vs. LVH (n = 9 in each group). B: female (F) vs. male (M) samples (n = 9 in each group). C: heat map generated from 24 differentially expressed genes comparing females with males (B) using unsupervised k-means clustering. D: principal component analysis plot of female and male samples from these 24 differentially expressed genes (B). E: differential expression profile of female NF (n = 4) vs. female LVH (n = 3). F: differential expression profile of male NF vs. male LVH (n = 3 in each group). Red dashed lines mark p_adj = 0.05. Dark dots indicate genes without significant changes in expression levels comparing 2 individual groups

(p_adj > 0.05). Red dots: significant genes (p_adj < 0.05) with abs(log2FC < 1); green dots with labels: significant genes with p_adj<0.05 and abs(log2FC) > 1. NF, nonfailed controls.

Figure 2: Body mass index (BMI)- and sex-specific LVH differential expression profiles (volcano)

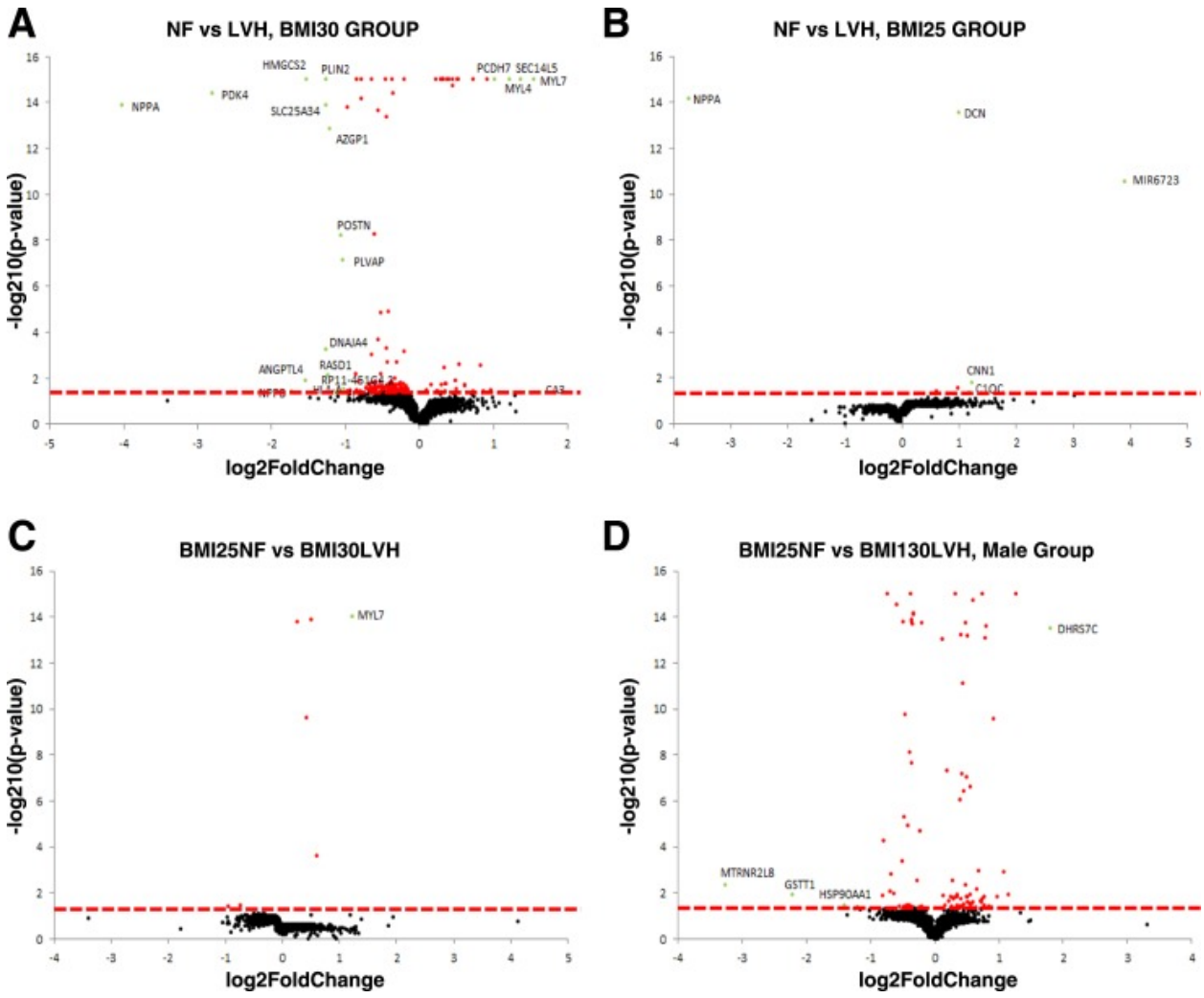

Figure 2. A: lean vs. obese samples (n = 9 in each group). B: obese NF vs. obese LVH (n = 4 in each group). C: lean NF vs. lean LVH (n = 3 in each group). D: lean NF vs. obese LVH (n = 3 in each group). Red dashed lines mark p_adj = 0.05. Dark dots indicate genes without significant changes in expression levels comparing 2 individual groups (p_adj > 0.05). Red dots: significant genes (p_adj < 0.05) with abs(log2FC < 1); green dots with labels: significant genes with p_adj < 0.05 and abs(log2FC) > 1.

Figure 3: Distribution of LVH differentially expressed genes under different conditions

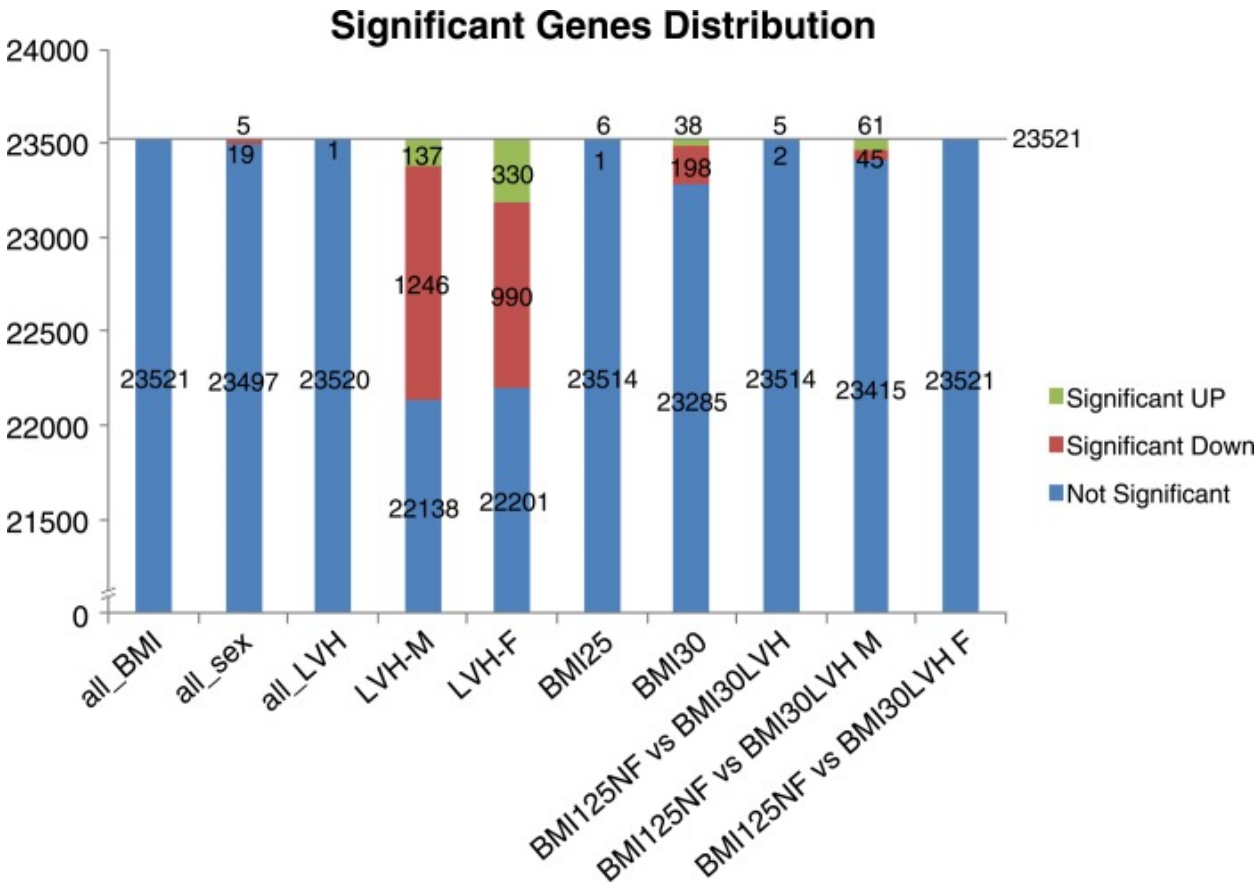

Figure 3. The number of significantly upregulated, downregulated, or non-significant genes when analyzed by different groupings (all_BMI = all samples, analyzed as lean versus obese; all_sex = all samples, analyzed as male versus female; all_LVH = all samples, analyzed as LVH versus non-failed control; LVH-M = male samples, analyzed as LVH versus non-failed control; LVH-F = female samples, analyzed as LVH versus non-failed control; BMI25 = samples with BMI<25, analyzed as LVH versus non-failed control; BMI30 = samples with BMI>30, analyzed as LVH versus non-failed control; BMI25NF vs BMI30LVH = non-failed control samples with BMI<25 versus LVH samples with BMI>30; BMI25NF vs BMI30LVH M = non-failed control samples with BMI<25 versus LVH samples with BMI>30, males only; BMI25NF vs

BMI30LVH F = non-failed control samples with BMI<25 versus LVH samples with BMI>30, females only). Green indicates upregulation, red indicates downregulation, and blue indicates no significant change.

Figure 4: Shared LVH differentially expressed (DE) genes in both sexes

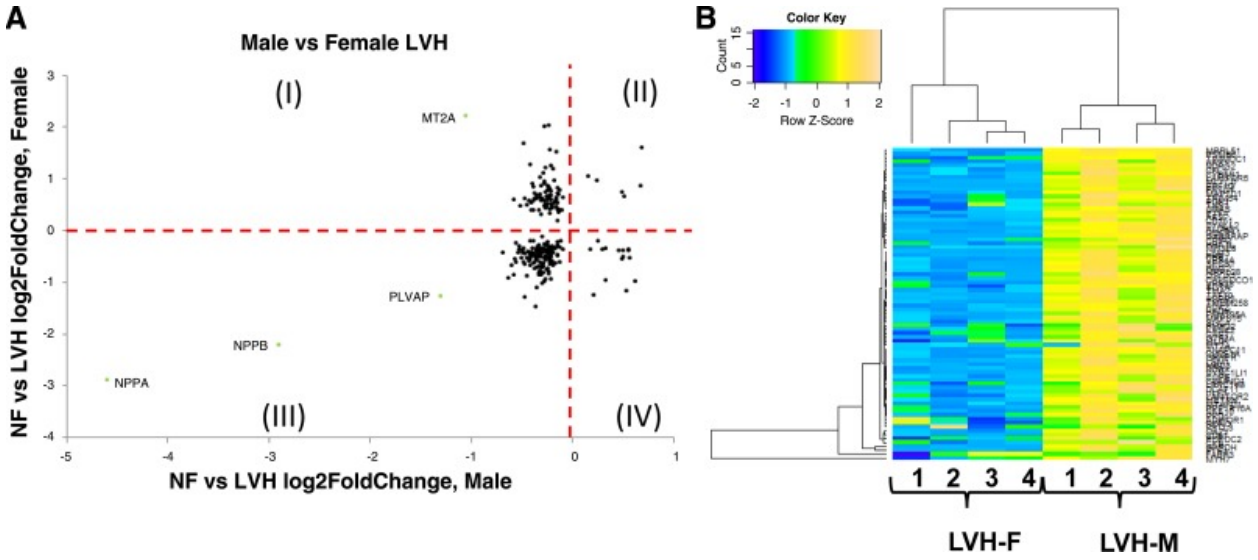

Figure 4. A: scatterplot of male vs. female LVH DE genes. Quadrant I contains DE genes upregulated in male LVH but downregulated in female LVH. Quadrant II contains DE genes downregulated in both male and female LVH. Quadrant III contains DE genes upregulated in both male and female LVH. Quadrant IV contains DE genes upregulated in female LVH but downregulated in male LVH. B: heat map from the 80 DE genes from quadrant I of male vs. female DE gene scatterplot.

Figure 5: Gene expression signature in LVH and HF

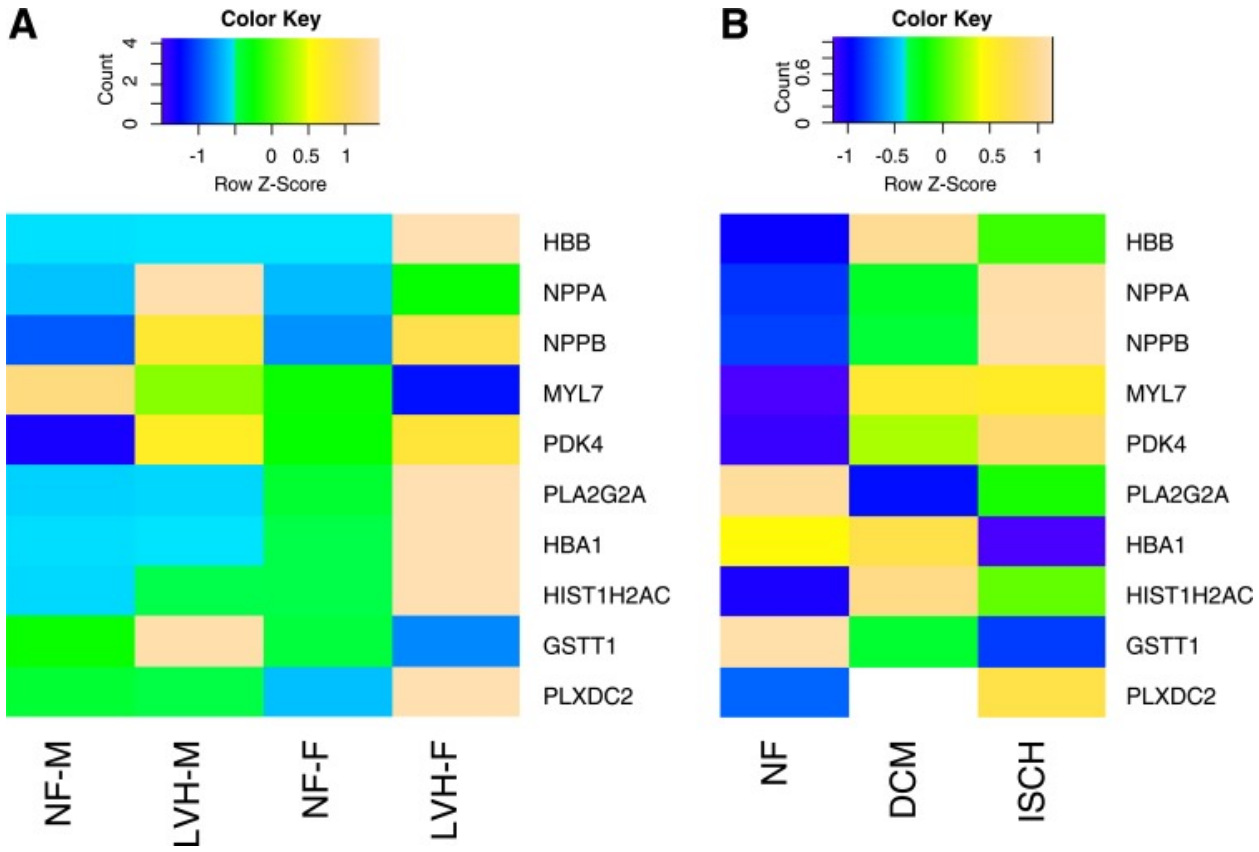

Figure 5. A: heat map of 10 DE genes in male and female LVH; B: heat map of 10 DE genes in ischemic cardiomyopathy (ISCH) and dilated cardiomyopathy (DCM).

Figure 6: Gene and protein expression of NPPA/ANP

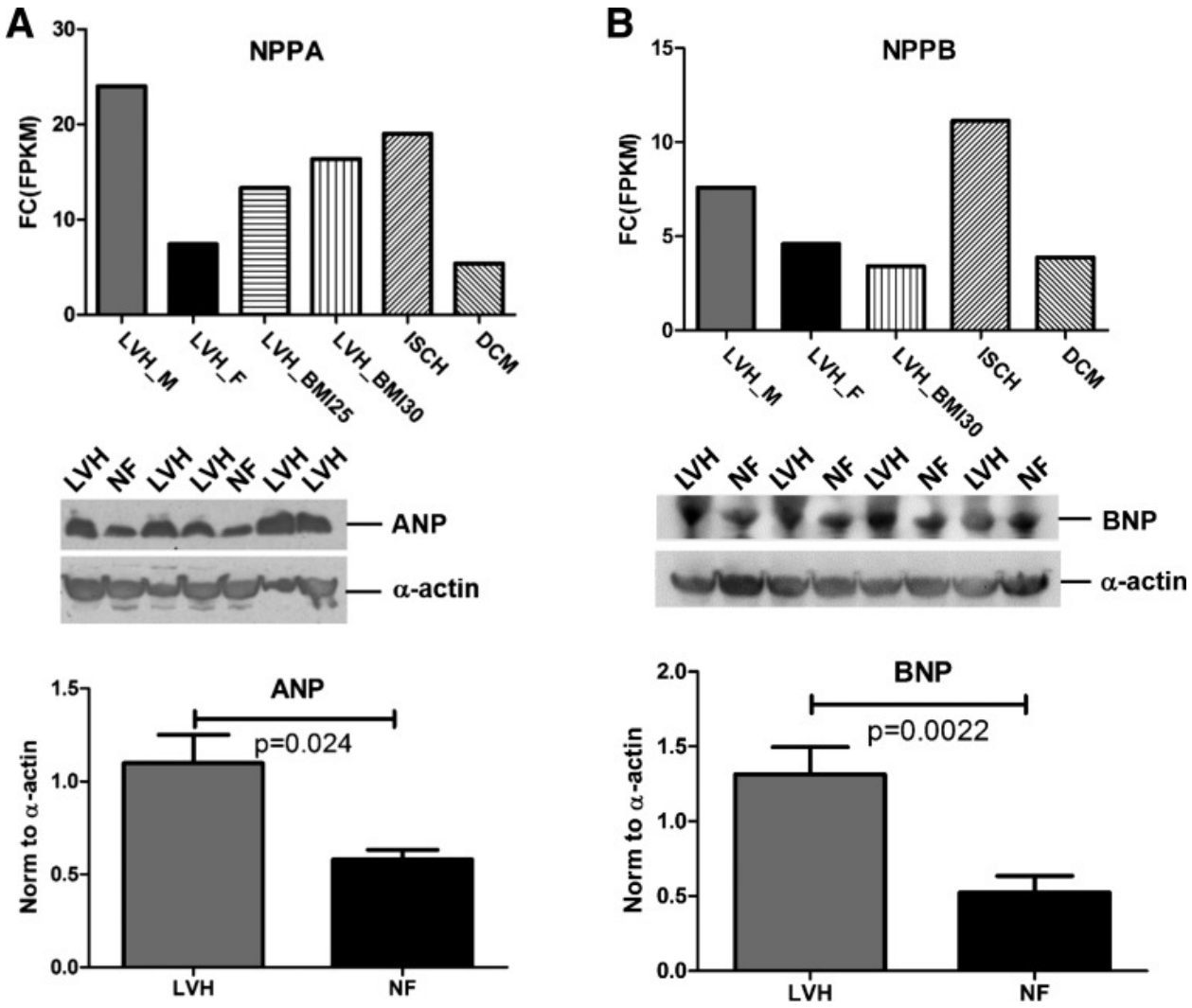

Figure 6. (A) and NPPB/BNP (B). Top: transcript expression of NPPA (A) or NPPB (B) in female and male LVH, ISCH, and DCM. Middle: ANP (A) or BNP (B) immunoblots in LVH and NF, α-actin was used as a loading control. Bottom: ANP (A) or BNP (B) protein expression normalized to α-actin in LVH and NF. ANP, NPPA, atrial natriuretic peptide A; BNP, NPPB, atrial natriuretic peptide B.

Figure 7: Gene and protein expression of HBA1 and HBB

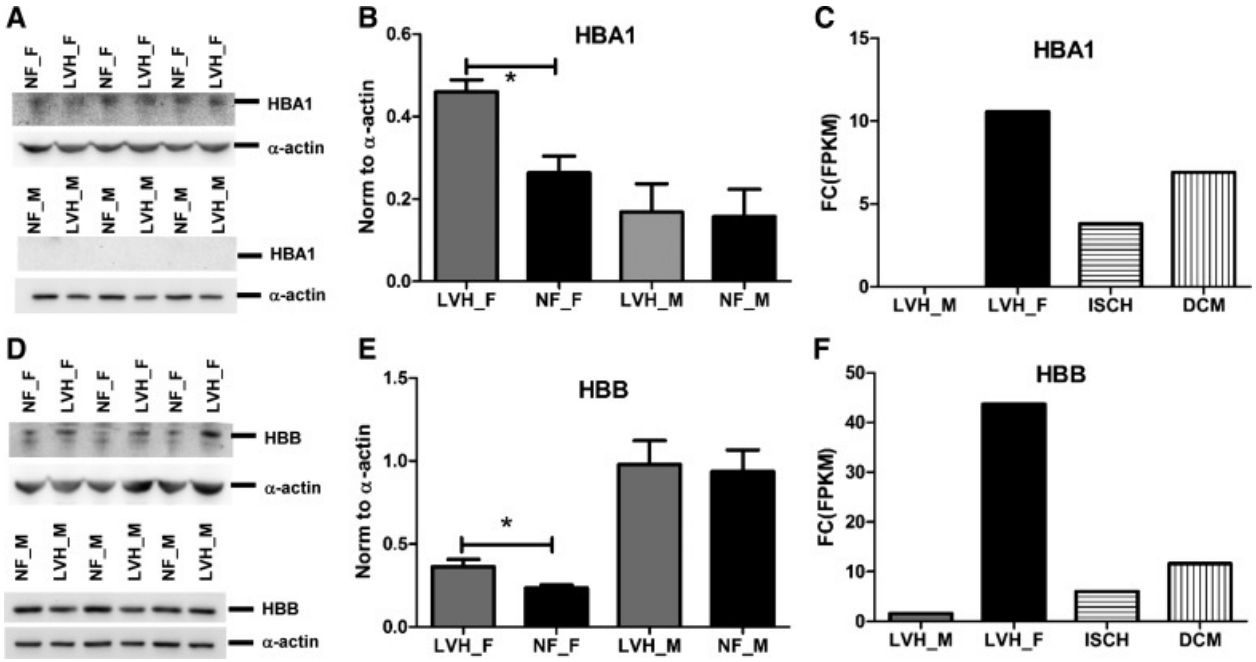

Figure 7. A: HBA1 immunoblots in female (top) and male (bottom) samples. α-Actin was used as a loading control. B: HBA1 protein expression normalized to α-actin in LVH and NF. C: HBA1 transcript changes in LVH over NF. D: HBB immunoblots in female (top) and male (bottom) samples. α-Actin was used as a loading control. E: HBB protein expression normalized to α-actin in LVH and NF. F: HBB transcript changes in LVH over NF. *Statistically significant difference between the 2 groups ($P < 0.05$). FC, fold change; FPKM, fragments per kilobase of transcript per million mapped reads.

Figure 8: Gene and protein expression of GSTT1 and PLA2G2A

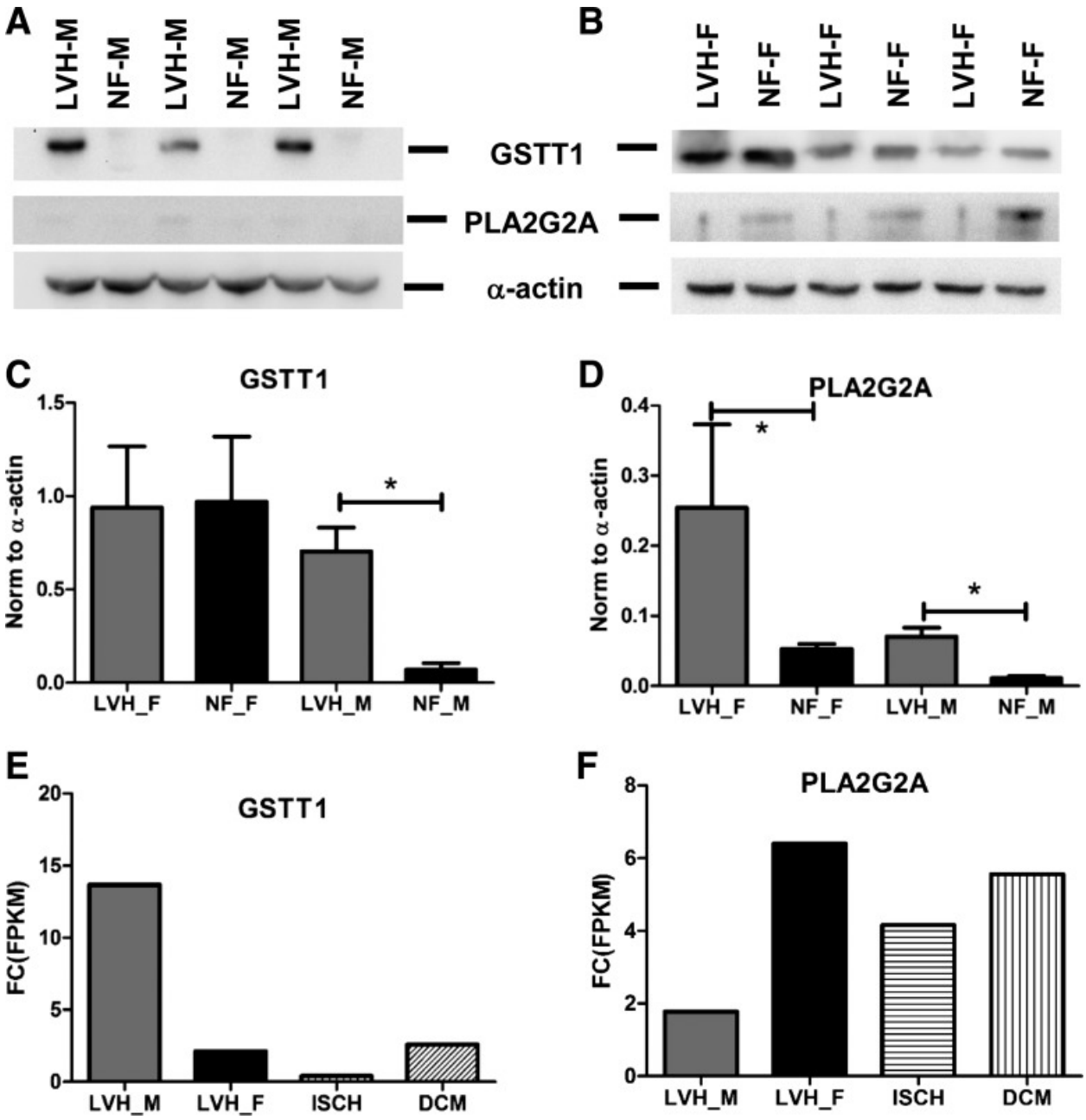

Figure 8. GSTT1 and PLA2G2A immunoblots in male (A) and female (B) samples. α-Actin was used as a loading control. C: GSTT1 protein expression normalized to α-actin in LVH and NF. D: PLA2G2A protein expression normalized to α-actin in LVH and NF. E: GSTT1 transcript changes in LVH over NF. F: PLA2G2A transcript changes in LVH over NF. *Statistically significant difference between the 2 groups ($P < 0.05$). FC, fold change.

Figure 9: Gene and protein expression of PDK4 and MYL7

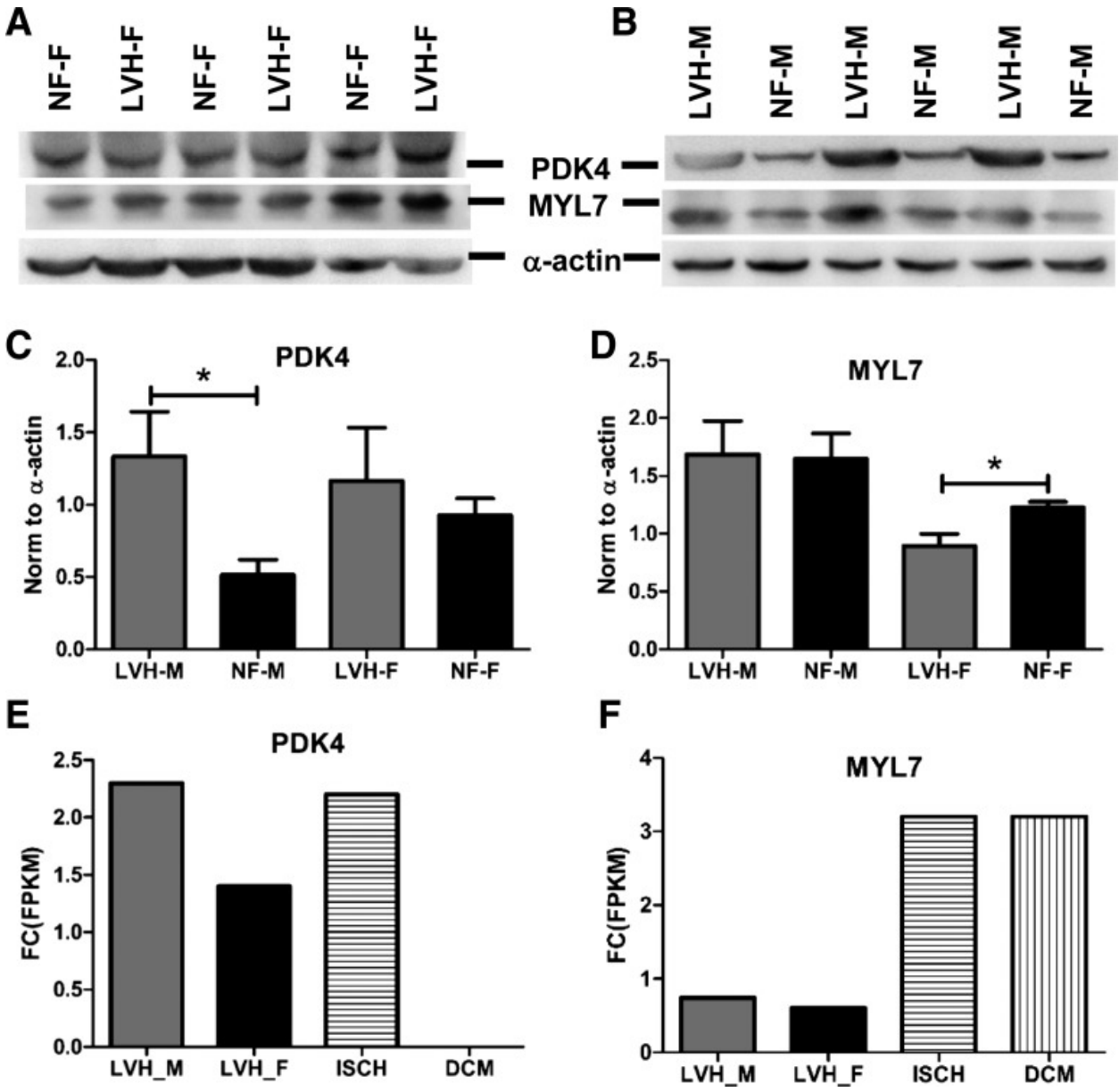

Figure 9. PDK4 and MYL7 immunoblots in female (A) and male (B) samples. α-Actin was used as a loading control. C: PDK4 protein expression normalized to α-actin in LVH and NF. D: MYL7 protein expression normalized to α-actin in LVH and NF. E: PDK4 transcript changes in LVH over NF. F: MYL7 transcript changes in LVH over NF. *Statistically significant difference between the 2 groups ($P < 0.05$). FC, fold change.

Figure 10: Gene and protein expression of HIST1H2AC

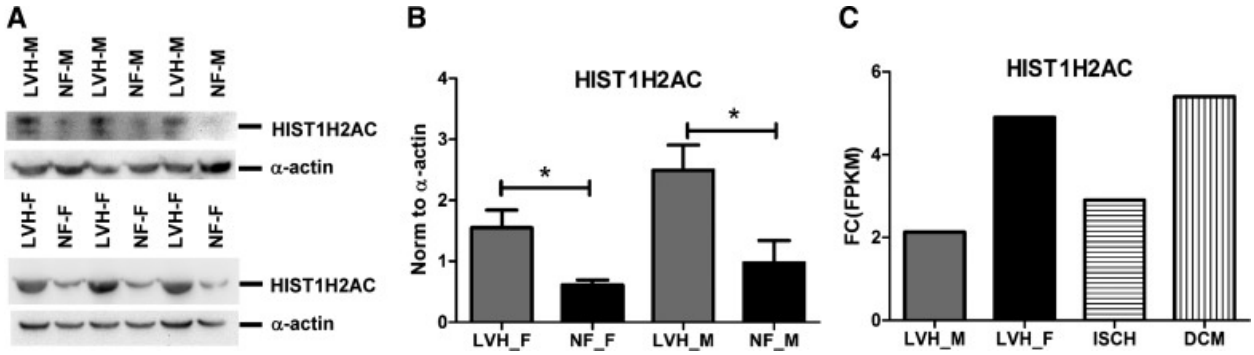

Figure 10. A: immunoblots in male (top) and female (bottom) samples. α-Actin was used as a loading control. B: HIST1H2AC protein expression normalized to α-actin in LVH and NF. C: HIST1H2AC transcript changes in LVH over NF. *Statistically significant difference between the 2 groups ($P < 0.05$). FC, fold change.

Tables

Table 1. Patient characterization

Human Sample	Sex	BMI	Age, yr	LV Mass, g	Path Report (LVH)
NF1	M	29.3	57	126	no
NF2	M	17.2	54	175	borderline
NF3	M	30.1	41	194	none to mild
NF4	M	22.5	67	97	no
NF5	M	34.9	38		none-mild
NF6	M	21.6	36	97	no
NF7	F	21.1	66		no
NF8	F	23	33		no
NF9	F	29.7	54	104	no
NF10	F	22.6	43	103	no
NF11	F	34.3	64		no
NF12	F	38.1	28	162	no
LVH1	M	23	53	378	moderate-severe
LVH2	M	51.1	54	300	moderate
LVH3	M	33.2	51	248	mild
LVH4	M	19	53	347	severe
LVH5	M	39.1	59	276	mild
LVH6	M	21.1	19	348	severe
LVH7	F	42.9	25		mild-moderate
LVH8	F	16.8	38	176	mild
LVH9	F	22.5	42	176	mild
LVH10	F	31.5	59	141	moderate
LVH11	F	33.5	49		severe
LVH12	F	19.5	50		moderate

BMI, body mass index; M, male; F, female; LVH, left ventricular hypertrophy; NF: non-LVH nonfailed left ventricular tissue.

Table 2. Significant differentially expressed genes in LVH [abs(log2FC) > 2, extreme small p_adj, also found in HF data set]

Gene	N/25	Y/30	log2FC	p_adj	Protein
HBB	5.385036	236.2845	−5.45543	0.000788	hemoglobin subunit beta
NPPA	28.79361	697.1588	−4.59767	0.018249	natriuretic peptides A
HBA1	2.670161	28.20004	−3.4007	0.001351	hemoglobin subunit alpha
NPPB	16.17904	120.645	−2.89857	0.013588	natriuretic peptides B
PDK4	66.72739	465.2543	−2.80167	4.00E-15	pyruvate dehydrogenase kinase isozyme 4
PLA2G2A	22.78948	142.7502	−2.64705	0.045658	phospholipase A2
HIST1H2AC	4.108	20.4747	−2.31733	0.003876	histone H2A type 1-C
GSTT1	2.927	13.489	−2.204	0.011703	glutathione S-transferase theta-1
PLXDC2	4.073109	16.66727	−2.03282	0.011265	plexin domain- containing protein 2
MYL7	493.851	205.222	1.267	<10E-20	myosin light chain 7

N, non-LVH nonfailed left ventricular tissue; 25, BMI 25; Y, LVH; 30, BMI 30; FC, fold-change.

References

(1) Abel ED, Litwin SE, Sweeney G. Cardiac remodeling in obesity. Physiol Rev 88: 389–419, 2008. doi:10.1152/physrev.00017.2007.

(2) Anders S, Huber W. Differential expression analysis for sequence count data. Genome Biol 11: R106, 2010. doi:10.1186/gb-2010-11-10-r106.

(3) Avelar E, Cloward TV, Walker JM, Farney RJ, Strong M, Pendleton RC, Segerson N, Adams TD, Gress RE, Hunt SC, Litwin SE. Left ventricular hypertrophy in severe obesity: interactions among blood pressure, nocturnal hypoxemia, and body mass. Hypertension 49: 34–39, 2007. doi:10.1161/01.HYP.0000251711.92482.14.

(4) Bernardo BC, Weeks KL, Pretorius L, McMullen JR. Molecular distinction between physiological and pathological cardiac hypertrophy: experimental findings and therapeutic strategies. Pharmacol Ther 128: 191–227, 2010. doi:10.1016/j.pharmthera.2010.04.005.

(5) Bharati S, Lev M. Cardiac conduction system involvement in sudden death of obese young people. Am Heart J 129: 273–281, 1995. doi:10.1016/0002-8703(95)90008-X.

(6) Bisping E, Wakula P, Poteser M, Heinzel FR. Targeting cardiac hypertrophy: toward a causal heart failure therapy. J Cardiovasc Pharmacol 64: 293–305, 2014. doi:10.1097/FJC.0000000000000126.

(7) Boheler KR, Volkova M, Morrell C, Garg R, Zhu Y, Margulies K, Seymour AM, Lakatta EG. Sex- and age-dependent human transcriptome variability: implications for chronic heart failure. Proc Natl Acad Sci USA 100: 2754–2759, 2003. doi:10.1073/pnas.0436564100.

(8) Bozkurt B, Mann DL. Use of biomarkers in the management of heart failure: are we there yet? Circulation 107: 1231–1233, 2003. doi:10.1161/01.CIR.0000057608.97285.20.

(9) Chadwick J, Mann W. Medical Works of Hippocrates. Oxford: Blackwell, 1950. [Google Scholar]

(10) Chen EY, Tan CM, Kou Y, Duan Q, Wang Z, Meirelles GV, Clark NR, Ma'ayan A. Enrichr: interactive and collaborative HTML5 gene list enrichment analysis tool. BMC Bioinformatics 14: 128, 2013. doi:10.1186/1471-2105-14-128.

(11) Cooper RS, Simmons BE, Castaner A, Santhanam V, Ghali J, Mar M. Left ventricular hypertrophy is associated with worse survival independent of ventricular function and number of coronary arteries severely narrowed. Am J Cardiol 65: 441–445, 1990. doi:10.1016/0002-9149(90)90807-D.

(12) Di Angelantonio E, Bhupathiraju ShN, Wormser D, Gao P, Kaptoge S, Berrington de Gonzalez A, Cairns BJ, Huxley R, Jackson ChL, Joshy G, Lewington S, Manson JE, Murphy N, Patel AV, Samet JM, Woodward M, Zheng W, Zhou M, Bansal N, Barricarte A, Carter B, Cerhan JR, Smith GD, Fang X, Franco OH, Green J, Halsey J, Hildebrand JS, Jung KJ, Korda RJ, McLerran DF, Moore SC, O'Keeffe LM, Paige E, Ramond A, Reeves GK, Rolland B, Sacerdote C, Sattar N, Sofianopoulou E, Stevens J, Thun M, Ueshima H, Yang L, Yun YD, Willeit P, Banks E, Beral V, Chen Zh, Gapstur SM, Gunter MJ, Hartge P, Jee SH, Lam TH, Peto R, Potter JD, Willett WC, Thompson SG, Danesh J, Hu FB; Global BMI Mortality Collaboration . Body-mass index and all-cause mortality: individual-participant-data meta-analysis of 239 prospective studies in four continents. Lancet 388: 776–786, 2016. doi:10.1016/S0140-6736(16)30175-1.

(13) Dobin A, Davis CA, Schlesinger F, Drenkow J, Zaleski C, Jha S, Batut P, Chaisson M, Gingeras TR. STAR: ultrafast universal RNA-seq aligner. Bioinformatics 29: 15–21, 2013. doi:10.1093/bioinformatics/bts635.

(14) Duflou J, Virmani R, Rabin I, Burke A, Farb A, Smialek J. Sudden death as a result of heart disease in morbid obesity. Am Heart J 130: 306–313, 1995. doi:10.1016/0002-8703(95)90445-X.

(15) England J, Loughna S. Heavy and light roles: myosin in the morphogenesis of the heart. Cell Mol Life Sci 70: 1221–1239, 2013. doi:10.1007/s00018-012-1131-1.

(16) Falcão LM, Pinto F, Ravara L, van Zwieten PA. BNP and ANP as diagnostic and predictive markers in heart failure with left ventricular systolic dysfunction. J Renin Angiotensin Aldosterone Syst 5: 121–129, 2004. doi:10.3317/jraas.2004.028.

(17) Frey N, Katus HA, Olson EN, Hill JA. Hypertrophy of the heart: a new therapeutic target? Circulation 109: 1580–1589, 2004. doi:10.1161/01.CIR.0000120390.68287.BB.

(18) Gaggin HK, Belcher AM, Gandhi PU, Ibrahim NE, Januzzi JL Jr. Serial echocardiographic characteristics, novel biomarkers and cachexia development in patients with stable chronic heart failure. J Cardiovasc Transl Res 9: 429–431, 2016. doi:10.1007/s12265-016-9710-4.

(19) Haddad GE, Saunders LJ, Crosby SD, Carles M, del Monte F, King K, Bristow MR, Spinale FG, Macgillivray TE, Semigran MJ, Dec GW, Williams SA, Hajjar RJ, Gwathmey JK. Human cardiac-specific cDNA array for idiopathic dilated cardiomyopathy: sex-related differences. Physiol Genomics 33: 267–277, 2008. doi:10.1152/physiolgenomics.00265.2007.

(20) Heckbert SR, Post W, Pearson GD, Arnett DK, Gomes AS, Jerosch-Herold M, Hundley WG, Lima JA, Bluemke DA. Traditional cardiovascular risk factors in relation to left ventricular mass, volume, and systolic function by cardiac magnetic resonance imaging: the Multiethnic Study of Atherosclerosis. J Am Coll Cardiol 48: 2285–2292, 2006. doi:10.1016/j.jacc.2006.03.072.

(21) Heidecker B, Lamirault G, Kasper EK, Wittstein IS, Champion HC, Breton E, Russell SD, Hall J, Kittleson MM, Baughman KL, Hare JM. The gene expression profile of patients with

new-onset heart failure reveals important gender-specific differences. Eur Heart J 31: 1188–1196, 2010. doi:10.1093/eurheartj/ehp549.

(22) Hulot JS, Ishikawa K, Hajjar RJ. Gene therapy for the treatment of heart failure: promise postponed. Eur Heart J 37: 1651–1658, 2016. doi:10.1093/eurheartj/ehw019.

(23) Kenchaiah S, Evans JC, Levy D, Wilson PWF, Benjamin EJ, Larson MG, Kannel WB, Vasan RS. Obesity and the risk of heart failure. N Engl J Med 347: 305–313, 2002. doi:10.1056/NEJMoa020245.

(24) Kittleson MM, Ye SQ, Irizarry RA, Minhas KM, Edness G, Conte JV, Parmigiani G, Miller LW, Chen Y, Hall JL, Garcia JG, Hare JM. Identification of a gene expression profile that differentiates between ischemic and nonischemic cardiomyopathy. Circulation 110: 3444–3451, 2004. doi:10.1161/01.CIR.0000148178.19465.11.

(25) Kuleshov MV, Jones MR, Rouillard AD, Fernandez NF, Duan Q, Wang Z, Koplev S, Jenkins SL, Jagodnik KM, Lachmann A, McDermott MG, Monteiro CD, Gundersen GW, Ma'ayan A. Enrichr: a comprehensive gene set enrichment analysis web server 2016 update. Nucleic Acids Res 44, W1: W90–W97, 2016. doi:10.1093/nar/gkw377.

(26) Lim D-S, Roberts R, Marian AJ. Expression profiling of cardiac genes in human hypertrophic cardiomyopathy: insight into the pathogenesis of phenotypes. J Am Coll Cardiol 38: 1175–1180, 2001. doi:10.1016/S0735-1097(01)01509-1.

(28) Liu Y, Morley M, Brandimarto J, Hannenhalli S, Hu Y, Ashley EA, Tang WH, Moravec CS, Margulies KB, Cappola TP, Li M; MAGNet Consortium . RNA-Seq identifies novel myocardial gene expression signatures of heart failure. Genomics 105: 83–89, 2015. doi:10.1016/j.ygeno.2014.12.002.

(29) Mahgerefteh B, Vigue M, Freestone Z, Silver S, Nguyen Q. New drug therapies for the treatment of overweight and obese patients. Am Health Drug Benefits 6: 423–430, 2013.

(30) Marfella R, Di Filippo C, Portoghese M, Barbieri M, Ferraraccio F, Siniscalchi M, Cacciapuoti F, Rossi F, D'Amico M, Paolisso G. Myocardial lipid accumulation in patients with pressure-overloaded heart and metabolic syndrome. J Lipid Res 50: 2314–2323, 2009. doi:10.1194/jlr.P900032-JLR200.

(31) McMurray JJ, Adamopoulos S, Anker SD, Auricchio A, Böhm M, Dickstein K, Falk V, Filippatos G, Fonseca C, Gomez-Sanchez MA, Jaarsma T, Køber L, Lip GY, Maggioni AP, Parkhomenko A, Pieske BM, Popescu BA, Rønnevik PK, Rutten FH, Schwitter J, Seferovic P, Stepinska J, Trindade PT, Voors AA, Zannad F, Zeiher A, Bax JJ, Baumgartner H, Ceconi C, Dean V, Deaton C, Fagard R, Funck-Brentano C, Hasdai D, Hoes A, Kirchhof P, Knuuti J, Kolh P, McDonagh T, Moulin C, Popescu BA, Reiner Z, Sechtem U, Sirnes PA, Tendera M, Torbicki A, Vahanian A, Windecker S, McDonagh T, Sechtem U, Bonet LA, Avraamides P, Ben Lamin HA, Brignole M, Coca A, Cowburn P, Dargie H, Elliott P, Flachskampf FA, Guida GF, Hardman S, Iung B, Merkely B, Mueller C, Nanas JN, Nielsen OW, Orn S, Parissis JT, Ponikowski P; ESC Committee for Practice Guidelines . ESC Guidelines for the diagnosis and treatment of acute and chronic heart failure 2012: The Task Force for the Diagnosis and Treatment of Acute and Chronic Heart Failure 2012 of the European Society of Cardiology. Developed in collaboration with the Heart Failure Association (HFA) of the ESC. Eur Heart J 33: 1787–1847, 2012. doi:10.1093/eurheartj/ehs104.

(32) Mosca L, Barrett-Connor E, Wenger NK. Sex/gender differences in cardiovascular disease prevention: what a difference a decade makes. Circulation 124: 2145–2154, 2011. doi:10.1161/CIRCULATIONAHA.110.968792.

(33) Nieminen MS, Harjola VP, Hochadel M, Drexler H, Komajda M, Brutsaert D, Dickstein K, Ponikowski P, Tavazzi L, Follath F, Lopez-Sendon JL. Gender related differences in patients presenting with acute heart failure. Results from EuroHeart Failure Survey II. Eur J Heart Fail 10: 140–148, 2008. doi:10.1016/j.ejheart.2007.12.012.

(34) Perego L, Pizzocri P, Corradi D, Maisano F, Paganelli M, Fiorina P, Barbieri M, Morabito A, Paolisso G, Folli F, Pontiroli AE. Circulating leptin correlates with left ventricular mass in morbid (grade III) obesity before and after weight loss induced by bariatric surgery: a potential role for leptin in mediating human left ventricular hypertrophy. J Clin Endocrinol Metab 90: 4087–4093, 2005. doi:10.1210/jc.2004-1963.

(35) Preston SH, Stokes A. Contribution of obesity to international differences in life expectancy. Am J Public Health 101: 2137–2143, 2011. doi:10.2105/AJPH.2011.300219.

(36) Razeghi P, Young ME, Alcorn JL, Moravec CS, Frazier OH, Taegtmeyer H. Metabolic gene expression in fetal and failing human heart. Circulation 104: 2923–2931, 2001. doi:10.1161/hc4901.100526.

(37) RStudio-Team. RStudio: Integrated Development for R. Boston, MA: RStudio, Inc. 2015.

(38) Simpson PC. Where are the new drugs to treat heart failure? Introduction to the special issue on “key signaling molecules in hypertrophy and heart failure”. J Mol Cell Cardiol 51: 435–437, 2011. doi:10.1016/j.yjmcc.2011.08.005.

(39) Son GH, Park SH, Kim Y, Kim JY, Kim JW, Chung S, Kim Y-H, Kim H, Hwang J-J, Seo J-S. Postmortem mRNA expression patterns in left ventricular myocardial tissues and their implications for forensic diagnosis of sudden cardiac death. Mol Cells 37: 241–247, 2014. doi:10.14348/molcells.2014.2344.

(40) Tan F-L, Moravec CS, Li J, Apperson-Hansen C, McCarthy PM, Young JB, Bond M. The gene expression fingerprint of human heart failure. Proc Natl Acad Sci USA 99: 11387–11392, 2002. doi:10.1073/pnas.162370099.

(41) Tarazona S, García-Alcalde F, Dopazo J, Ferrer A, Conesa A. Differential expression in RNA-seq: a matter of depth. Genome Res 21: 2213–2223, 2011. doi:10.1101/gr.124321.111.

(42) Trapnell C, Williams BA, Pertea G, Mortazavi A, Kwan G, van Baren MJ, Salzberg SL, Wold BJ, Pachter L. Transcript assembly and quantification by RNA-Seq reveals unannotated transcripts and isoform switching during cell differentiation. Nat Biotechnol 28: 511–515, 2010. doi:10.1038/nbt.1621.

(43) Twig G, Yaniv G, Levine H, Leiba A, Goldberger N, Derazne E, Ben-Ami Shor D, Tzur D, Afek A, Shamiss A, Haklai Z, Kark JD. Body-mass index in 2.3 million adolescents and cardiovascular death in adulthood. N Engl J Med 374: 2430–2440, 2016. doi:10.1056/NEJMoa1503840.

(44) van der Leeuw J, Beulens JWJ, van Dieren S, Schalkwijk CG, Glatz JFC, Hofker MH, Verschuren WMM, Boer JMA, van der Graaf Y, Visseren FLJ, Peelen LM, van der Schouw YT. Novel biomarkers to improve the prediction of cardiovascular event risk in type 2 diabetes mellitus. J Am Heart Assoc 5: e003048, 2016. doi:10.1161/JAHA.115.003048.

(45) Vest AR, Heneghan HM, Agarwal S, Schauer PR, Young JB. Bariatric surgery and cardiovascular outcomes: a systematic review. Heart 98: 1763–1777, 2012. doi:10.1136/heartjnl-2012-301778.

(46) Wang Z, Gerstein M, Snyder M. RNA-Seq: a revolutionary tool for transcriptomics. Nat Rev Genet 10: 57–63, 2009. doi:10.1038/nrg2484.

(47) Warde-Farley D, Donaldson SL, Comes O, Zuberi K, Badrawi R, Chao P, Franz M, Grouios C, Kazi F, Lopes CT, Maitland A, Mostafavi S, Montojo J, Shao Q, Wright G, Bader GD, Morris Q. The GeneMANIA prediction server: biological network integration for gene prioritization and predicting gene function. Nucleic Acids Res 38, suppl_2: W214–W220, 2010. doi:10.1093/nar/gkq537.

(48) Wong CY, O'Moore-Sullivan T, Leano R, Byrne N, Beller E, Marwick TH. Alterations of left ventricular myocardial characteristics associated with obesity. Circulation 110: 3081–3087, 2004. doi:10.1161/01.CIR.0000147184.13872.0F.

(49) Yancy CW, Jessup M, Bozkurt B, Butler J, Casey DE Jr, Drazner MH, Fonarow GC, Geraci SA, Horwich T, Januzzi JL, Johnson MR, Kasper EK, Levy WC, Masoudi FA, McBride PE, McMurray JJ, Mitchell JE, Peterson PN, Riegel B, Sam F, Stevenson LW, Tang WH, Tsai EJ, Wilkoff BL; American College of Cardiology Foundation/American Heart Association Task Force on Practice Guidelines . 2013 ACCF/AHA guideline for the management of heart failure: a report of the American College of Cardiology Foundation/American Heart Association Task Force on practice guidelines. Circulation 128: e240–e327, 2013. doi:10.1161/CIR.0b013e31829e8807.

(50) Yates A, Akanni W, Amode MR, Barrell D, Billis K, Carvalho-Silva D, Cummins C, Clapham P, Fitzgerald S, Gil L, Girón CG, Gordon L, Hourlier T, Hunt SE, Janacek SH, Johnson N, Juettemann T, Keenan S, Lavidas I, Martin FJ, Maurel T, McLaren W, Murphy DN, Nag R, Nuhn M, Parker A, Patricio M, Pignatelli M, Rahtz M, Riat HS, Sheppard D, Taylor K, Thormann A, Vullo A, Wilder SP, Zadissa A, Birney E, Harrow J, Muffato M, Perry E, Ruffier M, Spudich G, Trevanion SJ, Cunningham F, Aken BL, Zerbino DR, Flicek P. Ensembl 2016. Nucleic Acids Res 44, D1: D710–D716, 2016. doi:10.1093/nar/gkv1157.

Supplemental Figures

Supplemental Figure 1: Obese LVH DE genes found in HF patients

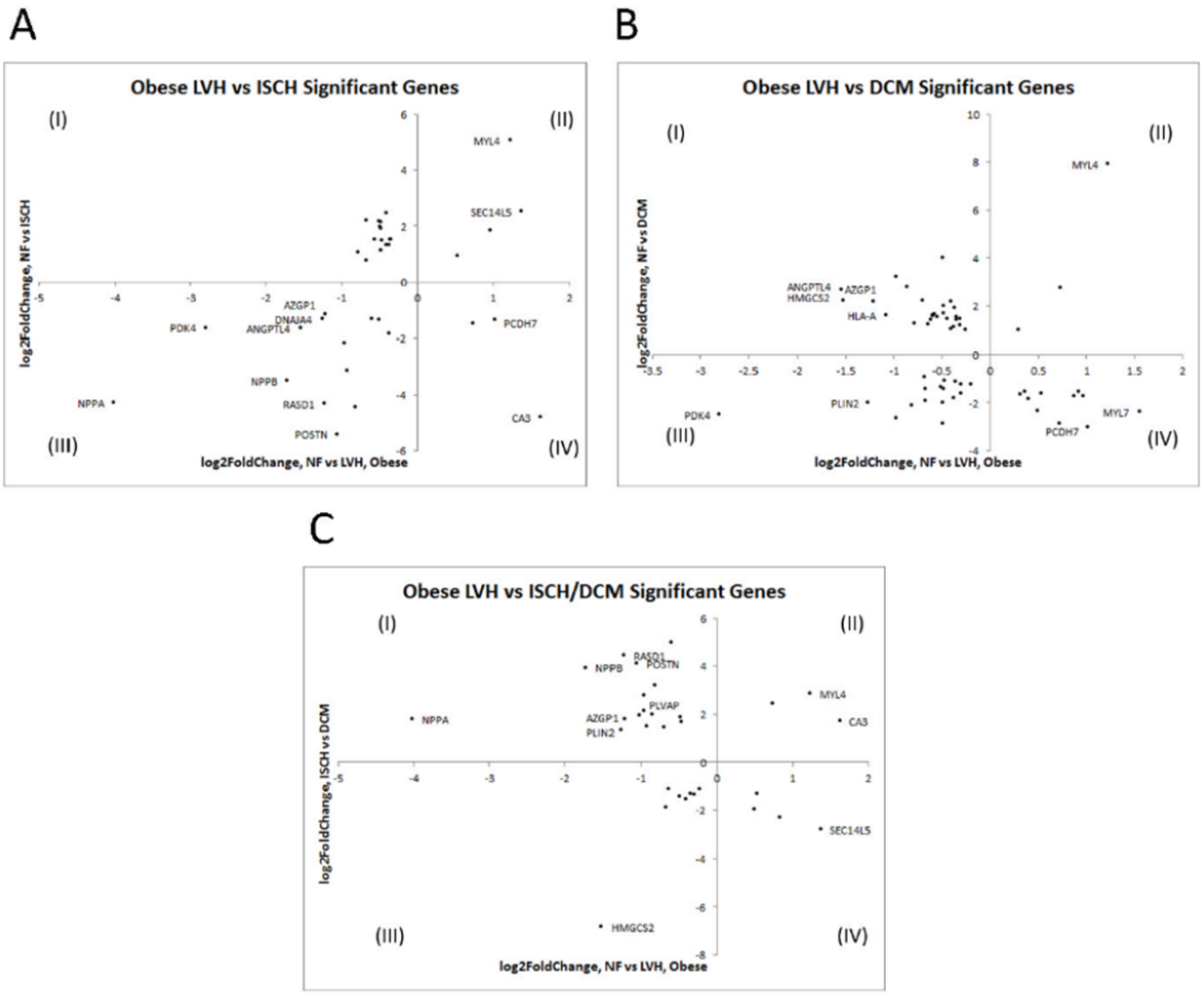

Supplementary Figure 1. A) Scatterplot of obese LVH and ischemia cardiomyopathy differentially expressed genes. Quadrant (I) contains DE genes upregulated in LVH but downregulated in ISCH. Quadrant (II) contains DE genes downregulated in both LVH and ISCH. Quadrant (III) contains DE genes upregulated in both LVH and ISCH. Quadrant (IV) contains DE genes upregulated in ISCH but downregulated in LVH. B) Scatterplot of obese LVH and dilated cardiomyopathy differentially expressed genes. Quadrant (I) contains DE genes upregulated in LVH but downregulated in DCM. Quadrant (II) contains DE genes

downregulated in both LVH and DCM. Quadrant (III) contains DE genes upregulated in both LVH and DCM. Quadrant (IV) contains DE genes upregulated in DCM but downregulated in LVH. C) Scatterplot of obese LVH and ISCH/DCM differentially expressed genes. Quadrant (I) contains DE genes upregulated in LVH but downregulated in ISCH/DCM. Quadrant (II) contains DE genes downregulated in both LVH and ISCH/DCM. Quadrant (III) contains DE genes upregulated in both LVH and ISCH/DCM. Quadrant (IV) contains DE genes upregulated in ISCH/DCM but downregulated in LVH.

Supplemental Figure 2: Sex-specific LVH DE genes found in HF patients

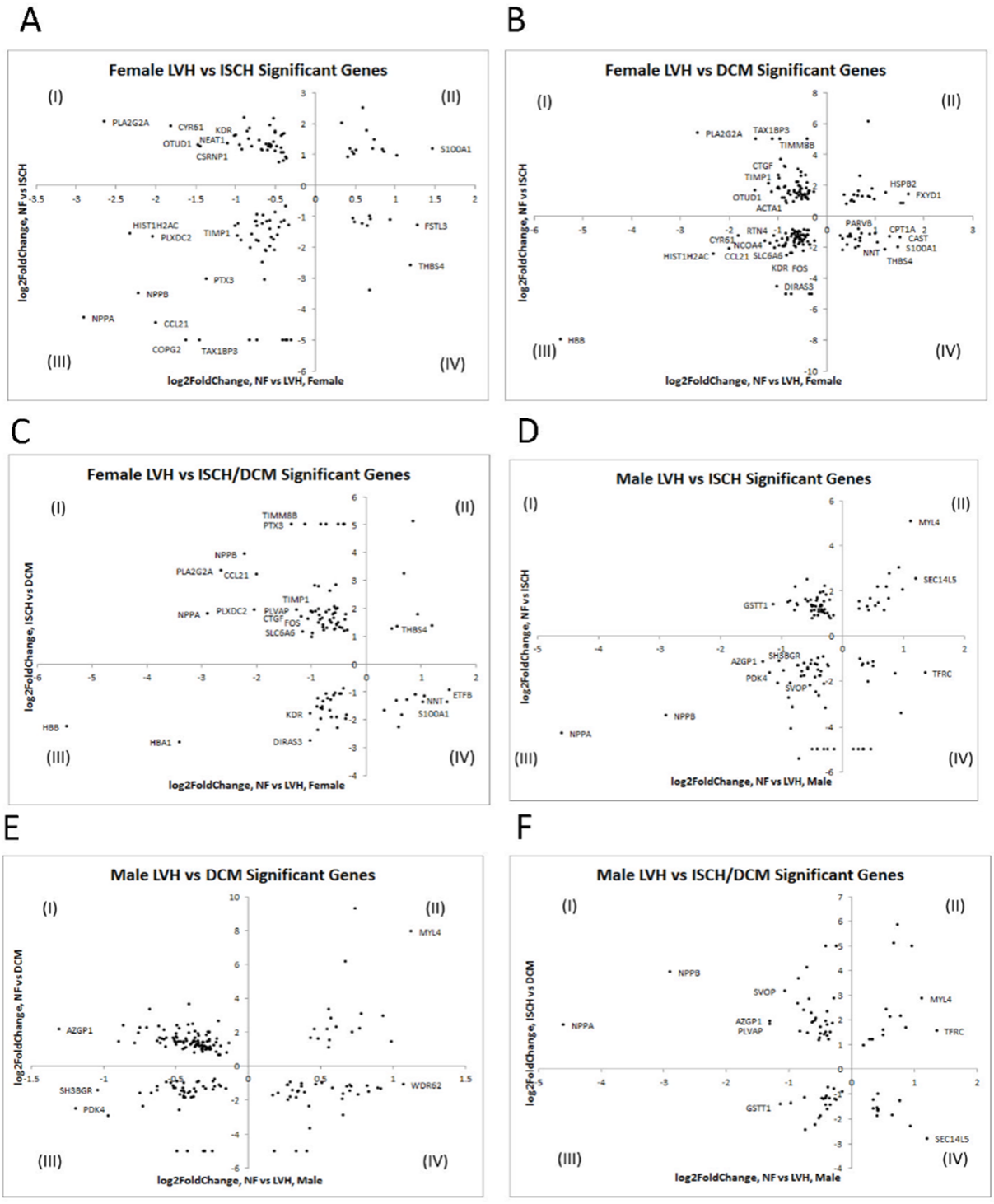

Supplementary Figure 2. A) Scatterplot of female LVH and ischemia cardiomyopathy differentially expressed genes. Quadrant (I) contains DE genes upregulated in LVH but

downregulated in ISCH. Quadrant (II) contains DE genes downregulated in both LVH and ISCH. Quadrant (III) contains DE genes upregulated in both LVH and ISCH. Quadrant (IV) contains DE genes upregulated in ISCH but downregulated in LVH. B) Scatterplot of female LVH and dilated cardiomyopathy differentially expressed genes. Quadrant (I) contains DE genes upregulated in LVH but downregulated in DCM. Quadrant (II) contains DE genes downregulated in both LVH and DCM. Quadrant (III) contains DE genes upregulated in both LVH and DCM. Quadrant (IV) contains DE genes upregulated in DCM but downregulated in LVH. C) Scatterplot of female LVH and ISCH/DCM differentially expressed genes. Quadrant (I) contains DE genes upregulated in LVH but downregulated in ISCH/DCM. Quadrant (II) contains DE genes downregulated in both LVH and ISCH/DCM. Quadrant (III) contains DE genes upregulated in both LVH and ISCH/DCM. Quadrant (IV) contains DE genes upregulated in ISCH/DCM but downregulated in LVH. D) Scatterplot of male LVH and ischemia cardiomyopathy differentially expressed genes. Quadrant (I) contains DE genes upregulated in LVH but downregulated in ISCH. Quadrant (II) contains DE genes downregulated in both LVH and ISCH. Quadrant (III) contains DE genes upregulated in both LVH and ISCH. Quadrant (IV) contains DE genes upregulated in ISCH but downregulated in LVH. E) Scatterplot of male LVH and dilated cardiomyopathy differentially expressed genes. Quadrant (I) contains DE genes upregulated in LVH but downregulated in DCM. Quadrant (II) contains DE genes downregulated in both LVH and DCM. Quadrant (III) contains DE genes upregulated in both LVH and DCM. Quadrant (IV) contains DE genes upregulated in DCM but downregulated in LVH. F) Scatterplot of male LVH and ISCH/DCM differentially expressed genes. Quadrant (I) contains DE genes upregulated in LVH but downregulated in ISCH/DCM. Quadrant (II) contains DE genes downregulated in both LVH and ISCH/DCM. Quadrant (III) contains DE genes

upregulated in both LVH and ISCH/DCM. Quadrant (IV) contains DE genes upregulated in ISCH/DCM but downregulated in LVH.

Supplemental Figure 3: nine DE genes interaction network analysis by GeneMANIA

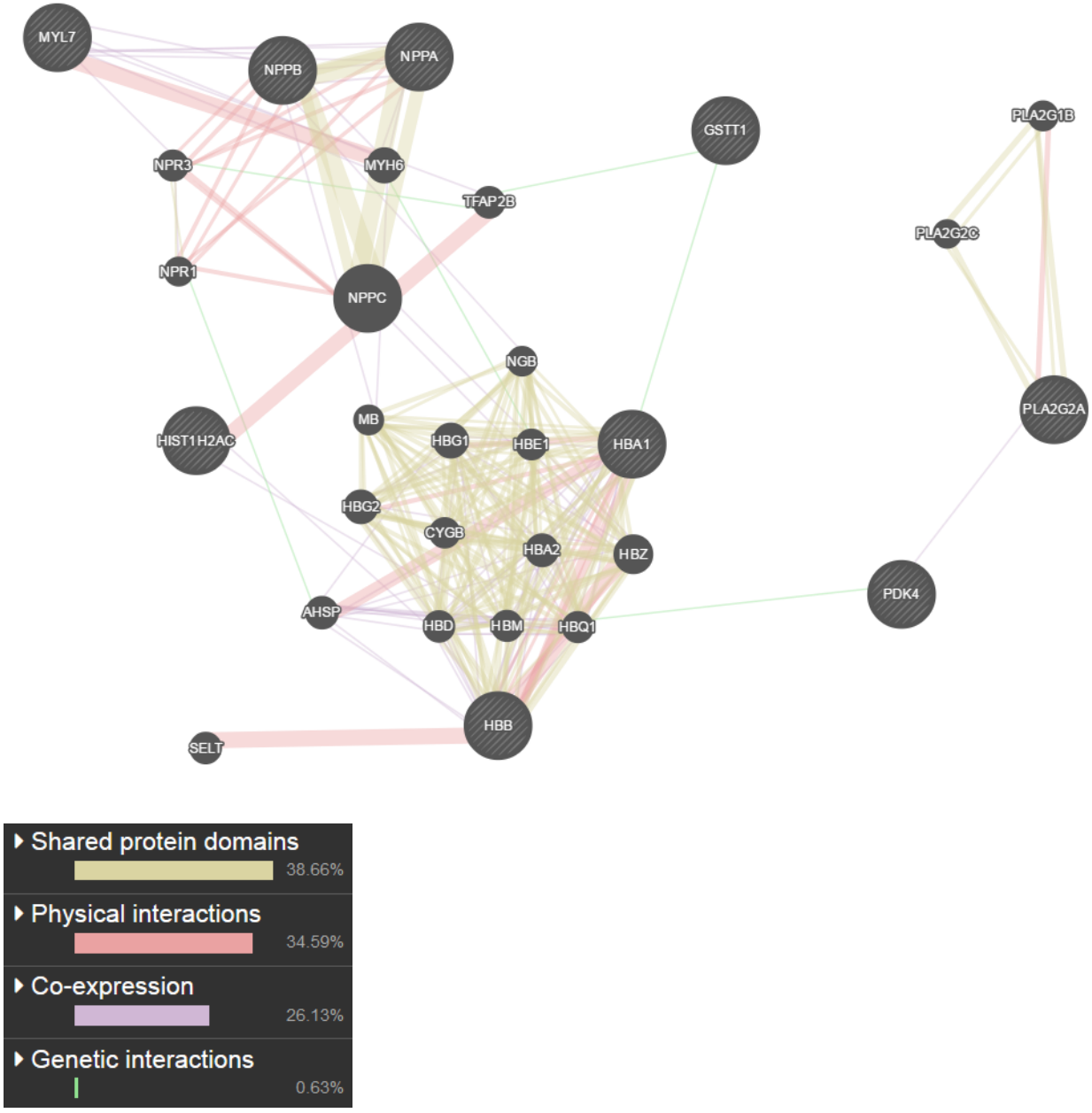

Supplementary Figure 3. Associations between the nine-gene panel with other genes estimated to have interactions were derived via GeneMANIA. Yellow indicates shared protein domains, red indicates physical interactions, purple indicates co-expression, and green indicates genetic interactions.

Supplemental Tables

Supplemental Table 1. DEG from comparing men to women (p_adj < 0.05)

GeneName	p_adj	log2FC
XIST	0	1.331247
DDX3Y	0	-2.28647
EIF1AY	0	-4.84517
RPS4Y1	0	-4.89043
FAM155B	0	-1.25799
KDM5D	5.00E-15	-1.59888
USP9Y	5.00E-15	-1.93858
TTTY14	1.52E-13	-1.70475
CCL2	0.000175	1.84234
ZFY	0.001617	-0.83281
EIF4EBP1	0.004783	-0.57846
COQ10A	0.008654	-0.61595
HPR	0.015133	-2.55647
HSPB6	0.020229	-0.83095
HS6ST3	0.02362	-0.98824
MBNL3	0.029631	-1.27373
ASIP	0.031702	-1.01184
EIF1B	0.03191	-0.60913
SFRP1	0.03445	-1.29097
SORBS1	0.036844	-0.45915
S100A9	0.040507	1.311026
FN1	0.041244	1.560714
LGALS1	0.042249	0.379527
ATP1A2	0.042719	-0.82381

Supplemental Table 2. DEG in females when comparing NF to LVH (p_adj < 0.05)

GeneName	p_adj	log2FC
ATP5F1	0	1.372359
COX5A	0	0.655162
NDUFAB1	2.00E-15	0.971683
UQCRC1	4.00E-15	0.78536
DCAF6	6.99E-15	0.894946
NDUFS2	7.99E-15	0.903111
TPM1	1.80E-14	0.852596
UQCRHL	3.00E-14	0.854599
ACADVL	1.30E-13	0.891492
CALM2	4.98E-09	0.48869
PGK1	1.52E-08	0.640531
RNF14	1.90E-07	1.344973
ANXA6	1.92E-07	0.346138
NFIX	1.93E-07	1.237286
AES	1.98E-07	0.773747
MYBPC3	3.07E-07	0.794732
TNS1	3.08E-07	0.423984
DBNDD2	3.19E-07	1.116301
TNNI3	3.21E-07	0.752848
TFG	2.12E-06	0.797028
SMIM4	4.14E-06	0.795172
RAB4A	5.53E-06	1.515827
MLYCD	6.48E-06	0.893457
PTPRM	7.06E-06	0.629126
NDUFV1	7.71E-06	0.442041
OAZ1	8.39E-06	0.687205
CAPZB	1.37E-05	0.593617
CKMT2	1.95E-05	0.826101
ANKRD9	2.22E-05	0.733555
CPT1A	2.31E-05	1.291808
MRPL16	3.43E-05	0.571236
COQ9	4.03E-05	0.591581
MRPL33	5.81E-05	0.685197
PDK2	0.000122	0.837148
TXLNB	0.000129	0.492954
EEF1G	0.000136	2.018869
DYNLL2	0.000138	0.593348
PTDSS1	0.00014	0.73936
CYR61	0.000146	-1.8073
PPP1R12B	0.000174	0.592238
MZT2A	0.000177	1.152776
FTH1	0.000189	0.948478
GATA6	0.000195	0.756302
TIMM21	0.00028	0.528606
PDHB	0.000373	0.973631
ATP6V1D	0.000455	0.531776
PSMB1	0.000497	-0.80433
TRAPPC5	0.000584	1.354619
DENND5A	0.000663	0.90012
HBB	0.000788	-5.45543
ABCF3	0.000789	1.080317
S100A1	0.000813	1.472048
COX6C	0.000854	0.434718
ASB8	0.000864	0.483151
SEPW1	0.000884	0.425352
C19orf43	0.001003	-0.58583
CSDE1	0.001139	0.58907
GNL3	0.001164	-0.81165
RPLP1	0.001217	0.862792
HBA1	0.001351	-3.4007
SDHC	0.001403	0.739299
SCARB2	0.00142	-0.49507
MCL1	0.001421	-0.55364
ADIPOR1	0.001502	1.190279
HNRNPA2B1	0.001525	1.093875
NDUFB1	0.001829	0.339606
ANKRD36B	0.001861	-3.04052
NNT	0.002013	1.040709
TTC21A	0.002043	-2.47755
SLC8A1	0.002115	0.685781
ATP5A1	0.002269	0.754705
GPR4	0.002359	-1.58775
ARL6IP4	0.002399	1.532074
NEAT1	0.002411	-1.10139
ETFB	0.002431	1.068367
TOM1L2	0.002475	0.570172

TFE3	0.002656	-0.80107
CCDC39	0.002766	-3.18253
SMARCA1	0.002783	0.990988
ETFA	0.003112	0.602531
GOT2	0.003261	0.596243
NCOA4	0.003347	-1.25799
TSFM	0.003479	1.156395
CAST	0.003565	1.515
TACC2	0.003703	0.563731
HIST1H2AC	0.003876	-2.31733
NDUFS6	0.004104	0.487713
PTGDS	0.004501	0.646333
MRPL41	0.004511	0.420448
ILK	0.004515	1.653967
FH	0.004539	0.588753
GIMAP6	0.004831	-0.94894
PFDN1	0.00486	-1.49717
LTBP1	0.004871	-1.15454
C1QTNF1	0.004932	-0.867
BOD1	0.005182	-0.51195
ATP5C1	0.005275	0.33629
NONO	0.005596	1.256768
AK1	0.005699	0.897919
TADA3	0.005769	-0.71523
MPC1	0.00577	0.985969
TRAP1	0.005888	0.768733
C15orf59	0.006123	0.693259
PARVB	0.006333	1.004308
COX7B	0.006368	1.091807
UCKL1	0.006433	-0.91676
MAGEF1	0.006657	-1.50688
ANXA2	0.006722	-0.7149
GABARAP	0.006902	2.005869
UBE2Q1	0.007324	-0.77789
TIMMDC1	0.007489	0.460374
MOB4	0.007926	-2.45158
GPRASP2	0.007945	-1.95928
ACAA1	0.008231	0.976931
MDH2	0.008315	1.042324
FXYD1	0.009307	1.676
MYL3	0.00939	0.551532
HNRNPH2	0.009874	-2.03727
VSTM5	0.010137	-1.45653
MRPL37	0.010439	0.571961
GABARAPL1	0.011234	-0.46525
PLXDC2	0.011265	-2.03282
SRSF1	0.01148	-0.72824
TIMM8B	0.012035	-1.1086
GNB1	0.012427	-0.47342
TCEAL8	0.012464	-0.48375
LMNA	0.012465	-0.36963
LINC00657	0.012465	-0.4487
ERCC1	0.012481	-0.63265
S100A8	0.012523	-0.84811
FAM46A	0.012548	-0.6472
NEMF	0.012557	-0.70149
ATP5E	0.01258	-0.94383
MRPL9	0.012593	-0.62379
RRAGA	0.012651	-0.42521
NTMT1	0.012669	-1.15378
POLR2J	0.012691	-1.02605
NPTN-IT1	0.012711	-1.49524
SDF4	0.012714	-0.47181
MIR4458HG	0.012752	-0.92531
RDH14	0.012763	-1.08698
AAMDC	0.012768	0.720372
MAT2A	0.012773	-3.98597
CD93	0.012803	-0.59718
FBLN5	0.012826	-0.55134
PDIA3P1	0.01289	-0.57568
SPARCL1	0.012917	-0.59801
C12orf57	0.013003	-0.54987
TMEM178B	0.013058	0.987441
TMEM14B	0.013071	-0.8565
TRIM35	0.013302	-1.52477
MB	0.013673	-0.36649
FAM162A	0.013689	0.502189
TNPO1	0.013703	-0.65171
ZNRF2P1	0.013769	-0.88818
ANAPC11	0.013918	1.566538
SHC1	0.014001	-0.77541
IDH3B	0.014044	0.416677

TUSC1	0.014086	-0.59556
MAGED2	0.014172	-0.74103
COX17	0.014284	-1.71685
GLRX5	0.014313	0.701564
SEPN1	0.014316	-0.44066
DEXI	0.01443	1.425424
SERTAD3	0.014546	-0.90384
NPPB	0.014572	-2.21326
TINAGL1	0.01468	0.714199
ATP5J	0.014702	0.284947
AKAP17A	0.014985	-1.03412
TGFBR3	0.014996	-0.6507
GMEB1	0.015111	-1.08091
FOXO3	0.015136	-0.76924
EHD2	0.015141	-0.48756
ANAPC2	0.015146	-1.12143
RNF185	0.01517	-0.83125
FAM217B	0.015182	-0.79726
NCBP2-AS2	0.015262	-0.9356
IPO8	0.015302	-0.77556
CCNG1	0.015352	-1.33632
GBGT1	0.015357	-1.08937
RFPL4AL1	0.015363	-1.82569
KLHDC3	0.015367	-0.74213
RAB12	0.015422	-0.67548
FANCI	0.015449	-1.70713
AP1S2	0.015457	-0.78901
PTGES3	0.015534	-0.50628
CD2BP2	0.015536	-0.58723
PSMB2	0.01563	-0.88634
RFTN1	0.015701	-0.77574
HMGN4	0.015742	-0.54851
A2M	0.015751	-0.41594
NES	0.015887	-0.88792
GNAT1	0.015907	-1.57915
SPRY1	0.01593	-0.99367
SOCS5	0.015948	-1.25689
ERLEC1	0.016148	-0.75281
PTBP3	0.016169	-0.95234
SLIRP	0.016174	0.781915
ZNF22	0.016207	-0.71381
ACSM1	0.016208	-2.13365
SMPX	0.016208	-0.5787
LARP1B	0.016209	-1.10904
ZSWIM1	0.01621	-1.14273
PBDC1	0.016215	-0.60672
SPRY4	0.016248	-1.08951
NDUFB8	0.016282	-0.7828
IFT52	0.016284	-0.80741
NEDD8	0.016298	-0.83441
IMMP1L	0.016304	-1.26851
RPS24	0.016319	-0.68556
SYNPO	0.016324	-0.61107
UQCC1	0.016391	-1.03014
PDIA4	0.016406	-0.53875
STAT1	0.016494	-0.6334
ARHGAP29	0.016538	-0.89775
MOGS	0.016616	-0.63599
MT1A	0.016679	-1.31961
PPIG	0.016724	-0.638
TRAM1	0.016725	-0.37237
LMF2	0.016726	-0.67529
OLFM1	0.016731	-0.87629
DHRS4L2	0.01678	-1.16709
A4GALT	0.016789	-0.51533
MEF2D	0.016819	-0.5289
FKBP8	0.016863	-0.58714
MYLIP	0.016882	-0.77689
SLC6A6	0.016902	-1.15071
HTR2B	0.016906	-1.63789
C14orf166	0.016924	0.698352
GAS7	0.016998	-0.83087
HNRNPDL	0.01702	-0.43099
MCCC2	0.017026	-0.90751
TXN	0.017065	-0.49235
PIN4P1	0.017103	-0.79958
POMP	0.017144	-0.38022
NCLN	0.017161	-0.6726
IGF2	0.017209	-1.4621
TPM3	0.017233	-0.81961
ANP32B	0.017281	-0.50937
PMEPA1	0.017309	-0.74767

FAM219A	0.017339	-0.54698
RNMTL1	0.017371	-0.74583
TMEM14C	0.017412	-0.60308
PUM2	0.017423	-0.45941
ZFP36	0.017465	-0.99179
SF1	0.017507	-1.01606
FAM160A2	0.017523	-0.96128
SERPINB1	0.017524	-0.63034
DENND2A	0.017611	-1.00146
PEF1	0.017654	-0.93352
EIF3I	0.017689	-0.81232
PLVAP	0.017747	-1.26576
LAMP2	0.017906	-0.9885
ZNF146	0.017951	-0.67501
SYPL1	0.017992	-0.31657
STK38	0.018017	-0.66665
EIF2B5	0.018254	-0.5767
CDC42EP1	0.018263	-0.60669
RBMS1	0.018418	-0.81146
MEA1	0.018451	-0.71157
MAPKAPK5-AS1	0.018459	-0.94441
SERINC1	0.018497	-0.664
PTX3	0.018539	-1.36678
BCAS2	0.018574	-0.83626
COL6A2	0.018589	-0.40003
OSBP	0.018598	-1.05728
ARHGDIA	0.018617	-0.83641
USP48	0.018636	-0.94575
RASSF3	0.018653	-0.75999
HTRA1	0.018696	-0.60734
PPIL4	0.018708	-0.9021
H6PD	0.01873	-0.69978
FUCA2	0.018749	-1.24515
AAR2	0.018794	-0.91337
PIP5K1C	0.018903	-0.63887
SAMHD1	0.018941	-0.5876
CNTRL	0.018993	-1.53438
DDX6	0.019062	-0.66268
PIP4K2A	0.019064	-0.86742
SLC45A3	0.019074	-1.48551
SAP18	0.019095	-0.46939
RFNG	0.019152	-0.98073
DCAF7	0.019219	-0.87273
PARK7	0.019226	-0.60096
CRKL	0.019327	-1.12111
CMYA5	0.019486	0.409973
EDN1	0.01956	-0.97511
APMAP	0.019589	-0.5634
PSIP1	0.019633	-0.76878
ATP1A1	0.01965	-1.06399
ARL6IP5	0.019765	-0.47494
GTPBP6	0.019788	-1.53881
ST13	0.019796	-0.40785
RN7SL2	0.019873	1.481054
FAM114A1	0.019887	-0.71223
CACFD1	0.01989	-0.89916
METTL7B	0.019927	-1.4323
NEK7	0.020017	1.095569
RARA	0.020098	-0.75894
FAM127B	0.020183	-0.71564
KLHDC8B	0.020214	-0.67781
EIF5	0.020246	-0.58398
TEAD4	0.02039	-0.83812
RD3L	0.020528	-0.84725
SLC25A5	0.020744	-0.24487
DENND6A	0.020744	-0.74386
CTNND1	0.020838	-0.49509
LMBRD1	0.020879	-0.75413
CRTAP	0.021056	-0.60928
MTURN	0.021131	-1.28667
CD59	0.021177	-0.57223
MTPN	0.021198	-2.09273
APOL1	0.021276	-0.78233
WDR61	0.021294	-1.02132
TMEM204	0.021325	-0.6529
UFM1	0.021325	-0.57161
ELOVL1	0.021326	-1.17358
H3F3B	0.02141	-0.61227
MKNK2	0.021436	-0.56249
PYURF	0.021461	1.332057
CKAP5	0.021646	1.106586

NDUFB9	0.021655	0.376823
ABL1	0.021665	-0.5416
RPS5	0.021779	0.882141
CSRP3	0.021814	-1.03479
PPP1R3F	0.021921	-0.75372
JAG1	0.021947	-0.64807
CBY1	0.021961	-0.81745
ALS2	0.0221	-0.83072
BTG2	0.022147	-0.54751
FSTL3	0.022169	1.277475
MGST2	0.022194	0.697938
SNRPN	0.022304	-1.23539
SRSF7	0.02232	-1.06689
SLC35D2	0.022325	-0.74864
NOP56	0.02236	-0.59664
CHST7	0.022374	-0.85819
TIMP3	0.02239	-0.39229
OSER1	0.022407	-0.54049
SLC19A2	0.022419	-0.7377
TLE1	0.022419	-0.82577
F11R	0.022427	-0.96876
DRAM2	0.022444	-0.72639
ASMTL	0.022448	-1.53306
ABCB7	0.022454	-0.73559
RBBP4	0.022462	-0.89412
MAGI1	0.022467	-1.14043
SLC7A2	0.02247	-0.88932
UGDH	0.022474	-0.74032
C10orf71	0.022517	0.497432
POPDC2	0.022602	0.851896
TRIM54	0.022801	0.39224
PHB	0.022854	0.58039
LDHB	0.023095	0.331912
TAX1BP3	0.023178	-1.44566
HAGH	0.023181	0.522402
BCKDHA	0.023183	1.361748
DGCR6L	0.023394	-0.86207
RBM18	0.023495	-0.88136
GNL2	0.023609	-0.56566
SAT1	0.023627	-0.40087
ZNF648	0.023648	-0.99854

ELK3	0.023721	-0.97643
HLA-DRB1	0.023762	-2.0529
RNF11	0.023794	-0.66954
ILF2	0.023796	-0.58265
AMOTL1	0.023841	-0.70949
POM121L10P	0.023984	-3.57981
HSPA14	0.024087	-0.88951
CES2	0.024136	0.651625
WDR89	0.024138	-1.19626
FAM134B	0.024207	-0.88409
CPXCR1	0.024216	-1.39867
ARHGEF15	0.024341	-0.67695
MFAP3	0.024431	-0.78174
PELI1	0.024498	-1.17581
PITPNA	0.024619	-0.55463
CNIH4	0.02465	-0.61098
SDHD	0.024683	-0.56053
CHTF8	0.024691	-0.48262
FABP3	0.024869	0.596267
TJP2	0.024913	-0.66178
C19orf53	0.02494	-0.83764
HSD17B11	0.02501	-0.69315
CLIC2	0.025025	-0.88174
OIP5-AS1	0.025046	-0.37826
TBCK	0.025073	-0.90682
TAF10	0.025111	0.9115
MYO1B	0.025112	-0.60631
TRPC4AP	0.025144	-0.4905
MAPRE1	0.025203	1.119034
CREM	0.025267	-2.14778
ALDH2	0.025329	0.862575
CYBRD1	0.025364	-0.90081
BRK1	0.025368	-0.6395
RPL9	0.025397	-1.02426
TOPORS	0.025448	-0.93365
SCNM1	0.025512	-0.93321
SH3BP4	0.025523	-0.70647
EDNRB	0.025631	-0.52333
ZBED1	0.025655	-1.19893
HNRNPF	0.025691	-0.95398
KLHDC2	0.025808	0.823827

RMDN1	0.025816	0.62209
CERK	0.025916	-0.34257
BOP1	0.025938	-0.50992
UBR4	0.02598	-0.87303
ANGPTL4	0.026011	-0.9783
RPN2	0.026012	-0.32802
CNPY3	0.02602	-1.06098
TMEM165	0.026022	1.050255
IL33	0.026093	-0.79908
NUMB	0.02612	-0.70918
NUDT15	0.026191	-0.84827
GTF3A	0.02623	0.395008
NUP153	0.026253	-0.59072
TMEM258	0.026373	0.779827
C1QBP	0.026389	0.445172
ARID4A	0.026396	-0.623
BLOC1S1	0.026446	-0.8507
TNFAIP1	0.026486	-1.42484
FNBP1	0.026615	-0.5942
RPS27A	0.026615	-0.50182
MAF1	0.026624	-0.37243
PCBP1	0.026636	1.265688
MYOZ2	0.026657	-0.55598
AKAP12	0.026665	-0.73199
YJEFN3	0.026669	-0.97526
TWF1	0.026748	-0.78106
AFG3L2	0.02694	0.504829
SNRPD3	0.026984	-0.90152
MGC16275	0.027125	-1.16985
LAMTOR3	0.027132	-0.73631
ATE1	0.02715	-0.82397
NFKBIB	0.027203	-0.63057
TP53RK	0.027302	-0.98484
LAMTOR2	0.027347	1.016552
C17orf58	0.027375	-0.97783
CC2D1A	0.02742	-0.61838
DCUN1D5	0.027445	-0.74856
KDR	0.027446	-1.01649
TCHH	0.027454	-1.91902
ANKRD10	0.027476	-0.70009
TRAPPC2	0.027511	-0.90358
SNTA1	0.027513	-0.50956
KCNH2	0.027536	0.701117
CHCHD3	0.027589	-1.8757
WAC	0.027652	-0.54735
RAI2	0.027658	-0.5362
ILF3	0.027679	-0.62026
UXT	0.02774	-0.443
VEZF1	0.027757	-0.62697
MAOA	0.027791	-0.67088
PRKACA	0.027812	0.296659
PRPF4B	0.027885	-0.56489
PALM	0.027912	-0.62806
ATG9A	0.028019	1.094103
CNN3	0.028099	-0.67041
NAT6	0.028176	-1.26624
SRF	0.028178	0.885317
SGCA	0.028242	0.496243
EDF1	0.028375	-0.81059
PDLIM7	0.028378	-0.57968
VBP1	0.028457	0.418934
CCDC3	0.028467	-1.26406
BCAM	0.028571	-0.62411
LAMTOR5	0.028573	0.967197
SEMA3G	0.028594	-0.65991
IQGAP1	0.028623	-0.86433
ACTG1	0.028634	-0.80754
PSPH	0.028652	-0.83482
GIMAP7	0.028666	-0.55439
RBM17	0.028738	-0.4027
ITM2B	0.028784	0.887048
RBP7	0.028813	-0.8759
KCTD11	0.028872	-1.32702
RETN	0.02888	-0.97095
TIMP1	0.028892	-1.00851
VAMP7	0.028929	-1.15256
DIRAS3	0.028944	-1.01864
MT2A	0.029011	2.208718
KCTD9	0.029115	-0.65237
GAS5	0.029155	-0.84549
CCNI	0.029275	-0.64834
MATR3	0.029278	1.100102

LRRFIP2	0.029348	0.529637
TMEM123	0.029487	-0.88018
SUPT4H1	0.02952	-0.44879
HNRNPA3	0.029563	-0.54081
COX6A2	0.029613	0.439694
ARL4A	0.029713	-0.87392
GCSHP3	0.029797	1.258673
COL6A1	0.029819	-0.56227
NPY6R	0.030041	-0.38687
EEF1B2	0.03009	-0.36574
MON1B	0.0301	-0.59648
IPO7	0.030296	-0.4767
CTGF	0.030305	-1.18947
TUBA8	0.030328	1.599595
CSRNP1	0.030347	-1.44187
MIR3147	0.030514	-1.29703
HBQ1	0.03057	-1.68139
ALG2	0.030579	-1.47132
SUMO1P3	0.030593	-0.87541
EFHD2	0.030605	-1.574
RAB28	0.030613	-0.47433
UTP11L	0.030623	-0.75675
C17orf62	0.030703	-0.72837
DCAF11	0.030771	0.664734
NDRG2	0.030812	0.411303
GSTK1	0.030825	0.410994
BOLA3	0.030894	0.76345
FUNDC2	0.030896	0.748066
COPG1	0.030907	-0.35733
ATP13A1	0.030911	-0.67598
MRPL4	0.030916	0.673332
PRELID1	0.030932	-0.60757
SDCBP	0.031003	-0.79818
DDX54	0.031005	-0.98504
MAPK14	0.031107	-0.55155
NBL1	0.03112	-0.79322
RBL1	0.031134	-0.87852
PHAX	0.031149	-0.50805
RBMS2	0.031211	-0.61912
EFNB2	0.031279	-0.5343
MEIS3P1	0.031286	-0.62686
ANXA9	0.031306	-0.63019
C12orf45	0.031349	-0.74622
HSPB2	0.031367	1.211078
UFL1	0.031372	-0.64279
UBB	0.03149	-0.31754
PPP2CA	0.03149	-0.71545
OSMR	0.031521	-0.68846
TSR1	0.031523	-0.67585
SDF2L1	0.031523	-0.49901
ST3GAL4	0.031551	-0.43762
5-Sep	0.031609	-1.92603
ZFP62	0.031615	-0.59505
ZNF436	0.031663	-0.85345
AGPAT2	0.031696	-0.86246
NDUFC1	0.031717	0.831897
SLC50A1	0.031719	-0.62206
GPR157	0.031724	-0.82673
PPP1R15A	0.031771	-0.60994
NCBP2	0.031874	-0.49276
CLIC5	0.031906	0.419942
SRSF4	0.032	-0.63244
ECSIT	0.032002	0.285857
PIR	0.032021	-0.62167
AP3S2	0.032022	-0.97934
SESTD1	0.032037	-1.46671
POT1	0.032046	-0.87773
MYL9	0.032117	0.544829
ZFAND5	0.032133	-0.76114
FAM129B	0.032265	-0.71755
HOMER2	0.032295	0.967059
PSAP	0.032314	0.423236
NPPA	0.032393	-2.89607
UTP14C	0.032418	-0.94049
ATF4	0.032427	-0.7596
PGM3	0.032448	-0.79205
SCN2B	0.032449	-0.81912
SLC39A1	0.03246	-0.37595
MIR3164	0.032498	-0.87443
HIAT1	0.032549	-0.40538
FAM73B	0.032558	-0.49709
TRIP4	0.032559	-0.47846

SOCS4	0.032568	-0.632
NDUFB5	0.032568	0.694388
NRAS	0.032582	-0.45616
PUS7	0.032602	-0.5256
BMI1	0.032605	-0.66256
EIF5AL1	0.032612	-0.47659
PTPDC1	0.032649	-0.62867
SEC14L1	0.03269	-0.42509
KLF8	0.032702	-2.63556
RBKS	0.032737	-0.81206
6-Sep	0.032737	-0.63976
CSNK1E	0.032738	-0.40218
ESPNP	0.032743	-2.91051
PDLIM3	0.032775	-0.56979
RBCK1	0.032778	-0.43379
GADD45B	0.032794	-0.53031
THOC2	0.032848	-0.54631
CCDC71L	0.032897	-0.64345
MPHOSPH8	0.032906	-0.49484
THAP10	0.032907	-0.73962
METTL9	0.032916	-0.4444
ARL5B	0.03292	-0.53217
CMC4	0.032923	1.087351
ALPK3	0.032942	-0.44771
RPL5	0.032976	-0.27665
GCA	0.033035	-0.53446
PRRC2B	0.033054	-0.64584
GDI2	0.033085	-0.41097
GBAS	0.033094	0.476362
YWHAH	0.033102	-0.32555
KIF5B	0.033119	-0.23947
KLHL11	0.033127	-0.78492
USP9X	0.033127	0.696856
MIR6766	0.033181	-1.11136
MTHFR	0.033204	-0.68037
GPR173	0.033213	-1.28738
REXO4	0.033222	-0.51427
SMIM13	0.033326	-0.85932
PTTG1IP	0.033331	-0.3002
UHMK1	0.033356	-0.51687
VPS29	0.033375	-0.31233
GCHFR	0.033375	-0.75276
ENG	0.033416	-0.57515
AZIN1	0.033503	-0.45722
HTATIP2	0.033517	-0.54413
DDI2	0.03353	-0.90494
CLINT1	0.033752	-0.69543
BZW2	0.033752	0.659553
SNORD116-24	0.033788	-0.91374
COQ10A	0.033817	0.483454
PKD1	0.033835	0.806112
P2RY8	0.033891	-0.76635
CDC73	0.033939	-0.47904
LDB1	0.033968	-0.37502
HIF1A-AS2	0.033996	-1.13095
RTN3	0.034032	-0.49811
MSANTD3	0.034098	-0.78896
EZR	0.034111	-0.37383
TMEM184B	0.034171	-0.44936
GABARAPL2	0.034229	-0.26784
MRPS10	0.034247	-0.5015
B2M	0.034341	-0.4811
CTNNAL1	0.034383	-0.66536
CCL21	0.034425	-1.99891
RPS3	0.034478	-0.40227
ARGLU1	0.034482	-0.49591
CX3CL1	0.034502	-0.86239
TRIM44	0.034555	-0.36939
PIAS1	0.034565	0.893026
FBXO21	0.034565	0.614546
MRPS15	0.034569	0.417615
KRBA2	0.034582	0.801596
IWS1	0.034587	-0.36654
PREX1	0.034587	-0.99797
HAX1	0.034595	0.354228
MRPL28	0.034597	0.448777
TBCE	0.034601	-0.45664
WWP1	0.034621	0.461459
KRTCAP2	0.034655	0.910631
CD302	0.034665	-0.72754
ELP3	0.034689	-0.55687

SCP2	0.034692	-0.63056
TBCA	0.034697	-0.48424
PSMB7	0.034751	-0.55098
LUC7L	0.03476	-0.66488
NDUFA5	0.034772	0.423046
POLDIP2	0.034779	-0.49773
MIR6723	0.034877	1.031906
MFGE8	0.034907	0.580005
MSANTD4	0.034921	-0.88134
PTPN18	0.034949	-0.67142
C10orf32	0.034966	-0.73241
HDLBP	0.034983	0.316667
MACROD1	0.035013	0.505591
GNAQ	0.035014	-0.81753
ALDH9A1	0.035017	-0.30472
EEF2	0.035026	-0.20504
SPEN	0.035042	-0.50484
ZNF516	0.035045	-0.59417
SLC7A8	0.035062	-0.97264
IFNGR1	0.035065	-0.64936
HIST1H4H	0.035099	-1.18434
TES	0.035128	-0.61007
VAMP8	0.035165	-0.56384
BTF3	0.035173	-0.36123
CKB	0.035218	0.524482
KLC1	0.035226	1.002591
ATG4D	0.035229	-0.43271
SEL1L	0.035252	-0.44253
HS2ST1	0.035255	-0.88546
PMP22	0.035297	0.650094
STOML2	0.035338	0.283353
RAD21	0.035372	0.391218
MCTS1	0.035379	-1.18667
IQCB1	0.035386	-0.57608
FIGF	0.035388	-1.15941
PPP1R2P3	0.035424	-0.80427
PGRMC2	0.035455	-0.42042
ARPP19	0.035456	-0.37512
EIF2S2	0.035465	-0.51712
QSOX1	0.035483	0.570679
NOP14	0.035532	-0.42275
HINT2	0.035535	0.617047
ZNF652	0.035536	-0.6381
NOLC1	0.03558	-0.51815
SSBP4	0.035593	-0.55126
RAP1A	0.035604	-0.42128
MFN2	0.035641	-0.7874
TREX1	0.035693	-0.7033
LY75	0.035726	-1.27058
STK39	0.035728	-0.61687
CEBPB	0.035736	-0.4419
AFAP1	0.035746	-0.60729
COPG2	0.035784	-1.62398
VPS4A	0.035788	0.72838
HSPA5	0.035795	1.758879
TGFB1	0.035802	-0.4841
CUTC	0.035822	-0.55877
SLC25A29	0.035854	-0.61363
ABCC2	0.035875	-0.87705
FAM84B	0.035885	-0.91927
GAS2L1	0.035893	-0.66278
NFYB	0.035894	-0.4614
TAF13	0.035928	-0.51109
CMAHP	0.035959	-0.86088
UBA52	0.035992	-0.33506
PTMS	0.035995	-0.42609
MCAM	0.036015	0.68023
ARF1	0.036022	-0.33003
PCBD1	0.03609	-0.40595
FOSL2	0.036099	-0.74138
HNRNPD	0.036109	-0.44658
CDV3	0.036113	-0.49624
PRELP	0.036116	-0.5701
SRPX	0.036118	-0.38798
THBS3	0.036129	-0.82807
STAT3	0.036138	-0.97262
PA2G4P4	0.036143	-0.6932
AGPAT9	0.036148	-0.65693
DBN1	0.036149	-0.64856
ADPRM	0.036149	-0.72515
SENP5	0.036158	-1.4376
SRGN	0.036167	-0.36339

NDUFA7	0.036176	1.782766
PHKA2	0.036178	0.764127
RARG	0.0362	-0.61422
IL6ST	0.036204	-0.34621
CANX	0.036208	-0.61134
MRPS36	0.036218	-0.4783
SNORD59A	0.036337	-0.74182
PFKP	0.036359	0.496966
TRIB1	0.036371	0.87391
TMEM120A	0.036375	-0.19527
GPATCH1	0.036451	-0.81312
SMC2	0.03646	-0.61163
COMMD1	0.036537	0.628965
LIMS2	0.036658	0.460768
USF1	0.036674	-0.78181
TAX1BP1	0.036848	0.279872
C17orf89	0.036896	-0.36637
TMA7	0.036909	0.615817
CCT3	0.036911	-0.20703
TRIM55	0.036942	-0.56786
C19orf18	0.037	-0.74323
LRPAP1	0.037026	-0.34356
FAM219B	0.037046	0.717804
CD151	0.037071	0.472685
SPTLC2	0.037092	-0.48621
APOD	0.037102	-0.89267
ADAM19	0.037114	-0.63014
FAM21A	0.037179	-0.91629
PIGU	0.037222	-0.48946
IL3RA	0.037239	-1.12638
GNG5	0.037263	-0.2129
TRUB2	0.037263	0.703895
CFL1	0.037271	0.512821
DDX19A	0.037332	-0.66125
FAM133DP	0.037353	-0.73167
MTX2	0.03736	-0.42275
GLIPR2	0.037362	-0.67926
SCAND1	0.037369	-0.34499
IDH3A	0.037432	0.65059
SBK2	0.037448	-0.71113
PEX6	0.037461	-0.49797
RNU6-7	0.037551	-1.09696
RSBN1L	0.03758	-0.60546
IL1R1	0.037637	-0.51121
OTUD1	0.037677	-1.47141
NAA10	0.03768	1.111668
PDLIM5	0.037684	-0.75044
C8orf4	0.03769	-0.88364
XRCC6	0.037731	-0.38855
MAP7D1	0.037767	0.542422
CEACAM3	0.037795	-0.83183
RGL1	0.037807	-1.12518
GLB1	0.037873	-0.55021
RWDD1	0.037879	0.742311
OAT	0.037903	-0.55549
IGSF8	0.037906	-0.43315
UBE2G2	0.037969	0.673819
C7orf55-LUC7L2	0.037975	-0.94018
NGRN	0.038009	0.494214
RNF145	0.038072	-0.50542
NDUFA12	0.038093	0.614495
NME4	0.038097	-0.48284
SUN1	0.038098	-0.45082
MMGT1	0.038143	-0.55294
MAP4	0.038209	-0.67629
RHOU	0.03821	-0.64759
HAND2	0.038228	0.564561
CUL4A	0.038228	0.372001
KLHL41	0.038234	-0.70921
PCF11	0.038267	-0.5163
ECI2	0.038296	0.474806
ZMAT3	0.038366	-0.65019
AIMP1	0.038396	-0.40934
SRPK2	0.038399	-0.56518
UBXN4	0.038413	-0.4632
TRA2A	0.038457	-0.55665
ENAH	0.038479	-0.95222
GAPDH	0.03848	0.825841
SORT1	0.038485	-0.68327
SPTSSA	0.038521	-0.72997
TLN1	0.038524	-0.39651

UQCRB	0.038548	0.451971
RPL38	0.038549	-0.33469
VGLL2	0.038578	-1.19911
CHURC1	0.038615	-0.7249
C22orf46	0.038672	-0.80934
TACC1	0.038676	-0.37055
P2RY2	0.038731	-0.64591
EGFL7	0.038757	-0.82415
PEBP1	0.038836	-0.40075
HMGN3	0.038909	-0.59267
NFIA	0.038917	-0.44679
GRIN2D	0.038948	-0.83435
UBIAD1	0.038962	-0.89191
SPCS1	0.038992	0.574248
SELE	0.039042	-0.7997
PLCB4	0.039118	-0.76018
TNFSF12	0.039249	-0.67128
GOLGA3	0.039346	-0.58309
RTN4	0.039426	-1.07648
ARFGAP3	0.039465	-0.59693
GSTP1	0.039562	-0.27793
TAF7	0.039646	-0.23116
HIF1A	0.039666	-0.79076
ZMIZ1	0.039673	-0.69877
GFM1	0.039675	0.593327
LINC00961	0.039683	-0.63191
TMEM100	0.039693	-0.62459
EMILIN1	0.039703	-0.57114
CDC42	0.039715	-0.44212
CNRIP1	0.039717	-0.8034
CXCL1	0.039718	-1.11979
RFC1	0.039781	-0.48255
MFAP4	0.039794	-0.52445
FAM168A	0.039818	-0.41783
ARL2BP	0.039899	1.290096
NAALADL2-AS3	0.039902	-0.92872
BEST4	0.039922	-1.08126
TBCC	0.039962	-0.44151
ETS2	0.039999	-0.55495
LRBA	0.040005	0.83503
GPRASP1	0.040016	-0.74586
STK25	0.040145	-0.47793
VSTM2L	0.04021	-0.86326
EIF3K	0.040228	0.330053
LLPH	0.040231	-0.65674
KIDINS220	0.040251	-0.33558
SPOP	0.040271	-0.39701
MED18	0.040278	-0.57297
ART4	0.04032	-0.71393
GNA13	0.040322	-0.90702
POU3F4	0.040361	-0.92947
PSMB4	0.040406	-0.2754
YIPF5	0.040414	-0.54419
C19orf47	0.040417	0.457919
WIPI1	0.040437	0.488378
AP1M1	0.040449	0.584028
SPRYD3	0.040467	-0.29592
SCO1	0.040469	0.476124
HIBCH	0.040508	0.61161
LAMC2	0.040528	-0.75161
ADNP	0.040531	-0.51295
C11orf68	0.040532	-0.37281
BTN2A3P	0.040561	-0.8744
RAVER2	0.040586	0.4035
PPP1R16A	0.040596	0.710287
DYNC1LI1	0.040613	0.455161
PSMC1	0.040634	0.78906
TP53BP2	0.040641	-0.57646
UBTD2	0.040645	-0.42758
FAM214B	0.04066	-0.55939
KLHL31	0.040682	-0.96742
ATP5J2	0.040698	1.053234
RNF144B	0.040792	-0.53885
LPL	0.040803	-0.43864
PRMT2	0.040809	-0.45257
CHCHD4	0.04081	0.979294
RPL18A	0.040965	0.921168
CLNS1A	0.040977	0.537933
HHATL	0.041005	0.690944
MLLT1	0.041049	-0.49458
ICA1L	0.041076	-0.64985

TMEM205	0.041111	0.656153
H2AFY	0.041137	0.600628
SKI	0.041146	0.527366
GRTP1	0.041158	-0.73563
PRPF6	0.041213	-0.3822
LYSMD1	0.041222	-0.51025
GNAS	0.041232	0.18082
ABCC4	0.041241	-0.73659
NHP2L1	0.041246	0.325181
USF2	0.041262	0.461716
SMARCA5	0.041267	-0.54153
AKAP8	0.041305	0.719672
ITGA6	0.041332	-0.38656
CHMP2B	0.041367	-0.4139
PSMB6	0.041415	0.38315
RNF146	0.041492	-0.37161
SZRD1	0.041493	-0.30777
TMEM59	0.041521	0.442592
LZTS1	0.041571	-0.84388
CLCC1	0.041678	-0.7063
HADHB	0.04173	0.454091
C1GALT1C1	0.041735	-0.50868
FAM3C	0.041765	0.732974
ANO5	0.04182	0.49683
CCL2	0.041833	0.861443
TRAM2	0.041837	-0.55606
FXYD6	0.041837	-0.61561
HSPA9	0.041839	0.33245
ATXN10	0.041858	-0.31479
CTNNA1	0.041888	0.216737
SPRYD4	0.04193	0.677688
PKM	0.041946	0.538092
LTV1	0.041958	-0.48423
SDHA	0.041978	0.649552
DCTN3	0.041992	0.483169
CMTM8	0.042006	-0.53464
KDM5C	0.042023	-0.45856
PLS3	0.042088	-0.59148
TCAP	0.042106	-0.13006
FXYD5	0.04211	-0.74162
PTPN11	0.042125	-0.40738
STX12	0.042183	-1.23808
ZNF777	0.042188	-0.65165
TEK	0.042213	-0.66509
HSPB6	0.04228	0.654175
KPNA6	0.042351	0.521901
ESF1	0.042366	-0.4259
EID1	0.042432	-0.4688
DENND5B-AS1	0.042446	-0.84422
CYB5R1	0.042453	0.622642
WASF2	0.042467	-0.61661
RAMP3	0.04247	-0.60506
ACTA1	0.042476	-1.1199
DDX42	0.042477	-0.42944
MYO18B	0.042532	-0.40501
ZCCHC24	0.04263	-0.4355
HSPA6	0.042634	-1.46953
GPR137B	0.042676	-0.41419
LPCAT3	0.042718	0.759429
PXYLP1	0.042773	-0.70605
MBTPS1	0.042804	0.439015
ABHD14B	0.042806	-0.79084
LAMB1	0.042876	-0.23987
PROS1	0.042894	-0.925
RNF10	0.042923	0.322112
PPIA	0.042948	-0.39158
ULK1	0.042966	0.844633
WDR5	0.043029	-0.35205
SGTA	0.043111	0.405405
NR1D2	0.043119	-0.36619
PSMB5	0.043129	0.264588
DNAJC11	0.043135	0.437261
SERPINH1	0.043145	-0.564
RPA1	0.043152	-0.34369
SPTAN1	0.043153	-0.35344
ZBTB21	0.043154	-0.573
S100P	0.043155	-0.62072
ANKRD11	0.043157	-0.4622
MIR621	0.043158	-0.65688
RPL28	0.04316	-0.35673
MED4	0.043166	-0.44131

CCNL2	0.043166	-0.60767
BACE2	0.043168	-0.47492
ST3GAL6	0.043173	-0.37651
NDUFAF1	0.043183	-0.445
LRRC2	0.043188	-0.51305
ATP5SL	0.04319	0.429372
TXNRD1	0.043213	-0.39736
PAFAH2	0.04322	-0.49065
HSPA8	0.043225	-0.35936
ISCA1	0.043227	-0.37738
CRIP2	0.043242	0.308317
SPOPL	0.043249	-0.48301
RHPN2	0.043263	-0.6109
IRS1	0.043275	-0.49894
CERS6	0.043281	0.829045
SLC35B3	0.0433	-0.43175
PRICKLE3	0.043329	-0.45225
TRIM65	0.043333	-0.51273
WAC-AS1	0.04334	-0.4838
B4GALT1	0.043353	-0.63432
FKBP5	0.043381	-0.51771
SLC35A2	0.043402	-0.41879
RIMS1	0.043419	-0.72291
ARV1	0.043446	-0.4904
SNORD63	0.043456	-0.60599
PANX1	0.043457	-0.64611
MYH7	0.043476	0.725402
ADPRH	0.043478	-0.73527
HCFC1	0.043483	-0.44703
GTPBP1	0.043497	-0.39791
UBE2A	0.043511	0.435335
UQCR11	0.043526	0.768241
TMEM70	0.043542	-0.43259
CYC1	0.04356	-0.51256
RHBDD1	0.043564	-0.53431
POLE3	0.043578	-0.30923
XPC	0.043598	-0.47842
LINC00998	0.043603	0.544187
ELK1	0.043625	-0.39441
FOS	0.043634	-1.05858
NCKIPSD	0.043648	-0.40907
ZNHIT2	0.043652	-0.96854
CASP3	0.043676	-0.66391
DENND4C	0.043721	-0.4932
RBMXL1	0.043723	-0.45167
RPS14	0.043761	0.724838
CALHM2	0.04377	-0.4685
FAM210B	0.043793	-0.36254
ATP8B2	0.043809	-0.42195
CTNNBL1	0.043831	-0.42786
TGFB3	0.043859	-0.45892
ROCK2	0.04386	-0.38353
SMIM3	0.043864	-0.3364
FAM8A1	0.043881	-0.428
SCO2	0.043892	-0.83004
DAAM2	0.043894	-0.50534
FAM78B	0.043911	-0.62746
DNMBP	0.043928	-0.53882
MYO10	0.04393	-0.53448
HDAC1	0.043974	-0.57812
UPP1	0.043985	-0.56422
LSM3	0.043996	0.678043
EPHA4	0.044019	-0.5129
BCAR3	0.044029	-0.79978
TRIP11	0.044051	-0.38457
KLF7	0.044053	-0.39001
MED6	0.044066	-0.68885
CLUH	0.044091	0.533426
DUSP27	0.044104	-0.54408
TSC1	0.044115	-0.53249
CDKN1A	0.044115	-0.42907
DGKE	0.044135	-0.55624
DYNLT3	0.044156	-0.34186
NFIB	0.044163	-0.29183
STX5	0.044175	-0.40774
PSMD11	0.044179	0.974021
CS	0.044195	0.634064
CYP20A1	0.044198	-0.60404
PPP1R17	0.044203	-1.20029
FAM98B	0.044205	-0.46231
C1orf43	0.044205	-0.23152
DPM1	0.044214	-0.44745

INTS10	0.044233	-0.43167
CRIPT	0.04425	-0.52125
SYT9	0.044262	-0.71172
SPSB1	0.044285	-0.41671
ODC1	0.044311	-0.25745
SAYSD1	0.044315	-0.49224
TECR	0.044317	0.682883
CNBP	0.044329	-0.36659
CD68	0.044368	0.939055
GAR1	0.044412	-0.42803
PPP1CC	0.044417	0.660556
DANCR	0.044424	0.485809
HSD3B7	0.044425	-0.59878
DDR2	0.044432	-0.52046
MYLK3	0.044447	-0.4339
CREB1	0.04448	-0.4684
PPP6R2	0.044507	-0.32101
NSMF	0.044562	-0.43373
TRMT61A	0.044654	-0.44573
GATAD2A	0.044678	-0.36954
TMEM167A	0.044683	-0.51829
FBXL7	0.044687	-0.37815
ARRDC1	0.044708	-0.44123
RHAG	0.044719	-0.83399
S100A9	0.044725	-0.93497
SFTPB	0.044732	-0.92639
THBS2	0.044745	-0.66519
BLOC1S2	0.044748	-0.37961
IKZF5	0.044775	-0.51802
NUPL1	0.044795	-0.41339
ZBTB44	0.044803	-0.42604
MTIF3	0.044814	-0.29802
CALM3	0.044816	-0.26617
CFDP1	0.04486	-0.3963
VPS28	0.044971	0.682919
NOP10	0.044991	-0.32865
DMWD	0.044996	-0.36496
HYPK	0.045092	0.872538
NR2F2	0.045107	-0.51244
MSMP	0.045127	0.807117
GPD2	0.045132	-0.62732
KLHL38	0.045138	0.335281
ZNF324B	0.045164	-0.84753
NDUFS3	0.045181	0.280477
RAI14	0.045196	-0.5097
GPKOW	0.045223	-0.35042
TRIM38	0.045223	-0.5031
SBDS	0.045268	-0.21392
EMCN	0.045297	-0.39739
FTL	0.045301	-0.67871
AKT1S1	0.045308	-0.3399
EFEMP1	0.04534	-0.72991
TM9SF3	0.045344	-0.294
RPS12	0.04535	-0.36671
MINPP1	0.045369	-0.5057
SGK223	0.04538	-0.59039
BTBD10	0.045469	-1.28796
THAP9-AS1	0.045504	-0.54543
LPAR1	0.045525	-0.46803
MAPK8IP3	0.045532	-0.58917
XPO7	0.045555	-0.35552
ARHGAP30	0.045572	-0.69869
GPATCH11	0.045615	-0.4265
LSM1	0.045632	0.470032
CXorf36	0.04564	-0.52947
PLA2G2A	0.045658	-2.64705
DYRK2	0.045658	-0.48669
CMAS	0.04569	-0.32507
ATXN3	0.04571	-2.43236
AAK1	0.045716	-1.78202
TUBA1B	0.045721	0.712811
FAF1	0.045739	0.416979
TCEAL7	0.045743	-0.55323
ENO2	0.045746	-0.61311
NUDT16P1	0.045758	-0.5736
CTTNBP2NL	0.045785	-0.53209
ZFYVE27	0.045792	-0.45599
PRKCDBP	0.045832	-0.26048
DGAT1	0.045874	-0.40077
LRRN4CL	0.045889	-0.74009
AC007392.3	0.045933	-0.82613
DUSP1	0.045995	-0.83021

ATN1	0.046005	-0.36858
DNAJB1	0.046029	-0.62176
CD81	0.046032	0.616659
PRDX2	0.046318	0.610194
RPL14	0.046364	0.820702
MIR568	0.046373	-0.46123
SIK3	0.046385	-0.53583
PBX4	0.046398	-0.8201
CHMP7	0.04643	-0.32032
PRKAA2	0.046432	-0.42629
NEDD9	0.046449	-0.52443
COPE	0.046456	0.427074
DLGAP4	0.046479	-0.46245
SLC11A2	0.046479	-0.71511
PSMD8	0.046502	-0.32555
DAPK2	0.046529	0.741447
SEC24A	0.046569	-0.50265
MYCT1	0.046578	-0.54874
ZNF793	0.046632	-0.78982
DNAJA2	0.046654	-0.309
E2F6	0.0467	-0.50392
RAB2A	0.046706	-0.35634
APP	0.046741	-0.19958
SLC25A37	0.046742	-0.54723
INPP5J	0.046762	-0.45787
MRPL51	0.046781	0.399561
MAML1	0.046807	-0.46279
LRRC14B	0.046813	0.601274
FBXO7	0.04684	-0.33304
RAB39B	0.046864	-0.6923
SNAPC2	0.046896	-0.41126
ATP5H	0.046897	1.01046
7-Mar	0.046901	-0.49283
MAP2K7	0.046903	-0.36906
PLAA	0.046927	-0.52849
CALCOCO1	0.047034	0.655995
ATP2B4	0.047037	-0.47315
YAE1D1	0.047064	-0.52899
SRL	0.047072	-0.49114
SLC29A3	0.047088	-0.56336
PPP1R15B	0.047125	-0.66899
RPL41	0.047202	-0.46263
CMC2	0.04727	0.928306
KANK2	0.047282	0.397004
KIAA0368	0.047288	-0.21364
NDUFA13	0.047299	0.553808
DHRS3	0.047324	-0.49842
COMMD10	0.047459	-0.75317
ATP6AP2	0.047549	-0.2996
MRPS6	0.047567	0.605533
TP53	0.04764	-0.47344
INPP5A	0.047664	0.353673
HIVEP1	0.047682	-0.57953
GRHPR	0.047712	0.471827
YDJC	0.047741	-0.4309
LRRC47	0.047796	-0.28552
SPANXC	0.047797	-0.76043
DOCK1	0.047808	-0.46818
NEXN	0.04781	-0.31415
MLIP	0.047821	0.32587
PCYT1A	0.047841	0.625988
KTN1-AS1	0.047945	-0.62535
C1orf52	0.04795	-0.45743
PCNXL2	0.047952	-0.98865
CIAPIN1	0.047955	-0.35584
SFXN1	0.047968	-0.43105
THBS1	0.048008	-0.37739
LTBP4	0.048019	-0.40618
FAM195A	0.048103	0.683693
CTNNB1	0.048125	-0.36302
FLAD1	0.048152	-0.44251
ATP6V0C	0.048154	0.795255
UQCRC2	0.048197	0.327542
MAFG	0.048208	-0.65158
TPI1	0.048222	0.369575
ZNF768	0.048268	-0.4432
FAM222B	0.048367	-0.55818
CRIM1	0.048377	-0.4341
WDR26	0.048381	0.434243
TIMM50	0.048402	0.469425
NMRK2	0.048413	0.585886
DDB1	0.048418	0.390274

CWF19L2	0.048419	-0.60657
GOLGA1	0.048422	0.732444
MORF4L2	0.048428	-0.51525
JAK1	0.048446	0.507475
RPRD1B	0.048459	-0.50933
MAGOH	0.048468	-0.30745
SNORA33	0.048468	-1.16312
NAAA	0.048474	-0.45585
CD1D	0.04848	-0.663
SOAT1	0.048506	-0.50051
SPG7	0.048523	0.461449
THBS4	0.048544	1.196572
MTHFD1	0.048549	0.512123
JAZF1	0.048565	-0.63113
NUCKS1	0.048583	-0.33916
ZSCAN26	0.04859	-0.48147
CLPTM1	0.048591	0.37098
MIR3936	0.048604	-0.71114
DFFA	0.048607	-0.45858
TRIM24	0.048612	0.630467
PECAM1	0.048628	-0.53376
HSBP1	0.048629	0.504809
SSH1	0.048667	-0.62376
CLEC10A	0.048724	-0.78745
GOLGA5	0.048731	-0.45546
TXNDC15	0.048733	-0.45751
GRAMD4	0.048737	-0.54644
CHTOP	0.048751	-0.42894
ASB1	0.048754	-0.4207
C4orf27	0.048773	-0.39327
CDH2	0.048778	-0.28261
PARS2	0.048787	-0.68577
TMEM181	0.048791	-0.58895
SUSD1	0.048805	-0.66238
RPE	0.048814	-0.62216
CAMK2D	0.048827	-0.51715
ZNF136	0.048863	-0.7799
MRTO4	0.048896	-0.51359
APLP2	0.048905	-0.31988
XIRP1	0.048919	-0.78224
MBD3	0.048919	0.640065
UBE2D3	0.048927	0.403792
HDHD2	0.048934	0.560806
ERRFI1	0.048981	-0.49895
POLR2M	0.049007	-0.52703
TLR4	0.049015	-0.51025
MTUS2	0.049071	0.370084
LARS	0.049073	-0.50774
TMSB4X	0.049079	-0.51899
CBLB	0.049091	-0.50192
POLI	0.049111	-0.65863
METRN	0.049113	0.568665
JUND	0.049129	-0.30596
TNFRSF10B	0.049134	-0.50488
PORCN	0.049136	-0.64084
PWAR1	0.049174	-1.02416
EGR1	0.049178	-0.77867
TTL	0.049195	0.703811
ASUN	0.049196	-0.39201
EIF4A3	0.04925	-0.43556
PITPNM1	0.049337	-0.57986
AVIL	0.049382	-0.61709
MPP1	0.049409	0.568199
NUDT4	0.049429	-0.57452
ATL3	0.04943	-0.54625
PNMAL1	0.049439	-0.63464
ZDHHC3	0.049442	-0.46304
FGD4	0.049444	-0.70371
FBXO40	0.049521	0.559935
NCS1	0.049573	-0.61313
DYNLL1	0.04959	-0.74122
RPS15A	0.049643	1.025891
RPL37A	0.049679	0.515517
GJA1	0.049747	-0.35022
GAS2	0.04977	-0.53259
SYNM	0.04979	0.325806
FASTKD1	0.049842	0.519079
ENPEP	0.049861	-0.57397
ZFAT	0.049905	-0.53663
CETN2	0.049919	-0.28869
PDE4D	0.04992	-0.51969
TOPORS-	0.04992	-0.55873

AS1		
PGRMC1	0.049922	-0.3399
RECK	0.049922	-0.42461
ANKIB1	0.049923	-0.38159
RAB6A	0.049923	-0.1895
ANGPTL1	0.049924	-0.41541
MGLL	0.049925	-0.37542
SLC25A16	0.049926	-0.49931
ZNF438	0.049926	-0.41161
ANKRD13C	0.049934	-0.42953
SLC31A1	0.049937	-0.47657
ENOSF1	0.049938	-0.51981
RBM12	0.049945	-0.38949
ZNF302	0.049949	-0.33246
DNAJC3	0.049951	-0.37766
LIMA1	0.049959	-0.57653
C14orf2	0.049972	0.367813
SLC25A38	0.049973	-0.42679
ZNF841	0.049978	-0.4047
ADAMTS9	0.049991	-0.42334

Supplemental Table 3. DEG in males when comparing NF to LVH (p_adj < 0.05)

GeneName	p_adj	log2FC
AZGP1	0	-1.30798
IGFBP2	0	-0.86226
ACKR3	0	0.671192
HSPG2	0	0.733618
PPP1R12C	0	-0.42178
DYNLRB1	0	-0.37811
IDH3A	0	0.511248
FKBP8	0	-0.42929
RAB11B	0	-0.48372
PSMA7	0	-0.33594
SLC5A1	0	0.724038
SOD1	0	-0.33697
GPNMB	0	0.834657
TTN	0	0.614038
NEXN	0	-0.52548
SRM	0	-0.35759
RHOC	0	-0.27958
C19orf53	0	-0.31797
PNRC1	0	-0.56502
HSD17B10	0	-0.27013
RAMP1	0	-0.59369
IDH2	0	0.289888
SPG21	2.00E-15	-0.50108
ARL2	2.00E-15	-0.47455
FAM50A	2.00E-15	-0.42732
UBL7	2.00E-15	-0.28434
UBXN6	2.00E-15	-0.45076
PCBD1	2.00E-15	-0.44015
LDHD	2.00E-15	-0.26791
PPAPDC3	2.00E-15	-0.22663
JUP	2.00E-15	-0.35173
IGSF8	3.00E-15	-0.49134
PLVAP	3.00E-15	-1.29896
CDIPT	3.00E-15	-0.29615
C10orf10	3.00E-15	-0.77617
UBL5	3.00E-15	-0.28347
PPP2R1A	3.00E-15	-0.27626
PACSIN3	3.00E-15	-0.34172
GPX4	3.00E-15	-0.22506
DUSP27	3.00E-15	-0.41684
TRIM63	3.00E-15	-0.64008
YPEL3	4.00E-15	-0.7847
HRSP12	4.00E-15	-0.4346
COPRS	4.00E-15	-0.35458
MPHOSPH8	4.00E-15	-0.40987
DAPK3	4.00E-15	-0.57591
LRPAP1	4.00E-15	-0.39917
CD151	4.00E-15	-0.51077
PEBP1	4.00E-15	-0.34523
LMOD2	4.00E-15	-0.63874
CLPP	5.00E-15	-0.34131
RBM42	5.00E-15	-0.35417
NUDC	5.00E-15	-0.52612
SF3B5	5.00E-15	-0.40871
ATP6V0E1	5.00E-15	-0.36647
RRAS	5.00E-15	-0.40779
PLEKHO1	6.00E-15	-0.59572
DYNLT1	6.00E-15	-0.44132
TRNP1	6.00E-15	-0.49843
EDF1	6.00E-15	-0.31412
RBPMS2	6.00E-15	-0.28934
DRG1	6.99E-15	-0.32335
ALDOC	6.99E-15	-0.45447
GIPC1	7.99E-15	-0.3734
FDFT1	7.99E-15	-0.52811
DIAPH1	7.99E-15	-0.39074
PPP1R7	7.99E-15	-0.33032
SGCA	7.99E-15	-0.45226
RBM3	7.99E-15	0.274338
GABARAPL1	7.99E-15	-0.31891
TCAP	7.99E-15	-0.29492
OS9	8.99E-15	-0.33479
PLA2G16	8.99E-15	-0.42933
ACTR1A	8.99E-15	-0.28631
TBC1D8	9.99E-15	-0.5583
PWAR5	9.99E-15	0.526286

DNASE2	1.10E-14	-0.45549
TMEM140	1.20E-14	-0.89372
TSPO	1.20E-14	-0.44565
NDUFAF3	1.30E-14	-0.24658
SDF4	1.30E-14	-0.3565
TRIM54	1.30E-14	-0.40356
PSMD4	1.40E-14	-0.36071
SORT1	1.40E-14	-0.41997
FBXW5	1.60E-14	-0.39062
SYNGR2	1.80E-14	-0.48952
PNPLA2	1.80E-14	-0.4725
HSPB8	2.00E-14	-0.30308
NUCB1	2.10E-14	-0.31163
EIF5A	2.40E-14	-0.38269
CTSD	2.60E-14	-0.47497
TRIP10	2.80E-14	-0.59969
EPN1	2.90E-14	-0.36742
BRK1	2.90E-14	-0.28194
PDHX	3.10E-14	0.25964
AC018464.3	3.20E-14	-0.27882
CCDC85B	3.60E-14	-0.62642
SNTA1	3.70E-14	-0.25705
KCNN2	3.90E-14	0.669077
CCDC124	4.10E-14	-0.48253
CDK2AP2	7.21E-14	-0.69732
BSG	1.07E-13	-0.40526
HIST2H2BE	1.11E-13	-0.52488
HSPB7	4.91E-13	-0.3482
WDR62	2.15E-12	1.07249
TALDO1	4.47E-12	-0.32684
RAB40B	1.33E-11	-0.49743
RPL35	1.57E-11	-0.26922
EMD	3.27E-11	-0.3251
BLVRA	2.66E-09	-0.31132
MT2A	7.38E-09	-1.04872
PEBP4	8.73E-09	-0.44419
S1PR3	1.29E-08	0.779523
PTPRB	1.29E-08	0.897076
TANGO2	1.46E-08	-0.40924
NCOA4	2.30E-08	0.20876
SCARA5	1.67E-07	0.976601

MYL4	1.01E-06	1.123475
ZBTB47	3.25E-06	-0.41997
CCL2	9.02E-06	0.671466
CD81	9.22E-06	-0.36777
PLP2	9.72E-06	-0.41521
LAMTOR5	1.83E-05	-0.17459
RRAD	1.96E-05	-0.58697
AURKAIP1	2.33E-05	-0.19937
SERF2	2.39E-05	-0.31704
MGAT4B	2.62E-05	-0.29272
MYH14	3.04E-05	-0.29136
DLAT	3.39E-05	0.330348
KCTD17	3.80E-05	-0.56372
ITM2A	4.45E-05	0.703263
PRPF6	5.66E-05	-0.32279
MXI1	5.68E-05	-0.44513
LRRC14B	6.69E-05	-0.58266
GTF3A	9.33E-05	-0.37791
FAM89B	9.57E-05	-0.44927
MASP1	9.84E-05	-0.6278
UXT	0.000104	-0.37965
MRPS23	0.000108	-0.33421
HDAC5	0.000133	-0.29006
ALDH2	0.000141	-0.30653
LRRC23	0.000151	-0.65684
ETFA	0.00019	-0.1549
SSB	0.000191	-0.3278
OSER1	0.00021	-0.45161
RSL24D1	0.000229	-0.32297
SLC6A8	0.000258	-0.35093
DUSP26	0.000341	-0.54462
SLC25A3	0.000341	0.25135
EMCN	0.000356	0.55574
CDC34	0.000616	-0.3254
B4GALT2	0.000621	-0.35529
HSP90B1	0.000756	-0.26208
RPL13A	0.000944	-0.18863
ZNF358	0.001	-0.31875
KEAP1	0.001042	-0.30105
INMT	0.001049	0.824406
PIN1	0.001078	-0.35181

WBP2	0.001109	-0.377
LAMTOR2	0.001135	-0.32041
C11orf68	0.001147	-0.31843
SQSTM1	0.001194	-0.39029
PIGT	0.001263	-0.25638
NRTN	0.001353	-0.74845
GYPC	0.001467	-0.25195
CKB	0.001634	-0.40248
ELN	0.001639	0.558139
ST3GAL4	0.001644	-0.68865
ANXA11	0.001677	-0.20158
PARK7	0.001698	-0.2137
ASIP	0.001734	-0.44131
SAT2	0.001785	-0.27437
FXR2	0.001807	-0.32765
ERP29	0.001823	-0.36148
C11orf31	0.001837	-0.51545
DAD1	0.001894	-0.25769
HTRA1	0.001916	-0.55285
MSRB1	0.001945	-0.47805
BRE	0.002095	-0.31542
VPS4A	0.002283	-0.26511
TERF2IP	0.002383	-0.38456
JOSD2	0.002388	-0.38476
TPRG1L	0.0024	-0.30609
CAMK2B	0.002571	-0.37192
SWI5	0.002661	-0.40895
EIF4B	0.002731	-0.25102
TMEM256	0.002757	-0.47367
LPL	0.003074	-0.52964
GSTP1	0.00341	-0.26256
COBL	0.003417	-0.36775
HIST1H1C	0.003543	-0.41015
ZNF204P	0.003762	-0.5165
GPS1	0.003858	-0.30609
SORBS1	0.00392	-0.11485
PIGQ	0.003927	-0.54206
NECAB3	0.003934	-0.24182
LSM10	0.003997	-0.27941
HRC	0.004002	-0.29343
UROD	0.004004	-0.33644
JUND	0.004008	-0.34378
TMEM14C	0.00412	-0.20294
TNIP2	0.004136	-0.43109
IK	0.004208	-0.28593
NKX2-5	0.004208	-0.2459
SGSM3	0.004221	-0.31954
DES	0.004376	-0.27321
NUPR1	0.004378	-0.71661
UQCR10	0.004388	-0.24074
ILVBL	0.004582	-0.26735
MIR4482	0.00467	-0.81714
ATP6AP1	0.004765	-0.30002
KARS	0.004848	-0.25315
GAPDH	0.004859	-0.14026
CYCS	0.004879	0.279535
PFDN5	0.004886	-0.22338
CHCHD2	0.00496	-0.21494
EIF3I	0.005083	-0.28683
NPTN	0.005114	0.209032
MYEOV2	0.005117	-0.34901
PABPC1	0.005194	-0.38188
CHPF	0.005284	-0.33398
SOD3	0.00539	-0.40206
SLC25A39	0.005428	-0.3899
LRP10	0.00543	-0.36537
PRKAG1	0.005935	-0.35304
MRPL28	0.005952	-0.24936
CERK	0.006085	-0.48008
PPP1R16A	0.006205	-0.37085
CSTB	0.00636	-0.39138
EXOSC1	0.006372	-0.39537
TMUB1	0.006399	-0.47745
TADA3	0.00641	-0.3553
MTA1	0.00647	-0.28772
VIPAS39	0.006582	-0.4012
CHMP2A	0.006599	-0.27158
LARP7	0.006649	-0.34372
SPARC	0.006824	0.610476
DDRGK1	0.006945	-0.42941
POLDIP2	0.006972	-0.14408
POLR2J	0.007028	-0.29525

HSPB1	0.00706	-0.58607
INPP5K	0.007167	-0.44067
SNRPD2	0.007275	-0.31241
ERI3	0.007414	-0.29734
GTF3C6	0.007485	-0.17151
TSPYL2	0.0075	-0.8597
ENO2	0.007665	-0.4759
SDC4	0.007675	-0.3726
POMP	0.007815	-0.23334
CIR1	0.007818	-0.37751
ANP32B	0.008025	-0.2556
SPR	0.008157	-0.57869
TRIM28	0.008165	-0.31917
WDR83OS	0.00831	-0.36759
DYNLL1	0.008446	-0.37751
PTGES3	0.008463	-0.34736
SAP18	0.008474	-0.1488
ALDH6A1	0.008789	-0.45957
RRAS2	0.008991	-0.4177
MXRA7	0.009181	-0.53303
PABPC4	0.009273	-0.26604
ATP6V0B	0.00929	-0.3209
GRHPR	0.0093	-0.20137
STX2	0.009303	-0.38346
PLEKHM2	0.009372	-0.27695
TMEM147	0.009384	-0.27193
FAM134B	0.009389	-0.44629
MRPL15	0.009423	-0.12168
IFT43	0.009442	-0.50101
MTRNR2L8	0.009458	-3.57542
RPS24	0.00946	-0.32826
VAMP2	0.00948	-0.16891
CCT3	0.00952	-0.41748
OTUD1	0.009595	-0.36497
LCMT1	0.009618	-0.23454
UFC1	0.009768	-0.23932
PSENEN	0.009805	-0.48937
C9orf78	0.009811	-0.32238
KIAA2013	0.009924	-0.26446
SPCS1	0.009987	-0.2743
PACS1	0.01	-0.26715
PSMB1	0.010017	-0.23548
LSM4	0.010025	-0.24831
NAP1L3	0.010078	-0.49295
TSG101	0.010191	-0.22809
CCT7	0.010264	-0.31043
TBC1D17	0.01028	-0.37313
SMARCC2	0.010316	-0.30411
GSTM4	0.010332	-0.26552
CCT4	0.01034	-0.25732
TMEM164	0.010365	-0.30622
ESF1	0.010457	-0.41539
COPA	0.010497	-0.26554
SNRPC	0.010573	-0.33658
AP2S1	0.010589	-0.31414
RNF181	0.01059	-0.26769
STAMBP	0.010618	-0.36705
CLU	0.010655	-1.00447
GCDH	0.010661	-0.34981
PCOLCE2	0.010665	-0.55002
POLRMT	0.010672	-0.42072
HHATL	0.010686	-0.32177
ZCRB1	0.010689	-0.27024
DPM3	0.01069	-0.37206
RNF20	0.010705	-0.28119
VPS28	0.010734	-0.21248
MLLT1	0.010817	-0.41122
TMEM127	0.010858	-0.19741
SLC25A5	0.010859	-0.5597
PLOD3	0.010886	-0.43705
GLUL	0.010959	-0.56715
GPC1	0.010965	-0.33923
POLD4	0.01097	-0.50326
GUK1	0.010998	-0.19952
TPT1	0.011014	-0.26429
FSTL3	0.011028	-0.41328
POLR2E	0.011031	-0.22606
ZNF688	0.011044	-0.42493
MYOF	0.011076	-0.39664
EI24	0.011102	-0.21384
IER5	0.011172	-0.51078
HOOK2	0.01119	-0.33956

C11orf24	0.011191	-0.33337
LAMTOR4	0.011205	-0.34185
PKIG	0.011212	-0.19222
PRDX1	0.01138	-0.42611
SDHAF1	0.011418	-0.31634
EIF3B	0.011534	-0.26048
RTFDC1	0.011569	-0.22657
C19orf43	0.011595	-0.22252
COPS6	0.01161	-0.16468
WBSCR16	0.01163	-0.24281
TCEAL4	0.011643	-0.23189
PCBP2	0.011658	-0.19845
YBX3	0.011689	-0.3657
PDAP1	0.01169	-0.25235
GDI1	0.011732	-0.28311
DKK3	0.011774	-0.74641
EIF3G	0.011847	-0.24517
NELFB	0.011884	-0.40404
TSR3	0.011897	-0.33253
C6orf1	0.011928	-0.50915
DBI	0.011937	-0.28167
RAB1B	0.011951	-0.173
IFT22	0.011969	-0.30612
PLEKHA6	0.011977	-0.42819
TTC38	0.01202	-0.61326
SLC27A6	0.012021	-0.72589
C1orf122	0.012048	-0.29349
SCYL1	0.012188	-0.2842
TTLL12	0.012313	-0.52602
TGM2	0.012428	-0.49285
TCEA3	0.012457	-0.33137
ARF5	0.012464	-0.25538
UCHL1	0.012504	-0.87673
CSNK2A2	0.012581	-0.34957
ACOT11	0.012581	-0.3613
PAIP2	0.012586	-0.25219
CTSF	0.012649	-0.60939
COMTD1	0.01268	-0.32352
MRPS21	0.012689	-0.26227
RTN2	0.012714	-0.31004
EFNA5	0.012737	-0.32865
EXOSC4	0.012762	-0.36018
ABTB1	0.012788	-0.46099
POP5	0.012837	-0.52448
RTCB	0.012912	-0.19915
ALDH4A1	0.012927	-0.53248
MRFAP1	0.01297	-0.12913
USP5	0.013017	-0.34138
CNBP	0.013039	-0.08732
ZER1	0.013115	-0.29479
EIF2S2	0.013166	-0.30553
PHLDA1	0.013169	-0.9679
GNAS	0.013184	-0.13999
COX14	0.013328	-0.25528
ATP6V1F	0.013414	-0.3454
ROGDI	0.01346	-0.27556
EIF2S3	0.013473	-0.27167
SCN1B	0.013482	-0.52847
RPS11	0.013484	-0.14012
MFAP4	0.013485	-0.36431
ULK1	0.013491	-0.38666
CHP1	0.013576	-0.30846
RALY	0.013578	-0.4703
NPPB	0.013588	-2.89857
RNF103	0.013768	-0.31533
SCAND1	0.013792	-0.35362
TST	0.013797	-0.72148
SYMPK	0.013798	-0.36044
PPCS	0.013805	-0.26008
ALDH1L1	0.013817	-0.42288
PAF1	0.013831	-0.23495
RABAC1	0.013844	-0.34446
ECHS1	0.013861	-0.25719
FAM58A	0.013924	-0.42815
SGTA	0.013971	-0.22424
RPS19BP1	0.013983	-0.40534
AGPAT2	0.014057	-0.30517
MRPL57	0.014129	-0.29881
SAMD1	0.014196	-0.44126
LSM7	0.014202	-0.56597
DYNLL2	0.014215	-0.20829
FASTK	0.014245	-0.27768

MAP3K3	0.014245	-0.35698
FXYD1	0.014267	-0.48232
EIF4A2	0.014294	-0.39294
LSM3	0.014327	-0.2158
EPDR1	0.014425	0.426137
HSF1	0.014428	-0.24261
POLR2G	0.014437	-0.31933
LYNX1	0.014458	-0.32746
C10orf76	0.014545	-0.37873
DNTTIP2	0.014579	-0.25529
NFE2L1	0.014752	-0.27819
MTURN	0.014763	-0.47446
KIAA1191	0.014774	-0.20948
PPP1R15A	0.014806	-0.32126
MB	0.014812	-0.22725
RPL36	0.014829	-0.21354
MTMR14	0.014979	-0.31443
NINJ1	0.014992	-0.43303
BOLA1	0.015013	-0.42337
CETN2	0.015106	-0.33188
CYB5R1	0.015145	-0.46927
ARF1	0.015199	-0.12529
RNPS1	0.015199	-0.29905
ST6GALNAC6	0.015234	-0.41203
ZBED5-AS1	0.015267	-0.6205
ST6GALNAC4	0.015328	-0.441
ATP6V1E1	0.015334	-0.24877
MRPL55	0.015397	-0.34849
CDK5	0.015408	-0.36628
EDNRB	0.015444	0.572002
MLIP	0.015451	-0.22347
TMEM120A	0.015642	-0.3858
CRCP	0.015655	-0.25161
CYSTM1	0.015682	-0.42572
FADS1	0.015691	-0.32319
CRELD1	0.015765	-0.57105
METRN	0.015824	-0.30801
UBXN1	0.015828	-0.37412
KCTD2	0.015842	-0.40662
LDHA	0.016036	-0.51813
CDKN2D	0.016106	-0.39297
MAF1	0.016223	-0.28331
FGF12	0.016281	0.915237
MIRLET7D	0.016287	-0.56492
SLC14A1	0.016378	0.566344
DRAP1	0.016476	-0.2622
GNG8	0.016495	1.058843
CAPN1	0.016533	-0.22307
UBC	0.016678	-0.49693
POLR1D	0.016683	-0.34645
EMC2	0.016794	-0.33008
ATRAID	0.016827	-0.33128
ELK1	0.016899	-0.34555
DGCR6L	0.016903	-0.3252
C12orf10	0.016919	-0.30345
HEPH	0.016989	-0.38567
TSSC4	0.017028	-0.41571
KLF15	0.017053	-0.70023
UBE2B	0.017103	-0.30749
DPP7	0.017114	-0.26966
MAFK	0.017121	-0.41121
PRDX6	0.017153	-0.41316
HINT2	0.017255	-0.35427
MBD3	0.017335	-0.31668
LIN52	0.017343	-0.40293
CFL1	0.017353	-0.2372
FBXW4	0.017386	-0.27573
HSPE1	0.017401	-0.62629
MAOA	0.017421	-0.29269
UBE2L3	0.017429	-0.31198
ADRM1	0.017531	-0.26227
SPTB	0.017546	-0.30281
HDGFRP2	0.017564	-0.29361
MRPS33	0.017572	-0.23304
CTNNBL1	0.017573	-0.32895
ITPA	0.017598	-0.54934
DDAH1	0.017604	-0.5688
RASL10B	0.017747	-0.60467
LYAR	0.017756	-0.50277
NEMF	0.017773	-0.28863
PPP1R1C	0.017784	0.517569
NHP2	0.017786	-0.26493

EIF1B	0.017796	-0.39273
RALBP1	0.017856	-0.26441
TCEAL3	0.017945	-0.35498
LRRC10	0.017955	-0.47799
DCAF11	0.017956	-0.23243
HMG20B	0.018001	-0.41925
ARL8A	0.018211	-0.16732
S100A13	0.018239	-0.37145
CCDC59	0.018244	-0.46895
NPPA	0.018249	-4.59767
ATG101	0.018275	-0.35859
PTMS	0.018308	-0.20457
TUSC2	0.018326	-0.24854
PCYT2	0.018328	-0.44157
ZC3H15	0.018443	-0.26553
ASNA1	0.018446	-0.22283
HSP90AA1	0.018487	-1.38355
DNAJB2	0.01849	-0.41515
BTF3	0.018499	-0.19986
RPLP2	0.018504	-0.20578
SRI	0.018627	-0.2971
KDELR1	0.018636	-0.36962
SLC25A38	0.018641	-0.43073
EIF5B	0.018641	-0.22733
DPM2	0.018683	-0.35311
TCEA2	0.018721	-0.38428
CTDSP1	0.018866	-0.26382
QSOX1	0.018983	-0.3826
CDC37	0.018999	-0.15495
RPS27A	0.019056	-0.32018
FNDC5	0.019081	0.420695
CALCRL	0.019111	0.604543
FHL2	0.01912	0.565827
BAD	0.019143	-0.29838
SBDS	0.019144	-0.10968
ASCC2	0.019171	-0.32559
ZSCAN18	0.019217	-0.29695
AHSA1	0.019274	-0.46542
RPL15	0.019279	-0.25243
BAMBI	0.019297	-0.4425
STMN1	0.01937	-0.58359
CES4A	0.019489	-0.70206
PPP1CA	0.019498	-0.34569
PSMB4	0.019554	-0.27062
EMC10	0.019562	-0.32654
DPH6-AS1	0.019774	-0.6062
GSTM3	0.019815	-0.53335
VWF	0.019926	0.704071
FKBP4	0.020063	-0.52346
ORMDL3	0.020082	-0.28424
C5orf15	0.020115	0.35937
SMG5	0.020116	-0.37037
DMWD	0.020142	-0.34524
C15orf65	0.020157	-0.40466
SND1	0.020159	-0.37093
NAP1L1	0.020236	-0.3132
PSMC5	0.020254	-0.27883
NT5M	0.020328	-0.38042
NPM1	0.020339	-0.26878
CD300LG	0.020405	0.770143
FBXO32	0.020543	-0.51296
ZNHIT1	0.020717	-0.31106
PLEKHA4	0.020773	-0.49707
APLP1	0.020786	-0.49427
DCBLD2	0.020852	-0.2775
NDUFS1	0.020927	0.309691
CD59	0.020933	-0.26825
OAZ1	0.021006	-0.13158
RNPEPL1	0.021057	-0.22856
ANAPC11	0.021095	-0.22134
POR	0.02111	-0.51248
SMYD1	0.021132	0.293732
FAM195A	0.021138	-0.35168
HFE2	0.021178	-0.41659
DBNL	0.021185	-0.43991
LINC01137	0.021186	-0.48382
COL4A3BP	0.021196	-0.30889
RRAGA	0.021263	-0.18647
UBE2Z	0.021294	-0.22151
RBM10	0.021521	-0.33803
SAE1	0.021552	-0.31922
GDI2	0.021604	-0.26871

B4GALNT3	0.021696	-0.43816
SNRPA	0.021733	-0.32029
UNC45B	0.021746	-0.90511
PACRG	0.021758	-0.45468
SLU7	0.021769	-0.29272
JAGN1	0.021776	-0.32502
HIST1H2BD	0.022086	-0.44462
SET	0.022102	-0.25376
HAX1	0.022118	-0.1331
MAPRE2	0.022163	-0.31408
SMTN	0.022189	0.264174
PRDX3	0.022218	0.14066
ITPKB	0.022309	0.683888
CTNNAL1	0.022452	-0.59542
PROS1	0.022481	-0.63447
FAM3A	0.022545	-0.42221
PLK2	0.022569	-0.74157
LSM1	0.022598	-0.27895
SERPINB6	0.022689	-0.2639
SOX12	0.022776	-0.4053
PTDSS1	0.022819	0.495418
RPL18	0.022836	-0.28869
RPL19	0.022951	-0.16645
CWC15	0.02303	-0.26389
IGFBP7	0.023042	-0.36395
COL23A1	0.023043	-0.75928
SURF1	0.023068	-0.25652
SKP1	0.023151	-0.16183
CYHR1	0.023158	-0.37718
CNPPD1	0.023171	-0.30237
SEC61G	0.02318	-0.29678
GTF2F1	0.02322	-0.22978
TRAPPC1	0.023272	-0.26542
UCK1	0.023313	-0.38595
HMCES	0.023375	-0.21037
TP53I13	0.023406	-0.36419
HSPBP1	0.02344	-0.32118
PDK4	0.023484	-1.19085
C11orf74	0.023496	-0.33449
AMZ2	0.023585	-0.35328
PYGM	0.023586	0.297264
TUBB6	0.023596	0.430748
RPS4X	0.023605	-0.17722
HSP90AB1	0.02364	-0.5772
CTSH	0.02375	0.322121
COX6A1	0.023755	-0.30993
HGS	0.023923	-0.45271
NENF	0.023928	-0.31267
PKN1	0.023964	-0.29225
TAF7	0.023997	-0.24279
COL15A1	0.024047	0.861246
MRPL14	0.024102	-0.28668
ITFG3	0.024142	-0.27646
PSMC3	0.024173	-0.23743
EEF1B2	0.024322	-0.25242
PLA2G15	0.024427	-0.42828
RPL36AL	0.024495	-0.21821
ERH	0.024512	-0.27679
SHB	0.024556	-0.38377
AAMP	0.024565	-0.32935
TBX20	0.0246	0.935813
MFGE8	0.02466	-0.42171
RP9	0.024743	-0.31803
NOL7	0.024744	-0.24137
DMPK	0.024775	-0.41788
C16orf13	0.024814	-0.29099
GSTO1	0.024931	-0.25031
FIS1	0.024969	-0.28059
ZFAND5	0.024971	-0.25691
C3	0.025013	0.990502
LRRC20	0.025057	-0.2855
SF3B6	0.025115	-0.34123
HINT1	0.025154	-0.21309
SLC27A1	0.025159	-0.45903
ZNF622	0.025306	-0.34891
DSP	0.025423	0.169735
FAM127B	0.025447	-0.29674
OST4	0.025479	-0.14268
DTNBP1	0.025485	-0.3453
C5orf46	0.025592	-0.63812
GRN	0.025626	-0.33901
CLTB	0.025627	-0.31529

SSR4	0.02579	-0.3286
LTBP3	0.025806	-0.31484
SEC14L5	0.025826	1.203995
BCAT2	0.025828	-0.39913
GAS6	0.025831	-0.27298
SPRYD3	0.025875	-0.23889
IQSEC1	0.025878	0.472077
MLYCD	0.025974	-0.39841
NSFL1C	0.026126	-0.27258
RRP12	0.026194	-0.50065
EMC3	0.026352	-0.39285
RPS12	0.026385	0.178465
NME3	0.026409	-0.42944
XIRP2	0.026453	0.508832
RAB13	0.026459	-0.35692
TNIP1	0.026482	-0.34038
PA2G4	0.026486	-0.26629
ERGIC3	0.026502	-0.27067
MPST	0.026537	-0.49941
GPR137B	0.026581	-0.33007
CHST9	0.026745	0.537514
HIPK3	0.026941	0.347339
CTSA	0.02735	-0.22709
SLITRK4	0.027366	-0.72626
WIPI2	0.027404	-0.24828
SARS	0.027439	-0.21692
ST3GAL3	0.027532	-0.29576
SYNJ2BP	0.027682	0.275491
APLN	0.027729	0.4261
INSR	0.027943	-0.25008
PMP22	0.027949	-0.25453
RPL24	0.028027	-0.20131
EIF2B4	0.028117	-0.29439
GMPR	0.028127	-0.12988
HCFC1R1	0.028189	-0.26988
POPDC2	0.028197	-0.24067
GPR137	0.028202	-0.33936
ISCU	0.028242	-0.13404
DNAJA1	0.028375	-0.3996
BUD31	0.028401	-0.3016
ZNF444	0.028468	-0.32209
MAP1LC3A	0.028534	-0.23328
UQCR11	0.028558	-0.20712
THBS1	0.028597	-0.52502
NUTF2	0.028654	-0.22124
KIF1B	0.028657	0.307622
OSER1-AS1	0.028788	-0.39574
RPS27	0.028815	-0.3501
COMMD6	0.028834	-0.28021
METTL5	0.028893	-0.34246
CBX7	0.028918	-0.1791
SUMO1	0.029073	-0.2358
CBR1	0.029114	-0.35687
MGLL	0.029221	0.557831
TSPAN15	0.029257	0.632717
TJP2	0.029268	-0.2175
NAA10	0.029307	-0.28236
FAM180A	0.029324	-0.92246
COMMD7	0.029367	-0.32804
RNF126	0.029394	-0.40166
FBL	0.029427	-0.22109
TIMM17B	0.029525	-0.22288
YPEL2	0.029564	-0.29997
MOB2	0.029577	-0.35481
AGTRAP	0.029608	-0.43219
SURF2	0.029614	-0.3161
SSNA1	0.029669	-0.15168
BCL7C	0.029712	-0.26555
FABP3	0.029774	-0.24525
AGPAT9	0.029837	-0.47228
HSPB2	0.029863	-0.26549
TEAD1	0.029968	0.289096
FIBP	0.030052	-0.27112
COA3	0.030084	-0.24036
JTB	0.030102	-0.29281
TOM1	0.030337	-0.40531
FAM228B	0.030479	-0.44692
SLC38A10	0.030654	-0.31889
GSS	0.030691	-0.32203
CCDC167	0.030783	-0.27559
WDR45	0.030806	-0.38495
PRMT5	0.030842	-0.30563

APEX1	0.030872	-0.26722
UBA52	0.030973	-0.18546
ALDH1L1-AS2	0.031011	-0.56135
RUVBL1	0.031159	-0.31242
PXDNL	0.031173	-0.58521
HIF3A	0.031215	-0.36726
LPAR5	0.031229	0.49944
MKRN1	0.03124	-0.2462
SUGT1	0.031268	-0.3227
CEBPB	0.031278	-0.46473
PSMD13	0.03144	-0.16577
STX8	0.031652	-0.26619
CLSTN1	0.031657	-0.17756
SRP14	0.031665	-0.16348
GATA6-AS1	0.031717	-0.23575
MTCH1	0.031753	-0.44486
ADO	0.0318	-0.25563
ACOT9	0.031855	-0.18189
CYB5D2	0.031951	-0.5814
RPL26	0.031971	-0.14777
RUVBL2	0.032053	-0.37922
NEAT1	0.032055	-0.35596
SPATA24	0.032056	-0.31896
CHN1	0.032057	-0.34155
POLR2L	0.032057	-0.26405
KANK2	0.032067	-0.32401
TUFM	0.032069	-0.14371
TMEM258	0.032069	-0.24075
SSBP1	0.032073	-0.28029
PSMA5	0.032107	-0.22166
PERM1	0.03213	-0.24044
WISP2	0.032136	-0.61489
TYRP1	0.032138	-0.2615
ABCF2	0.03214	-0.29159
AP2A1	0.032148	-0.27227
OARD1	0.032151	-0.30922
CD55	0.032166	-0.25869
COPE	0.03217	-0.26005
ABHD11	0.032183	-0.29422
SLC25A29	0.032238	-0.36921
TIMMDC1	0.032249	-0.15166
RPL13	0.03225	-0.25975
VPS45	0.032287	-0.23252
ARHGAP24	0.032372	-0.44656
PPP2R4	0.032413	-0.24363
ITGA6	0.032435	0.499611
P4HB	0.032444	-0.27061
RPL34	0.032458	-0.19978
TOMM40	0.032473	-0.27085
CCNB1IP1	0.032583	-0.20411
TOMM7	0.032642	-0.18831
PHLDA3	0.032697	-0.31311
SEMA5A	0.0327	-0.35377
IFI6	0.032703	-0.34789
ISG15	0.032719	-0.4353
DDX54	0.032735	-0.27439
CDKN2AIPNL	0.032748	-0.25254
CIZ1	0.032753	-0.25381
SYF2	0.032798	-0.3305
TAF10	0.032805	-0.27692
CNN2	0.032806	-0.23453
PES1	0.032812	-0.34474
APLP2	0.032846	-0.21945
WDTC1	0.032879	-0.24767
GPIHBP1	0.032929	0.716162
SLC2A4RG	0.032933	-0.31134
ADIPOR1	0.032961	-0.19009
NSMCE2	0.033041	-0.2607
ANTXR2	0.033088	-0.23948
TXN	0.033112	-0.32177
HAGH	0.033144	-0.26948
CERS4	0.03322	-0.42398
CCDC107	0.033226	-0.28906
THYN1	0.033229	-0.26346
RPL28	0.033283	-0.21538
ZNF394	0.033332	-0.30539
ARHGAP10	0.033369	-0.2098
TUBA8	0.033375	0.687207
GSTT1	0.033376	-1.14097
UBA1	0.033394	-0.17864
MAP7D1	0.033484	-0.17939

TMEM106C	0.033492	-0.33189
NSA2	0.033509	-0.61507
PHB	0.033533	-0.1705
GABARAP	0.033543	-0.27524
RAI2	0.033563	-0.27666
ZC3H13	0.03359	-0.24509
IPO13	0.033605	-0.19624
RHOBTB1	0.033645	-0.34881
MORN4	0.033678	-0.41256
ZRSR2	0.03368	-0.30277
FKBP2	0.03378	-0.28402
IMP4	0.033791	-0.2654
CD320	0.033797	-0.39382
CEP85	0.033799	-0.35432
NDUFA2	0.033836	-0.21085
EIF3D	0.033886	-0.21668
NUDT16P1	0.033931	-0.35165
PNMA1	0.033934	-0.2806
TAF1D	0.033934	-0.33269
NFIC	0.033942	-0.21991
BCAP31	0.03395	-0.25814
ADCY5	0.033955	-0.22636
ARMCX2	0.033972	-0.35739
SF3A2	0.033972	-0.25171
MT1E	0.03398	-0.37435
TIMM9	0.033989	-0.24866
FLNC	0.033991	-0.29921
COG4	0.034012	-0.28871
ZMAT2	0.034018	-0.25549
TMEM219	0.034024	-0.2405
MRPL40	0.034028	-0.18299
FTSJ3	0.034082	-0.32143
TNPO3	0.034111	-0.24098
ARHGAP1	0.034159	-0.2206
C1orf35	0.034189	-0.29119
BRMS1	0.034189	-0.35444
FAM177A1	0.03419	-0.3486
TMEM109	0.034242	-0.1514
TTF1	0.034247	-0.28503
ARFRP1	0.034255	-0.22561
CBY1	0.034258	-0.33169
AAGAB	0.034268	-0.27342
EFTUD2	0.03428	-0.28831
ENKD1	0.03433	-0.45241
STK40	0.034331	-0.38054
SVOP	0.034337	-1.06419
CREG1	0.034368	-0.14789
TMEM44-AS1	0.034374	-0.45809
DEDD2	0.034377	-0.26013
IL11RA	0.034381	-0.34646
BOP1	0.034388	-0.33889
NABP2	0.034394	-0.30164
PSMB6	0.034398	-0.10589
RPP25L	0.034401	-0.25943
PTRF	0.03446	-0.13256
MAP2K7	0.034484	-0.2147
MYH7	0.034499	-0.14756
PIK3IP1	0.034509	-0.51557
MAGED2	0.034542	-0.24398
GPAA1	0.034604	-0.189
OXLD1	0.034606	-0.33125
MARK4	0.034611	-0.33795
CUEDC2	0.034613	-0.16919
ATG14	0.034698	-0.24888
SF3B2	0.034737	-0.2289
COPG1	0.034749	-0.16548
TBCA	0.034805	-0.26488
COMMD1	0.034815	-0.15443
GADD45B	0.034827	-0.49784
SHISA4	0.034849	-0.19029
CRNDE	0.034849	-0.52827
AHCY	0.03485	-0.3178
RBX1	0.034867	-0.22541
RPL10A	0.034873	-0.17068
ODF2	0.034886	-0.31579
NFKBIB	0.034893	-0.38029
HACL1	0.034896	-0.35284
IFT46	0.034921	-0.31926
ARID5B	0.03493	-0.36754
ANKH	0.034957	-0.25857
JMJD8	0.034976	-0.31651
PGK1	0.03498	-0.09618

RHEB	0.034982	-0.29912
BRSK1	0.034994	-0.3673
THOC5	0.03501	-0.39403
RBMS3-AS3	0.035034	-0.51495
ZNF524	0.035041	-0.33402
KPNB1	0.035045	-0.20564
WDR18	0.035078	-0.42631
ANKZF1	0.035082	-0.27192
UBAC2	0.035092	-0.2381
SUPV3L1	0.035109	-0.2505
CALCOCO1	0.035111	-0.21693
CTDNEP1	0.035115	-0.17151
EMC9	0.035121	-0.27157
RNF26	0.035136	-0.31242
ATXN10	0.035143	-0.19459
NDRG2	0.035152	-0.14695
NCL	0.035189	-0.18666
SCCPDH	0.03519	-0.20731
GLTP	0.035217	-0.27896
NUBP2	0.035226	-0.28845
ORAI3	0.035237	-0.41031
NAB2	0.03527	-0.35302
AIP	0.035335	-0.39889
TBL3	0.035351	-0.32247
BABAM1	0.03536	-0.21146
UBALD1	0.035361	-0.30137
UBE2Q2	0.035361	-0.21968
TWF2	0.035362	-0.32439
GNB2	0.035362	-0.28174
FLOT2	0.035363	-0.24019
ANKRD1	0.035363	-0.60096
CTIF	0.035364	-0.34031
CEBPZ	0.03537	-0.25298
CWC27	0.035398	-0.25741
CD99L2	0.03543	-0.21221
MPG	0.035503	-0.28327
RRP9	0.035529	-0.36141
RORC	0.035537	-0.43576
UBE2T	0.035552	-0.44856
LRP3	0.03561	-0.24281
RIOK3	0.035647	-0.24306

ABAT	0.035648	-0.43632
RPL37	0.035649	-0.15853
SDF2L1	0.035695	-0.39462
USP11	0.035701	-0.32699
LAMTOR1	0.035708	-0.17128
C14orf1	0.035729	-0.27531
CEBPD	0.035732	-0.49284
FAU	0.035748	-0.15049
RPL39	0.035752	-0.28673
DYNC1LI1	0.035781	-0.15102
RPL23A	0.03584	-0.22563
BTBD2	0.03585	-0.38041
C11orf73	0.035856	-0.24875
GTF2F2	0.035857	-0.24101
COMMD9	0.035885	-0.29688
RAD23A	0.035914	-0.15544
PRPF19	0.035933	-0.16993
PLBD1	0.03597	-0.24267
RPUSD3	0.035973	-0.24711
DVL1	0.036015	-0.20339
POLR3GL	0.036017	-0.2946
COPS3	0.036025	-0.17417
NONO	0.036063	-0.20707
AP2M1	0.036118	-0.21351
SNRPB2	0.036128	-0.2526
TMEM203	0.036133	-0.17728
H1FX	0.036183	-0.38973
TXNRD1	0.036189	-0.49065
ZDHHC2	0.036191	-0.26944
SCAF1	0.036192	-0.17292
NOP16	0.036193	-0.36398
C1orf226	0.036197	-0.34229
GOLGA2	0.036199	-0.19635
EDEM2	0.0362	-0.33971
GLE1	0.036204	-0.26479
HARS	0.036207	-0.25595
CTSB	0.03621	-0.22159
FBXL15	0.036216	-0.30803
PKD1	0.036223	-0.22321
ABHD8	0.036223	-0.27618
NCBP2-AS2	0.03623	-0.20476

SNCA	0.036233	-0.48798
PDK2	0.036234	-0.23697
XIRP1	0.036235	-0.31783
CDKN1B	0.036237	-0.28838
MMGT1	0.036237	-0.2194
MAX	0.036242	-0.33015
FAM96B	0.036243	-0.2586
ELOF1	0.036243	-0.2683
BANF1	0.036243	-0.31316
TNK2	0.036253	-0.31504
CALR	0.036253	-0.20634
TMUB2	0.036254	-0.2077
ARHGAP5-AS1	0.036256	-0.36162
PRAF2	0.036294	-0.33803
CDK4	0.036296	-0.23838
TCP1	0.036297	-0.2326
COMMD3	0.036309	-0.26026
RNF167	0.036315	-0.18438
DNAJC6	0.036332	0.473468
LAPTM4A	0.036384	-0.09958
CAMK2G	0.036408	-0.30398
MEAF6	0.036434	-0.25225
ARPC4	0.036517	-0.35209
PPID	0.036546	-0.3233
RFXANK	0.036547	-0.26278
COX7A2L	0.036559	-0.23144
AKR7A2	0.036639	-0.26411
PDCD5	0.036652	-0.18871
MKNK2	0.036684	-0.56656
MIF4GD	0.036688	-0.34444
PREB	0.036703	-0.20891
SNAP47	0.036703	-0.44979
SHMT2	0.036704	-0.29907
PFDN2	0.036764	-0.18553
HIGD2A	0.036793	-0.1969
A4GALT	0.036802	-0.21474
SYNPO	0.036819	-0.12529
PKDCC	0.036829	-0.50866
TP53TG1	0.036838	-0.28175
EIF1	0.03684	-0.22448
UGT2B4	0.036872	0.96781
AES	0.036878	-0.12894
TRAM1	0.036889	0.303004
NOL3	0.036899	-0.28388
OGFR	0.036914	-0.28894
NCAM1	0.036984	-0.17442
LYSMD1	0.036994	-0.34905
TOX4	0.037001	-0.21988
PPP2R5B	0.037015	-0.27286
NOC2L	0.037018	-0.2637
ABHD4	0.037021	-0.32842
WBSCR22	0.037038	-0.22916
CCND2	0.037071	-0.33213
C19orf24	0.037155	-0.44343
MARK2	0.037193	-0.19623
NUDT16L1	0.037198	-0.1828
LMAN2	0.037204	-0.24025
HTATSF1	0.037221	-0.17907
CDK5RAP3	0.037227	-0.30484
CRIP2	0.037283	-0.31158
ABHD12	0.037286	-0.27832
PLIN4	0.037297	-0.34226
MRFAP1L1	0.037329	-0.19483
VPS51	0.037355	-0.19631
FGFRL1	0.037363	-0.32622
BCL7B	0.037446	-0.21312
TPD52L2	0.037452	-0.23359
YPEL1	0.037534	-0.31246
MYLK3	0.037545	-0.29417
RBCK1	0.037584	-0.32562
MLF2	0.037649	-0.16014
ELP3	0.037705	-0.21595
UBB	0.037717	-0.19496
NDUFB2	0.037727	0.167528
XAB2	0.037745	-0.24261
NDUFA1	0.037752	-0.23606
RAB20	0.037768	-0.38825
ILKAP	0.037808	-0.28373
LRRC47	0.037826	-0.14233
LDB3	0.037827	-0.19309
MEA1	0.037845	-0.29351

VPS16	0.037848	-0.33445
KLHL21	0.03786	-0.30959
FMOD	0.03788	-0.66788
HSPD1	0.037896	-0.40253
ITPRIP	0.037923	-0.39424
ATOX1	0.037927	-0.25732
CD2BP2	0.037935	-0.21861
CTSL	0.037947	-0.16436
EPN2	0.037971	-0.25437
CCDC53	0.037993	-0.44427
TMEM160	0.037993	-0.30858
GPX3	0.037995	-0.28328
RSL1D1	0.038042	-0.19426
GRINA	0.03811	-0.182
PRKCSH	0.038133	-0.19147
RPL11	0.038158	-0.12005
GPR22	0.038161	0.72637
NKIRAS2	0.03819	-0.21491
FAM98C	0.038198	-0.29988
LAD1	0.038212	-0.70958
SLC25A34	0.038229	-0.6356
RP11-451G4.2	0.038241	-0.6335
VPS72	0.038241	-0.28147
TSC22D4	0.038241	-0.19438
ITGB1BP1	0.038246	-0.3411
POLR2K	0.038276	-0.25759
ADAM9	0.038311	0.324659
SLCO2A1	0.038314	-0.40719
PHC2	0.038315	-0.25133
YIPF3	0.038328	-0.23518
TCEB2	0.038371	-0.26271
C1orf115	0.038375	0.560171
NUDT16	0.038384	-0.31382
MIR126	0.038384	0.588636
PTOV1	0.038386	-0.40275
CDC16	0.038389	-0.20721
MAPKAPK5-AS1	0.038403	-0.26467
LMBRD2	0.03841	0.45269
RPS19	0.038423	-0.36706
FTH1	0.038454	-0.27768
PDZD2	0.038455	0.357551
SART1	0.038459	-0.25815
TMEM129	0.038468	-0.20959
DCTN2	0.038477	-0.18366
DGUOK	0.038496	-0.31123
CYB5R3	0.038505	-0.22288
ARVCF	0.038517	-0.3541
UBALD2	0.038531	-0.32891
GSK3A	0.03855	-0.23396
CDKN1A	0.03855	-0.3932
CCS	0.038581	-0.2738
TNS1	0.038613	-0.19777
MAP2K3	0.038615	-0.31403
ACOX2	0.038629	-0.31187
RPL8	0.038643	-0.1336
PMM1	0.038654	-0.44972
EHD3	0.038657	-0.41696
TIMM10	0.038672	-0.32651
MIR5690	0.038673	-1.01813
MRPL51	0.038675	-0.1205
H2AFX	0.038681	-0.23258
CCDC9	0.038686	-0.31105
AP3D1	0.038688	-0.23903
EGLN3	0.038702	-0.36243
SMPD1	0.038714	-0.20845
GKAP1	0.038723	-0.33471
IDH1-AS1	0.038727	-0.43623
SERGEF	0.03873	-0.32063
SETD3	0.038731	-0.20027
C1QTNF1	0.038739	-0.5785
TMA7	0.038743	-0.29814
MAD2L2	0.038743	-0.41339
PLD3	0.038744	-0.22871
DDOST	0.038749	-0.14211
RPF1	0.038758	-0.20963
POLE4	0.038764	-0.30762
C19orf70	0.038769	-0.26739
CCM2	0.038772	-0.27933
CTF1	0.038807	-0.37463
NAT14	0.038835	-0.45773
NDUFAB1	0.038846	0.249002

DCAKD	0.038868	-0.26436
DNAJC21	0.038868	-0.26833
EIF3H	0.038869	-0.12197
RNF208	0.038875	-0.21658
RPS27L	0.038886	-0.45338
RABGGTB	0.038889	-0.29911
CDK18	0.038997	-0.20614
EEF1A1	0.039115	-0.29709
ATP5J2	0.039351	0.152296
MTSS1	0.039649	0.405886
PFKFB2	0.03972	-0.50091
CD248	0.039828	0.682005
COMP	0.039889	-0.84929
UTRN	0.039902	0.391413
SYNE1	0.039974	0.420362
NDUFA11	0.040079	-0.27112
XPR1	0.040079	-0.40453
PKIA	0.040133	0.190573
DUSP23	0.040206	-0.3803
ARPC2	0.04023	-0.18688
IVNS1ABP	0.040303	-0.50274
ZMYND19	0.040303	-0.32232
AKT1S1	0.040327	-0.30619
APOPT1	0.040328	-0.31231
MANBAL	0.040437	-0.31077
HIST3H2A	0.040552	-0.39049
SNAP29	0.040615	-0.26867
NCEH1	0.040649	0.47032
TIMP3	0.040691	0.458962
TUBB4B	0.040782	0.721508
HMGN4	0.04093	-0.21951
AQP7	0.040948	-0.33909
TXN2	0.040982	-0.2091
NR1H2	0.041104	-0.33779
JAM3	0.0412	-0.45255
TSR2	0.04123	-0.23005
MAP7D3	0.041242	-0.3786
P4HTM	0.04128	-0.23929
SH3BGR	0.041381	-1.03842
ETNPPL	0.041395	0.520276
HMGA1	0.041419	-0.19421
CHMP1A	0.04147	-0.3999
MIIP	0.041477	-0.58435
MT1X	0.041477	-0.82048
EML1	0.041581	0.398453
OPA1	0.041586	0.179787
TAOK1	0.041596	0.273087
TMEM261	0.04169	-0.23682
KLHL31	0.041734	0.331983
EXOSC5	0.04175	-0.33487
TFRC	0.041854	1.359095
MAN2C1	0.042233	-0.27072
ZNF41	0.042259	0.340503
ABCA8	0.042578	0.648874
FRA10AC1	0.042611	-0.32812
RBPMS	0.042622	-0.19739
SPC24	0.042623	-0.42661
CLNS1A	0.042626	-0.14629
PTGR2	0.042626	-0.24052
GALNT18	0.042629	-0.27594
KRI1	0.04263	-0.3348
NAPA	0.042632	-0.1559
C18orf8	0.042648	-0.32397
ARHGEF17	0.042658	-0.2543
NUCB2	0.04266	-0.22229
SNX17	0.042689	-0.24286
VPS35	0.042693	-0.16446
LINC00847	0.042694	-0.30445
RTF1	0.042714	-0.15155
GRK6	0.042721	-0.27522
ASUN	0.042725	-0.21673
TMEM141	0.042731	-0.18739
UBE2MP1	0.042739	-0.20882
PFN1	0.042746	-0.18697
BSDC1	0.042749	-0.16824
SNHG8	0.042777	-0.34416
R3HDM4	0.042781	-0.20931
TSPAN17	0.042792	-0.26126
PAFAH1B1	0.042805	0.142887
OSGIN1	0.042848	-0.45382
KLHDC8B	0.042867	-0.18668
VEGFB	0.042867	-0.20507

KCND3	0.04292	0.403417
ITGB1	0.042933	0.292811
4-Sep	0.042957	-0.21332
MIEN1	0.04298	-0.21318
C7orf26	0.042984	-0.21517
TM4SF1	0.04299	0.367067
EMILIN3	0.042993	0.743265
FAM127A	0.043012	-0.13189
GPR153	0.043028	-0.68191
PTS	0.043102	-0.26375
LOH12CR1	0.043119	-0.26707
CAST	0.043171	-0.1509
POSTN	0.043196	-0.71602
MAP3K10	0.043217	-0.28638
NSRP1	0.043228	-0.22539
ADAMTS15	0.043257	0.546947
TAF3	0.043265	-0.23352
TCOF1	0.043275	-0.24971
PPM1G	0.043291	-0.18035
STRA13	0.043304	-0.34545
GARS	0.043332	-0.16787
DHX29	0.043332	-0.19836
RBM24	0.043341	-0.24186
EML2	0.043345	-0.2887
IRX3	0.043472	-0.40778
ZNF579	0.043485	-0.24029
IRS2	0.043535	-0.44685
PRDX5	0.043545	-0.12374
ORC3	0.043559	-0.17899
F3	0.043564	-0.26721
LSAMP	0.04362	0.662075
ANKRD12	0.043635	-0.22516
MIR6748	0.043642	0.576951
BCCIP	0.043651	-0.23845
RXRG	0.043663	-0.43099
EXOSC7	0.04368	-0.31322
OTUB1	0.043746	-0.18332
YIF1B	0.043766	-0.26359
ADCK3	0.043788	-0.32058
MRPS26	0.043817	-0.16512
MRPS15	0.043821	-0.13981

ZNF274	0.043824	-0.22026
PPIG	0.043832	-0.1633
GLG1	0.043851	-0.1679
FOXN3-AS1	0.043859	-0.3671
TMOD1	0.043875	-0.12936
PSME1	0.044005	-0.18707
ATP5G1	0.044025	0.252811
CCT8	0.044075	-0.23011
SSRP1	0.044078	-0.22359
DNAJB1	0.044088	-0.19553
POLR1E	0.04409	-0.2488
OGDH	0.044109	0.164603
KIAA1462	0.044113	0.656201
C19orf54	0.044118	-0.37015
VPS13D	0.044122	0.260475
FIGF	0.044151	0.53526
SHARPIN	0.044177	-0.1874
RPS13	0.044187	-0.11095
PPP2R3C	0.044233	-0.25372
LPAR3	0.044328	0.474278
DDB1	0.044389	-0.12906
IFITM1	0.044422	-0.27235
SOBP	0.044503	-0.25994
AZIN1	0.044509	-0.23306
MYPOP	0.044571	-0.19777
PPP1R3G	0.044642	-0.36934
IGBP1	0.04468	-0.181
GOLGB1	0.044739	-0.23189
LONP1	0.044766	-0.2357
SLC12A4	0.044854	-0.21426
PPP4C	0.044869	-0.26589
PDE6D	0.044909	-0.30053
ENO1	0.045018	0.368078
CBX3	0.045028	-0.23295
CYGB	0.045147	0.484722
PTTG1IP	0.045153	-0.14804
EEF1G	0.045169	-0.23034
C11orf96	0.045204	-0.28625
DHPS	0.045206	-0.17092
PGLS	0.045295	-0.31026
SMAP1	0.045427	-0.21296

TMEM245	0.045476	0.238885
CDPF1	0.045552	-0.27819
TRAPPC6A	0.04559	-0.32744
TBC1D22A	0.045678	-0.22663
URM1	0.045749	-0.23648
PPP1R35	0.04587	-0.43023
DNAJA4	0.045952	-0.73967
MFSD6	0.045963	0.455339
KAT2B	0.045965	0.276942
YWHAB	0.046168	-0.09964
RAPGEF2	0.046195	0.348173
FGFBP2	0.046198	0.626356
ST3GAL6	0.046284	-0.24462
TAF11	0.046295	-0.24922
TRPC4AP	0.046408	-0.20512
TRDN	0.046461	-0.15193
TMEM71	0.046493	-0.33857
TMED9	0.046493	-0.23333
ALDH7A1	0.046532	-0.28075
CSNK1E	0.046613	-0.19763
RPPH1	0.046663	-0.44324
ARL3	0.046702	-0.227
ATP6V1H	0.046822	-0.20221
RSG1	0.046887	-0.35664
MAP3K7CL	0.046917	-0.50744
NT5C1A	0.046935	0.656828
NAA20	0.046991	-0.14086
STARD10	0.047049	-0.29455
CRYAB	0.047064	-0.4513
C22orf39	0.047064	-0.22494
ATP13A3	0.047239	-0.30394
SCARNA7	0.047274	-0.32296
INTS10	0.047293	-0.23943
SAFB	0.047321	-0.19663
EEFSEC	0.047366	-0.33974
FBXW11	0.047424	-0.19659
KLC2	0.047432	-0.27713
CREB3L2	0.047452	0.320287
GNPAT	0.047476	-0.14615
SGCG	0.047528	-0.22029
BNIP3	0.047535	-0.15576
ETV1	0.047575	-0.34829
PAX8-AS1	0.047598	0.515569
CTNNA3	0.047603	0.420902
TLR4	0.047667	0.507093
C1orf43	0.047679	-0.14213
EHBP1L1	0.047699	-0.22378
UBE3A	0.047775	-0.14015
CDH5	0.047911	0.7136
SLC16A1	0.047959	0.342604
ZNF667-AS1	0.047976	-0.3176
PRKAR2B	0.048108	-0.28691
ELK3	0.048157	0.621871
AIF1L	0.04817	0.760357
MYCT1	0.048203	0.49137
APRT	0.048238	-0.26923
NEDD8	0.048326	-0.23093
ZNF404	0.048442	-0.30295
RPA1	0.048614	-0.28105
APOOL	0.048967	0.380361
NT5C	0.049081	-0.24269
LINC00957	0.049119	-0.32978
HDDC2	0.04915	-0.26761
HLA-B	0.049228	0.583581
SHISA3	0.049266	0.929802
TNNI1	0.049448	0.738987
MTHFD1	0.049485	-0.20469
NDUFS5	0.049485	-0.15074
GLTSCR2	0.049597	-0.1596
NMT1	0.049633	-0.13706
VPS4B	0.049698	0.267645
QTRT1	0.049764	-0.27948
ELOVL2	0.049783	0.395433
CAMK2A	0.049788	-0.25057
APP	0.04983	0.252107
NEIL2	0.049882	-0.37047
PPAP2B	0.049882	0.270841
GSR	0.049948	-0.21135
IL6ST	0.049957	0.330776
ALYREF	0.049987	-0.2162

Supplemental Table 4. DEG in obese samples when comparing NF to LVH, (p_adj < 0.05)

GeneName	p_adj	log2FC
HMGCS2	0	-1.52337
NUPR1	0	-0.84992
MLYCD	0	-0.63952
SEC14L5	0	1.368913
PCDH7	0	1.017951
PLIN2	0	-1.26669
TINAGL1	0	-0.45178
PDHB	0	0.283917
SUCLA2	0	0.381001
NDUFS1	0	0.45615
ACADM	0	0.311292
DLD	0	0.313703
CLIC5	0	0.403322
NDUFS2	0	0.220307
RGS5	0	0.517071
GPNMB	0	0.917826
MYL4	0	1.223488
FAM129A	0	0.530084
UBC	0	-0.78413
ACADVL	0	-0.20461
NEXN	0	-0.36827
IDH2	0	0.329235
RYR2	0	0.722121
MYL7	0	1.550622
AGT	2.00E-15	0.45158
PDK4	4.00E-15	-2.80167
TAF7	4.00E-15	-0.35599
CDKN1A	6.99E-15	-0.78787
SLC25A34	1.40E-14	-1.2642
NPPA	1.40E-14	-4.02274
GADD45G	1.60E-14	-0.97254
TRIM63	2.20E-14	-0.55388
CTSD	4.60E-14	-0.4451
AZGP1	1.46E-13	-1.21571
CEBPB	5.28E-09	-0.61231
POSTN	5.92E-09	-1.06062
PLVAP	7.69E-08	-1.02931
FABP3	1.33E-05	-0.4155
TRIP10	1.47E-05	-0.51549
HSP90AB1	0.000225	-0.55578
RPS24	0.000506	-0.44797
DNAJA4	0.000586	-1.25998
MRFAP1	0.000686	-0.20271
SNHG5	0.000939	-0.65023
PABPC1	0.002124	-0.43332
ANXA11	0.002186	-0.31079
ATP11A	0.002511	0.533909
TBX20	0.002823	0.827152
PPIF	0.003478	0.342752
ZNF622	0.007096	-0.51671
FKBP5	0.007155	-0.86411
RASD1	0.007468	-1.23112
TSPO	0.010087	-0.32877
PDE3A	0.012594	0.494364
ANGPTL4	0.012837	-1.54119
DNAJB1	0.014125	-0.59205
SS18L2	0.014448	-0.53527
CCL21	0.014933	-0.81735
RPS19BP1	0.015094	-0.37503
SPSB1	0.015303	-0.62767
ETFA	0.016655	-0.253
EIF4A2	0.017004	-0.36697
TST	0.017433	-0.6759
PGAM2	0.017968	0.356582
SLC16A1	0.01809	0.359136
RPL10A	0.018447	-0.22134
PLA2G16	0.018502	-0.4033
COX6A1	0.018897	-0.27185
TSR3	0.019015	-0.31082
SDHA	0.019244	0.2945
THSD4	0.01937	0.612104
JTB	0.019502	-0.35856
TXNIP	0.019841	-0.67479
ATP5B	0.020097	0.160013
SF3B5	0.020807	-0.3282
C6orf1	0.021257	-0.44422

C10orf10	0.02189	-0.50913
GPR22	0.021962	0.6118
AMOTL2	0.022329	-0.4103
EIF3D	0.022381	-0.25298
PNRC1	0.022442	-0.32237
BTF3	0.022593	-0.1762
SPR	0.023243	-0.54463
NSA2	0.023588	-0.65499
CLPP	0.023947	-0.32218
HDDC2	0.024731	-0.3461
PIM3	0.025119	-0.48626
CHP1	0.025409	-0.35118
CES2	0.025626	-0.59991
ILF3-AS1	0.026093	-0.60451
DDIT4	0.026101	-0.5924
DNAJB2	0.026361	-0.48136
KLF15	0.02653	-0.70413
GLUL	0.026805	-0.57424
APOPT1	0.026905	-0.40913
LAD1	0.026985	-0.72085
HIST1H2BD	0.026992	-0.37751
HIGD2A	0.027319	-0.20007
MAP3K7CL	0.027687	-0.5808
P4HA2	0.027888	-0.51364
ETFB	0.028124	-0.22952
FAM212B	0.028241	-0.58876
SCARB2	0.028244	-0.19712
BCS1L	0.028414	-0.31361
AGTRAP	0.028565	-0.42563
FTL	0.028623	-0.35963
CERK	0.028674	-0.47531
SRSF3	0.028815	-0.37009
TAF11	0.029432	-0.32988
B3GALT2	0.029454	0.496169
LMAN2	0.029648	-0.22971
ENO2	0.029835	-0.40776
NDUFA1	0.030201	-0.14984
SLC25A20	0.030399	-0.63407
BRK1	0.030816	-0.16216
DUSP1	0.031356	-0.47569
FLOT2	0.031435	-0.17131
SQSTM1	0.031502	-0.29943
PTGES3	0.031626	-0.26122
RP11-451G4.2	0.031715	-1.02284
RPS4X	0.031805	-0.17197
SNRNP70	0.032196	-0.30914
GNL3	0.032279	-0.386
MT1M	0.032563	-0.60151
PSME1	0.032774	-0.20252
TXNRD1	0.032906	-0.68006
CLU	0.033301	-0.8501
GSS	0.033486	-0.42971
CCDC85B	0.033578	-0.35189
HIF3A	0.0337	-0.48731
HSPA4	0.033707	-0.24471
TMEM109	0.033713	-0.20255
C11orf24	0.033819	-0.37851
HLA-A	0.033857	-1.07959
CYSTM1	0.034106	-0.47757
HS6ST1	0.034253	-0.34455
CCT3	0.03428	-0.41886
KEAP1	0.034344	-0.22295
ATP6V1G1	0.034351	-0.15847
PSMB4	0.03439	-0.16743
MANBAL	0.034404	-0.32331
TSSC4	0.034527	-0.33444
EEF1B2	0.034575	-0.22103
HSPE1	0.034606	-0.66784
CRYAB	0.034918	-0.64407
LRRC4	0.035271	-0.49529
PLEKHO1	0.035305	-0.59406
ADAM11	0.035425	0.963323
PEBP1	0.035486	-0.18038
TNNC1	0.035576	0.099498
FDFT1	0.035763	-0.35421
YBX3	0.035845	-0.31249
MT1X	0.036025	-0.93198
IMPDH2	0.036094	-0.39243
TRIM54	0.036123	-0.31441
NGFR	0.036183	0.731879
SLC25A3	0.036573	0.232832

SPRYD3	0.036704	-0.26283
TUBA3E	0.036916	-0.48888
GGPS1	0.037146	-0.23481
GGTA1P	0.037154	0.872429
SND1	0.0372	-0.3163
C10orf54	0.037269	-0.31484
POLR3GL	0.037398	-0.38815
LSM7	0.037624	-0.58806
GOT2	0.037858	0.255418
MRFAP1L1	0.037936	-0.26112
DUSP23	0.038242	-0.48478
ITGB5	0.038249	-0.3956
MYO1C	0.038317	-0.21544
APOOL	0.038404	0.351662
SCN1B	0.038415	-0.50331
KLHL36	0.038418	-0.48906
RSL1D1	0.038745	-0.21678
HADHA	0.038791	-0.34315
CHCHD2	0.038807	-0.15763
TTLL12	0.039027	-0.62207
ADCK3	0.039031	-0.5208
SLC25A39	0.039036	-0.32232
CCT7	0.039088	-0.28018
ADO	0.039112	-0.29512
MIR5690	0.039171	-0.61361
TERF2IP	0.039215	-0.26911
PRDX1	0.039357	-0.41997
NPPB	0.039417	-1.72874
STIP1	0.039604	-0.39623
H1FX	0.039639	-0.79503
FAM96B	0.039689	-0.25402
VSTM2L	0.039785	-0.97141
C11orf68	0.039816	-0.24351
FIS1	0.040053	-0.18151
DYNLRB1	0.040103	-0.23809
OSER1	0.040119	-0.40278
SAMD1	0.040196	-0.42475
MAF1	0.040273	-0.2453
MPST	0.04035	-0.39317
SRM	0.040441	-0.28869
PLOD1	0.04053	-0.46537
KANK2	0.040589	-0.29737
CHURC1	0.040622	-0.34072
KLF10	0.040722	-0.49371
CENPB	0.040746	-0.27682
IMP4	0.040824	-0.30508
PHF5A	0.040864	-0.35502
HSPB2	0.041105	-0.34623
SIAE	0.041108	-0.30127
SNHG8	0.041204	-0.37071
UBXN6	0.041528	-0.26849
CA3	0.041911	1.622109
POPDC2	0.042035	-0.2717
LAMTOR4	0.042074	-0.21479
ABCF2	0.042127	-0.27423
HSPA2	0.042397	-0.67426
PSMA7	0.042442	-0.23883
RABAC1	0.043129	-0.31624
DRAP1	0.043515	-0.29077
PLEKHA4	0.043644	-0.47818
GDI2	0.043684	-0.21875
NABP2	0.043803	-0.31278
MORN4	0.04407	-0.48357
NGFRAP1	0.044122	0.294436
CMYA5	0.044239	0.34836
HMGA1	0.044499	-0.27266
DBI	0.045126	-0.2712
FLJ42969	0.045495	-1.10766
PLIN5	0.045642	-0.36538
FAM3A	0.04754	-0.35208
SDPR	0.047867	-0.3549
CSNK2A2	0.04787	-0.28847
ORAI3	0.047875	-0.42071
ACSL1	0.047905	-0.3018
NOP10	0.047961	-0.24819
LARP7	0.048245	-0.31615
TP53I13	0.048609	-0.30731
TADA3	0.04919	-0.31025
NANOS1	0.049464	-0.94055

Supplemental Table 5. DEG in all lean samples when comparing NF to LVH (p_adj < 0.05)

GeneName	p_adj	log2FC
NPPA	6.99E-15	-3.73254
DCN	2.90E-14	1.003963
MIR6723	2.71E-11	3.901165
CNN1	0.015874	1.230719
C1QA	0.027665	0.985104
SPARCL1	0.038244	0.600471
C1QC	0.043925	1.175501

Supplemental Table 6. DEG in when comparing lean NF to obese LVH samples (p_adj < 0.05)

GeneName	p_adj	log2FC
MYL7	0	1.231699
MYL9	1.30E-14	0.501845
TPM1	1.60E-14	0.26546
TPM2	2.49E-10	0.422366
ACTC1	0.00024	0.611517
ECHDC3	0.035165	-0.73491
RASD1	0.037077	-0.94223

Supplemental Table 7. DEG in when comparing lean NF to obese LVH samples, males only (p_adj < 0.05)

GeneName	p_adj	log2FC
SLC16A7	0	0.739186
DANCR	0	-0.371
IRX3	0	-0.72525
MYL7	0	1.26689
PRKAR1A	0	0.331577
SLC38A1	2.00E-15	0.602805
FAM155B	3.00E-15	-0.59298
HSPB3	6.99E-15	-0.32055
PPAPDC3	7.99E-15	-0.33143
FAM107A	1.30E-14	-0.35431
NINJ1	1.60E-14	-0.48848
SAT2	1.70E-14	-0.35145
BSG	1.90E-14	-0.20203
NRAP	1.90E-14	0.489586
LDHD	2.10E-14	-0.33736
LGR4	2.60E-14	0.811303
DHRS7C	3.10E-14	1.799902
NEBL	5.90E-14	0.406793
ACTN2	6.49E-14	0.514332
ABCA8	8.50E-14	0.783352
NDUFS5	9.10E-14	0.130064
FAM129A	7.66E-12	0.445771
UBXN6	1.75E-10	-0.45321
NR1D2	2.66E-10	0.916154
ECH1	7.66E-09	-0.3775
HYAL1	2.32E-08	-0.3605
MFN2	4.96E-08	0.19523
MYL12A	6.60E-08	0.433722
RYR2	9.76E-08	0.502612
EGLN1	2.47E-07	0.555696
OIP5-AS1	3.69E-07	0.45973
PDLIM5	8.57E-07	0.395338
C17orf89	5.14E-06	-0.47029
C10orf54	1.24E-05	-0.41807
PEBP1	2.12E-05	-0.22826
VSTM2L	5.47E-05	-0.7891
ID3	0.0004	-0.49882
CPT1A	0.001089	0.684059
AGPAT9	0.001219	1.075068
CIRBP	0.001488	-0.66858
GBAS	0.002905	0.285877
SLC2A4	0.003014	-0.26979
HNRNPH1	0.004275	0.48207
MTRNR2L8	0.004412	-3.25627
PDE3A	0.006769	0.664528
ASS1	0.008458	-0.69383
NFIL3	0.010733	-0.63558
GSTT1	0.011703	-2.20421
HOPX	0.011744	1.145151
RB1CC1	0.012092	0.556311
DECR1	0.012308	0.357415
SPR	0.012736	-0.80244
UQCR11	0.013373	0.134543
CFL2	0.015294	0.336491
PPAP2B	0.015298	0.495698
ACE2	0.015324	0.775487
AREG	0.015347	0.979501
LMOD3	0.015389	0.254639
ZNF844	0.015429	0.511165
MYOM2	0.015505	0.360828
MTUS1	0.017233	0.294426
TRAK2	0.017693	0.412516
C3	0.017999	0.745286
GOLGA4	0.018802	0.297001
RPS12	0.022689	0.22347
DPY19L2	0.022967	0.713779
ASB11	0.024143	0.518274
GATM	0.024475	0.600525
NR1D1	0.024778	0.726608
PPARGC1A	0.028884	0.53886
TNNT1	0.03236	0.454654
ADRB1	0.032499	0.578817
DHCR7	0.035029	-0.42659
HINT2	0.035032	-0.38789
NPY6R	0.035286	0.161042
HSP90AA1	0.035951	-1.39985

FAM124A	0.036349	0.772011
HDDC2	0.03684	-0.40888
PALMD	0.036931	0.36049
PLOD1	0.037799	-0.53847
FABP3	0.037937	-0.19022
UBE2D1	0.038221	0.407133
TOMM22	0.038638	-0.36846
PIK3IP1	0.039085	0.851293
SUCLG2	0.039289	0.429302
PDXK	0.040214	0.395105
NACA	0.040426	0.261319
HIST2H2BE	0.04072	-0.47358
MRPS26	0.041411	-0.24566
SRM	0.041446	-0.33945
GJA1	0.042569	0.458062
KLHL24	0.043239	0.648831
F2RL3	0.04369	-1.20011
C8orf4	0.04381	-0.41677
GAPDH	0.043989	-0.21032
IFITM1	0.044485	-0.32031
SFRP1	0.044853	0.897901
YBEY	0.045711	0.543591
SNTA1	0.045962	-0.21448
RXRG	0.047003	-0.75542
PFKFB3	0.047302	0.721138
PDE7B	0.047321	0.646953
POPDC2	0.047669	-0.43408
PIK3R3	0.048177	-0.68814
HK2	0.049065	-0.71184
AHCY	0.049348	-0.38926

Supplemental Table 8. Sex- and BMI-specific DEG with (p_adj < 0.05) and absolute value of log2 fold change > 1

GeneName	p_adj	log2FC	Origin
AAK1	0.045716	-1.78202	LVH-F
ABCF3	0.000789	1.080317	LVH-F
ACSM1	0.016208	-2.13365	LVH-F
ACTA1	0.042476	-1.1199	LVH-F
ADIPOR1	0.001502	1.190279	LVH-F
AGPAT9	0.001219	1.075068	BMI25NF vs BMI30LVH M
AKAP17A	0.014985	-1.03412	LVH-F
ALG2	0.030579	-1.47132	LVH-F
ANAPC11	0.013918	1.566538	LVH-F
ANAPC2	0.015146	-1.12143	LVH-F
ANGPTL4	0.012837	-1.54119	BMI30
ANKRD36B	0.001861	-3.04052	LVH-F
ARL2BP	0.039899	1.290096	LVH-F
ARL6IP4	0.002399	1.532074	LVH-F
ASMTL	0.022448	-1.53306	LVH-F
ATG9A	0.028019	1.094103	LVH-F
ATP1A1	0.01965	-1.06399	LVH-F
ATP5F1	0	1.372359	LVH-F
ATP5H	0.046897	1.01046	LVH-F
ATP5J2	0.040698	1.053234	LVH-F
ATXN3	0.04571	-2.43236	LVH-F
AZGP1	1.46E-13	-1.21571	BMI30
AZGP1	0	-1.30798	LVH-M
BCKDHA	0.023183	1.361748	LVH-F
BEST4	0.039922	-1.08126	LVH-F
BTBD10	0.045469	-1.28796	LVH-F
C1QC	0.043925	1.175501	BMI25
CA3	0.041911	1.622109	BMI30
CAST	0.003565	1.515	LVH-F
CCDC3	0.028467	-1.26406	LVH-F
CCDC39	0.002766	-3.18253	LVH-F
CCL21	0.034425	-1.99891	LVH-F
CCNG1	0.015352	-1.33632	LVH-F
CHCHD3	0.027589	-1.8757	LVH-F
CKAP5	0.021646	1.106586	LVH-F
CLU	0.010655	-1.00447	LVH-M

CMC4	0.032923	1.087351	LVH-F
CNN1	0.015874	1.230719	BMI25
CNPY3	0.02602	-1.06098	LVH-F
CNTRL	0.018993	-1.53438	LVH-F
COPG2	0.035784	-1.62398	LVH-F
COX17	0.014284	-1.71685	LVH-F
COX7B	0.006368	1.091807	LVH-F
CPT1A	2.31E-05	1.291808	LVH-F
CPXCR1	0.024216	-1.39867	LVH-F
CREM	0.025267	-2.14778	LVH-F
CRKL	0.019327	-1.12111	LVH-F
CSRNP1	0.030347	-1.44187	LVH-F
CSRP3	0.021814	-1.03479	LVH-F
CTGF	0.030305	-1.18947	LVH-F
CXCL1	0.039718	-1.11979	LVH-F
CYR61	0.000146	-1.8073	LVH-F
DBNDD2	3.19E-07	1.116301	LVH-F
DCN	2.90E-14	1.003963	BMI25
DENND2A	0.017611	-1.00146	LVH-F
DEXI	0.01443	1.425424	LVH-F
DHRS4L2	0.01678	-1.16709	LVH-F
DHRS7C	3.10E-14	1.799902	BMI25NF vs BMI30LVH M
DIRAS3	0.028944	-1.01864	LVH-F
DNAJA4	0.000586	-1.25998	BMI30
EEF1G	0.000136	2.018869	LVH-F
EFHD2	0.030605	-1.574	LVH-F
ELOVL1	0.021326	-1.17358	LVH-F
ESPNP	0.032743	-2.91051	LVH-F
ETFB	0.002431	1.068367	LVH-F
F2RL3	0.04369	-1.20011	BMI25NF vs BMI30LVH M
FANCI	0.015449	-1.70713	LVH-F
FIGF	0.035388	-1.15941	LVH-F
FLJ42969	0.045495	-1.10766	BMI30
FOS	0.043634	-1.05858	LVH-F
FSTL3	0.022169	1.277475	LVH-F
FUCA2	0.018749	-1.24515	LVH-F
FXYD1	0.009307	1.676	LVH-F
GABARAP	0.006902	2.005869	LVH-F
GBGT1	0.015357	-1.08937	LVH-F
GCSHP3	0.029797	1.258673	LVH-F

GMEB1	0.015111	-1.08091	LVH-F
GNAT1	0.015907	-1.57915	LVH-F
GNG8	0.016495	1.058843	LVH-M
GPR173	0.033213	-1.28738	LVH-F
GPR4	0.002359	-1.58775	LVH-F
GPRASP2	0.007945	-1.95928	LVH-F
GSTT1	0.011703	-2.20421	BMI25NF vs BMI30LVH M
GSTT1	0.033376	-1.14097	LVH-M
GTPBP6	0.019788	-1.53881	LVH-F
HBA1	0.001351	-3.4007	LVH-F
HBB	0.000788	-5.45543	LVH-F
HBQ1	0.03057	-1.68139	LVH-F
HIF1A-AS2	0.033996	-1.13095	LVH-F
HIST1H2AC	0.003876	-2.31733	LVH-F
HIST1H4H	0.035099	-1.18434	LVH-F
HLA-A	0.033857	-1.07959	BMI30
HLA-DRB1	0.023762	-2.0529	LVH-F
HMGCS2	0	-1.52337	BMI30
HNRNPA2B1	0.001525	1.093875	LVH-F
HNRNPH2	0.009874	-2.03727	LVH-F
HOPX	0.011744	1.145151	BMI25NF vs BMI30LVH M
HSP90AA1	0.035951	-1.39985	BMI25NF vs BMI30LVH M
HSP90AA1	0.018487	-1.38355	LVH-M
HSPA5	0.035795	1.758879	LVH-F
HSPA6	0.042634	-1.46953	LVH-F
HSPB2	0.031367	1.211078	LVH-F
HTR2B	0.016906	-1.63789	LVH-F
IGF2	0.017209	-1.4621	LVH-F
IL3RA	0.037239	-1.12638	LVH-F
ILK	0.004515	1.653967	LVH-F
IMMP1L	0.016304	-1.26851	LVH-F
KCTD11	0.028872	-1.32702	LVH-F
KDR	0.027446	-1.01649	LVH-F
KLC1	0.035226	1.002591	LVH-F
KLF8	0.032702	-2.63556	LVH-F
LAMTOR2	0.027347	1.016552	LVH-F
LARP1B	0.016209	-1.10904	LVH-F
LTBP1	0.004871	-1.15454	LVH-F
LY75	0.035726	-1.27058	LVH-F

MAGEF1	0.006657	-1.50688	LVH-F
MAGI1	0.022467	-1.14043	LVH-F
MAPRE1	0.025203	1.119034	LVH-F
MAT2A	0.012773	-3.98597	LVH-F
MATR3	0.029278	1.100102	LVH-F
MCTS1	0.035379	-1.18667	LVH-F
MDH2	0.008315	1.042324	LVH-F
METTL7B	0.019927	-1.4323	LVH-F
MGC16275	0.027125	-1.16985	LVH-F
MOB4	0.007926	-2.45158	LVH-F
MT1A	0.016679	-1.31961	LVH-F
MT2A	0.029011	2.208718	LVH-F
MT2A	7.38E-09	-1.04872	LVH-M
MTPN	0.021198	-2.09273	LVH-F
MTRNR2L8	0.004412	-3.25627	BMI25NF vs BMI30LVH M
MTRNR2L8	0.009458	-3.57542	LVH-M
MTURN	0.021131	-1.28667	LVH-F
MYL4	0	1.223488	BMI30
MYL4	1.01E-06	1.123475	LVH-M
MYL7	0	1.231699	BMI25NF vs BMI30LVH
MYL7	0	1.26689	BMI25NF vs BMI30LVH M
MYL7	0	1.550622	BMI30
MZT2A	0.000177	1.152776	LVH-F
NAA10	0.03768	1.111668	LVH-F
NAT6	0.028176	-1.26624	LVH-F
NCOA4	0.003347	-1.25799	LVH-F
NDUFA7	0.036176	1.782766	LVH-F
NEAT1	0.002411	-1.10139	LVH-F
NEK7	0.020017	1.095569	LVH-F
NFIX	1.93E-07	1.237286	LVH-F
NNT	0.002013	1.040709	LVH-F
NONO	0.005596	1.256768	LVH-F
NPPA	0.004457	-3.54329	All_LVH
NPPA	6.99E-15	-3.73254	BMI25
NPPA	1.40E-14	-4.02274	BMI30
NPPA	0.032393	-2.89607	LVH-F
NPPA	0.018249	-4.59767	LVH-M
NPPB	0.039417	-1.72874	BMI30
NPPB	0.014572	-2.21326	LVH-F

NPPB	0.013588	-2.89857	LVH-M
NPTN-IT1	0.012711	-1.49524	LVH-F
NTMT1	0.012669	-1.15378	LVH-F
OSBP	0.018598	-1.05728	LVH-F
OTUD1	0.037677	-1.47141	LVH-F
PARVB	0.006333	1.004308	LVH-F
PCBP1	0.026636	1.265688	LVH-F
PCDH7	0	1.017951	BMI30
PDK4	4.00E-15	-2.80167	BMI30
PDK4	0.023484	-1.19085	LVH-M
PELI1	0.024498	-1.17581	LVH-F
PFDN1	0.00486	-1.49717	LVH-F
PLA2G2A	0.045658	-2.64705	LVH-F
PLIN2	0	-1.26669	BMI30
PLVAP	7.69E-08	-1.02931	BMI30
PLVAP	0.017747	-1.26576	LVH-F
PLVAP	3.00E-15	-1.29896	LVH-M
PLXDC2	0.011265	-2.03282	LVH-F
POLR2J	0.012691	-1.02605	LVH-F
POM121L10P	0.023984	-3.57981	LVH-F
POSTN	5.92E-09	-1.06062	BMI30
PPP1R17	0.044203	-1.20029	LVH-F
PTX3	0.018539	-1.36678	LVH-F
PWAR1	0.049174	-1.02416	LVH-F
PYURF	0.021461	1.332057	LVH-F
RAB4A	5.53E-06	1.515827	LVH-F
RASD1	0.007468	-1.23112	BMI30
RDH14	0.012763	-1.08698	LVH-F
RFPL4AL1	0.015363	-1.82569	LVH-F
RGL1	0.037807	-1.12518	LVH-F
RN7SL2	0.019873	1.481054	LVH-F
RNF14	1.90E-07	1.344973	LVH-F
RNU6-7	0.037551	-1.09696	LVH-F
RP11-451G4.2	0.031715	-1.02284	BMI30
RPL9	0.025397	-1.02426	LVH-F
RPS15A	0.049643	1.025891	LVH-F
RTN4	0.039426	-1.07648	LVH-F
S100A1	0.000813	1.472048	LVH-F
SEC14L5	0	1.368913	BMI30
SEC14L5	0.025826	1.203995	LVH-M

SENP5	0.036158	-1.4376	LVH-F
5-Sep	0.031609	-1.92603	LVH-F
SESTD1	0.032037	-1.46671	LVH-F
SF1	0.017507	-1.01606	LVH-F
SH3BGR	0.041381	-1.03842	LVH-M
SLC25A34	1.40E-14	-1.2642	BMI30
SLC45A3	0.019074	-1.48551	LVH-F
SLC6A6	0.016902	-1.15071	LVH-F
SNORA33	0.048468	-1.16312	LVH-F
SNRPN	0.022304	-1.23539	LVH-F
SOCS5	0.015948	-1.25689	LVH-F
SPRY4	0.016248	-1.08951	LVH-F
SRSF7	0.02232	-1.06689	LVH-F
STX12	0.042183	-1.23808	LVH-F
SVOP	0.034337	-1.06419	LVH-M
TAX1BP3	0.023178	-1.44566	LVH-F
TCHH	0.027454	-1.91902	LVH-F
TFRC	0.041854	1.359095	LVH-M
THBS4	0.048544	1.196572	LVH-F
TIMM8B	0.012035	-1.1086	LVH-F
TIMP1	0.028892	-1.00851	LVH-F
TMEM165	0.026022	1.050255	LVH-F
TNFAIP1	0.026486	-1.42484	LVH-F
TRAPPC5	0.000584	1.354619	LVH-F
TRIM35	0.013302	-1.52477	LVH-F
TSFM	0.003479	1.156395	LVH-F
TTC21A	0.002043	-2.47755	LVH-F
TUBA8	0.030328	1.599595	LVH-F
UQCC1	0.016391	-1.03014	LVH-F
VAMP7	0.028929	-1.15256	LVH-F
VGLL2	0.038578	-1.19911	LVH-F
VSTM5	0.010137	-1.45653	LVH-F
WDR61	0.021294	-1.02132	LVH-F
WDR62	2.15E-12	1.07249	LVH-M
WDR89	0.024138	-1.19626	LVH-F
ZBED1	0.025655	-1.19893	LVH-F
ZSWIM1	0.01621	-1.14273	LVH-F

Supplemental Table 9. Sex- and BMI-specific DEG with (p_adj < 0.05) and absolute value of log2 fold change > 2

GeneName	p_adj	log2FC	Origin
HBB	0.000788	-5.45543	LVH-F
NPPA	0.018249	-4.59767	LVH-M
NPPA	1.40E-14	-4.02274	BMI30
MAT2A	0.012773	-3.98597	LVH-F
NPPA	6.99E-15	-3.73254	BMI25
POM121L10P	0.023984	-3.57981	LVH-F
MTRNR2L8	0.009458	-3.57542	LVH-M
NPPA	0.004457	-3.54329	All_LVH
HBA1	0.001351	-3.4007	LVH-F
MTRNR2L8	0.004412	-3.25627	BMI25NF vs BMI30LVH M
CCDC39	0.002766	-3.18253	LVH-F
ANKRD36B	0.001861	-3.04052	LVH-F
ESPNP	0.032743	-2.91051	LVH-F
NPPB	0.013588	-2.89857	LVH-M
NPPA	0.032393	-2.89607	LVH-F
PDK4	4.00E-15	-2.80167	BMI30
PLA2G2A	0.045658	-2.64705	LVH-F
KLF8	0.032702	-2.63556	LVH-F
TTC21A	0.002043	-2.47755	LVH-F
MOB4	0.007926	-2.45158	LVH-F
ATXN3	0.04571	-2.43236	LVH-F
HIST1H2AC	0.003876	-2.31733	LVH-F
NPPB	0.014572	-2.21326	LVH-F
MT2A	0.029011	2.208718	LVH-F
GSTT1	0.011703	-2.20421	BMI25NF vs BMI30LVH M
CREM	0.025267	-2.14778	LVH-F
ACSM1	0.016208	-2.13365	LVH-F
MTPN	0.021198	-2.09273	LVH-F
HLA-DRB1	0.023762	-2.0529	LVH-F
HNRNPH2	0.009874	-2.03727	LVH-F
PLXDC2	0.011265	-2.03282	LVH-F
EEF1G	0.000136	2.018869	LVH-F
GABARAP	0.006902	2.005869	LVH-F

Supplemental Table 10. DEG shared between obesity-related LVH and ischemic heart datasets with (p_adj < 0.05)

Gene	log2FC NF vs LVH, BMI30	p_adj	log2FC NF vs ISCH	p_adj
ADAM11	0.963323248	0.035425	1.859819771	1.99E-05
AMOTL2	-0.410297052	0.022329	2.454941712	1.72E-09
ANGPTL4	-1.541190467	0.012837	-1.62521166	0.046472
ATP11A	0.533909197	0.002511	0.933140384	0.011395
AZGP1	-1.215705163	0	-1.138888768	0.040662
C10orf10	-0.509127057	0.02189	2.175525819	1.54E-07
CA3	1.622109468	0.041911	-4.806058253	1.20E-09
CCL21	-0.817354828	0.014933	-4.445963698	4.26E-13
CDKN1A	-0.787871528	0	1.066409299	0.042891
CES2	-0.599913795	0.025626	-1.29788074	0.000568
DNAJA4	-1.259979001	0.000586	-1.318690893	0.005975
DUSP1	-0.475690762	0.031356	1.50041234	0.002321
ENO2	-0.407758301	0.029835	1.329284641	0.01159
GADD45G	-0.972541723	0	-2.141900654	8.62E-06
GLUL	-0.574244275	0.026805	1.511265015	4.26E-05
HIF3A	-0.487311467	0.0337	1.90209774	2.88E-11
HIST1H2BD	-0.377505615	0.026992	-1.819527247	0.008223
KLF10	-0.493714422	0.040722	1.981681166	2.83E-06
KLHL36	-0.489064934	0.038418	1.118522643	0.044766
MT1X	-0.931977954	0.036025	-3.148047139	3.10E-06
MYL4	1.223488273	0	5.061522714	0
NGFR	0.731879187	0.036183	-1.468816887	0.006195
NPPA	-4.022740194	0	-4.275261149	0
NPPB	-1.728742349	0.039417	-3.478505958	1.79E-13
P4HA2	-0.513644739	0.027888	-1.327847131	0.000437
PCDH7	1.017950806	0	-1.342352722	0.001533
PDK4	-2.801668723	0	-1.621761989	0.003644
PIM3	-0.486255599	0.025119	1.148851509	0.031203
PLIN5	-0.365375409	0.045642	1.522271323	0.000835
POSTN	-1.060620451	6.00E-09	-5.398096936	0
RASD1	-1.231118925	0.007468	-4.302868698	0
SDPR	-0.354902106	0.047867	1.540942135	0.001267
SEC14L5	1.368913328	0	2.532045159	4.07E-09
SNHG8	-0.370713939	0.041204	1.326354211	0.025361
TUBA3E	-0.488877251	0.036916	2.13283323	3.49E-07
TXNIP	-0.67478941	0.019841	2.215508659	4.64E-06

TXNRD1	-0.6800562	0.032906	0.786257974	0.033516

Supplemental Table 11. DEG shared between obesity-related LVH and dilated cardiomyopathy datasets with (p_adj < 0.05)

Gene	log2FC NF vs LVH, BMI30	p_adj	log2FC NF vs DCM	p_adj
ACADM	0.311292269	0	-1.635131511	0.024369
ACSL1	-0.301796691	0.047905	-1.237893201	0.028694
ADAM11	0.963323248	0.035425	-1.705143444	0.000396
ANGPTL4	-1.541190467	0.012837	2.676261492	7.52E-07
AZGP1	-1.215705163	0	2.180581657	2.13E-06
C10orf54	-0.314841388	0.037269	1.198134446	0.039901
C11orf24	-0.37851224	0.033819	1.146685791	0.045062
C6orf1	-0.444222465	0.021257	1.462087575	0.00141
CCDC85B	-0.351885521	0.033578	1.451714992	0.003356
CCL21	-0.817354828	0.014933	-2.08871703	0.010486
CDKN1A	-0.787871528	0	1.293184109	0.041044
CEBPB	-0.612313557	5.00E-09	1.446932885	0.038798
CES2	-0.599913795	0.025626	1.624109893	3.83E-05
CLIC5	0.403321879	0	-1.829084965	0.024395
DUSP1	-0.475690762	0.031356	-1.092128327	0.041697
ENO2	-0.407758301	0.029835	2.196136473	0.0023
FAM129A	0.530083934	0	-1.595061831	0.010247
FAM96B	-0.254020969	0.039689	1.007933098	0.042718
FKBP5	-0.864105785	0.007155	2.79848211	1.39E-10
GADD45G	-0.972541723	0	-2.628999414	2.73E-09
GGTA1P	0.872428613	0.037154	-1.706254443	0.012987
GLUL	-0.574244275	0.026805	1.664537577	5.94E-08
GPNMB	0.91782649	0	-1.545983281	0.000353
HIF3A	-0.487311467	0.0337	2.0184829	6.70E-10
HIST1H2BD	-0.377505615	0.026992	-1.796075408	0.0122
HLA-A	-1.079594248	0.033857	1.632995353	0.003143
HMGCS2	-1.523371969	0	2.238661292	2.33E-06
HSPA2	-0.6742577	0.042397	-1.921073556	0.005923
HSPB2	-0.346226709	0.041105	1.552376496	0.031126
HSPE1	-0.66784361	0.034606	-1.424482306	0.044167
KLF10	-0.493714422	0.040722	-2.844803667	7.04E-09
KLF15	-0.70413339	0.02653	2.244450656	6.56E-06
KLHL36	-0.489064934	0.038418	-1.997317857	0.006246
MLYCD	-0.639518345	0	1.255474711	0.025587
MYL4	1.223488273	0	7.928132761	0
MYL7	1.550621715	0	-2.355940042	1.32E-09

NGFR	0.731879187	0.036183	2.775612164	1.05E-07
NGFRAP1	0.29443617	0.044122	1.03562481	0.043437
P4HA2	-0.513644739	0.027888	-1.327516966	0.022345
PCDH7	1.017950806	0	-3.01148407	5.79E-13
PDE3A	0.494363508	0.012594	-2.310334066	2.07E-05
PDK4	-2.801668723	0	-2.495837398	3.53E-08
PIM3	-0.486255599	0.025119	-1.433797174	0.004027
PLA2G16	-0.403295041	0.018502	1.062296467	0.006247
PLEKHA4	-0.478182032	0.043644	1.715005619	0.002446
PLEKHO1	-0.594058511	0.035305	1.581454714	0.030276
PLIN2	-1.26669077	0	-1.979051483	5.95E-05
PSME1	-0.20251521	0.032774	-1.220196145	0.026897
RABAC1	-0.316244037	0.043129	1.466716007	0.048405
RYR2	0.722120711	0	-2.846601211	0.001689
SDPR	-0.354902106	0.047867	-1.109838725	0.036961
SIAE	-0.301274805	0.041108	-1.596753323	0.029123
SLC16A1	0.359135811	0.01809	-1.5319772	0.015032
SNHG8	-0.370713939	0.041204	1.921250812	0.000585
SPR	-0.544625322	0.023243	1.53937965	0.003249
TUBA3E	-0.488877251	0.036916	4.00419486	1.18E-11
TXNRD1	-0.6800562	0.032906	-0.917006565	0.005121
VSTM2L	-0.971412272	0.039785	3.223903018	5.23E-06

Supplemental Table 12. DEG shared between obesity-related LVH and both dilated ischemia and cardiomyopathy datasets with (p_adj < 0.05)

Gene	log2FC NF vs LVH, BMI30	p_adj	log2FC ISCH vs DCM	p_adj
ACSL1	-0.301796691	0.047905	-1.36779967	0.040646
AMOTL2	-0.410297052	0.022329	-1.54606353	0.000364
ATP11A	0.533909197	0.002511	-1.31543383	0.000361
AZGP1	-1.215705163	0	1.813024958	0.000192
CA3	1.622109468	0.041911	1.717173576	0.00744
CCL21	-0.817354828	0.014933	3.211259363	1.73E-08
ETFB	-0.229518502	0.028124	-1.136020685	0.039885
FKBP5	-0.864105785	0.007155	1.999049339	1.19E-05
GADD45G	-0.972541723	0	2.127923456	0.000128
HMGCS2	-1.523371969	0	-6.83427681	0
KLF10	-0.493714422	0.040722	-1.429708621	0.00882
KLF15	-0.70413339	0.02653	1.466101481	0.017679
MLYCD	-0.639518345	0	-1.107128992	0.038156
MT1M	-0.601514184	0.032563	5	0.027723
MT1X	-0.931977954	0.036025	1.515877998	0.048194
MYL4	1.223488273	0	2.866610047	1.24E-05
NGFR	0.731879187	0.036183	2.460128189	3.52E-06
NPPA	-4.022740194	0	1.804016681	0.002728
NPPB	-1.728742349	0.039417	3.95062945	1.28E-12
PDE3A	0.494363508	0.012594	-1.958909858	0.000798
PLEKHA4	-0.478182032	0.043644	1.693949792	0.000295
PLIN2	-1.26669077	0	1.361068302	0.012164
PLVAP	-1.029311185	7.70E-08	1.949632993	0.001075
POSTN	-1.060620451	6.00E-09	4.131445065	0
RASD1	-1.231118925	0.007468	4.447645806	0
SDPR	-0.354902106	0.047867	-1.293987604	0.023136
SEC14L5	1.368913328	0	-2.791126985	9.97E-09
TBX20	0.827151711	0.002823	-2.297082344	1.42E-06
TUBA3E	-0.488877251	0.036916	1.87136163	0.00554
TXNIP	-0.67478941	0.019841	-1.869992367	0.002275
VSTM2L	-0.971412272	0.039785	2.777014645	6.09E-05

Supplemental Table 13. DEG shared between female obesity-related LVH and ischemia datasets with (p_adj < 0.05)

Gene	log2FC NF vs LVH_F	p_adj	log2FC NF vs ISCH	p_adj
ADAM19	-0.630142749	0.037114	-3.048888723	1.74E-10
AKAP12	-0.731993228	0.026665	-1.298370962	0.01369
AKAP8	0.719672413	0.041305	1.190883805	0.022442
AMOTL1	-0.709487539	0.023841	-1.806957882	0.00021
ANGPTL4	-0.978298815	0.026011	-1.62521166	0.046472
ANO5	0.496829866	0.04182	-1.194968001	0.010258
APOD	-0.892669878	0.037102	2.188726773	4.39E-07
ATE1	-0.823974167	0.02715	-5	2.25E-07
ATP2B4	-0.473150152	0.047037	-1.590706441	0.000121
AZIN1	-0.457215273	0.033503	-1.355458125	0.00242
B2M	-0.481096356	0.034341	1.263669684	0.019571
BCAR3	-0.799783333	0.044029	1.256167644	0.020878
BTG2	-0.547514523	0.022147	-1.680509038	0.000236
CBLB	-0.501922722	0.049091	1.736718946	0.000114
CCL21	-1.998910656	0.034425	-4.445963698	4.26E-13
CD151	0.472684984	0.037071	-1.076847186	0.003615
CD68	0.939054502	0.044368	-1.102746724	0.045551
CDKN1A	-0.429068187	0.044115	1.066409299	0.042891
CES2	0.651625466	0.024136	-1.29788074	0.000568
COPG2	-1.623978704	0.035784	-5	1.32E-05
COQ10A	0.483453731	0.033817	1.023565636	0.025646
COX6A2	0.439693907	0.029613	1.183127397	0.036892
CSRNP1	-1.441867051	0.030347	1.25190798	0.017483
CYR61	-1.807300387	0.000146	1.922649835	1.06E-05
DAAM2	-0.505335353	0.043894	1.699349677	0.000119
DAPK2	0.74144734	0.046529	1.472556324	0.003215
DRAM2	-0.726386837	0.022444	-5	2.46E-05
DUSP1	-0.830211926	0.045995	1.50041234	0.002321
DYNLL1	-0.741219481	0.04959	-1.775643022	3.34E-05
EDNRB	-0.523326087	0.025631	2.168141571	1.62E-11
EFEMP1	-0.729911964	0.04534	-0.95010613	0.030239
ELK1	-0.394407987	0.043625	1.055086757	0.0086
EMILIN1	-0.571141425	0.039703	-1.138198488	0.04197
ENG	-0.575150638	0.033416	1.319210813	0.010059
ENO2	-0.613111978	0.045746	1.329284641	0.01159
EPHA4	-0.512902526	0.044019	-2.090495025	0.000511

ETS2	-0.554950903	0.039999	1.228682928	0.014796
FBLN5	-0.551338968	0.012826	1.290762964	0.006991
FSTL3	1.277475497	0.022169	-1.278100975	0.030781
FXYD5	-0.741622441	0.04211	-1.168609909	0.049289
GIMAP6	-0.948944237	0.004831	1.309671928	0.000231
GIMAP7	-0.554386987	0.028666	1.30526632	0.021863
GPR157	-0.826733847	0.031724	1.844800392	0.002285
HIST1H2AC	-2.317333894	0.003876	-1.555247681	0.043713
IL33	-0.799078418	0.026093	-1.589206695	0.028392
IL6ST	-0.346209222	0.036204	-5	1.55E-14
ITGA6	-0.386557844	0.041332	-1.132163475	0.020601
KDR	-1.01649251	0.027446	1.609651748	0.000579
KIDINS220	-0.335580105	0.040251	-1.272954014	0.017108
KLHL31	-0.967419601	0.040682	-1.242447658	0.022627
KLHL38	0.335280765	0.045138	2.014012569	2.44E-06
LIMS2	0.460768094	0.036658	1.077500891	0.013085
LRRC14B	0.601273929	0.046813	2.497809238	2.29E-09
MAGOH	-0.307452819	0.048468	-5	2.79E-06
MAOA	-0.670884366	0.027791	1.156827805	0.033939
MFAP4	-0.524445582	0.039794	-1.750721346	0.002055
MON1B	-0.59647824	0.0301	1.135406402	0.042159
MRPL33	0.685197212	5.81E-05	-3.374524114	0
MYO1B	-0.606313032	0.025112	-1.152455909	0.026489
NCKIPSD	-0.409067028	0.043648	1.647170331	5.65E-07
NDRG2	0.411302702	0.030812	0.914021945	2.83E-06
NEAT1	-1.101387739	0.002411	1.359837777	0.042058
NEDD9	-0.524428571	0.046449	1.403249907	0.001187
NPPA	-2.896073668	0.032393	-4.275261149	0
NPPB	-2.213258402	0.014572	-3.478505958	1.79E-13
NR1D2	-0.366189625	0.043119	-5	8.32E-11
OTUD1	-1.471407718	0.037677	1.307614166	0.008755
PLA2G2A	-2.647052214	0.045658	2.063800018	9.32E-07
PLXDC2	-2.032815142	0.011265	-1.64696227	0.027561
PMEPA1	-0.747667125	0.017309	-1.156183207	0.005308
PPP1R12B	0.592237795	0.000174	-1.241293709	0.000151
PRELP	-0.570100677	0.036116	1.943073151	5.58E-07
PREX1	-0.997966408	0.034587	1.63079897	0.000293
PRKAA2	-0.426292519	0.046432	-1.187609705	0.026793
PROS1	-0.92499567	0.042894	-1.777064031	0.000208
PTGDS	0.646333156	0.004501	1.774781138	0.001074
PTMS	-0.426086888	0.035995	1.586696097	0.000379

PTX3	-1.366782142	0.018539	-3.020915462	0.000259
RNF146	-0.371611904	0.041492	-0.664744793	0.048359
RPL28	-0.356732224	0.04316	0.86291538	0.047925
RPL37A	0.515517464	0.049679	1.124108637	0.031403
RPLP1	0.862792317	0.001217	1.078124335	0.002645
RPS15A	1.025890917	0.049643	0.955141541	0.018754
RTN3	-0.498114556	0.034032	-0.871600672	0.016901
S100A1	1.472047839	0.000813	1.194716866	0.038654
S100A8	-0.848107813	0.012523	1.735255886	0.006747
SAMHD1	-0.58759924	0.018941	1.250344989	0.014341
SCN2B	-0.819119857	0.032449	-2.022686998	3.54E-05
SEC14L1	-0.425089014	0.03269	1.207579863	0.003966
SEMA3G	-0.659911145	0.028594	1.140983505	0.031186
SERPINH1	-0.564001102	0.043145	-1.417623133	0.004327
SLC8A1	0.685780929	0.002115	-0.988155998	0.006057
SPEN	-0.504840729	0.035042	1.112858292	0.042159
STK38	-0.666653177	0.018017	-1.23246269	0.04036
STK39	-0.616865536	0.035728	-2.1051715	0.000835
SUN1	-0.450823867	0.038098	0.750215245	0.022747
TACC1	-0.370545039	0.038676	0.91919359	0.006701
TAX1BP3	-1.445656879	0.023178	-5	5.68E-07
THBS2	-0.665188472	0.044745	-2.475548465	7.80E-08
THBS4	1.196572038	0.048544	-2.581450709	1.48E-09
TIMP1	-1.008514924	0.028892	-1.301912191	0.012381
TIMP3	-0.392285917	0.02239	1.659800666	0.004458
TMEM100	-0.624594284	0.039693	-2.083667615	0.01159
TNPO1	-0.651711854	0.013703	-0.97428252	0.044435
TXNRD1	-0.397359953	0.043213	0.786257974	0.033516
UCKL1	-0.916759905	0.006433	1.164593946	0.006452
ULK1	0.844633034	0.042966	1.158112048	0.027754
USP9X	0.696855665	0.033127	-1.085170923	0.041503
VAMP8	-0.563839444	0.035165	-1.974598288	0.008887
ZMIZ1	-0.698773614	0.039673	1.461323404	0.004155
ZNF438	-0.411605766	0.049926	-5	2.62E-11

Supplemental Table 14. DEG shared between female obesity-related LVH and dilated cardiomyopathy datasets with (p_adj < 0.05)

Gene	log2FC NF vs LVH_F	p_adj	log2FC NF vs DCM	p_adj
ACAA1	0.976931371	0.008231	1.073799181	0.04415
ACTA1	-1.119896192	0.042476	1.585652186	0.035032
AGPAT2	-0.862461622	0.031696	1.173437054	0.014742
AGPAT9	-0.656929279	0.036148	-1.692568564	0.017186
AKAP12	-0.731993228	0.026665	-2.360153532	1.43E-05
AKAP8	0.719672413	0.041305	-1.108378062	0.027646
AMOTL1	-0.709487539	0.023841	-2.394648442	0.000287
ANAPC11	1.56653796	0.013918	0.824630217	0.002557
ANGPTL4	-0.978298815	0.026011	2.676261492	7.52E-07
ANXA2	-0.714896823	0.006722	-1.291176926	0.006209
APOD	-0.892669878	0.037102	-1.945149012	5.02E-05
ARHGEF15	-0.676954813	0.024341	0.955448515	0.014902
ARL6IP4	1.532074342	0.002399	0.839194224	0.013855
ATE1	-0.823974167	0.02715	-5	2.59E-05
ATP2B4	-0.473150152	0.047037	-2.249432133	1.86E-06
AZIN1	-0.457215273	0.033503	-1.234736437	0.014779
B2M	-0.481096356	0.034341	-1.838140453	0.002514
BCAR3	-0.799783333	0.044029	-1.55715444	0.04658
BTG2	-0.547514523	0.022147	1.569479725	0.002223
C17orf89	-0.36636919	0.036896	1.628093417	0.023999
C1QTNF1	-0.866995909	0.004932	1.86440586	0.000983
CALHM2	-0.468504076	0.04377	-1.19644797	0.049581
CALM2	0.488690339	4.98E-09	-1.133345004	0.049818
CAMK2D	-0.517152358	0.048827	-1.21846042	0.005703
CAST	1.51500001	0.003565	-1.367834595	0.000208
CBLB	-0.501922722	0.049091	-1.541442813	0.002264
CCL2	0.861442892	0.041833	6.143199949	0.000908
CCL21	-1.998910656	0.034425	-2.08871703	0.010486
CD151	0.472684984	0.037071	-1.317019331	2.63E-06
CD68	0.939054502	0.044368	1.772692722	0.000442
CDKN1A	-0.429068187	0.044115	1.293184109	0.041044
CEBPB	-0.441897123	0.035736	1.446932885	0.038798
CES2	0.651625466	0.024136	1.624109893	3.83E-05
CLIC5	0.419941576	0.031906	-1.829084965	0.024395
CLINT1	-0.69542973	0.033752	-0.858279003	0.046264
COL6A2	-0.400028873	0.018589	-1.204770251	0.036974

CPT1A	1.291808397	2.31E-05	-1.279781009	0.007423
CRIM1	-0.434102162	0.048377	1.256178203	0.006172
CTGF	-1.189465404	0.030305	2.120582413	0.001288
CXorf36	-0.529466638	0.04564	1.723076035	7.56E-05
CYBRD1	-0.900806819	0.025364	1.184422202	0.02653
CYR61	-1.807300387	0.000146	-1.254650049	0.019218
DAAM2	-0.505335353	0.043894	1.768775305	2.20E-05
DAPK2	0.74144734	0.046529	1.303940902	0.016556
DCAF11	0.664734382	0.030771	-0.8027819	0.034408
DCAF6	0.894946081	6.99E-15	-1.170334921	0.002897
DIRAS3	-1.018644618	0.028944	-4.507392284	9.26E-13
DNAJC3	-0.377663049	0.049951	-1.638522404	0.02877
DRAM2	-0.726386837	0.022444	-5	0.000183
DUSP1	-0.830211926	0.045995	-1.092128327	0.041697
DYRK2	-0.486689622	0.045658	-1.634574589	0.00945
EDF1	-0.810589432	0.028375	0.831908111	0.040718
EDNRB	-0.523326087	0.025631	2.827625448	7.91E-13
EFEMP1	-0.729911964	0.04534	1.409250958	0.000575
EFNB2	-0.534300677	0.031279	-1.403835955	0.019655
EHD2	-0.487559748	0.015141	1.398161943	0.004582
ELK1	-0.394407987	0.043625	1.195326989	0.002194
EMILIN1	-0.571141425	0.039703	1.95821404	5.42E-05
ENG	-0.575150638	0.033416	-1.014972805	0.026503
ENO2	-0.613111978	0.045746	2.196136473	0.0023
ETS2	-0.554950903	0.039999	-1.676128716	0.000133
FAM134B	-0.884094691	0.024207	-1.884835279	0.00021
FAM46A	-0.647202094	0.012548	-1.451241958	0.04004
FBLN5	-0.551338968	0.012826	-1.514662511	0.003136
FBXL7	-0.378152289	0.044687	-1.181297147	0.039006
FKBP5	-0.517708568	0.043381	2.593668358	2.22E-11
FOS	-1.058578228	0.043634	-2.021564297	0.000552
FXYD1	1.676000427	0.009307	1.416270491	0.002163
FXYD6	-0.615605462	0.041837	1.19541486	0.000825
GADD45B	-0.530310364	0.032794	1.914790207	0.00068
GAS2L1	-0.662780815	0.035893	1.569622643	0.009101
GAS5	-0.845491655	0.029155	-1.886659007	0.02464
GAS7	-0.830867293	0.016998	0.970841425	0.003611
GFM1	0.593327245	0.039675	-1.50539242	0.044621
GIMAP6	-0.948944237	0.004831	5	9.08E-12
GIMAP7	-0.554386987	0.028666	-1.410024917	0.009221
GJA1	-0.35022164	0.049747	-1.825553014	0.00178

GPR157	-0.826733847	0.031724	-1.730715343	0.036692
HAGH	0.522401715	0.023181	1.028491735	0.03694
HBB	-5.455425115	0.000788	-7.950773935	7.01E-06
HIST1H2AC	-2.317333894	0.003876	-2.444267659	0.002105
HSPB2	1.21107834	0.031367	1.552376496	0.031126
HSPB6	0.654174777	0.04228	-1.92991699	0.001118
IL6ST	-0.346209222	0.036204	-5	1.49E-05
IQGAP1	-0.864329128	0.028623	-1.914008486	0.002439
JAG1	-0.648073868	0.021947	-1.500158672	0.004055
JAK1	0.507474682	0.048446	-1.291085313	0.010722
KCTD9	-0.652371069	0.029115	-1.588741638	0.045577
KDR	-1.01649251	0.027446	-1.618120478	0.001516
KIDINS220	-0.335580105	0.040251	-1.826845671	0.002914
KIF5B	-0.239468754	0.033119	-1.602393975	0.02837
KLHL31	-0.967419601	0.040682	-1.879304514	0.001189
KLHL38	0.335280765	0.045138	-2.19231975	0.001188
MAFG	-0.651584295	0.048208	-1.010092131	0.009541
MAGOH	-0.307452819	0.048468	-5	3.86E-05
METRN	0.568665031	0.049113	1.393969653	0.016556
MFAP4	-0.524445582	0.039794	1.412504009	0.002207
MGLL	-0.375416043	0.049925	1.082085931	0.021445
MKNK2	-0.562491586	0.021436	-0.940147819	0.03771
MLYCD	0.893456574	6.48E-06	1.255474711	0.025587
MON1B	-0.59647824	0.0301	-1.329558764	0.016891
MRPL33	0.685197212	5.81E-05	2.628185807	0.001411
MTUS2	0.370084163	0.049071	1.366734076	0.005888
MYLK3	-0.433901967	0.044447	-1.349636972	0.037659
NBL1	-0.793221485	0.03112	-1.407958502	0.039406
NCKIPSD	-0.409067028	0.043648	1.807487423	0.000159
NCOA4	-1.257988904	0.003347	-1.608733137	0.004488
NDRG2	0.411302702	0.030812	0.796941477	0.019726
NDUFAF1	-0.444998855	0.043183	1.320804879	0.031125
NNT	1.040709158	0.002013	-1.685801348	0.004346
NUDT4	-0.57452292	0.049429	-1.175784242	0.014874
OTUD1	-1.471407718	0.037677	1.656789936	0.002426
P2RY2	-0.645910688	0.038731	-0.949886077	0.044382
PALM	-0.628062223	0.027912	-1.462084762	0.004055
PARVB	1.004307731	0.006333	-1.086567828	0.006525
PDLIM3	-0.569792209	0.032775	-1.308620279	0.034935
PDLIM7	-0.579683763	0.028378	2.236962747	1.13E-06
PECAM1	-0.533763511	0.048628	1.602886378	0.0135

PEX6	-0.497972807	0.037461	1.100292214	0.041317
PLA2G2A	-2.647052214	0.045658	5.409285129	0
PNMAL1	-0.634642632	0.049439	-1.964423567	0.004
PPP1R12B	0.592237795	0.000174	-2.028461332	0.000287
PRELP	-0.570100677	0.036116	1.33153185	0.000945
PRKCDBP	-0.26048416	0.045832	1.595793765	0.02828
PTGDS	0.646333156	0.004501	1.322718047	0.028126
PTMS	-0.426086888	0.035995	2.640986855	3.74E-05
PUM2	-0.45940875	0.017423	-1.520513073	0.025117
QSOX1	0.570678641	0.035483	1.402760158	0.000116
RAMP3	-0.605059906	0.04247	-1.03432831	0.046878
RFTN1	-0.775743929	0.015701	1.628866348	0.000266
RNF146	-0.371611904	0.041492	-0.889268847	0.026133
RNF185	-0.83124553	0.01517	-5	1.80E-07
RPL28	-0.356732224	0.04316	1.619734681	0.00747
RPLP1	0.862792317	0.001217	1.300726888	0.046657
RPS27A	-0.501818519	0.026615	1.226988387	0.024042
RTN4	-1.076477799	0.039426	-1.258282951	0.00121
S100A1	1.472047839	0.000813	-2.005092261	0.000204
S100A8	-0.848107813	0.012523	3.192432432	1.63E-05
S100A9	-0.934970606	0.044725	3.700776981	2.27E-06
SAMHD1	-0.58759924	0.018941	3.066923442	5.41E-10
SCN2B	-0.819119857	0.032449	-2.524350286	1.94E-05
SDCBP	-0.798182227	0.031003	-1.469515535	0.006884
SEC14L1	-0.425089014	0.03269	1.182266352	0.042053
SEL1L	-0.44253006	0.035252	-1.241379115	0.017791
SEMA3G	-0.659911145	0.028594	-1.095365967	0.02975
SERPINH1	-0.564001102	0.043145	-1.80990502	0.00023
SERTAD3	-0.903840592	0.014546	-1.43676246	0.013748
SGCA	0.496242738	0.028242	0.975357587	0.00212
SLC25A29	-0.613634157	0.035854	1.485004892	0.035932
SLC6A6	-1.150709242	0.016902	-1.743431244	0.00046
SLC7A8	-0.972640406	0.035062	2.456764225	1.18E-07
SLC8A1	0.685780929	0.002115	-1.420048399	0.000244
SPARCL1	-0.598007079	0.012917	1.47024442	0.003893
SPOP	-0.397007271	0.040271	5	9.57E-10
SRGN	-0.363394399	0.036167	1.540982699	0.011232
SRPX	-0.387977389	0.036118	1.429851664	0.023931
STAT1	-0.633400793	0.016494	-1.272018841	0.003775
STAT3	-0.972618741	0.036138	1.755397946	4.58E-07
SUN1	-0.450823867	0.038098	-0.872885661	0.043073

SYNM	0.325806265	0.04979	-1.464381185	0.005351
TACC1	-0.370545039	0.038676	1.464658566	1.73E-05
TACC2	0.563731348	0.003703	0.951365548	0.043192
TAX1BP1	0.279872161	0.036848	-1.262935914	0.024751
TAX1BP3	-1.445656879	0.023178	5	7.34E-06
TEAD4	-0.838120353	0.02039	1.917580892	0.000583
TEK	-0.665089599	0.042213	-1.904942937	0.000222
TGFB1	-0.48409647	0.035802	-1.545663311	0.005583
THBS4	1.196572038	0.048544	-2.120653978	0.002596
TIMM8B	-1.108598614	0.012035	5	5.43E-10
TIMP1	-1.008514924	0.028892	1.840233596	0.006884
TIMP3	-0.392285917	0.02239	2.182312486	4.85E-06
TMEM204	-0.652903815	0.021325	1.673222066	0.016904
TMSB4X	-0.518989998	0.049079	-1.498036021	0.0037
TSC1	-0.532485732	0.044115	-0.986793547	0.020307
TXNRD1	-0.397359953	0.043213	-0.917006565	0.005121
USP9X	0.696855665	0.033127	-1.591714262	0.022522
VSTM2L	-0.863262469	0.04021	3.223903018	5.23E-06
WDR26	0.434242526	0.048381	-1.326486608	0.015158
XIRP1	-0.78224014	0.048919	1.476941227	0.000878
ZFP36	-0.991785116	0.017465	1.859309472	0.002371
ZMIZ1	-0.698773614	0.039673	-1.134288226	0.033385

Supplemental Table 15. DEG shared between female obesity-related LVH and both dilated ischemia and cardiomyopathy datasets with (p_adj < 0.05)

Gene	log2FC NF vs LVH_F	p_adj	log2FC ISCH vs DCM	p_adj
ADAM19	-0.630142749	0.037114	1.489280792	0.002551
AKAP12	-0.731993228	0.026665	-1.06178257	0.015975
AP1S2	-0.789011417	0.015457	1.309426583	0.020855
APOD	-0.892669878	0.037102	-1.524595823	0.000468
APOL1	-0.782334647	0.021276	1.393911307	0.011075
ATE1	-0.823974167	0.02715	-1.582781094	0.001702
BCAR3	-0.799783333	0.044029	-1.610550008	0.004017
BTG2	-0.547514523	0.022147	1.982556367	0.000194
C1QTNF1	-0.866995909	0.004932	1.983690511	0.000181
C8orf4	-0.883640814	0.03769	-2.378198117	1.06E-06
CASP3	-0.66390716	0.043676	1.569891424	0.004874
CAST	1.51500001	0.003565	-0.923186229	0.005729
CCL2	0.861442892	0.041833	5.109077051	0.012536
CCL21	-1.998910656	0.034425	3.211259363	1.73E-08
CD151	0.472684984	0.037071	1.258355253	0.00377
CD68	0.939054502	0.044368	1.783816809	0.00035
CD93	-0.59718142	0.012803	1.638558045	0.000696
COL6A2	-0.400028873	0.018589	1.196810429	0.046365
CRIM1	-0.434102162	0.048377	1.280530737	0.0142
CTGF	-1.189465404	0.030305	1.712090851	0.00187
CXorf36	-0.529466638	0.04564	1.404338257	0.005522
DAPK2	0.74144734	0.046529	-1.29432394	0.012646
DIRAS3	-1.018644618	0.028944	-2.755293509	1.15E-09
DRAM2	-0.726386837	0.022444	5	1.19E-05
DYRK2	-0.486689622	0.045658	-1.060596127	0.047844
EFEMP1	-0.729911964	0.04534	1.867728848	3.00E-06
EFNB2	-0.534300677	0.031279	-1.914497416	0.000313
EGR1	-0.778673334	0.049178	-1.332175587	0.016758
EMILIN1	-0.571141425	0.039703	2.041043672	8.13E-06
ETFB	1.068367319	0.002431	-1.136020685	0.039885
FAM114A1	-0.712234668	0.019887	1.298243506	0.023462
FAM134B	-0.884094691	0.024207	-1.226478006	0.004017
FBXO40	0.559934599	0.049521	-1.302725083	0.048941
FKBP5	-0.517708568	0.043381	1.999049339	1.19E-05
FOS	-1.058578228	0.043634	1.617142342	0.021996
GADD45B	-0.530310364	0.032794	1.423620172	0.03675

GJA1	-0.35022164	0.049747	-1.835417002	0.000968
GLIPR2	-0.67926169	0.037362	1.940228249	0.005741
GPR157	-0.826733847	0.031724	-1.956324683	0.003773
HBA1	-3.400698784	0.001351	-2.7929336	4.60E-12
HBB	-5.455425115	0.000788	-2.22489195	1.09E-07
IL1R1	-0.511212184	0.037637	1.483566641	0.024324
IL33	-0.799078418	0.026093	1.634526823	0.021856
IL6ST	-0.346209222	0.036204	1.207790986	0.000608
IQGAP1	-0.864329128	0.028623	1.474355992	0.009234
ITGA6	-0.386557844	0.041332	1.585582568	0.000365
JAG1	-0.648073868	0.021947	-1.288054053	0.02486
KDR	-1.01649251	0.027446	-1.766277418	0.000681
KLHL38	0.335280765	0.045138	-1.661614181	0.001099
LAMP2	-0.988496109	0.017906	0.967998379	0.031384
LRRC14B	0.601273929	0.046813	-2.25222654	2.04E-06
MAPK8IP3	-0.589170794	0.045532	-1.122339641	0.000425
MLYCD	0.893456574	6.48E-06	-1.107128992	0.038156
MRPL33	0.685197212	5.81E-05	3.24989797	5.31E-05
MYO1B	-0.606313032	0.025112	1.770265741	0.000998
NCKIPSD	-0.409067028	0.043648	-0.881265111	0.048721
NEDD9	-0.524428571	0.046449	-2.282312678	1.31E-07
NNT	1.040709158	0.002013	-1.370583183	0.001314
NPPA	-2.896073668	0.032393	1.804016681	0.002728
NPPB	-2.213258402	0.014572	3.95062945	1.28E-12
NR1D2	-0.366189625	0.043119	1.769391525	0.000757
PDLIM3	-0.569792209	0.032775	-1.051610175	0.033209
PDLIM7	-0.579683763	0.028378	1.237640222	0.003134
PLA2G2A	-2.647052214	0.045658	3.345485111	2.17E-08
PLVAP	-1.265760002	0.017747	1.949632993	0.001075
PLXDC2	-2.032815142	0.011265	1.934162391	0.005957
PNMAL1	-0.634642632	0.049439	-1.904599535	0.000101
PROS1	-0.92499567	0.042894	1.897009877	9.67E-05
PTGDS	0.646333156	0.004501	-1.841490956	0.001027
PTX3	-1.366782142	0.018539	5	2.34E-05
QSOX1	0.570678641	0.035483	1.356787899	0.000798
RFTN1	-0.775743929	0.015701	1.201772963	0.036786
RNF145	-0.505423328	0.038072	5	1.05E-10
RNF185	-0.83124553	0.01517	5	7.02E-08
S100A1	1.472047839	0.000813	-1.356663715	0.0142
S100A9	-0.934970606	0.044725	2.81213663	0.000516
SAMHD1	-0.58759924	0.018941	1.816578453	0.002707

SDCBP	-0.798182227	0.031003	-1.519540572	3.79E-05
SERPINH1	-0.564001102	0.043145	1.273626761	0.012686
SLC6A6	-1.150709242	0.016902	1.147020506	0.034305
SLC7A8	-0.972640406	0.035062	1.870262997	0.000332
SPOP	-0.397007271	0.040271	5	2.65E-11
STAT3	-0.972618741	0.036138	1.106890148	0.003681
SUN1	-0.450823867	0.038098	-1.068370923	0.000884
TCEAL7	-0.553228932	0.045743	2.828337491	0.009234
TEAD4	-0.838120353	0.02039	1.594275865	0.009234
TEK	-0.665089599	0.042213	-1.674114374	0.001404
TGFB1	-0.48409647	0.035802	1.319426652	0.027066
THBS1	-0.377386586	0.048008	-1.958430312	6.76E-05
THBS2	-0.665188472	0.044745	2.628736021	1.33E-08
THBS4	1.196572038	0.048544	1.363856989	0.026136
TIMM8B	-1.108598614	0.012035	5	3.34E-11
TIMP1	-1.008514924	0.028892	1.891597357	0.000442
VAMP8	-0.563839444	0.035165	1.823924832	0.024876
VSTM2L	-0.863262469	0.04021	2.777014645	6.09E-05
ZMIZ1	-0.698773614	0.039673	-1.238874926	0.040865
ZNF436	-0.853453662	0.031663	1.7512317	0.03428
ZNF438	-0.411605766	0.049926	5	1.04E-11

Supplemental Table 16. DEG shared between male obesity-related LVH and ischemia datasets with (p_adj < 0.05)

Gene	log2FC NF vs LVH_M	p_adj	log2FC NF vs ISCH	p_adj
ABTB1	-0.460991597	0.012788	0.899951705	0.012014
ADAM9	0.324658867	0.038311	-1.296514971	0.0169
ADAMTS15	0.546947449	0.043257	1.328317163	0.004927
AIF1L	0.760356543	0.04817	1.666590241	0.000101
ALDH6A1	-0.459566879	0.008789	1.123273643	0.036902
ANTXR2	-0.239481735	0.033088	1.006537036	0.018857
APLN	0.42609975	0.027729	-2.034721693	0.001492
APLP1	-0.494267388	0.020786	-5	1.01E-09
AQP7	-0.339087891	0.040948	1.111539965	0.040004
ATP13A3	-0.303941208	0.047239	-2.110450865	6.16E-06
AZGP1	-1.307980325	0	-1.138888768	0.040662
AZIN1	-0.233055614	0.044509	-1.355458125	0.00242
B4GALNT3	-0.438156567	0.021696	1.300729904	0.006208
C10orf10	-0.776170461	3.00E-15	2.175525819	1.54E-07
C11orf96	-0.286254062	0.045204	2.224645005	5.09E-06
C3	0.99050202	0.025013	2.045972787	1.21E-05
CD151	-0.510771364	4.00E-15	-1.076847186	0.003615
CD300LG	0.770142832	0.020405	2.773023736	0
CDKN1A	-0.393196018	0.03855	1.066409299	0.042891
CEP85	-0.354319987	0.033799	1.377027078	0.004362
COL15A1	0.861245935	0.024047	-1.666558498	0.000493
COL4A3BP	-0.308889968	0.021196	-5	6.23E-08
COMMD6	-0.280205666	0.028834	-3.151519642	3.22E-07
COMP	-0.849294671	0.039889	-4.065207514	2.18E-07
CRNDE	-0.528269658	0.034849	-2.186615542	0.004521
CTIF	-0.340308488	0.035364	1.15914319	0.000568
DDAH1	-0.568797795	0.017604	-1.393084172	0.021863
DNAJA4	-0.739665528	0.045952	-1.318690893	0.005975
DYNLL1	-0.377506314	0.008446	-1.775643022	3.34E-05
EDNRB	0.572001611	0.015444	2.168141571	1.62E-11
ELK1	-0.345545015	0.016899	1.055086757	0.0086
ENO2	-0.475902084	0.007665	1.329284641	0.01159
ETV1	-0.348286938	0.047575	-1.585575868	0.000271
FLNC	-0.299205249	0.033991	1.534788946	0.000252
FMOD	-0.667877526	0.03788	-1.556832307	0.004055
FNDC5	0.420695209	0.019081	-1.197431896	0.003018

FSTL3	-0.413282056	0.011028	-1.278100975	0.030781
GLUL	-0.567151422	0.010959	1.511265015	4.26E-05
GPIHBP1	0.716162309	0.032929	2.175472642	1.92E-07
GPR153	-0.681905951	0.043028	-1.810031993	0.001268
GSTT1	-1.140967802	0.033376	1.379716623	0.004122
HCFC1R1	-0.269876232	0.028189	1.813783392	4.68E-09
HDAC5	-0.290056255	0.000133	1.016822647	0.003741
HEPH	-0.385669396	0.016989	-2.635587422	7.15E-08
HFE2	-0.416585779	0.021178	-5	2.01E-15
HIF3A	-0.36726417	0.031215	1.90209774	2.88E-11
HIPK3	0.347338792	0.026941	-5	1.85E-10
HIST1H2BD	-0.444623519	0.022086	-1.819527247	0.008223
HLA-B	0.583581342	0.049228	1.447469619	0.002137
IER5	-0.5107848	0.011172	1.11415786	0.032784
IGFBP2	-0.862259937	0	-2.089911786	5.79E-06
IL6ST	0.33077625	0.049957	-0.96627322	0.007438
IRX3	-0.407781337	0.043472	1.642289454	0.000158
ITGA6	0.49961087	0.032435	-1.130173886	0.004787
ITGB1	0.292811102	0.042933	-1.012564118	0.006673
ITPKB	0.68388826	0.022309	1.136878349	0.031003
JUP	-0.351730759	2.00E-15	1.340514078	0.000647
KCTD17	-0.563715606	3.80E-05	-1.477646367	0.021895
KLHL21	-0.309586543	0.03786	1.946075397	3.75E-05
KLHL31	0.331983204	0.041734	-1.242447658	0.022627
LDB3	-0.193086896	0.037827	0.780896708	0.021489
LDHA	-0.518131046	0.016036	-1.229179915	0.019527
LRRC14B	-0.582658557	6.69E-05	2.497809238	2.29E-09
MAOA	-0.292685908	0.017421	1.156827805	0.033939
MASP1	-0.627801182	9.84E-05	-1.201667492	0.015218
MFAP4	-0.36430884	0.013485	-1.750721346	0.002055
MT1X	-0.820480928	0.041477	-3.148047139	3.10E-06
MTMR14	-0.314430647	0.014979	1.060913826	0.00318
MTSS1	0.405885732	0.039649	1.302231648	0.008775
MYL4	1.123474745	1.01E-06	5.061522714	0
NAP1L1	-0.313200929	0.020236	-0.910734866	0.027081
NCEH1	0.470319732	0.040649	-5	1.70E-07
NDRG2	-0.146954763	0.035152	0.914021945	2.83E-06
NEAT1	-0.355959133	0.032055	1.359837777	0.042058
NPPA	-4.597666596	0.018249	-4.275261149	0
NPPB	-2.898570787	0.013588	-3.478505958	1.79E-13
NRTN	-0.748451624	0.001353	1.414942419	0.045468

OPA1	0.179786546	0.041586	-1.003990391	0.003612
OTUD1	-0.364965273	0.009595	1.307614166	0.008755
PDK4	-1.190849404	0.023484	-1.621761989	0.003644
PHLDA1	-0.967904287	0.013169	-1.533891972	0.00837
PIK3IP1	-0.515566884	0.034509	1.573888462	0.000162
PLEKHA6	-0.428192332	0.011977	1.556511571	0.00051
PLK2	-0.741565424	0.022569	1.372546472	0.009604
POR	-0.512484111	0.02111	1.351443234	0.004687
POSTN	-0.716023612	0.043196	-5.398096936	0
PPAP2B	0.270841062	0.049882	1.203371662	0.018584
PROS1	-0.634473414	0.022481	-1.777064031	0.000208
PTMS	-0.204572767	0.018308	1.586696097	0.000379
RASL10B	-0.604665337	0.017747	1.614289113	0.000481
RBM3	0.274338467	7.99E-15	1.527018038	0.000788
RPL28	-0.215383175	0.033283	0.86291538	0.047925
RPS27L	-0.453376267	0.038886	-1.237217046	0.026793
RRAS2	-0.417699346	0.008991	-5	9.89E-07
RXRG	-0.430989662	0.043663	-2.486881571	0.001101
SEC14L5	1.203995176	0.025826	2.532045159	4.07E-09
SH3BGR	-1.038419793	0.041381	-1.126205863	0.042774
SHISA3	0.929801987	0.049266	3.030175389	1.33E-08
SLC27A6	-0.725885867	0.012021	-1.314110357	0.029792
SLCO2A1	-0.40718502	0.038314	1.689613686	0.000169
SNHG8	-0.344159108	0.042777	1.326354211	0.025361
SOD3	-0.402059082	0.00539	-1.490774626	0.002217
SVOP	-1.064191722	0.034337	-2.07588899	0.003099
TFRC	1.359094592	0.041854	-1.626296372	0.000835
TGM2	-0.492854217	0.012428	1.284423864	0.028545
TIMM9	-0.248657524	0.033989	-5	1.94E-05
TIMP3	0.458961699	0.040691	1.659800666	0.004458
TMEM140	-0.89371551	1.20E-14	1.502983443	0.001443
TOM1	-0.405308093	0.030337	0.901618286	0.045771
TSPYL2	-0.85969565	0.0075	1.54357506	0.000704
TUBB6	0.430747751	0.023596	1.122036783	0.036911
TXNRD1	-0.490654157	0.036189	0.786257974	0.033516
UBAC2	-0.238098048	0.035092	-1.270103527	0.015028
UBE3A	-0.140145749	0.047775	-5	2.61E-09
UCHL1	-0.876726333	0.012504	-2.745991144	0.002544
UGT2B4	0.967809667	0.036872	-3.395510497	1.03E-05
ULK1	-0.386662051	0.013491	1.158112048	0.027754
VPS13D	0.260474561	0.044122	-5	6.36E-07

XIRP2	0.508831734	0.026453	-1.338335243	0.00205
XPR1	-0.404531859	0.040079	-0.992860816	0.035245
YPEL3	-0.784698444	4.00E-15	1.140709773	0.018303

Supplemental Table 17. DEG shared between male obesity-related LVH and dilated cardiomyopathy datasets with (p_adj < 0.05)

Gene	log2FC NF vs LVH_M	p_adj	log2FC NF vs DCM	p_adj
ABAT	-0.436324244	0.035648	-1.855169072	0.000245
ABCA8	0.648874255	0.042578	-1.940300807	0.002435
ABHD11	-0.294215215	0.032183	0.953401699	0.034878
ACOT11	-0.361296457	0.012581	-1.52973733	0.000207
ADAMTS15	0.546947449	0.043257	2.160891353	6.59E-06
AGPAT2	-0.305168768	0.014057	1.173437054	0.014742
AGPAT9	-0.472276352	0.029837	-1.692568564	0.017186
AIF1L	0.760356543	0.04817	-1.690830076	5.89E-05
ALDH1L1	-0.422880657	0.013817	1.464875776	0.00475
ALDH6A1	-0.459566879	0.008789	-1.487913517	0.003356
ANAPC11	-0.221336121	0.021095	0.824630217	0.002557
ANTXR2	-0.239481735	0.033088	-0.934274411	0.046
APLN	0.42609975	0.027729	-3.647631894	1.65E-07
APLP1	-0.494267388	0.020786	-5	3.22E-07
APRT	-0.2692331	0.048238	1.479862863	0.036549
AQP7	-0.339087891	0.040948	1.320446161	0.012755
AZGP1	-1.307980325	0	2.180581657	2.13E-06
AZIN1	-0.233055614	0.044509	-1.234736437	0.014779
B4GALNT3	-0.438156567	0.021696	-1.571730374	0.002181
BAMBI	-0.442504318	0.019297	1.432540867	0.011909
C10orf76	-0.378725282	0.014545	-1.837503291	0.007708
C11orf24	-0.333366417	0.011191	1.146685791	0.045062
C11orf96	-0.286254062	0.045204	1.838403629	0.010094
C1orf115	0.560171498	0.038375	1.522052774	0.004354
C1orf122	-0.293493497	0.012048	1.113214233	0.036556
C1QTNF1	-0.578503513	0.038739	2.113417594	0.001372
C3	0.99050202	0.025013	1.430493191	0.005785
C6orf1	-0.509148869	0.011928	1.462087575	0.00141
CAMK2B	-0.371924966	0.002571	0.782785864	0.024498
CAST	-0.150895471	0.043171	-1.367834595	0.000208
CCDC85B	-0.626416075	3.60E-14	1.451714992	0.003356
CCL2	0.671466177	9.02E-06	6.143199949	0.000908
CD151	-0.510771364	4.00E-15	-1.317019331	2.63E-06
CD300LG	0.770142832	0.020405	2.221769286	1.13E-11
CDH5	0.713600224	0.047911	-1.238663795	0.005578
CDK18	-0.206138497	0.038997	0.661435315	0.028167

CDKN1A	-0.393196018	0.03855	1.293184109	0.041044
CEBPB	-0.464728923	0.031278	1.446932885	0.038798
CEBPD	-0.492843424	0.035732	1.639611818	0.015646
CNN2	-0.234532303	0.032806	1.205382083	0.042821
COL23A1	-0.759281134	0.023043	1.965826273	0.00649
COL4A3BP	-0.308889968	0.021196	-5	1.04E-06
COMMD6	-0.280205666	0.028834	1.986287051	0.003216
CRELD1	-0.571053939	0.015765	1.119429701	0.003928
CTF1	-0.374627485	0.038807	1.46343487	0.003932
CTIF	-0.340308488	0.035364	-0.901524118	0.031209
CTNNA3	0.420902413	0.047603	-2.358489586	0.000779
CTSF	-0.609388393	0.012649	1.636528981	0.001335
CYGB	0.484721501	0.045147	1.603747399	0.000827
DCAF11	-0.23242679	0.017956	-0.8027819	0.034408
DKK3	-0.746405642	0.011774	-1.591477235	5.19E-05
DPM3	-0.372064209	0.01069	-1.330865471	0.04489
DSP	0.169735277	0.025423	-1.738090398	0.024171
EDF1	-0.314122494	6.00E-15	0.831908111	0.040718
EDNRB	0.572001611	0.015444	2.827625448	7.91E-13
EGLN3	-0.362429875	0.038702	1.213162938	0.017311
ELK1	-0.345545015	0.016899	1.195326989	0.002194
ELN	0.558139214	0.001639	3.353674038	7.56E-10
ENO1	0.36807835	0.045018	-1.04443571	0.039006
ENO2	-0.475902084	0.007665	2.196136473	0.0023
EPN1	-0.367415216	2.90E-14	1.140407858	0.034801
FAM134B	-0.446289424	0.009389	-1.884835279	0.00021
FAM58A	-0.428148244	0.013924	1.589540039	0.008686
FAM96B	-0.258604662	0.036243	1.007933098	0.042718
FAM98C	-0.299884112	0.038198	-5	0.00225
FGF12	0.915237306	0.016281	-1.357459243	0.041842
FMOD	-0.667877526	0.03788	-1.629519375	0.032014
FXYD1	-0.482324859	0.014267	1.416270491	0.002163
GADD45B	-0.497838091	0.034827	1.914790207	0.00068
GLUL	-0.567151422	0.010959	1.664537577	5.94E-08
GPIHBP1	0.716162309	0.032929	1.997394735	0.000878
GPNMB	0.834656999	0	-1.545983281	0.000353
GPR153	-0.681905951	0.043028	3.330351255	1.19E-10
HAGH	-0.269484135	0.033144	1.028491735	0.03694
HCFC1R1	-0.269876232	0.028189	2.009929055	7.11E-08
HDAC5	-0.290056255	0.000133	0.998631607	0.036506
HFE2	-0.416585779	0.021178	-5	9.12E-07

HIF3A	-0.36726417	0.031215	2.0184829	6.70E-10
HIST1H2BD	-0.444623519	0.022086	-1.796075408	0.0122
HIST3H2A	-0.390486066	0.040552	-1.888931371	0.048405
HLA-B	0.583581342	0.049228	-1.295070572	0.016126
HSPB2	-0.265488233	0.029863	1.552376496	0.031126
HSPBP1	-0.321175159	0.02344	1.023892449	0.014184
HSPE1	-0.626289358	0.017401	-1.424482306	0.044167
IER5	-0.5107848	0.011172	1.61853436	0.023403
IFI6	-0.347885446	0.032703	1.410291788	0.002942
IFT43	-0.501012542	0.009442	1.37413865	0.020028
IL6ST	0.33077625	0.049957	-5	1.49E-05
INMT	0.824405867	0.001049	-1.18429467	0.014254
IRX3	-0.407781337	0.043472	1.929352226	2.35E-05
ISCU	-0.134040132	0.028242	1.33769501	0.01322
ITGB1	0.292811102	0.042933	-0.980421554	0.045357
ITM2A	0.703262638	4.45E-05	-1.478001876	0.031951
ITPKB	0.68388826	0.022309	-1.228955592	0.023999
JOSD2	-0.384763927	0.002388	2.475679235	0.001562
JUP	-0.351730759	2.00E-15	-0.947178548	0.021847
KAT2B	0.27694211	0.045965	-1.988769812	0.003654
KCND3	0.403416768	0.04292	-5	1.18E-05
KIAA1462	0.656200891	0.044113	-1.673784644	0.019311
KIF1B	0.307621803	0.028657	-1.420263708	0.020581
KLC2	-0.277130347	0.047432	1.010816551	0.028992
KLF15	-0.700234622	0.017053	2.244450656	6.56E-06
KLHL21	-0.309586543	0.03786	-1.209988358	0.023398
KLHL31	0.331983204	0.041734	-1.879304514	0.001189
LDB3	-0.193086896	0.037827	0.661937621	0.036828
LDHA	-0.518131046	0.016036	-1.193485774	0.036046
LRRC10	-0.477986329	0.017955	-2.556754092	9.14E-05
MAFK	-0.41121213	0.017121	-1.600385839	0.000849
MASP1	-0.627801182	9.84E-05	-1.236931196	0.011745
METRN	-0.308008848	0.015824	1.393969653	0.016556
MFAP4	-0.36430884	0.013485	1.412504009	0.002207
MGLL	0.557831017	0.029221	1.082085931	0.021445
MKNK2	-0.56656081	0.036684	-0.940147819	0.03771
MLYCD	-0.398413389	0.025974	1.255474711	0.025587
MRPL55	-0.348486272	0.015397	1.25082383	0.000798
MTMR14	-0.314430647	0.014979	0.984248097	0.015083
MXI1	-0.44513223	5.68E-05	-1.014610918	0.034023
MXRA7	-0.533026994	0.009181	-1.012060794	0.014742

MYL4	1.123474745	1.01E-06	7.928132761	0
MYLK3	-0.294168859	0.037545	-1.349636972	0.037659
NCEH1	0.470319732	0.040649	-1.070742336	0.035032
NCOA4	0.20875989	2.30E-08	-1.608733137	0.004488
NDRG2	-0.146954763	0.035152	0.796941477	0.019726
NENF	-0.312674229	0.023928	1.113785717	0.041455
NOL3	-0.283878573	0.036899	1.412768463	0.000199
NRTN	-0.748451624	0.001353	2.237726854	0.013565
NT5C1A	0.656828147	0.046935	-2.854945342	0.0023
OPA1	0.179786546	0.041586	-5	4.03E-09
ORMDL3	-0.28424199	0.020082	1.083147377	0.040718
OTUD1	-0.364965273	0.009595	1.656789936	0.002426
PACS1	-0.267153098	0.01	1.081585456	0.020732
PDK4	-1.190849404	0.023484	-2.495837398	3.53E-08
PEBP4	-0.444188822	8.73E-09	1.357320348	0.002526
PHLDA1	-0.967904287	0.013169	-2.900790044	9.89E-09
PIK3IP1	-0.515566884	0.034509	1.628750929	0.000141
PLA2G16	-0.429325781	8.99E-15	1.062296467	0.006247
PLEKHA4	-0.4970689	0.020773	1.715005619	0.002446
PLEKHO1	-0.595716203	6.00E-15	1.581454714	0.030276
PLIN4	-0.342258388	0.037297	1.770077196	0.005091
PLP2	-0.41520749	9.72E-06	2.438307418	0.000171
PPAP2B	0.270841062	0.049882	-1.148180528	0.012479
PSME1	-0.187065181	0.044005	-1.220196145	0.026897
PTGR2	-0.240516468	0.042626	-1.384657793	0.018137
PTMS	-0.204572767	0.018308	2.640986855	3.74E-05
PTPRB	0.897075719	1.29E-08	-1.293901464	0.028365
QSOX1	-0.382599933	0.018983	1.402760158	0.000116
RAB40B	-0.497432018	1.33E-11	1.260992128	0.03673
RABAC1	-0.344457803	0.013844	1.466716007	0.048405
RAPGEF2	0.348172878	0.046195	-1.486548606	0.029188
RASL10B	-0.604665337	0.017747	1.34844708	0.010022
RBM3	0.274338467	7.99E-15	-1.142839467	0.013191
RHOC	-0.279578803	0	1.024149951	0.003138
RPL13	-0.259754186	0.03225	0.96882753	0.038432
RPL28	-0.215383175	0.033283	1.619734681	0.00747
RPL34	-0.19977586	0.032458	-1.135965587	0.045212
RPPH1	-0.443235403	0.046663	-1.490980417	0.007622
RPS27A	-0.320176756	0.019056	1.226988387	0.024042
RRP12	-0.500648788	0.026194	-1.312136309	0.00381
S1PR3	0.77952287	1.29E-08	3.072552131	9.00E-10

SGCA	-0.452258165	7.99E-15	0.975357587	0.00212
SGCG	-0.220288165	0.047528	1.390817319	0.00745
SH3BGR	-1.038419793	0.041381	-1.456364189	0.004471
SHISA3	0.929801987	0.049266	2.945548655	2.73E-05
SHISA4	-0.190293722	0.034849	1.167445824	0.012045
SLC16A1	0.342603538	0.047959	-1.5319772	0.015032
SLC25A29	-0.369212061	0.032238	1.485004892	0.035932
SLC27A6	-0.725885867	0.012021	-2.371207698	5.90E-05
SLCO2A1	-0.40718502	0.038314	3.644338952	4.74E-08
SNAP47	-0.449792851	0.036703	-1.291372522	0.025832
SNHG8	-0.344159108	0.042777	1.921250812	0.000585
SPARC	0.610476051	0.006824	2.314285316	0.00014
SPR	-0.578686275	0.008157	1.53937965	0.003249
ST6GALNAC4	-0.440998042	0.015328	1.038108792	0.027679
TCEAL3	-0.354979559	0.017945	1.259083776	0.040293
TCEB2	-0.262708567	0.038371	1.00029373	0.029824
TEAD1	0.289096382	0.029968	-1.8094642	0.003053
TGM2	-0.492854217	0.012428	2.399523907	0.001434
TIMM9	-0.248657524	0.033989	-5	0.006
TIMP3	0.458961699	0.040691	2.182312486	4.85E-06
TM4SF1	0.367067279	0.04299	-1.212879539	0.037013
TMEM140	-0.89371551	1.20E-14	1.440124571	0.005012
TNK2	-0.315040377	0.036253	1.394373146	0.042979
TNNI1	0.738987233	0.049448	9.276823467	0
TRNP1	-0.498430701	6.00E-15	1.369548495	0.014466
TSPYL2	-0.85969565	0.0075	2.390733186	2.13E-05
TUBB6	0.430747751	0.023596	1.642746812	0.030168
TXNRD1	-0.490654157	0.036189	-0.917006565	0.005121
UTRN	0.391412756	0.039902	-1.589898147	0.013508
VWF	0.704070796	0.019926	-1.135546205	0.027555
WDR62	1.072490247	2.15E-12	-1.109653992	0.011913
WISP2	-0.614891518	0.032136	2.328288849	0.002022
XIRP1	-0.317827132	0.036235	0.949858802	0.011572
XIRP2	0.508831734	0.026453	-1.017910018	0.001751
XPR1	-0.404531859	0.040079	-1.53208742	0.000285
YIF1B	-0.263588099	0.043766	1.10697907	0.029123
YPEL3	-0.784698444	4.00E-15	1.326294057	0.037659

Supplemental Table 18. DEG shared between male obesity-related LVH and both dilated ischemia and cardiomyopathy datasets with (p_adj < 0.05)

Gene	log2FC NF vs LVH_M	p_adj	log2FC ISCH vs DCM	p_adj
ABAT	-0.436324244	0.035648	1.402124026	0.014941
ABCA8	0.648874255	0.042578	-1.84507599	0.000274
ACOT11	-0.361296457	0.012581	1.184750634	0.014629
ADAM9	0.324658867	0.038311	1.186817111	0.031098
APLN	0.42609975	0.027729	-1.612910202	0.002372
AQP7	-0.339087891	0.040948	-1.44003696	0.001261
ATP13A3	-0.303941208	0.047239	1.838355362	0.000121
AZGP1	-1.307980325	0	1.813024958	0.000192
C1QTNF1	-0.578503513	0.038739	1.983690511	0.000181
C5orf46	-0.638118011	0.025592	2.279946307	0.048626
CAMK2B	-0.371924966	0.002571	-0.758761378	0.020855
CAST	-0.150895471	0.043171	-0.923186229	0.005729
CCL2	0.671466177	9.02E-06	5.109077051	0.012536
CD151	-0.510771364	4.00E-15	1.258355253	0.00377
CD300LG	0.770142832	0.020405	-1.275290819	0.007124
CHPF	-0.333975406	0.005284	1.502751997	0.018214
COL15A1	0.861245935	0.024047	1.680275526	0.000418
COL23A1	-0.759281134	0.023043	2.384872695	2.68E-05
COMMD6	-0.280205666	0.028834	2.877074001	3.04E-06
COMP	-0.849294671	0.039889	3.672769871	1.37E-06
CTNNA3	0.420902413	0.047603	-1.665848899	0.004357
DKK3	-0.746405642	0.011774	-1.17219224	0.001464
ELN	0.558139214	0.001639	2.405718414	2.62E-07
FAM134B	-0.446289424	0.009389	-1.226478006	0.004017
GADD45B	-0.497838091	0.034827	1.423620172	0.03675
GPR153	-0.681905951	0.043028	2.838701409	5.12E-07
GSTT1	-1.140967802	0.033376	-1.408853917	0.010118
HEPH	-0.385669396	0.016989	2.343603804	5.93E-07
HIPK3	0.347338792	0.026941	-1.575941651	6.26E-05
HIST3H2A	-0.390486066	0.040552	-1.597503693	0.044378
IGFBP2	-0.862259937	0	2.645422346	4.96E-07
IL6ST	0.33077625	0.049957	1.207790986	0.000608
ILVBL	-0.267348022	0.004582	-1.210007211	0.012376
IRX3	-0.407781337	0.043472	-1.18400673	0.014833
ITGA6	0.49961087	0.032435	1.585582568	0.000365
ITGB1	0.292811102	0.042933	1.208608991	0.000586

JOSD2	-0.384763927	0.002388	1.795954224	0.018766
KCND3	0.403416768	0.04292	-1.876821251	0.001093
KCTD17	-0.563715606	3.80E-05	2.047177058	0.002859
KLF15	-0.700234622	0.017053	1.466101481	0.017679
LDHA	-0.518131046	0.016036	1.163646348	0.034742
LRRC14B	-0.582658557	6.69E-05	-2.25222654	2.04E-06
MAFK	-0.41121213	0.017121	-1.418199767	0.005203
MLYCD	-0.398413389	0.025974	-1.107128992	0.038156
MRPL55	-0.348486272	0.015397	-1.182167424	0.001452
MT1X	-0.820480928	0.041477	1.515877998	0.048194
MTSS1	0.405885732	0.039649	-1.550740075	0.00301
MYL4	1.123474745	1.01E-06	2.866610047	1.24E-05
NOL3	-0.283878573	0.036899	-0.792023062	0.048467
NPPA	-4.597666596	0.018249	1.804016681	0.002728
NPPB	-2.898570787	0.013588	3.95062945	1.28E-12
PFKFB2	-0.500907657	0.03972	-1.879265511	2.54E-08
PHLDA1	-0.967904287	0.013169	-1.366898072	0.013516
PKIA	0.190572744	0.040133	0.958191615	0.03428
PLEKHA4	-0.4970689	0.020773	1.693949792	0.000295
PLK2	-0.741565424	0.022569	-2.454955955	5.88E-07
PLP2	-0.41520749	9.72E-06	1.488051412	0.015975
PLVAP	-1.298964363	3.00E-15	1.949632993	0.001075
PNPLA2	-0.47250156	1.80E-14	-1.203871191	0.03428
POSTN	-0.716023612	0.043196	4.131445065	0
PROS1	-0.634473414	0.022481	1.897009877	9.67E-05
QSOX1	-0.382599933	0.018983	1.356787899	0.000798
RAPGEF2	0.348172878	0.046195	-1.258547528	0.029287
RBM24	-0.241858165	0.043341	-1.241857132	0.035328
RRAS2	-0.417699346	0.008991	5	2.41E-05
S1PR3	0.77952287	1.29E-08	2.144826087	0.000239
SEC14L5	1.203995176	0.025826	-2.791126985	9.97E-09
SLCO2A1	-0.40718502	0.038314	1.954725266	0.004097
SPARC	0.610476051	0.006824	2.112232792	0.000418
SVOP	-1.064191722	0.034337	3.167780548	4.70E-05
SYNE1	0.420361736	0.039974	-1.017437725	0.025506
TBX20	0.935812719	0.0246	-2.297082344	1.42E-06
TFRC	1.359094592	0.041854	1.549593619	0.001462
THBS1	-0.525021016	0.028597	-1.958430312	6.76E-05
TIMM9	-0.248657524	0.033989	5	1.32E-05
TNNI1	0.738987233	0.049448	5.839519429	0
UGT2B4	0.967809667	0.036872	5	6.76E-05

WDR18	-0.426309848	0.035078	-1.180729841	0.024547
WISP2	-0.614891518	0.032136	1.907856911	0.005317
XIRP2	0.508831734	0.026453	1.365025666	0.000972

Supplemental Table 19. Gene ontology results for "biological processes" from Ingenuity Pathway Analysis

Term	Overlap	P-value	Adjusted P-value	Z-score	Combined Score	Genes
receptor guanylyl cyclase signaling pathway (GO:0007168)	2/11	9.9E-06	0.000403093	-2.73352782	21.36619446	NPPB; NPPA
oxygen transport (GO:0015671)	2/16	2.2E-05	0.000531633	-2.64329808	19.92929626	HBB; HBA1
cGMP biosynthetic process (GO:0006182)	2/16	2.2E-05	0.000531633	-2.62154671	19.76530058	NPPB; NPPA
hydrogen peroxide catabolic process (GO:0042744)	2/20	3.4E-05	0.000631627	-2.61014597	19.22949714	HBB; HBA1
gas transport (GO:0015669)	2/20	3.4E-05	0.000631627	-2.55343897	18.81172467	HBB; HBA1
regulation of blood vessel size (GO:0050880)	3/63	2.5E-06	0.000264119	-2.26273855	18.64295124	NPPB; NPPA; HBB
regulation of tube size (GO:0035150)	3/64	2.6E-06	0.000264119	-2.24830864	18.52406162	NPPB; NPPA; HBB
vascular process in circulatory system (GO:0003018)	3/86	6.3E-06	0.000322775	-2.29516194	18.44978297	NPPB; NPPA; HBB
reactive oxygen species metabolic process (GO:0072593)	3/84	5.9E-06	0.000322775	-2.24768357	18.06812556	PDK4; HBB; HBA1
cGMP metabolic process (GO:0046068)	2/24	4.9E-05	0.000840276	-2.45121922	17.35899443	NPPB; NPPA
circulatory system process (GO:0003013)	3/130	2.2E-05	0.000531633	-2.2966276	17.31555443	NPPB; NPPA; HBB
regulation of blood pressure (GO:0008217)	3/133	2.3E-05	0.000531633	-2.2953209	17.30570248	NPPB; NPPA; HBB
cyclic purine nucleotide metabolic process (GO:0052652)	2/33	9.4E-05	0.001277978	-2.52856174	16.84648204	NPPB; NPPA
cyclic nucleotide biosynthetic process (GO:0009190)	2/34	0.0001	0.001277978	-2.52746357	16.83916551	NPPB; NPPA
hydrogen peroxide metabolic process (GO:0042743)	2/33	9.4E-05	0.001277978	-2.45103358	16.3299525	HBB; HBA1
regulation of anatomical structure size (GO:0090066)	3/232	0.00012	0.001475084	-2.41140828	15.72006712	NPPB; NPPA; HBB
bicarbonate transport (GO:0015701)	2/31	8.3E-05	0.001277978	-2.32083616	15.46251535	HBB; HBA1
organophosphate biosynthetic process	3/436	0.00078	0.006685052	-2.38238235	11.93068786	NPPB; PLA2G2A;

(GO:0090407)						NPPA
cellular response to hydrogen peroxide (GO:0070301)	2/62	0.00034	0.003603955	-2.09511044	11.78651171	HBB; HBA1
cyclic nucleotide metabolic process (GO:0009187)	2/58	0.00029	0.003328491	-2.05442688	11.72099042	NPPB; NPPA
renal system process (GO:0003014)	2/71	0.00044	0.004489781	-2.16591455	11.70882865	NPPB; HBB
protein heterooligomerization (GO:0051291)	2/81	0.00057	0.005562119	-2.18198987	11.32840277	HBB; HBA1
cellular response to reactive oxygen species (GO:0034614)	2/89	0.00069	0.00640506	-2.17389801	10.97963498	HBB; HBA1
response to hydrogen peroxide (GO:0042542)	2/95	0.00079	0.006685052	-2.18694825	10.95197708	HBB; HBA1
purine ribonucleotide biosynthetic process (GO:0009152)	2/126	0.00138	0.011237257	-2.18473896	9.806245641	NPPB; NPPA
purine nucleotide biosynthetic process (GO:0006164)	2/132	0.00151	0.011846304	-2.20857659	9.796670106	NPPB; NPPA
response to reactive oxygen species (GO:0000302)	2/141	0.00172	0.01238831	-2.22873446	9.786377434	HBB; HBA1
cellular response to oxidative stress (GO:0034599)	2/148	0.00189	0.01238831	-2.22195018	9.756587623	HBB; HBA1
purine-containing compound biosynthetic process (GO:0072522)	2/146	0.00184	0.01238831	-2.20400803	9.677803611	NPPB; NPPA
ribose phosphate biosynthetic process (GO:0046390)	2/144	0.00179	0.01238831	-2.19585593	9.642007714	NPPB; NPPA
ribonucleotide biosynthetic process (GO:0009260)	2/140	0.0017	0.01238831	-2.19114785	9.621334546	NPPB; NPPA
negative regulation of cell growth (GO:0030308)	2/150	0.00194	0.01238831	-2.17058903	9.531060743	NPPB; NPPA
cellular response to external stimulus (GO:0071496)	2/185	0.00294	0.018147129	-2.27974751	9.140061513	NPPA; PDK4
nucleotide biosynthetic process (GO:0009165)	2/208	0.00369	0.02112531	-2.30417853	8.887869651	NPPB; NPPA
nucleoside phosphate biosynthetic process (GO:1901293)	2/209	0.00373	0.02112531	-2.3023159	8.880684986	NPPB; NPPA
positive regulation of renal sodium excretion (GO:0035815)	1/14	0.00628	0.02563726	-2.36912468	8.679782303	NPPB
cellular modified amino acid metabolic process (GO:0006575)	2/199	0.00339	0.020321255	-2.18054286	8.495586698	PLA2G2A; GSTT1

regulation of fatty acid oxidation (GO:0046320)	1/24	0.01075	0.029401443	-2.39620447	8.450721933	PDK4
response to insulin (GO:0032868)	2/246	0.00512	0.025330625	-2.28482003	8.398406997	NPPA; PDK4
negative regulation of growth (GO:0045926)	2/221	0.00416	0.022924024	-2.2225645	8.391447455	NPPB; NPPA
positive regulation of urine volume (GO:0035810)	1/13	0.00584	0.025330625	-2.26932608	8.341455256	NPPB
regulation of homeostatic process (GO:0032844)	2/314	0.00822	0.027502741	-2.30668843	8.289014758	NPPB; PDK4
regulation of renal sodium excretion (GO:0035813)	1/22	0.00986	0.029401443	-2.34779171	8.279984113	NPPB
regulation of sulfur metabolic process (GO:0042762)	1/17	0.00763	0.026820941	-2.28302805	8.261302138	PDK4
renal absorption (GO:0070293)	1/13	0.00584	0.025330625	-2.24317347	8.245325008	HBB
regulation of urine volume (GO:0035809)	1/18	0.00807	0.027446534	-2.29288751	8.244112312	NPPB
regulation of coenzyme metabolic process (GO:0051196)	1/14	0.00628	0.02563726	-2.24966527	8.242117842	PDK4
regulation of vascular permeability (GO:0043114)	1/27	0.01209	0.029401443	-2.32303767	8.192683755	NPPB
response to oxidative stress (GO:0006979)	2/290	0.00705	0.026820941	-2.25935012	8.175621808	HBB; HBA1
regulation of cofactor metabolic process (GO:0051193)	1/14	0.00628	0.02563726	-2.22720499	8.159829903	PDK4
phosphatidylglycerol acyl-chain remodeling (GO:0036148)	1/17	0.00763	0.026820941	-2.24878469	8.137390053	PLA2G2A
response to inorganic substance (GO:0010035)	2/370	0.01128	0.029401443	-2.29825494	8.105282199	HBB; HBA1
regulation of excretion (GO:0044062)	1/25	0.0112	0.029401443	-2.28068583	8.043321033	NPPB
negative regulation of anoikis (GO:2000811)	1/16	0.00718	0.026820941	-2.21378836	8.010753305	PDK4
regulation of acyl-CoA biosynthetic process (GO:0050812)	1/13	0.00584	0.025330625	-2.17524596	7.995641076	PDK4
response to peptide hormone (GO:0043434)	2/364	0.01093	0.029401443	-2.25871606	7.96583997	NPPA; PDK4
negative regulation of systemic arterial blood pressure (GO:0003085)	1/13	0.00584	0.025330625	-2.15854699	7.934259986	NPPA
response to peptide (GO:1901652)	2/384	0.01211	0.029401443	-2.23645603	7.887335279	NPPA; PDK4
regulation of anoikis (GO:2000209)	1/20	0.00897	0.028139038	-2.20456099	7.871599745	PDK4
regulation of acetyl-CoA biosynthetic process from	1/12	0.00539	0.025330625	-2.1368309	7.85443726	PDK4

pyruvate (GO:0010510)						
regulation of cell growth (GO:0001558)	2/322	0.00863	0.028139038	-2.19686961	7.844136932	NPPB; NPPA
positive regulation of macrophage derived foam cell differentiation (GO:0010744)	1/15	0.00673	0.026820941	-2.16462201	7.832841304	PLA2G2A
phosphatidylcholine acyl-chain remodeling (GO:0036151)	1/26	0.01164	0.029401443	-2.21865045	7.824540131	PLA2G2A
organic anion transport (GO:0015711)	2/328	0.00895	0.028139038	-2.18397702	7.798102678	HBB; HBA1
phosphatidylinositol acyl-chain remodeling (GO:0036149)	1/16	0.00718	0.026820941	-2.15382746	7.793780434	PLA2G2A
phosphatidylserine acyl-chain remodeling (GO:0036150)	1/17	0.00763	0.026820941	-2.14615106	7.766002824	PLA2G2A
phosphatidylethanolamine acyl-chain remodeling (GO:0036152)	1/23	0.0103	0.029401443	-2.1875258	7.714772466	PLA2G2A
carbohydrate derivative biosynthetic process (GO:1901137)	2/377	0.01169	0.029401443	-2.16057823	7.619736157	NPPB; NPPA
cellular response to fatty acid (GO:0071398)	1/27	0.01209	0.029401443	-2.15589578	7.603222498	PDK4
protein oligomerization (GO:0051259)	2/366	0.01104	0.029401443	-2.1468579	7.571348505	HBB; HBA1
protein-lipid complex remodeling (GO:0034368)	1/23	0.0103	0.029401443	-2.14232935	7.55537763	PLA2G2A
regulation of macrophage derived foam cell differentiation (GO:0010743)	1/28	0.01253	0.029727456	-2.14517339	7.541752258	PLA2G2A
phosphatidylserine metabolic process (GO:0006658)	1/27	0.01209	0.029401443	-2.13577782	7.532272253	PLA2G2A
low-density lipoprotein particle remodeling (GO:0034374)	1/11	0.00494	0.025330625	-2.04798395	7.527858869	PLA2G2A
macromolecular complex remodeling (GO:0034367)	1/23	0.0103	0.029401443	-2.13154487	7.517343872	PLA2G2A
cardiac muscle adaptation (GO:0014887)	1/13	0.00584	0.025330625	-2.0425056	7.507721883	NPPA
plasma lipoprotein particle remodeling (GO:0034369)	1/23	0.0103	0.029401443	-2.12240361	7.485105269	PLA2G2A
positive regulation of nitric oxide biosynthetic process (GO:0045429)	1/32	0.01431	0.03199631	-2.16432542	7.449899633	HBB
cellular amino acid metabolic process (GO:0006520)	2/421	0.01443	0.03199631	-2.15253741	7.409323703	PLA2G2A; GSTT1

muscle hypertrophy in response to stress (GO:0003299)	1/13	0.00584	0.025330625	-2.01519176	7.407323274	NPPA
cardiac muscle hypertrophy (GO:0003300)	1/17	0.00763	0.026820941	-2.03932258	7.379436253	NPPA
regulation of fatty acid biosynthetic process (GO:0042304)	1/29	0.01298	0.03042917	-2.09889379	7.330079239	PDK4
cardiac muscle hypertrophy in response to stress (GO:0014898)	1/13	0.00584	0.025330625	-1.96695067	7.230001514	NPPA
regulation of bone resorption (GO:0045124)	1/33	0.01476	0.032022137	-2.09602489	7.213108818	PDK4
striated muscle hypertrophy (GO:0014897)	1/18	0.00807	0.027446534	-2.00283531	7.201225173	NPPA
glutathione derivative biosynthetic process (GO:1901687)	1/27	0.01209	0.029401443	-2.0370459	7.184073249	GSTT1
glutathione derivative metabolic process (GO:1901685)	1/27	0.01209	0.029401443	-2.03284516	7.16925846	GSTT1
striated muscle adaptation (GO:0014888)	1/23	0.0103	0.029401443	-2.03178992	7.165536941	NPPA
regulation of vasodilation (GO:0042312)	1/39	0.01742	0.035889962	-2.14413362	7.13417069	NPPB
muscle hypertrophy (GO:0014896)	1/20	0.00897	0.028139038	-1.9959265	7.126649966	NPPA
phosphatidic acid metabolic process (GO:0046473)	1/31	0.01387	0.031430911	-2.05771477	7.119617883	PLA2G2A
phosphatidic acid biosynthetic process (GO:0006654)	1/31	0.01387	0.031430911	-2.05288489	7.102906657	PLA2G2A
anion transport (GO:0006820)	2/443	0.0159	0.03343286	-2.0855864	7.087273147	HBB; HBA1
alditol phosphate metabolic process (GO:0052646)	1/35	0.01564	0.033242025	-2.06963168	7.044902841	PLA2G2A
muscle adaptation (GO:0043500)	1/28	0.01253	0.029727456	-1.98762912	6.987876347	NPPA
phosphatidylglycerol metabolic process (GO:0046471)	1/34	0.0152	0.032638693	-2.0191409	6.910018702	PLA2G2A
plasma lipoprotein particle organization (GO:0071827)	1/31	0.01387	0.031430911	-1.99698297	6.909488048	PLA2G2A
protein-lipid complex subunit organization (GO:0071825)	1/33	0.01476	0.032022137	-1.97523612	6.797435056	PLA2G2A
negative regulation of blood pressure (GO:0045776)	1/39	0.01742	0.035889962	-2.03903955	6.784491452	NPPA
regulation of bone	1/40	0.01786	0.036074095	-	6.697027835	PDK4

remodeling (GO:0046850)				2.01585324		
regulation of nitric oxide biosynthetic process (GO:0045428)	1/44	0.01963	0.038879911	-1.97249456	6.405237357	HBB
platelet aggregation (GO:0070527)	1/40	0.01786	0.036074095	-1.89768215	6.304442187	HBB
somatic stem cell maintenance (GO:0035019)	1/44	0.01963	0.038879911	-1.88279094	6.113944817	PLA2G2A
glutathione metabolic process (GO:0006749)	1/49	0.02184	0.042838953	-1.87070624	5.893299843	GSTT1
response to fatty acid (GO:0070542)	1/50	0.02228	0.043288255	-1.85563355	5.826455398	PDK4
regulation of tissue remodeling (GO:0034103)	1/58	0.0258	0.048294438	-1.87961093	5.696046012	PDK4
regulation of pH (GO:0006885)	1/52	0.02316	0.044160653	-1.80164344	5.620985349	PDK4
regulation of fatty acid metabolic process (GO:0019217)	1/72	0.03194	0.055696595	-1.9297141	5.572698345	PDK4
defense response to Gram-positive bacterium (GO:0050830)	1/52	0.02316	0.044160653	-1.76201285	5.497341041	PLA2G2A
body fluid secretion (GO:0007589)	1/71	0.03151	0.055407562	-1.89751252	5.489578097	NPPB
negative regulation of angiogenesis (GO:0016525)	1/64	0.02844	0.052267585	-1.83661158	5.420536652	NPPB
negative regulation of blood vessel morphogenesis (GO:2000181)	1/66	0.02932	0.053398367	-1.8467018	5.410790326	NPPB
cellular response to mechanical stimulus (GO:0071260)	1/67	0.02976	0.053716999	-1.84921783	5.407160611	NPPA
homotypic cell-cell adhesion (GO:0034109)	1/57	0.02536	0.047910801	-1.75912968	5.344964784	HBB
negative regulation of vasculature development (GO:1901343)	1/70	0.03107	0.055407562	-1.84564916	5.339535356	NPPB
cellular response to starvation (GO:0009267)	1/74	0.03282	0.056735959	-1.85678295	5.32775474	PDK4
positive regulation of inflammatory response (GO:0050729)	1/88	0.03892	0.065075659	-1.93289789	5.281072705	PLA2G2A
phosphatidylcholine metabolic process (GO:0046470)	1/62	0.02756	0.051114936	-1.74559521	5.190838994	PLA2G2A
monovalent inorganic cation homeostasis (GO:0055067)	1/82	0.03631	0.061723153	-1.84987596	5.15208244	PDK4
pyruvate metabolic process (GO:0006090)	1/71	0.03151	0.055407562	-1.77809292	5.144092529	PDK4

female pregnancy (GO:0007565)	1/85	0.03761	0.063414586	-1.85992222	5.129779653	NPPA
cellular response to nutrient levels (GO:0031669)	1/99	0.04369	0.071871484	-1.93686747	5.09953128	PDK4
regulation of glucose metabolic process (GO:0010906)	1/94	0.04152	0.068865042	-1.90292583	5.091480909	PDK4
ethanolamine-containing compound metabolic process (GO:0042439)	1/81	0.03587	0.061495055	-1.79894728	5.016901485	PLA2G2A
regulation of lipid biosynthetic process (GO:0046890)	1/113	0.04973	0.078635729	-1.95971673	4.98342072	PDK4
negative regulation of epithelial cell proliferation (GO:0050680)	1/110	0.04843	0.077800036	-1.93886197	4.951103869	PLA2G2A
response to starvation (GO:0042594)	1/106	0.04671	0.07623123	-1.91045262	4.917474601	PDK4
cellular response to extracellular stimulus (GO:0031668)	1/119	0.0523	0.082075886	-1.93929572	4.848454594	PDK4
positive regulation of homeostatic process (GO:0032846)	1/130	0.05701	0.08551943	-1.94446727	4.781467733	NPPB
cellular response to acid chemical (GO:0071229)	1/147	0.06425	0.091587408	-1.98818964	4.752690749	PDK4
phosphatidylinositol metabolic process (GO:0046488)	1/125	0.05487	0.083540694	-1.91436713	4.752265974	PLA2G2A
positive regulation of response to wounding (GO:1903036)	1/130	0.05701	0.08551943	-1.92665788	4.737674233	PLA2G2A
peptide metabolic process (GO:0006518)	1/113	0.04973	0.078635729	-1.85387676	4.714277173	GSTT1
stem cell maintenance (GO:0019827)	1/109	0.048	0.077720098	-1.84172747	4.704953231	PLA2G2A
cellular biogenic amine metabolic process (GO:0006576)	1/125	0.05487	0.083540694	-1.88164422	4.671033906	PLA2G2A
cellular amine metabolic process (GO:0044106)	1/125	0.05487	0.083540694	-1.87913714	4.664810279	PLA2G2A
insulin receptor signaling pathway (GO:0008286)	1/148	0.06467	0.091587408	-1.94291262	4.644457778	PDK4
multi-multicellular organism process (GO:0044706)	1/121	0.05316	0.082785256	-1.8619101	4.638958887	NPPA
regulation of cellular carbohydrate metabolic process (GO:0010675)	1/137	0.06	0.088694451	-1.90665765	4.618988666	PDK4
amine metabolic process (GO:0009308)	1/134	0.05872	0.087437681	-1.88203617	4.586200233	PLA2G2A
regulation of carbohydrate metabolic	1/145	0.0634	0.091084176	-1.91022418	4.576842093	PDK4

process (GO:0006109)						
carbohydrate homeostasis (GO:0033500)	1/143	0.06255	0.090500943	-1.90358622	4.573166033	PDK4
glucose homeostasis (GO:0042593)	1/143	0.06255	0.090500943	-1.90108069	4.567146763	PDK4
regulation of ion homeostasis (GO:2000021)	1/160	0.06975	0.096798699	-1.95252547	4.559384651	NPPB
glucose metabolic process (GO:0006006)	1/149	0.0651	0.091587408	-1.89429783	4.528246002	PDK4
regulation of cellular ketone metabolic process (GO:0010565)	1/178	0.07732	0.103654301	-1.99449004	4.520898482	PDK4
multi-organism reproductive process (GO:0044703)	1/140	0.06128	0.08993087	-1.87348024	4.512678108	NPPA
xenobiotic metabolic process (GO:0006805)	1/156	0.06806	0.095100819	-1.86636234	4.391210346	GSTT1
regulation of blood circulation (GO:1903522)	1/204	0.08816	0.111704914	-1.99570569	4.374376481	NPPB
positive regulation of response to external stimulus (GO:0032103)	1/201	0.08691	0.111345309	-1.98683895	4.361347956	PLA2G2A
response to mechanical stimulus (GO:0009612)	1/176	0.07648	0.103654301	-1.91921018	4.350262098	NPPA
cellular response to insulin stimulus (GO:0032869)	1/195	0.08442	0.110396313	-1.97115366	4.343789029	PDK4
regulation of angiogenesis (GO:0045765)	1/179	0.07774	0.103654301	-1.91256909	4.335208772	NPPB
cellular amide metabolic process (GO:0043603)	1/177	0.0769	0.103654301	-1.90686125	4.322270856	GSTT1
hexose metabolic process (GO:0019318)	1/187	0.08109	0.106719788	-1.92848107	4.315070283	PDK4
defense response to bacterium (GO:0042742)	1/179	0.07774	0.103654301	-1.89719298	4.300355833	PLA2G2A
response to hypoxia (GO:0001666)	1/241	0.10339	0.1240641	-2.03780663	4.252814632	NPPA
response to decreased oxygen levels (GO:0036293)	1/245	0.10502	0.124557829	-2.03765987	4.244415298	NPPA
regulation of vasculature development (GO:1901342)	1/197	0.08525	0.110774178	-1.91926706	4.222889581	NPPB
response to oxygen levels (GO:0070482)	1/259	0.11071	0.128326022	-2.0533001	4.215797179	NPPA
glycerophospholipid biosynthetic process (GO:0046474)	1/178	0.07732	0.103654301	-1.85850686	4.212666243	PLA2G2A
response to bacterium (GO:0009617)	1/201	0.08691	0.111345309	-1.9173704	4.208856224	PLA2G2A
transcription initiation from RNA polymerase II promoter (GO:0006367)	1/187	0.08109	0.106719788	-1.88035219	4.207379574	NPPA

cellular response to abiotic stimulus (GO:0071214)	1/232	0.0997	0.121793771	-1.97971767	4.168149185	NPPA
regulation of lipid metabolic process (GO:0019216)	1/245	0.10502	0.124557829	-1.98657852	4.138013601	PDK4
regulation of epithelial cell proliferation (GO:0050678)	1/258	0.11031	0.128326022	-2.01373413	4.134561082	PLA2G2A
regulation of inflammatory response (GO:0050727)	1/247	0.10583	0.124799244	-1.98605804	4.133083846	PLA2G2A
response to acid chemical (GO:0001101)	1/275	0.11718	0.132070091	-2.02976969	4.109111444	PDK4
cellular response to peptide hormone stimulus (GO:0071375)	1/261	0.11152	0.128535376	-1.99780837	4.098605974	PDK4
monosaccharide metabolic process (GO:0005996)	1/221	0.09518	0.118399598	-1.92031113	4.09734855	PDK4
glycerolipid biosynthetic process (GO:0045017)	1/202	0.08733	0.111345309	-1.86097981	4.085072172	PLA2G2A
cellular response to peptide (GO:1901653)	1/273	0.11637	0.131890227	-1.99892269	4.049388232	PDK4
DNA-templated transcription, initiation (GO:0006352)	1/220	0.09477	0.118399598	-1.89256968	4.038156913	NPPA
phospholipid biosynthetic process (GO:0008654)	1/206	0.08899	0.112059235	-1.84130636	4.030118151	PLA2G2A
positive regulation of defense response (GO:0031349)	1/272	0.11597	0.131890227	-1.98124152	4.013569974	PLA2G2A
single organismal cell-cell adhesion (GO:0016337)	1/235	0.10093	0.122561368	-1.90358593	3.995899863	HBB
muscle system process (GO:0003012)	1/237	0.10175	0.122824304	-1.89958782	3.98343636	NPPA
positive regulation of secretion (GO:0051047)	1/273	0.11637	0.131890227	-1.96230497	3.975208583	NPPB
glycerophospholipid metabolic process (GO:0006650)	1/229	0.09847	0.121748516	-1.88193914	3.962983126	PLA2G2A
lipid catabolic process (GO:0016042)	1/232	0.0997	0.121793771	-1.87427142	3.946139893	PLA2G2A
cellular response to lipid (GO:0071396)	1/315	0.13317	0.145271214	-2.04511867	3.945346484	PDK4
response to nutrient levels (GO:0031667)	1/291	0.12361	0.137789387	-1.98911959	3.942492597	PDK4
single organism cell adhesion (GO:0098602)	1/259	0.11071	0.128326022	-1.89852701	3.898019985	HBB
response to extracellular stimulus (GO:0009991)	1/313	0.13237	0.145271214	-1.9809919	3.821636155	PDK4
phospholipid metabolic process (GO:0006644)	1/288	0.1224	0.137199649	-1.89627255	3.766600533	PLA2G2A
regulation of response to wounding (GO:1903034)	1/347	0.14577	0.156508623	-1.99853017	3.706562333	PLA2G2A

glycerolipid metabolic process (GO:0046486)	1/296	0.1256	0.139257235	-1.87625128	3.69890266	PLA2G2A
sulfur compound metabolic process (GO:0006790)	1/314	0.13277	0.145271214	-1.87362498	3.614508959	GSTT1
defense response to other organism (GO:0098542)	1/328	0.1383	0.150075488	-1.89956945	3.602755435	PLA2G2A
regulation of system process (GO:0044057)	1/371	0.15511	0.165669999	-1.99392402	3.584591709	NPPB
cellular response to organonitrogen compound (GO:0071417)	1/411	0.17049	0.181140749	-2.06158381	3.522176632	PDK4
alcohol metabolic process (GO:0006066)	1/340	0.14303	0.154376223	-1.87990284	3.512340243	PLA2G2A
cellular response to nitrogen compound (GO:1901699)	1/438	0.18072	0.191021163	-2.05282397	3.398185388	PDK4
cellular response to hormone stimulus (GO:0032870)	1/462	0.18972	0.197615928	-2.00324322	3.248118432	PDK4
cation homeostasis (GO:0055080)	1/465	0.19084	0.197615928	-1.92251321	3.117220381	PDK4
response to other organism (GO:0051707)	1/462	0.18972	0.197615928	-1.92119481	3.115082683	PLA2G2A
nitrogen compound transport (GO:0071705)	1/464	0.19047	0.197615928	-1.89214096	3.067973915	HBB
blood coagulation (GO:0007596)	1/472	0.19345	0.197615928	-1.88619266	3.058329153	HBB
coagulation (GO:0050817)	1/472	0.19345	0.197615928	-1.88360204	3.054128643	HBB
hemostasis (GO:0007599)	1/478	0.19568	0.197615928	-1.87614674	3.042040403	HBB
monocarboxylic acid metabolic process (GO:0032787)	1/473	0.19382	0.197615928	-1.8611017	3.017645924	PDK4
lipid biosynthetic process (GO:0008610)	1/491	0.20049	0.201474791	-1.88047736	3.012695878	PLA2G2A
organic hydroxy compound metabolic process (GO:1901615)	1/476	0.19494	0.197615928	-1.85637011	3.009973985	PLA2G2A
gene expression (GO:0010467)	1/672	0.26483	0.264834524	-1.84167319	2.446939247	NPPA

Supplemental Table 20. Gene ontology results for "cellular component" from Ingenuity Pathway Analysis

Term	Overlap	P-value	Adjusted P-value	Z-score	Combined Score	Genes
endocytic vesicle lumen (GO:0071682)	2/16	2.2E-05	0.000387551	-2.4661	19.37315594	HBB; HBA1
hemoglobin complex (GO:0005833)	2/12	1.2E-05	0.000387551	-2.4402	19.16928532	HBB; HBA1
extracellular region (GO:0005576)	5/1585	0.0003	0.003581419	-2.6121	14.71140055	NPPB; NPPA; PLA2G2A; HBB; HBA1
cytoplasmic membrane-bounded vesicle lumen (GO:0060205)	2/76	0.0005	0.00363052	-2.137	12.00654638	HBB; HBA1
vesicle lumen (GO:0031983)	2/76	0.0005	0.00363052	-2.1108	11.85949491	HBB; HBA1
blood microparticle (GO:0072562)	2/161	0.00223	0.013404023	-2.522	10.87518376	HBB; HBA1
cytosolic part (GO:0044445)	2/198	0.00335	0.0161741	-2.1824	9.000859897	HBB; HBA1
extracellular vesicular exosome (GO:0070062)	5/2717	0.00361	0.0161741	-2.1092	8.699115282	PLA2G2A; HBB; GSTT1; HBA1; HIST1H2AC
cytoplasmic vesicle part (GO:0044433)	2/363	0.01087	0.034211899	-2.2201	7.493233854	HBB; HBA1
extracellular space (GO:0005615)	3/1120	0.0114	0.034211899	-2.0031	6.760721979	NPPB; NPPA; PLA2G2A
mast cell granule (GO:0042629)	1/18	0.00807	0.029061036	-1.8919	6.694189763	NPPA
cytosolic small ribosomal subunit (GO:0022627)	1/39	0.01742	0.048232212	-1.8421	5.584864766	HBA1
dendritic spine (GO:0043197)	1/71	0.03151	0.061430179	-1.8738	5.227635379	MYL7
neuron spine (GO:0044309)	1/74	0.03282	0.061430179	-1.8378	5.127284847	MYL7
myosin complex (GO:0016459)	1/64	0.02844	0.061430179	-1.8348	5.118816301	MYL7
small ribosomal subunit (GO:0015935)	1/62	0.02756	0.061430179	-1.7713	4.941658002	HBA1
nucleosome (GO:0000786)	1/71	0.03151	0.061430179	-1.7524	4.888981784	HIST1H2AC
DNA packaging complex (GO:0044815)	1/77	0.03413	0.061430179	-1.7301	4.826699714	HIST1H2AC
DNA bending complex (GO:1990104)	1/71	0.03151	0.061430179	-1.7266	4.816889438	HIST1H2AC
protein-DNA complex (GO:0032993)	1/98	0.04325	0.074149599	-1.7808	4.633022425	HIST1H2AC
A band (GO:0031672)	1/9	0.00404	0.0161741	-1.0513	4.336048765	MYL7

contractile fiber part (GO:0044449)	1/167	0.0727	0.113794974	-1.834	3.985955491	MYL7
secretory granule (GO:0030141)	1/176	0.07648	0.114725126	-1.8347	3.972485589	PLA2G2A
ribosomal subunit (GO:0044391)	1/135	0.05915	0.096785732	-1.6955	3.959505965	HBA1
mitochondrial matrix (GO:0005759)	1/208	0.08982	0.129335749	-1.8608	3.805919731	PDK4
mitochondrion (GO:0005739)	2/1269	0.10762	0.138442768	-1.8445	3.647181286	PLA2G2A; PDK4
lytic vacuole (GO:0000323)	1/261	0.11152	0.138442768	-1.799	3.557232948	NPPA
lysosome (GO:0005764)	1/261	0.11152	0.138442768	-1.7797	3.519025579	NPPA
vacuole (GO:0005773)	1/293	0.12441	0.149286509	-1.7819	3.388910633	NPPA
cytosol (GO:0005829)	3/2529	0.09443	0.130743337	-1.6311	3.318418288	HBB; GSTT1; HBA1
mitochondrial inner membrane (GO:0005743)	1/341	0.14342	0.166549167	-1.7749	3.181532604	PDK4
organelle inner membrane (GO:0019866)	1/360	0.15084	0.169696037	-1.777	3.151907437	PDK4
perinuclear region of cytoplasm (GO:0048471)	1/411	0.17049	0.185984084	-1.7534	2.949390315	NPPA
mitochondrial membrane (GO:0031966)	1/457	0.18786	0.193223696	-1.7167	2.822023032	PDK4
cytoplasmic membrane-bounded vesicle (GO:0016023)	1/492	0.20086	0.200856006	-1.7176	2.757096016	PLA2G2A
endoplasmic reticulum membrane (GO:0005789)	1/449	0.18486	0.193223696	-1.6636	2.734740612	PLA2G2A

Supplemental Table 21. Gene ontology results for "molecular function" from Ingenuity Pathway Analysis

Term	Overlap	P-value	Adjusted P-value	Z-score	Combined Score	Genes
oxidoreductase activity, acting on peroxide as acceptor (GO:0016684)	3/42	7.17024E-07	8.60429E-06	-2.456896157	28.65539296	HBB; GSTT1; HBA1
peroxidase activity (GO:0004601)	3/42	7.17024E-07	8.60429E-06	-2.4349774	28.39974903	HBB; GSTT1; HBA1
oxygen transporter activity (GO:0005344)	2/14	1.6335E-05	9.801E-05	-2.775041681	25.6148578	HBB; HBA1
antioxidant activity (GO:0016209)	3/70	3.39748E-06	2.71798E-05	-2.280737145	23.97747229	HBB; GSTT1; HBA1
oxygen binding (GO:0019825)	2/37	0.000118911	0.000570771	-2.395657228	17.89202107	HBB; HBA1
hormone activity (GO:0005179)	2/122	0.001291935	0.00516774	-2.332161538	12.27957659	NPPB; NPPA
tetrapyrrole binding (GO:0046906)	2/146	0.001842388	0.005527164	-2.271718933	11.80857763	HBB; HBA1
heme binding (GO:0020037)	2/137	0.001624924	0.005527164	-2.266033372	11.77902362	HBB; HBA1
iron ion binding (GO:0005506)	2/172	0.00254417	0.006784455	-2.29969838	11.48267312	HBB; HBA1
glutathione peroxidase activity (GO:0004602)	1/18	0.00807251	0.01614502	-2.574585679	10.62311032	GSTT1
peptide hormone receptor binding (GO:0051428)	1/17	0.007625562	0.01614502	-2.364306114	9.755466632	NPPA
glutathione transferase activity (GO:0004364)	1/25	0.011196142	0.020669801	-2.511179384	9.741069625	GSTT1
phospholipase A2 activity (GO:0004623)	1/29	0.012977146	0.022246536	-2.390870595	9.098622916	PLA2G2A
calcium-dependent phospholipase A2 activity (GO:0047498)	1/9	0.004043525	0.00970446	-1.704169377	7.899114285	PLA2G2A
transferase activity, transferring alkyl or aryl (other than	1/54	0.024043964	0.038470342	-2.029011138	6.610249768	GSTT1

methyl) groups (GO:0016765)						
calcium ion binding (GO:0005509)	2/698	0.037207026	0.055810538	-2.186146214	6.308764498	MYL7; PLA2G2A
phospholipase activity (GO:0004620)	1/90	0.039786418	0.056169061	-2.073175967	5.969480469	PLA2G2A
lipase activity (GO:0016298)	1/105	0.046278873	0.061705164	-2.100801189	5.851545715	PLA2G2A
carboxylic ester hydrolase activity (GO:0052689)	1/111	0.048864909	0.061724095	-2.056264556	5.726863137	PLA2G2A
hormone receptor binding (GO:0051427)	1/160	0.069752004	0.083702404	-2.116892259	5.250924951	NPPA
phospholipid binding (GO:0005543)	1/296	0.125604565	0.143548074	-2.270665579	4.407555553	PLA2G2A
protein heterodimerization activity (GO:0046982)	1/408	0.169341136	0.184735784	-2.209302288	3.73113304	HIST1H2AC
protein serine/threonine kinase activity (GO:0004674)	1/449	0.184858766	0.192896104	-2.252252364	3.706314502	PDK4
ATP binding (GO:0005524)	1/1494	0.5028586	0.5028586	-2.111794514	1.451745246	PDK4

CHAPTER 3

Obese Zucker Rats Share Similar Sex- and BMI-Specific Gene-Expression Signature with Human Left Ventricular Hypertrophy

Mackenzie S. Newman[1], Janelle Stricker[1,2,#], Han-Gang Yu[1,*]

[1] Physiology and Pharmacology, West Virginia University, Morgantown, WV, USA

[2] Exercise Physiology, West Virginia University, Morgantown, WV, USA

[#] present address: Pharmacology, California Institute for Biomedical Research, La Jolla, CA, USA

Abstract

Background: We recently identified in human cardiac hypertrophy a gene expression signature containing nine differentially-expressed genes (DEG) that are body-mass index (BMI) and sex-dependent. To study mechanistic roles of these genes in hypertrophy, we asked whether these nine genes are differentially expressed in OZR known to develop cardiac hypertrophy.

Results: Rat LV were grouped according to sex (male, female) and obesity (obese, lean). OZR hypertrophy was characterized by increased left ventricular (LV) mass, LV inner diameter, inter-ventricular septum, and LV wall thickness in a sex-specific manner. Altered electrophysiology in OZR was characterized by decreased resting heart rate, increased ST elevation, and suppressed sympathetic activity. 89 DEG were found when comparing all samples for obesity, but males alone had 2859 DEG and females had 826. Obese humans and rats shared 337 DEG. Five DEG in human LVH previously identified (Hbb, Hist1h2ac, Nppa, Nppb, Pdk4) were validated by qPCR and protein expression in OZR.

Conclusions: We identified a five-gene expression signature that is shared between rat and human LVH in an obesity and sex-specific manner. Expression of established biomarkers Anp/Nppa and Bnp/Nppb were already significantly increased in hypertrophy compared to controls, with the absolute levels of Nppa significantly higher than Nppb. New genes (Hbb, Hist1h2ac, Pdk4) may provide potential new targets for early prognostic diagnosis in sex-dependent obesity-related cardiac LVH.

Background

Obesity has been recognized as an independent risk for cardiovascular disease (1, 34). In fact, a high rate of sudden cardiac death in morbid obesity had been recognized in ancient times (13). High prevalence of sudden cardiac death also occurs in young obese people (7). For every 1

kg/m^2 increase in body mass index (BMI), the HF risk is increased by 5% in men and 7% in women (37). In ventricular biopsy samples from obese patients, the number of adipocytes increases as the ejection fraction decreases (46). How these excessive adipocytes contribute to HF is unknown on the molecular level.

While HF is frequently the final state of cardiovascular disease, cardiac hypertrophy is a major independent predictor of progressive heart disease and increased mortality (15). Cardiac hypertrophy is also one of the most common independent features in obesity, even in the absence of hypertension or diabetes mellitus (1, 3, 31, 58, 76, 79). Myocyte hypertrophy has been found to be the most common cause of sudden cardiac death in morbid obese patients (19). Advances in studies of signaling pathways in both physiological and pathological hypertrophies have led to a recent proposal that aims to treat cardiac hypertrophy as a new therapeutic target (10, 25). Development of cardiac hypertrophy in obesity, especially in a sex-dependent manner, is an important question with significant clinical relevance.

Our previous study has found left ventricular myocyte hypertrophy in OZR, a common animal model for studies of obesity and metabolic syndrome (45). We have recently identified a sex-dependent gene expression signature for obesity-related human cardiac hypertrophy (56). To understand the genetic mechanisms that may mediate obesity-induced changes in cardiac electrophysiology and hypertrophy, we set out to identify an obese animal model associated with cardiac hypertrophy. We also noticed that almost all the previous studies used only male OZR. In this study, we examined the gene expression profile of OZR relative to the lean Zucker rats (LZR) in both sexes. We focused on genes that exhibited similar expression patterns from human heart, related to ventricular hypertrophy in obesity in a sex-dependent manner.

Methods

Animals

Lean and obese Zucker rats of both sexes (Charles River) were purchased at age of 8-10 weeks old. Experiments were performed when rats were at 14-17 weeks old. They were given access to food and water *ad libitum*. Proposed research using animals in this work was approved by West Virginia University Institutional Animal Care and Use Committee.

Euthanasia and heart collection

Animals were maintained for up to 10 days during the experiments. After echocardiography recordings, surgery was performed to insert the electrical leads. Recovery takes at least two days to warrant full recovery before electrocardiography recordings for up to 48 hours. Animals were sacrificed immediately following final electrocardiography data collection. Then, hearts were removed under deep anesthesia (3-5% isoflurane), exsanguinated in Tyrode's solution, then flash-frozen and stored in liquid nitrogen until further RNA isolation and protein chemistry experiments.

Echocardiography

Echocardiography was performed using Vevo 2100 Micro-Ultrasound Imaging System (VisualSonics). An MS200 transducer (9-18 MHz) was used to obtain high-resolution heart images. Animals were anesthetized (2-3% isoflurane) for 1-2 hours. Supplemental heat and close monitoring of temperature, pulse, and respiration were provided during study. LVH was identified as significantly increased left ventricular (LV) mass (animal body sized corrected, M=mode) (24). Other measured ventricular parameters included left ventricular internal diameter (diastole) (*LVID, d*), inter ventricular septum (diastole) (*IVS, d*), and left ventricular posterior wall (diastole) (*LVPW, d*).

Telemetry Electrocardiography

Surgical procedure, Post-surgical recovery

All survival surgeries were performed accordance with the WVU IACUC policy on Rodent Surgery and Post-Operative Care as well as the Pain and Distress Policy. Rats were weighed and anesthetized using an isoflurane (3-5%) induction chamber. Sterile ophthalmic ointment was applied to the eyes of the animal to reduce corneal desiccation. Animals were shaved in relevant areas then transferred to the surgical area and externally heated with a temperature-controlled warming pad. Deep anesthesia was maintained with isoflurane. After disinfecting relevant areas with Betadine and 70% isopropanol, surgery was performed.

Animals were implanted with telemetry transmitters (Data Science Inc., St. Paul, MN) according to manufacturer's specifications. Briefly, a small midline incision was made below the xiphoid process to expose the abdominal muscles and a small pocket was made on the animals' left side, just slightly larger than the body of the transmitter. The pocket was then filled with sterile saline and the transmitter body inserted into the pocket. The ECG leads were then cut to allow for them to be placed subcutaneously while remaining flat along the muscle wall and with enough length to allow for normal animal movement. The red lead was then placed at the lowest rib and a 4-0 suture was used to secure the lead to the abdominal wall muscle. The clear lead was positioned on top of the right pectoral muscle. The leads were sutured into the subcutaneous muscle as described above. The skin was then sutured shut after gently cleaning up any excess blood and applying antibiotic ointment. Carprofen (5 mg/kg subcutaneous) was administered parenterally to ensure pain relief without suppressing respiration. Animals were monitored for signs of pain twice daily post-surgery for five days and analgesics (stated above) were given during this period. Animals were then put on a 24-hour acquisition schedule to collect ECG data.

Data acquisition and analysis were performed using the Ponemah 5.20 platform (Data Sciences International). A pair of lean and obese rats was studied simultaneously under identical conditions. Heart rate variability data analysis was performed according to procedures recommended directly by the manufacturer. ECG recordings of five minutes in length were isolated if they contained no signs of inconsistencies in the data or arrhythmias. Data were interpolated at 20Hz and the Hanning method was applied for windowing. Default rate frequency bins were used, VLF (very low frequency): 0.05-0.25, LF (low frequency): 0.25-1, HF (high frequency): 1-3. LF and HF data were normalized to the sum of original LF and HF data. Graphs were produced by inserting raw R-wave interval (R-R) data from Ponemah into Kubios HRV Standard v. 3.0.0 (72, 73).

Transcriptome (RNA-Seq), bioinformatics analysis, and RT-qPCR

Total RNA was isolated using an RNA Fibrous tissue miniprep kit (Qiagen). Quality of RNA was tested and passed with (1) Nanodrop for purity (OD260/OD280), (2) Agarose gel electrophoresis for RNA degradation and potential contamination, and (3) an Agilent 2100 Bioanalyzer for RNA integrity. Only samples that had RNA Integrity Number (RIN)>7.0 were submitted for sequencing.

After the QC procedures, mRNA was enriched using oligo (dT) beads and then fragmented randomly in fragmentation buffer, followed by cDNA synthesis using random hexamers and reverse transcriptase. After first-strand synthesis, a custom second-strand synthesis buffer (Illumina) was added with dNTPs, RNase H and *Escherichia coli* polymerase I to generate the second strand by nick-translation. The final cDNA library was generated after purification, terminal repair, A-tailing, ligation of sequencing adapters, size selection, and PCR enrichment. Library concentration was first quantified using a Qubit 2.0 fluorometer (Life Technologies), and

then diluted to 1 ng/μl before checking insert size on an Agilent 2100 and quantifying to greater accuracy by quantitative PCR (qPCR) (library activity >2 nM).

Single-end sequencing with 20 million raw reads was performed using HiSeq™ PE150 (Illumina). The raw data were transformed to sequenced reads by base calling and converted to FastQ using onboard instrument software. Reads were mapped to human reference genome (hg38) using TopHat2 (39).

Differential expression analysis was performed with NOISeq (v.2.14.1) (71) using RStudio version 0.99.879 (65). NOISeq is a newly-developed tool for differential expression analysis. Compared to the commonly used DeSeq (2), NOISeq offered a set of tools for better quality control to avoid false positive discoveries (71). Gene annotation information was obtained from the Ensembl Biomart database, release 85 (80). Gene expression levels are indicated by FPKM (fragments Per Kilobase of transcript per Million mapped reads) (74). FPKM was then normalized for batch effect using the ARSyNseq module included with the NOISeq package. Data were analyzed using the noiseqbio method under default conditions. The CPM filtering method was used for differential analyses where at least one group contained five or fewer replicates; otherwise, the Wilcoxon test was used for filtering.

RT-qPCR was run on either a BioRad CFX96 Real Time System or Applied Biosystems 7500 using a Luna Universal One-Step RT-qPCR Kit (NEB E3005L) according to the manufacturer's instruction. Briefly, components were prepared for a 20μL reaction volume per well using 100-300ng template RNA and primers at 10μM concentration (primer sequences are listed in Supplemental Table 1). Each sample was prepared as two technical replicates, with three biological replicates total per group. GAPDH was used as a loading control on each plate. Reverse transcription was run at 55°C for 10 minutes, followed by one cycle of initial

denaturation at 95ºC. This was followed by 40 cycles of 95ºC denaturation (10 seconds) and 60ºC extension (30 seconds). After the plate was read, melt curves were recorded using a 0.5ºC step from 60-95ºC.

Gene expression levels were plotted in log2-fold (y-axis) from both transcriptome and qPCR.

Immunoblotting

Tissues sections were submerged in minimal lysis buffer (fresh protease and phosphatase inhibitors (Sigma), 20mM Tris, 150mM NaCl, 10mM EGTA and 10mM EDTA at pH 7.4) on ice and homogenized briefly at high speed. Samples were then centrifuged for 15 minute increments at 10,000 x g to pellet debris. Supernatants were placed into new tubes and protein concentration was recorded using Bradford's method on an Eppendorf Biophotometer.

For Western blotting procedures, protein concentrations were normalized between samples to 10 μg and mixed with Non-Reducing Lane Marker (Thermo Scientific) with 5% β-mercaptoethanol. After heating in a water bath to 95ºC for five minutes, samples were cooled to 4ºC then loaded into a 4-12% bis-tris gel (Invitrogen). Electrophoresis was carried out at 80V for 30 minutes then 140V for the remainder.

Proteins were transferred to pre-wetted nitrocelluose membranes at 30V for one hour. Blots were blocked with 3% BSA-V in TBS-T for one hour before primary antibody (1:1000 dilution; Cell Signaling) was added on a shaker at 4ºC overnight. Primary antibody solution was replaced with fresh 3% BSA-V in TBS-T containing secondary antibodies at 1:10,000 dilution for one hour at room temperature on a shaker. After five washes with TBS-T, blots were developed with a standard ECL kit (Life Technologies) on x-ray film or using a G:BOX digital imaging system (Syngene).

Statistics

Data are presented as mean ± SD. Student's *t* test was used for statistical analysis on paired groups, with $p<0.05$ being considered as statistically significant, marked with the symbol *. One-way ANOVA with Tukey's post-hoc test was used for statistical analyses on more than two groups. Blinding and randomization was not performed during *in vivo* analysis due to the small number of animals in the study. For gene expression, gene size adjusted p-value (FDR – false discovery rate) less than 0.05 was used ($p\_adj<0.05$) to identify significant genes.

Results

Characterization of OZR

Table 1 shows that in both sexes, body and heart weight in OZR are significantly increased compared to age-matched LZR. Echocardiogram (Echo) recordings revealed that although heart rate is decreased in OZR, it is statistically not significantly altered compared to lean controls of both sexes. On the other hand, left ventricular (LV) mass was significantly increased in OZR compared to LZR in both sexes: 32.7% increase in male and 59.1% increase in female, consistent with the enlarged heart. In comparison to LZR, the interventricular septum at diastole (*IVS;d*) was increased in OZR, but reached statistically significance only in female. Left ventricular internal diameter at diastole (*LVID;d*) was increased by 24.2% in male OZR, but the increase in female OZR was not statistically significant compared to LZR. Left ventricular posterior wall thickness at diastole (*LVPW;d*) thickness was increased in OZR in OZR compared to their lean controls. We found no changes in OZR contractility since both ejection fraction (EF) and fraction shortening (FS) were not statistically significant.

Altered heart rate, ST elevation, and heart rate variability in OZR from ECG recordings

To investigate potential electrical abnormalities in OZR, we performed telemetry ECG recordings on paired OZR and LZR. A representative set of recordings is shown in Figure 1. In addition to apparent slowing in heart rate, the R-wave amplitude is larger in OZR than in LZR, especially in male OZR compared to male LZR (1A), which is a strong indicator of LVH (12, 17). However, averaged peaks of R-wave between obese and lean rats showed no statistical difference, although R-wave mean value in OZR-M is more than doubled than in LZR-M (OZR-M: 0.862, LZR-M: 0.367, $p=0.065$, $n=4$. OZR-F: 0.761±0.416, LZR-F: 0.696±0.158, $p=0.813$, $n=4$)

Table 2 summarized the most significant changes from ECG recordings. In comparison to age-matched male LZR controls, resting heart rate was significantly decreased, while ST elevation (STe) was significantly increased in male OZR. These changes were not observed in female OZR.

Heart rate variability also showed sex-dependent changes. To eliminate large inter-subject variability in the total raw heart rate variability spectral power, we used normalized frequency power (11). Normalized low-frequency (nLF) power (11, 21) were decreased by 67% in male and by 40% in female obese rats compared to LZR controls, respectively. Normalized high-frequency (nHF) power was increased by 110% in male and by 57% in female obese rats. The ratio of LF/HF was decreased by 61% in female, but insignificantly decreased by 86% in male obese rats (possibly due to small number of animals).

Identification of Differentially Expressed Genes (DEG) in OZR

When comparing obese to lean left ventricular samples, 89 DEG (75 down, 14 up) associated with LVH were found (Figure 2). However, when female and male samples were separated, 826 female DEG (138 down, 688 up in obesity) and 2859 male DEG (1239 down,

1620 up in obesity) were identified (Figure 2). There are 43 DEG that were upregulated in both sexes, whereas 253 DEG downregulated in both, and another 83 that were up in one sex and down in the other (Supplemental Table 2).

PCA plots to show cohesion of males and females are shown in Supplemental Figure 1. Detailed upregulation and downregulation of these DEG are shown in the volcano plots (Supplemental Figure 3) and heatmaps (Supplemental Figure 3).

Shared Differentially Expressed Genes between rat and human obesity-related cardiac hypertrophy

We have recently identified an RNA expression signature in LV for obesity-related human cardiac hypertrophy from 12 males and 12 females (Male BMI: 31.08±12.49 (LVH), n=6; 25.93±6.57 (non-failure, NF, controls), n=6. Female BMI: 27.78±9.92 (LVH), n=6; 28.13±7.02 (NF controls), n=6. Male age: 48.17±14.54 (LVH), n=6; 48.83±12.38 (NF controls), n=6. Female age: 43.83±11.72 (LVH), n=6; 48.00±15.91 (NF controls), n=6) (56). The expression signature contains nine genes (HBA1, HBB, HIST1H2AC, GSTT1, MYL7, NPPA, NPPB, PDK4, PLA2G2A) with altered expression levels in a BMI- and sex-dependent manner (56). We compared expression profiles between rat and human heart samples and identified 337 shared DEG. In female hypertrophied samples (Figure 3A), 6 DEG are upregulated in both rat and human (lower left), 27 DEG are downregulated in both rat and human (upper right), 5 DEG are upregulated in rat but downregulated in human (lower right), and 55 DEG are downregulated in rat but upregulated in human (upper left). In male hypertrophied samples (Figure 3B), 28 DEG are upregulated in both rat and human (lower left), 22 DEG are downregulated in both rat and human (upper right), 8 DEG are upregulated in rat but downregulated in human (lower right), and 193 DEG are downregulated in rat but upregulated in human (upper left).

Among the nine-gene expression signature (HBA1, HBB, HIST1H2AC, GSTT1, MYL7, NPPA, NPPB, PDK4, PLA2G2A) identified in obesity-related human cardiac hypertrophy (56), seven DEG (Nppa, Nppb, Gstt1, Hbb, Hba1, Myl7, Pdk4) are potential DEG found in OZR compared to LZR in a sex-dependent manner. Figure 4 compares the expression levels of seven DEG in rat and human LVH. NPPA and NPPB expression levels were significantly increased in LVH of both rat and human of either sex. However, NPPA levels are notably higher than NPPB in rat and human of either sex. HBB gene expression was also drastically upregulated in rat and human LVH, but only in female. Upregulation of PDK4 is more significant in female than in male in both rat and human. MYL7 was upregulated in male but downregulated in female human LVH. In rats, Myl7 expression levels were significantly increased in females, inconsistent with that in human LVH. In human, GSTT1 and HBA1 levels were very low compared the other DEG.

Validation of differentially expressed genes shared in OZR and obese human hypertrophied heart

We set out to validate six DEG expression using qPCR and protein expression using western blotting. We did not include Hba1 due to very low expression in human heart (Figure 4 bottom) (but dramatically high expression in rat heart (Figure 4 top)) and we could not detect protein expression in human heart. We included Gstt1 because it has a similar low expression pattern in both rat and human heart.

Figure 5A indicates a significant increase in Nppa transcript levels in OZR of both sexes from transcriptome experiment. Quantitative PCR experiments confirmed the statistically significant increase in male OZR, but not in female OZR (Figure 5B). At protein expression levels, Anp are remarkably higher in obese than in lean rats of both sexes (Figure 5C). The

results are statistically significant (male: p=0.007, n=3; female: p=0.01, n=3) (Figure 5D), similar to human ANP protein expression patterns (56).

Figure 6A shows Nppb transcriptional level from transcriptome experiment, suggesting a higher expression in obese than in lean rats of both sexes, which was confirmed by quantitative PCR (Figure 6B). However, immunoblots (Figure 6C) did not reveal statistical difference in protein expression levels in either sex (Figure 6D) ($p>0.05$, n=3).

Figure 7 shows Gstt1 transcript levels that are not significantly altered in OZR of both sexes (upper panel). Quantitative PCR also revealed insignificant changes of gene expression levels between OZR and LZR in both sexes (lower panel). We did not perform immunoblot experiments due to lack of justification.

Figure 8A shows an increase in Hbb transcriptional level only female OZR over LZR, which was confirmed by quantitative PCR (Figure 8B). However, immunoblots (Figure 8C) suggested that the protein expression levels are increased in OZR compared to LZR in both sexes (Figure 8D), which are statistically significant (male: p=0.007, n=3; female: p=0.0003, n=3).

Figure 9A shows a dramatic increase in Myl7 transcript levels in OZR compared to LZR in both sexes. However, quantitative PCR failed to validate increased gene expression, although very close in female OZR (Figure 9B) (p=0.0608). Immunoblots (Figure 9C) confirmed a significantly increased protein expression in female OZR compared to female LZR (Figure 9D) (OZR-F: 1.693, LZR-F: 0.769, $p<0.05$, n=3).

Figure 10A shows an increase in Pdk4 transcript levels in OZR compared to LZR in both sexes. Quantitative PCR validated these increases at gene expression levels (Figure 10B). Immunoblots (Figure 10C) confirmed an increased protein expression in female OZR, but not in male OZR, compared to LZR (Figure 10D) (male: p=0.092, n=3; female: $p<0.0001$, n=3).

Sex- and obesity-dependent NPPA/NPPB expression

Figure 11A shows that NPPA gene expression levels are higher in obese female than in obese male rat and human with LVH. NPPB levels are higher only in obese female human compared to obese male human LVH; its levels are lower in obese female than in obese male rat. Figure 11B shows that in addition to LVH-mediated increase in expression of both NPPA and NPPB in human heart, obesity is associated with a significantly decreased expression of NPPB in both sexes, decreased expression of NPPA in male, but increased expression of NPPA in female human with LVH.

Discussion

Obesity drastically increases the risk of sudden cardiac death and HF, with severity varying in a sex-specific manner. Cardiac hypertrophy is an independent feature from obesity but is the most common cause of sudden cardiac death in morbidly obese patients. Discovery of cross-species DEG validates an animal model to study how individual genes may contribute to sex-specific obesity-related cardiac hypertrophy *in vivo*. Novel biomarkers of cardiac hypertrophy should allow early intervention to delay or even prevent sudden cardiac death and HF.

In the present work, we investigated gene expression profiles of LV from OZR and LZR to test a hypothesis that OZR can serve as an animal model to study sex-specific obesity-related cardiac hypertrophy.

Echocardiography and electrophysiological characterizations of OZR

Enlargement of heart associated with obesity in Zucker rats can be detected at 12-weeks old and established in 14 weeks old of age (62). Our data on heart weight and LV mass in OZR of 14-17 weeks of age showed significant hypertrophy in both sexes, which is consistent with the

cellular hypertrophy in OZR we previously reported (45). Although female hearts are smaller and lighter compared to males, the percent increase in LV mass is larger in female (59%) than in male (33%) (Table 1). The LVID is significantly increased in male OZR over LZR, but not in female OZR/LZR, although there is a tendency to increase. An increased IVS was found in female, but not in male, OZR compared to the respective LZR controls. OZR of both sexes showed an increased LVPW.

OZR has been known to have dysfunctional cardiac functions such as reduced contractility (81). However, we do not detect statistically significant changes in this study. Studies showing reduced contractility used old OZR (e.g. 20 weeks) (81), while younger OZR (e.g. 10-12 weeks old) do not exhibit altered contractility (40, 51). It is possible that while there is no significant difference in contractility between obese and lean rats at the tissue or whole-heart level, depressed contraction at the level of myocytes has already occurred (62).

ECG recordings showed that in comparison to LZR the resting heart rate was decreased in male but not in female OZR, although there is a statistically insignificant decrease in female OZR. ST elevation was also found to increase only in male OZR (Table 2). In OZR of both sexes LF (a combination of sympathetic and parasympathetic activities) was decreased, while HF (predominately vagal modulation) was increased, in agreement with reduced sympathetic baroreflex sensitivity in OZR due to leptin receptor dysfunction (14, 28, 33, 60). Increased HF component is more significant in male than in female OZR (Table 2). Reduced ratio of LF/HF further supported that the sympathetic tone in the obese heart was suppressed (21). It has been well established that reduced heart rate variability is a powerful independent risk factor for cardiovascular diseases such as hypertrophic cardiomyopathy and sudden cardiac death (16, 35,

41, 42, 57), type 2 diabetes and metabolic disorders (6, 70), as well as in the general population (63, 75).

Differentially expressed genes associated with sex-specific obesity-related cardiac hypertrophy

It is not surprising for significantly increased Anp expression levels in both sexes of OZR compared to LZR, similar to what we found in obesity-related human cardiac hypertrophy (56). Consistent with human data, the Anp increase in LVH is significantly larger than Bnp, which has been clinically used as biomarker for diagnosis of HF (5, 22, 54, 61).

ANP can directly modulate all voltage-dependent ion channels known to control heart rate and action potential duration (52, 59), yet, yields inconsistent results in experimental models and in humans. Nonetheless, ANP was found anti-arrhythmic, since a protein degradation-resistant mutant can trigger atrial fibrillation (32). ANP can potentiate isoproterenol stimulation of the L-type voltage-gated calcium channel, while mutant ANP cannot (32).

While the mechanistic roles of ANP in cardiac electrophysiology and especially on ion channels remain to be clarified, the roles of ANP in hypertrophy and HF has been extensively studied and well defined (38, 61, 69, 77). ANP is predominantly released from atria, while it was later found also present in the ventricle (A:V ratio 40:1) (27). The synthesis of ANP is dramatically increased in the ventricle in response to hypertrophy, making it one of the surrogate markers (other than BNP) in advanced HF patients (54, 69). It was noted that the total amount of ANP in the failing ventricles is about 9-fold higher than BNP (ANP: 135±31 pmol/g; BNP: 16.9±4.2) (54). In Anp knockout mice, overload volume-induced cardiac hypertrophy was worsened, indicating that Anp protects the heart from hypertrophy development (53). Additionally, Anp protection is independent of blood pressure. Protective roles of ANP and BNP

have recently been found in human studies. Increased LV mass and wall thickness were found in patients who carried allele 664C>G in the ANP promoter, which results in lower levels of circulating ANP (66). On the other hand, patients with the rs5068 allele at the NPPA-NPPB locus, which results in higher circulating levels of ANP and BNP, had reduced LVH (36).

Consistent with our previous findings in obese human hypertrophied hearts (56), ANP expression levels are significantly increased in OZR of both sexes compared to LZR. Particular, ANP gene expression levels are higher in female than in male LZR and OZR, respectively (Figure 5), also in agreement with our previous findings in obese human hypertrophied heart (56). Unlike human hypertrophied heart, significant increases in BNP gene expression levels were found only in male OZR, which failed to be validated in protein expression (Figure 6). In both obese rat and human hypertrophied heart of both sexes, ANP expression levels are significantly higher than BNP. Thus, ANP not only can be used as an early biomarker in obesity-related cardiac hypertrophy, but also a potential target to study how ANP affects cardiac electrophysiology during early development of hypertrophy under obesity condition.

Interestingly, we found several genes that were previously understudied or unknown with regard to their respective roles in cardiac hypertrophy and arrhythmias (Figure 4). In female (but not male) obese human hypertrophied heart, HBB expression was upregulated (56). In female OZR, Hbb gene expression was significantly upregulated compared to female LZR (Figure 8). Interestingly, immunoblots confirmed upregulated protein expression in both male and female OZR. The Hbb gene encodes β-globin, a subunit of hemoglobin. Its upregulation along with α-globin (encoded by Hba1 gene) may help explain the increased oxygen transport to peripheral tissues in obesity-related cardiac hypertrophy.

Myosin light chain 7 (MYL7) was identified as a DEG in female (but not male) obese human hypertrophied heart (56). In OZR, Myl7 gene expression was significantly increased in both sexes, particularly in female (64-fold). Both quantitative PCR and immunoblots validated its upregulated expression in female OZR, in agreement with human data. MYL7 encodes myosin regulatory light chain protein, atrial isoform (MLC2a) in humans. Its expression is restricted to atria in healthy individuals, modulating cardiac development and contractility (23). In hypertrophic cardiomyopathy, MYL7 expression is readily detected in the ventricle (30). Its gene expression levels are very low in LZR of both sexes, but dramatically increased in OZR, consistent with its expression pattern in obese-related human cardiac hypertrophy (56).

We found PDK4 was significantly upregulated in male (but not female) obese human hypertrophied heart (56). In OZR, however, PDK4 was significantly upregulated in both male and male) heart (Figure 10). Its upregulation was validated by qPCR. PDK4 encodes a mitochondrial enzyme pyruvate dehydrogenase kinase 4. PDK4 downregulates glucose utilization and increases fat metabolism by decreasing glucose conversion to acetyl-CoA (43), resulting in a decreased production of ATP. Therefore, its upregulation may be resulted in increased demand for fat metabolism in obesity.

Currently, we do not know the biological roles of upregulated expression of Hbb, Myl7, and Pdk4, in association of obesity-related cardiac hypertrophy. Neither do we know whether these DEG might be used as potential new sex-dependent biomarkers for cardiac hypertrophy in obesity.

Unexpectedly, we did not detect the anticipated alterations of expression levels of genes that have been well documented in their contributions to development of cardiac hypertrophy and arrhythmia. Early study in mice identified that the expressions of 25 genes were altered in

cardiac hypertrophy induced by angiotensin II and isoproterenol and that of 30 distinct genes were changed during regression of hypertrophy (26). Recently, using personalized and multi-omics approaches in 100+ strains of genetically distance mice, 36 differentially expressed genes were identified (67). Microarray studies in a young hypertrophied heart rat model in the absence of hypertension, 65 genes altered their expression levels, and significantly more genes (390) changed their expression levels in the old hypertrophied heart (20). Notably, the Ras/mitogen-activated protein kinase (MAPK) signaling pathway and the tumor necrosis factor (TNF) receptor-mediated activation of nuclear factor-κB (NF-κB) were found to play a crucial role in the development of hypertrophy (20). In human patients with cardiac hypertrophy, PCR screening found 35 (the article stated 36) genes were increased compared to normal human heart (44).

It is imperative to point out that hypertrophy has diverse phenotypes revealed by cardiac magnetic resonance imaging (47-49, 68). Pathologic hypertrophy caused by genetic mutations in sarcomere proteins are rare, representing 0.6% of prevalence in 3,600 unrelated subjects from the Framingham Heart Study and Jackson Heart Study cohorts (8, 68). The majority (88.8%) of hypertrophic patients have benign mutations or variant of uncertain significance (8, 68). Cellular hypertrophy should occur earlier than changes in phenotype detected by echocardiography or cardiac magnetic imaging. Thus, altered gene expression patterns are important early markers during development of hypertrophy.

It is interesting to notice that obesity seems to inhibit gene expression of human NPPA and NPPB, except that in female with LVH obesity increased gene expression of NPPA (Figure 11B). Currently, we do not know the mechanism and how significant it may be in clinical settings.

Genes related to cardiac arrhythmias

Electrical disturbance can be triggered by heart remodeling such as hypertrophy. Alterations of gene expression levels of membrane ion transporters including ion channels, pumps, and exchangers cause ionic imbalance which can trigger arrhythmias. Studies from experimental animal models demonstrated that ion channel remodeling occurs preceding clinical hypertrophy phenotype is diagnosed (9), since properties of ion channels can be altered when myocytes are enlarged (cellular hypertrophy).

We did not find changes in expression of genes that encode ion channels controlling the heart rate, such as hyperpolarization-activated, cyclic-nucleotide modulated (HCN) and voltage-gated calcium channels (Cav1.2, Cav3.1) (64). Lack of heart rate-related ion channel gene expression changes supports the notion that the decreased heart rate in OZR is more likely caused by post-translational modulation under the hypertrophy conditions. Clinically, elevated ST segment is frequently associated with acute ischemic conditions such as acute coronary syndrome (29), however, it often occurs in healthy male individuals (78). In this study, STe was increased with statistical significance only in male OZR, but not in female OZR. ST elevation is associated with myocardial infarction (55). Recently, ST elevation is found to also occur in LVH (55) and in obesity (4, 18). The likely explanation for increased STe in male OZR is the LVH-related cardiovascular dysfunction (50), female OZR may be more resistant to ischemic conditions at this age group (14-17 weeks).

Limitations of the study

The sample size is small (four animals per each group), which may have caused insignificant changes in expression levels for many genes related to cardiac hypertrophy and arrhythmias as well as in many ECG and Echo parameters. However, the small sample size also

provided us an opportunity to focus on genes with significant alteration of expression levels. If confirmed in large samples of obese human cardiac hypertrophy, these genes (particularly the new genes) may represent novel targets for exploring early pharmacological treatment of sex-specific cardiac hypertrophy in obesity.

Conclusions

We identified five differentially expressed genes in LVH shared between OZR and human heart in obesity in a sex-dependent manner. ANP has the highest expression levels in LVH in both sexes. Future investigations of these five DEG may provide mechanistic insights in early development of hypertrophy in obesity in a sex-dependent manner.

Figures

Figure 1: Representative ECG recordings of male (A) and female (B) Zucker rats

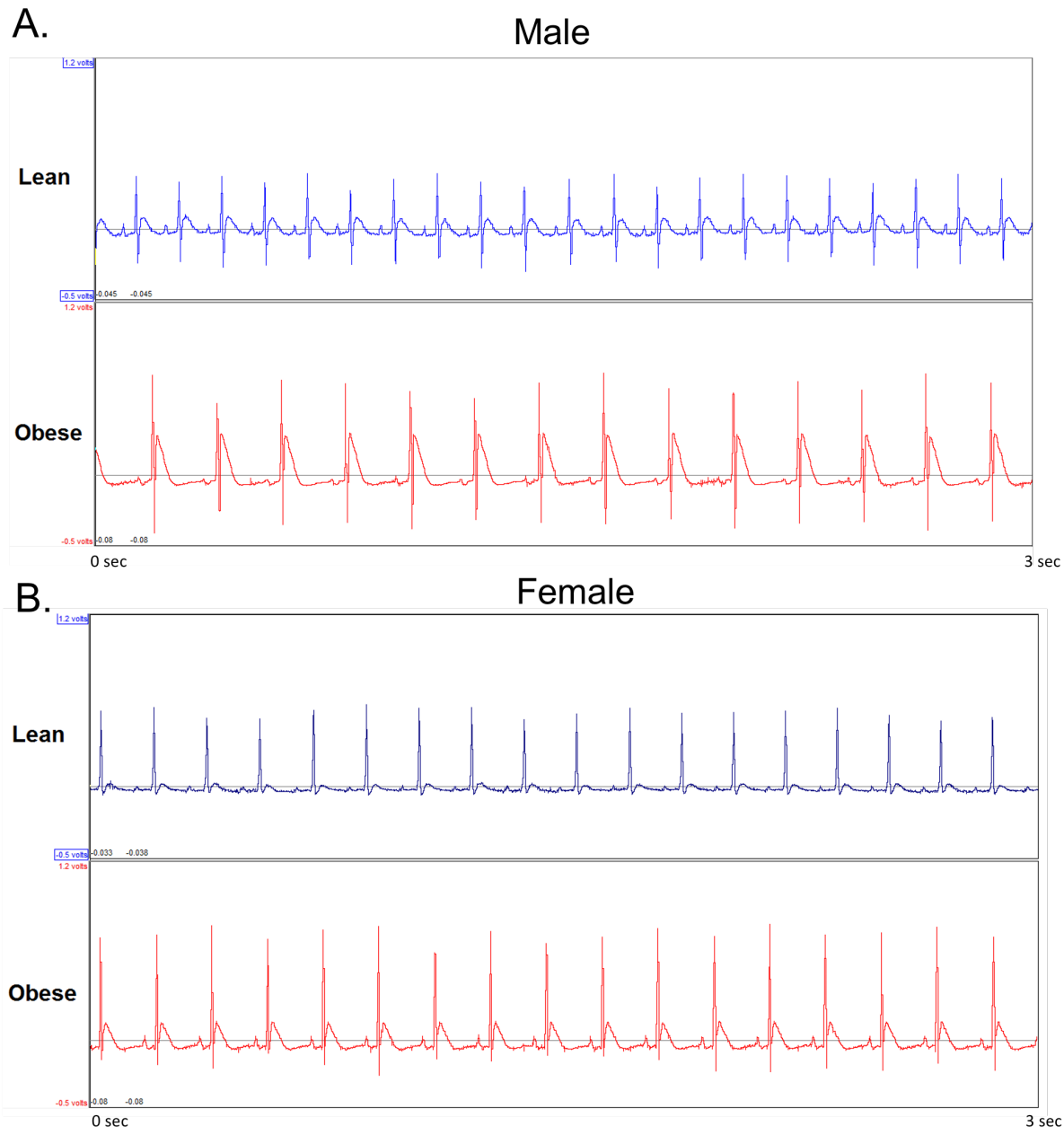

Figure 1A: Representative ECG data from males; B: Representative ECG data from females. Each X-axis ranges from 0 to 3 seconds and each Y-axis ranges from -0.5 to 1.2V.

Figure 2: Sex-specific distribution of significant genes in Zucker rat LVH

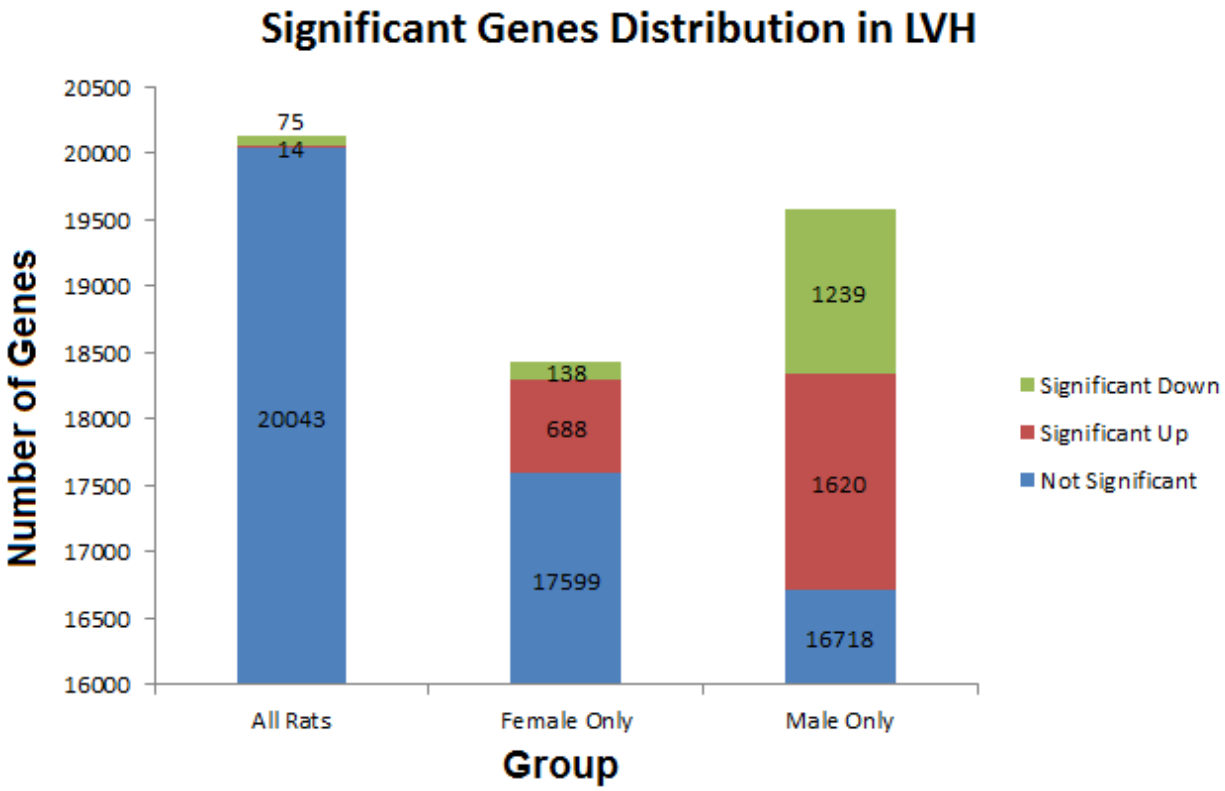

Figure 2. Significantly upregulated, downregulated, or not statistically significantly different total gene expression when comparing A) all rats; B) females only, and C) males only. The discrepancy in total number of genes between analyses is due to sex-specific expression: some genes are exclusively expressed in either males or females. If a gene had 0 expression in all samples, it was removed from analysis.

Figure 3: Sex-specific differentially expressed genes shared between human and rat

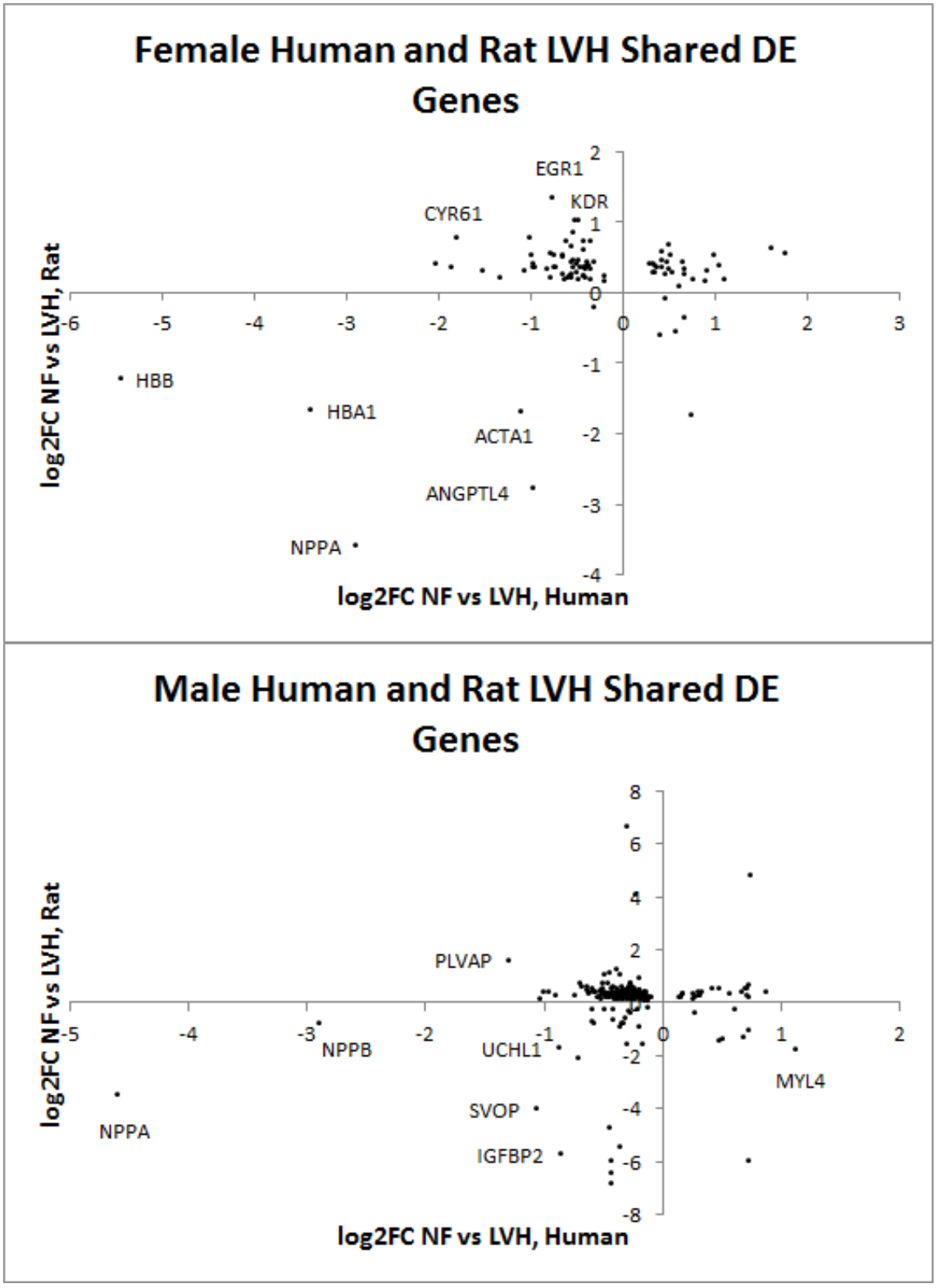

Figure 3. A: female, B: male. Bottom-left quadrants represent genes upregulated in human and rat LVH; upper-right quadrants represent genes downregulated in human and rat LVH; bottom-right quadrants represent genes upregulated in rats but downregulated in humans; top-left quadrants represent genes upregulated in humans but downregulated in rats.

Figure 4. Comparison of seven obesity- and LVH-related differentially expressed genes levels between human and rat.

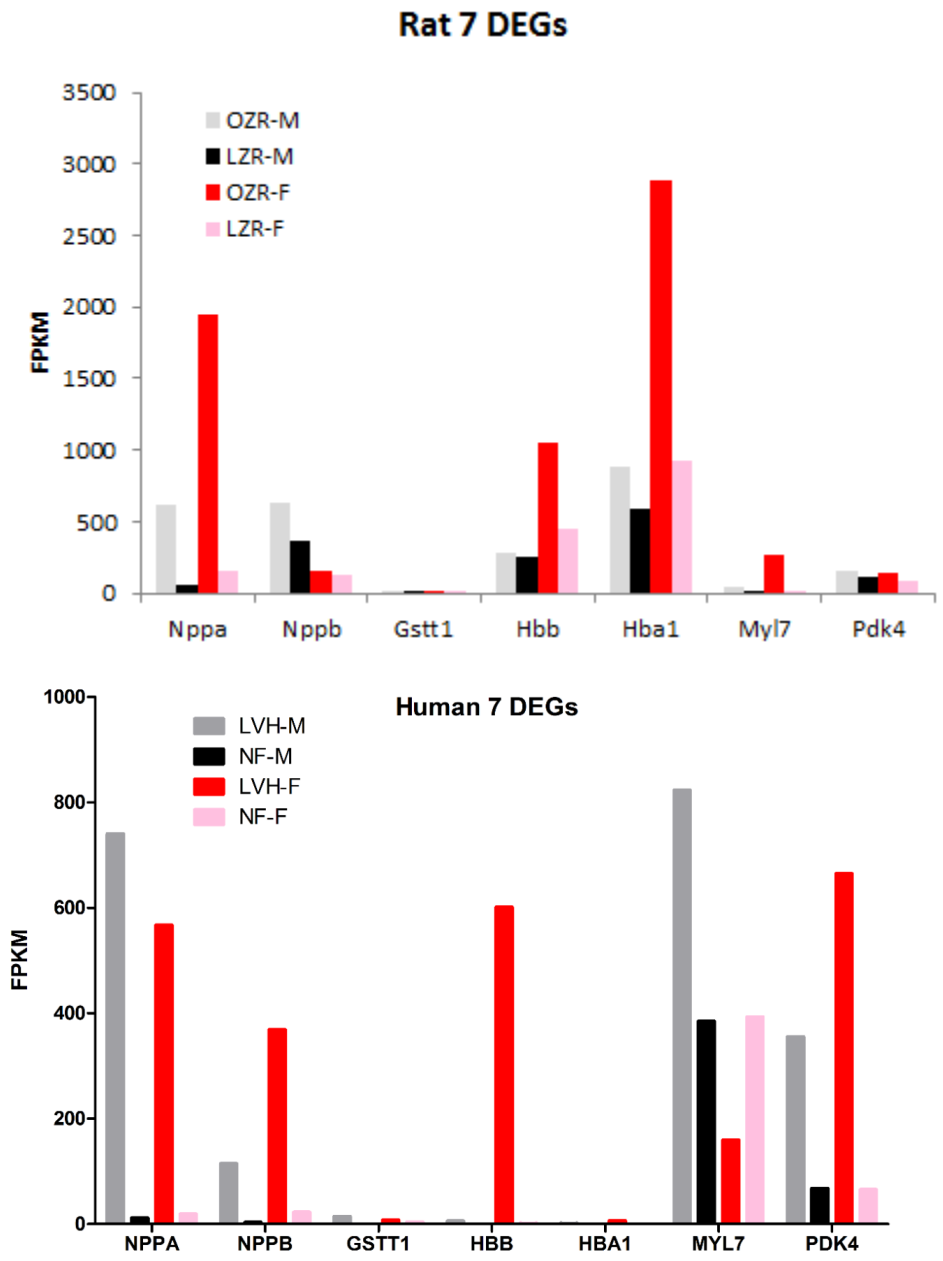

Figure 4. Gene panel transcript levels from transcriptome dataset in rats (top) and humans (bottom). The original nine-gene panel from humans was reduced to seven because two of the genes in humans were significant in neither male nor female Zucker rats.

Figure 5: Nppa validation

A. Transcriptome

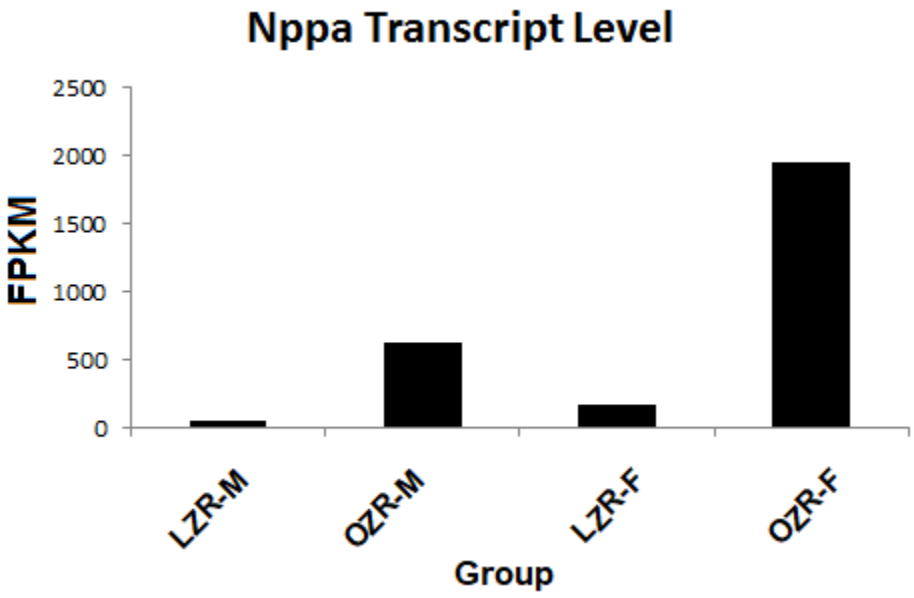

B. RT-qPCR

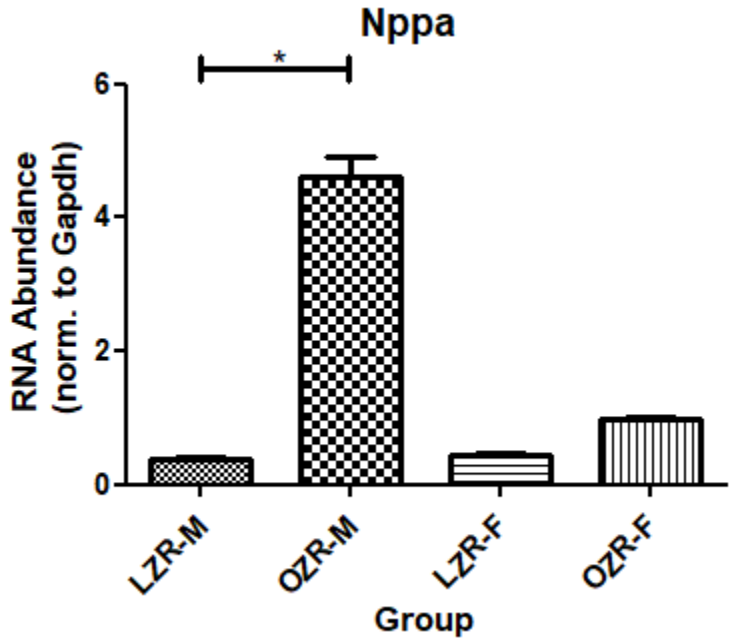

C. Western blots

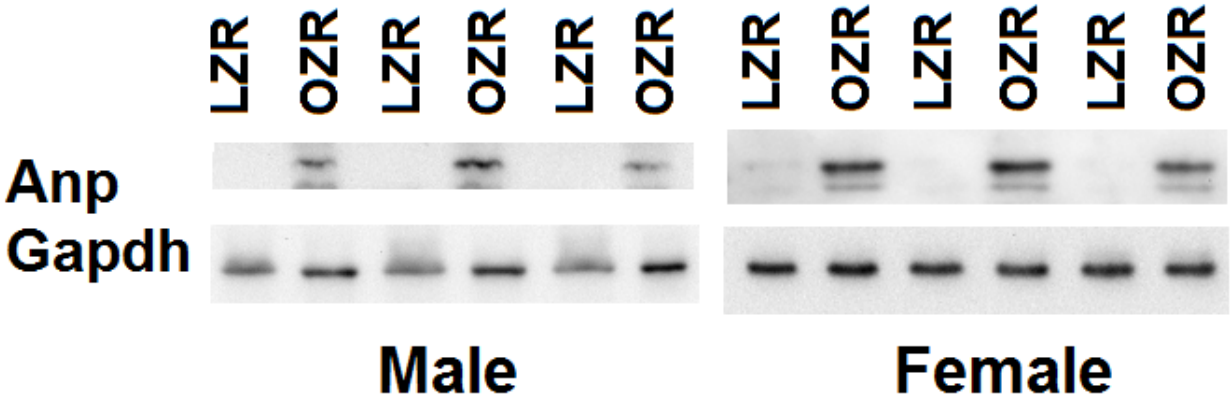

D. Protein quantification

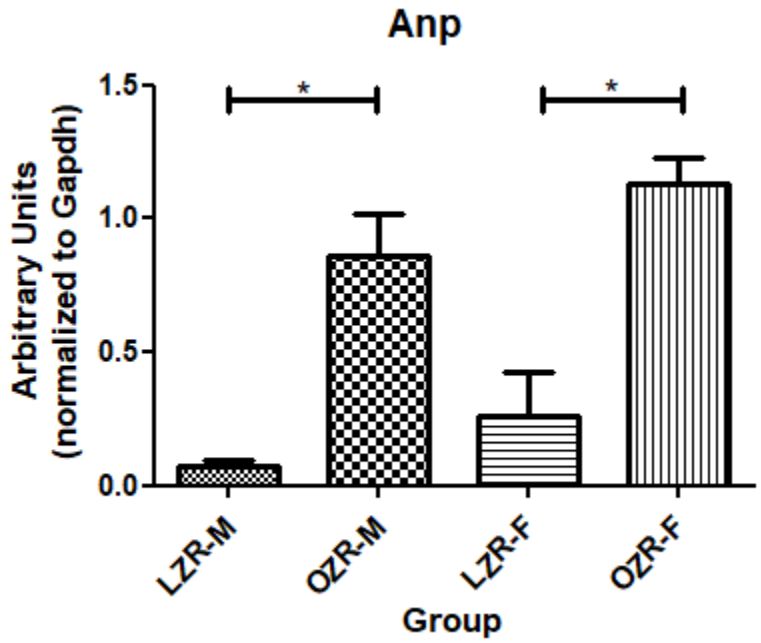

Figure 5. A: Gene expression from transcriptome. B: Gene expression from qPCR. C: Protein expression. D: Protein expression quantification. Protein level was normalized to α-actin. * indicates statistically significant ($p<0.05$).

Figure 6: Nppb validation

A. Transcriptome

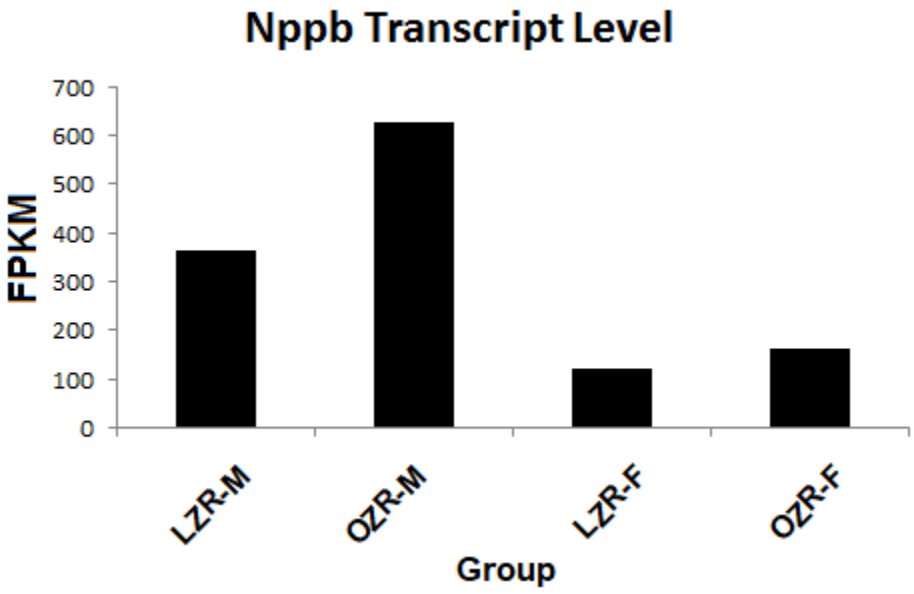

B. RT-qPCR

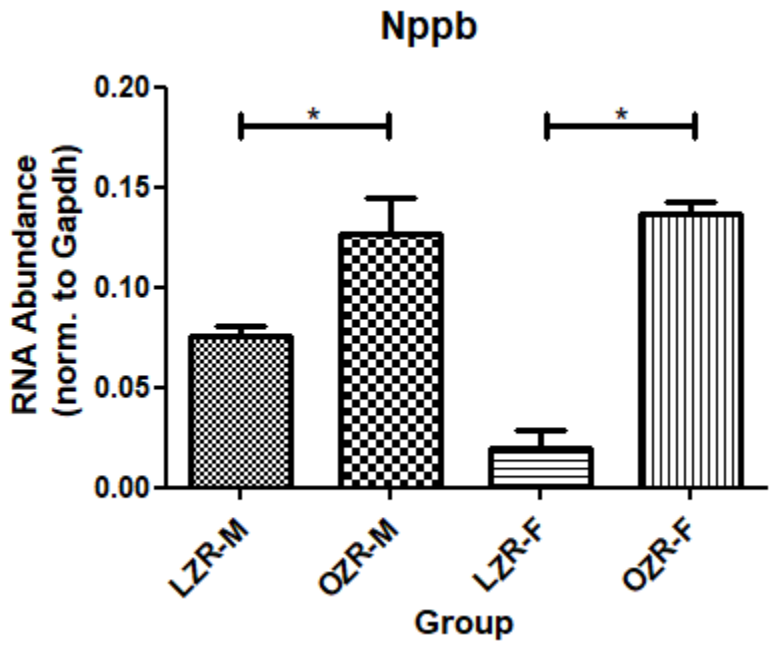

C. Western blots

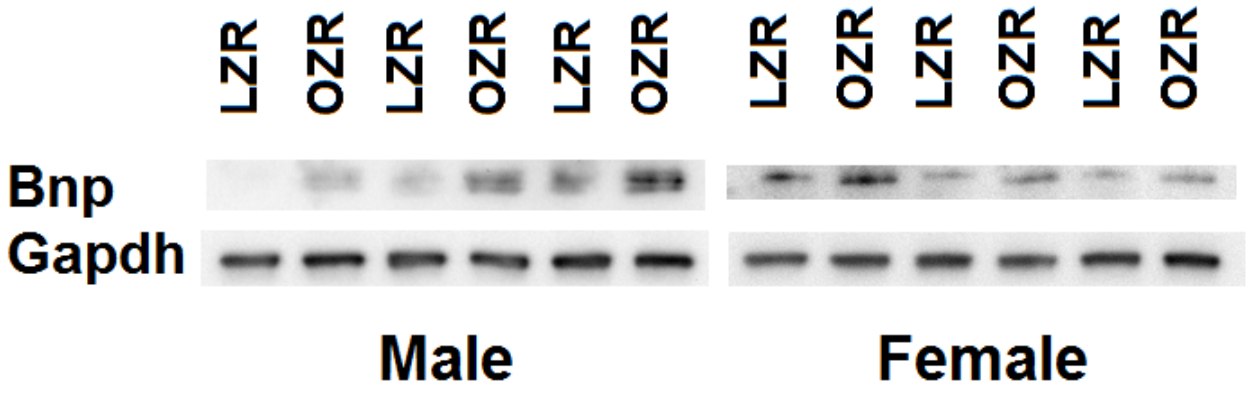

D. Protein quantification

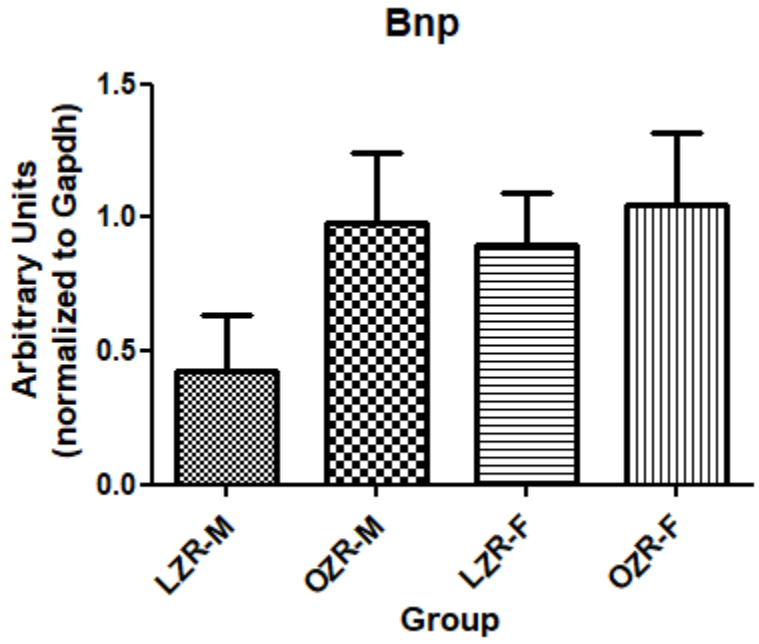

Figure 6. A: Gene expression from transcriptome. B: Gene expression from qPCR. C: Protein expression. D: Protein expression quantification. Protein level was normalized to α-actin. * indicates statistically significant ($p<0.05$).

Figure 7: Gstt1 validation

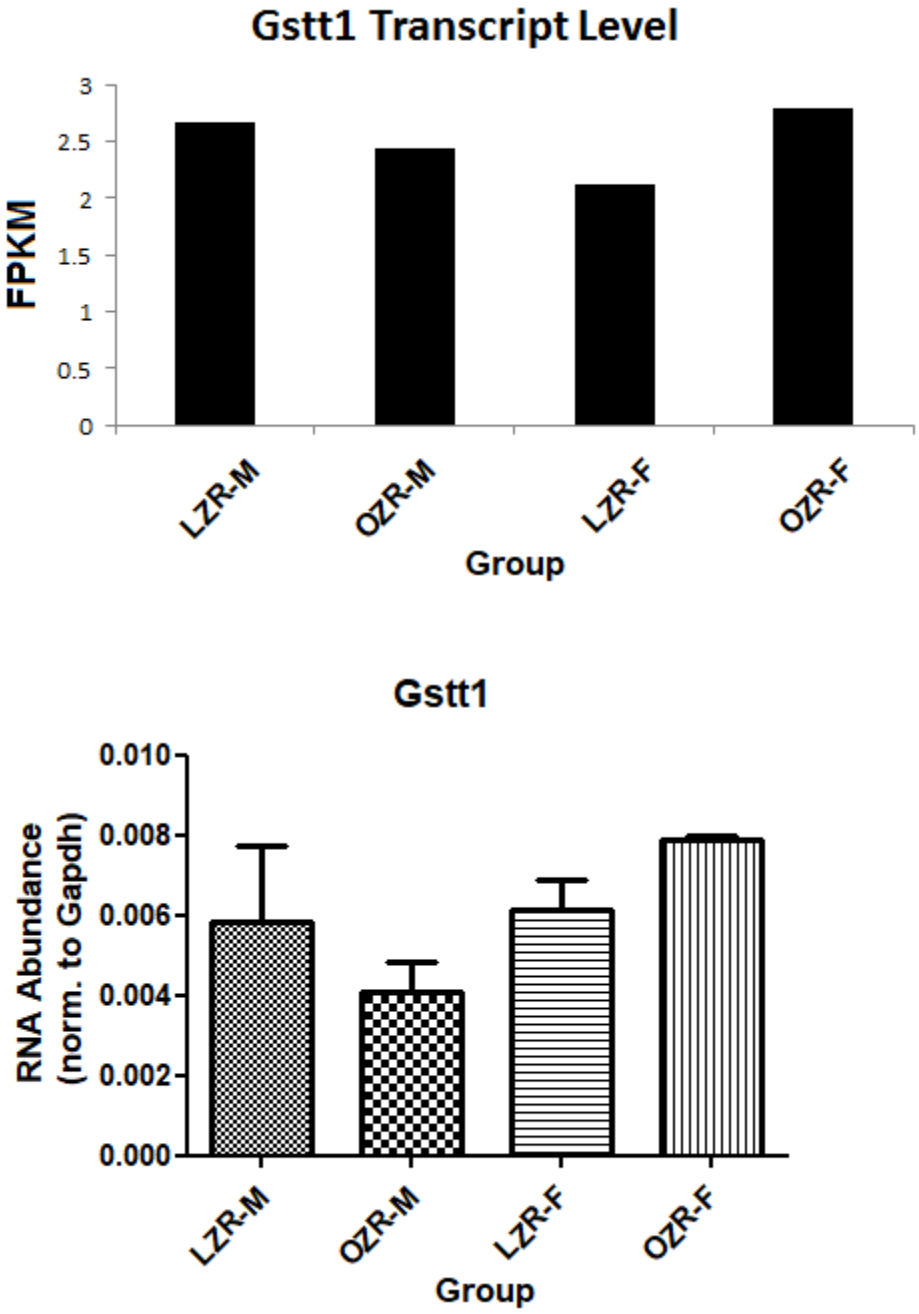

Figure 7. Upper: Gene expression from transcriptome, lower: Gene expression from qPCR.

Figure 8: Hbb validation

A. Transcriptome

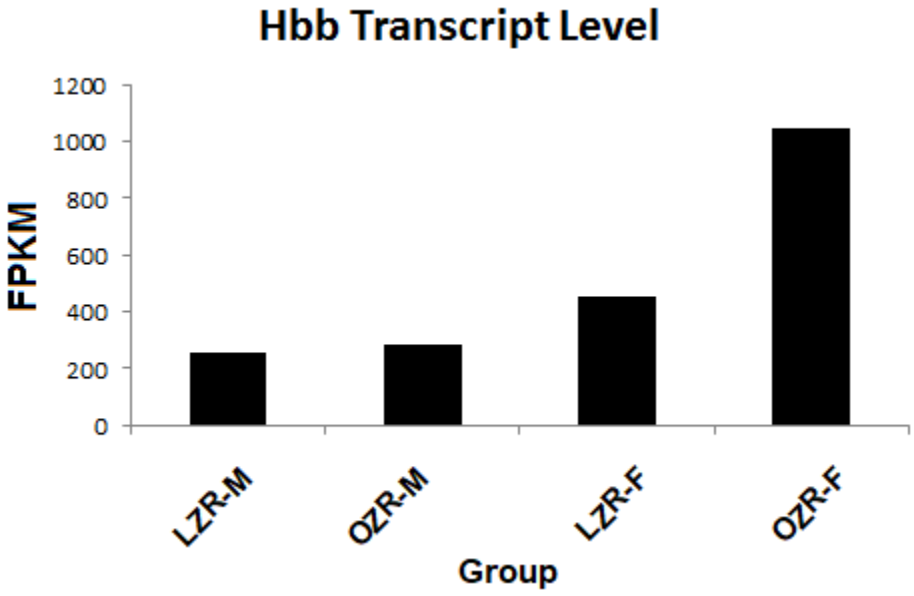

B. RT-qPCR

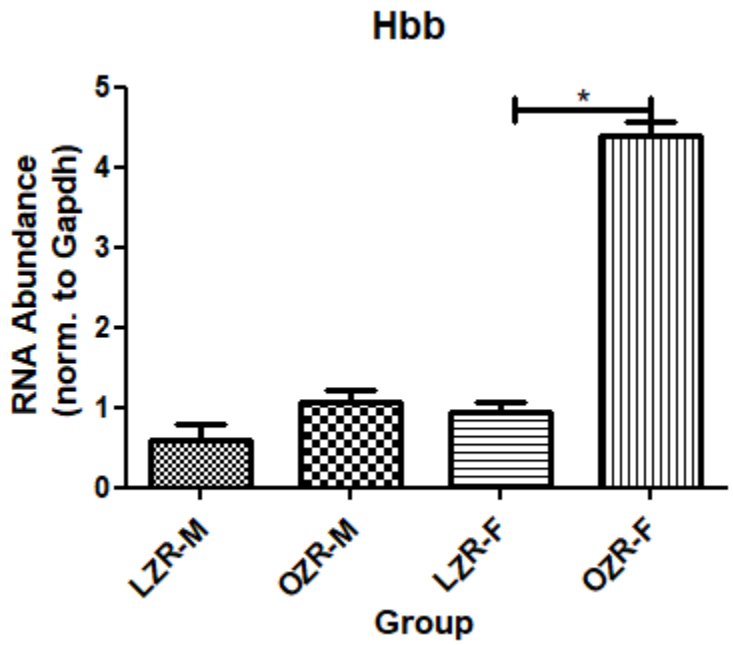

C. Western blots

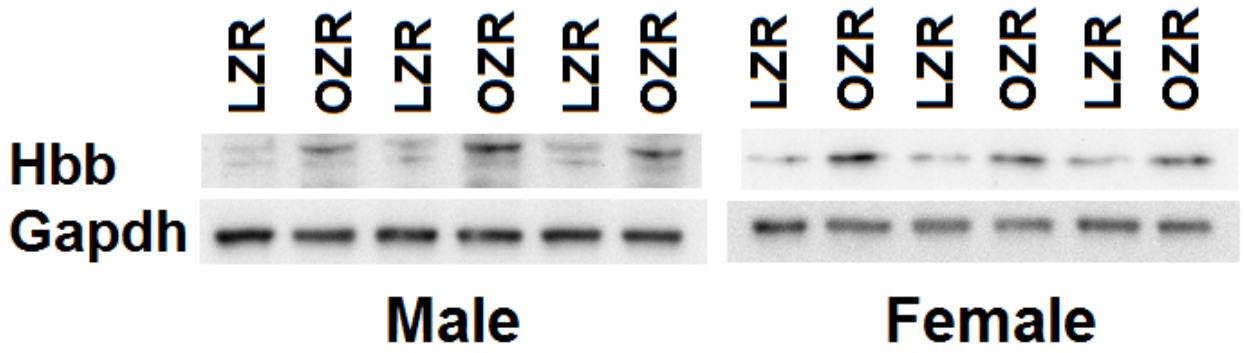

D. Protein quantification

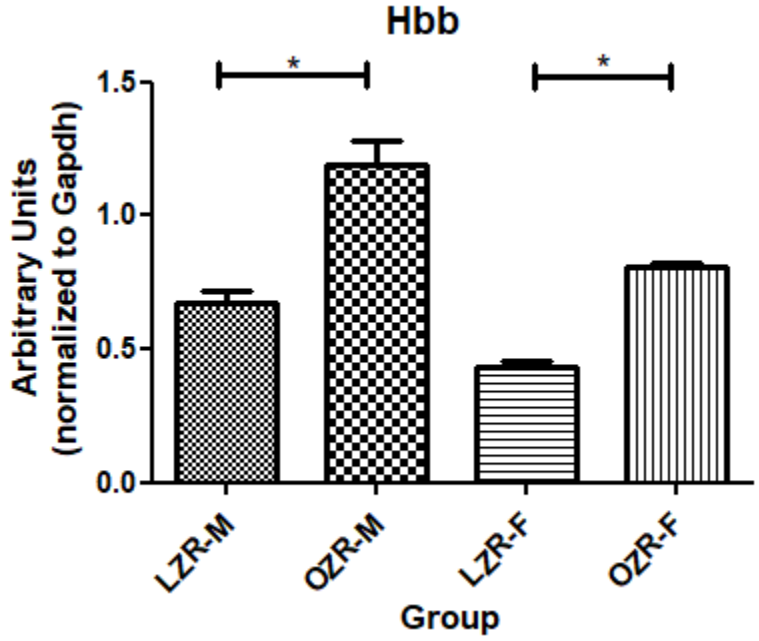

Figure 8. A: Gene expression from transcriptome. B: Gene expression from qPCR. C: Protein expression. D: Protein expression quantification. Protein level was normalized to α-actin. * indicates statistically significant ($p<0.05$).

Figure 9: Myl7 validation

A. Transcriptome

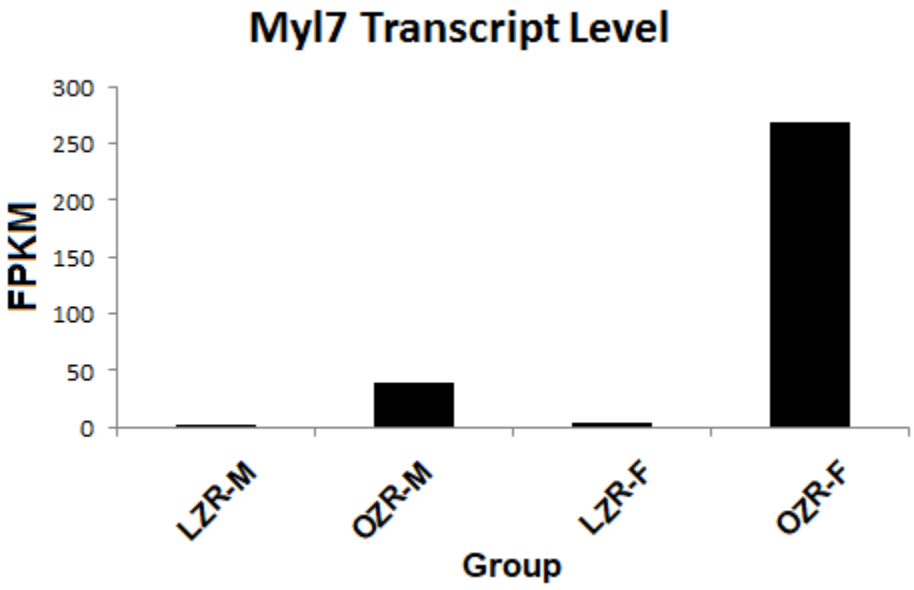

B. RT-qPCR

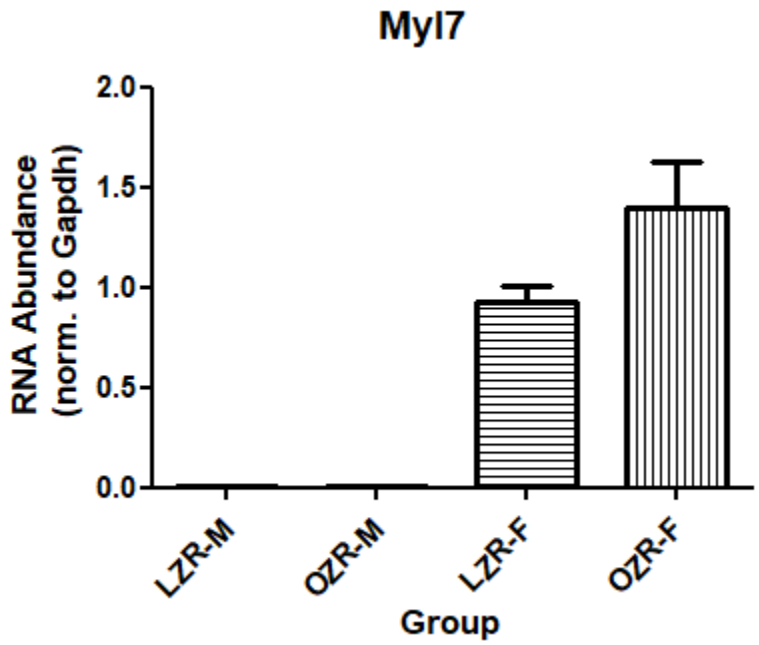

C. Western blots

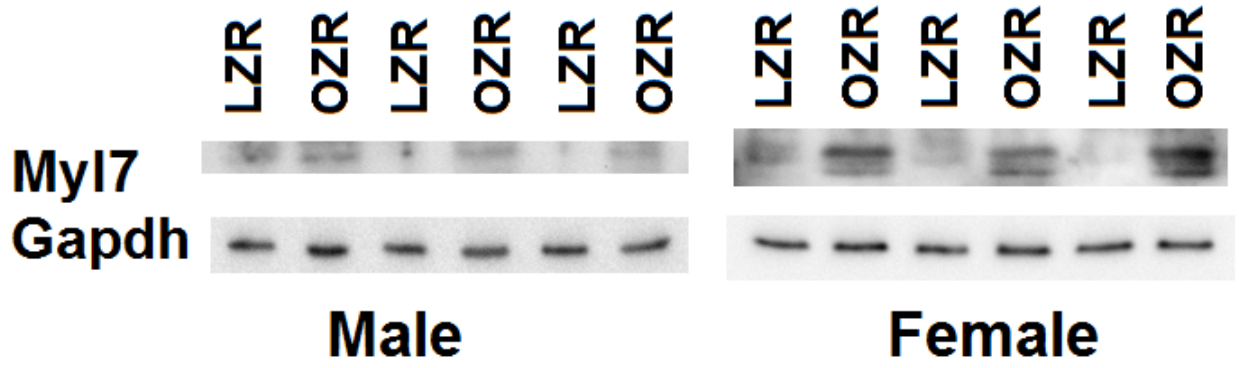

D. Protein quantification

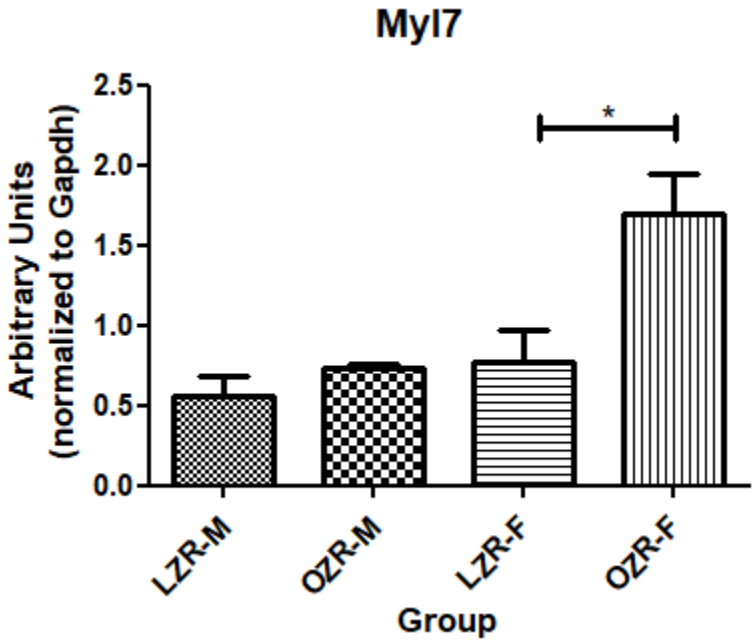

Figure 9. A: Gene expression from transcriptome. B: Gene expression from qPCR. C: Protein expression. D: Protein expression quantification. Protein level was normalized to α-actin. * indicates statistically significant ($p<0.05$).

Figure 10: Pdk4 validation

A. Transcriptome

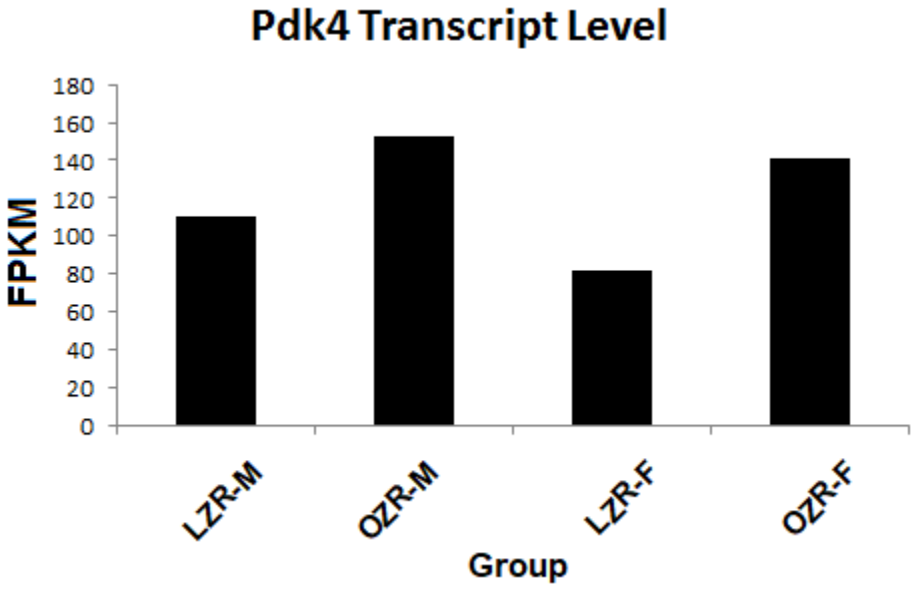

B. RT-qPCR

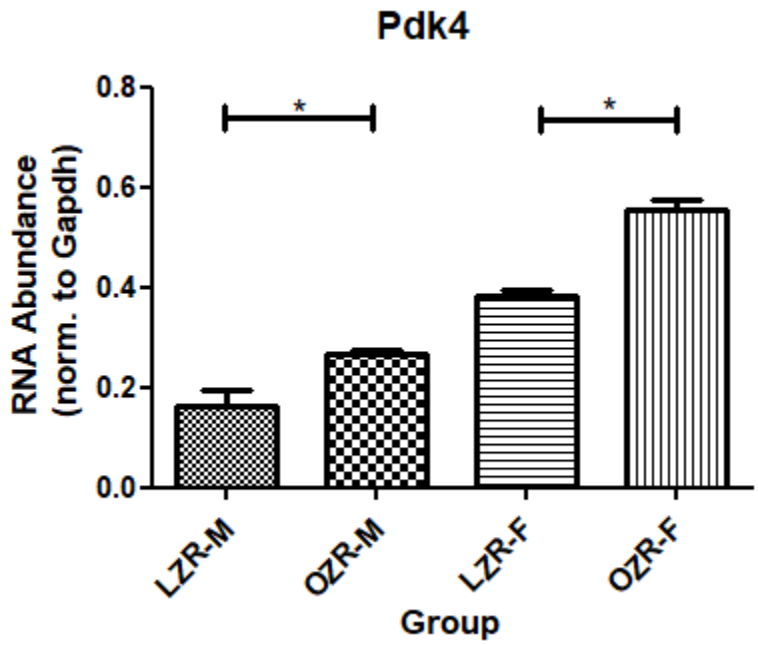

C. Western blots

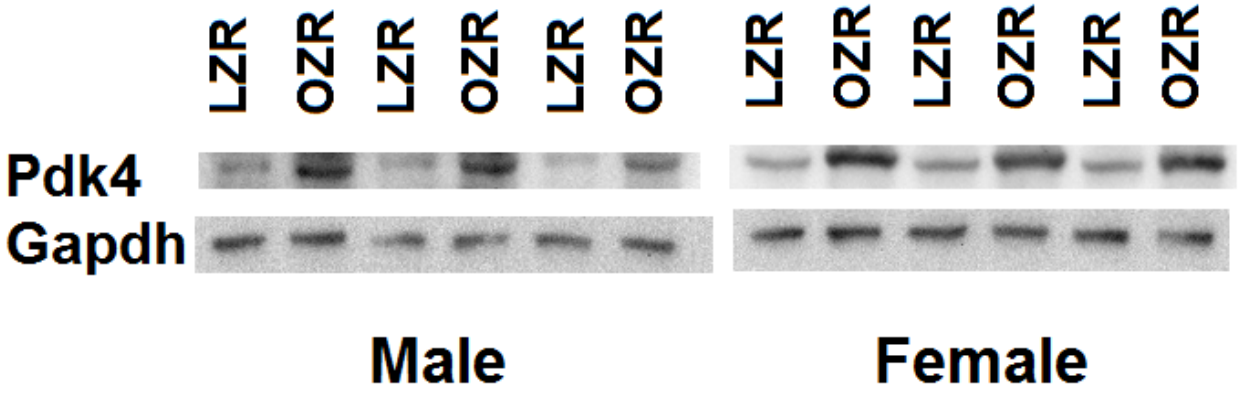

D. Protein quantification

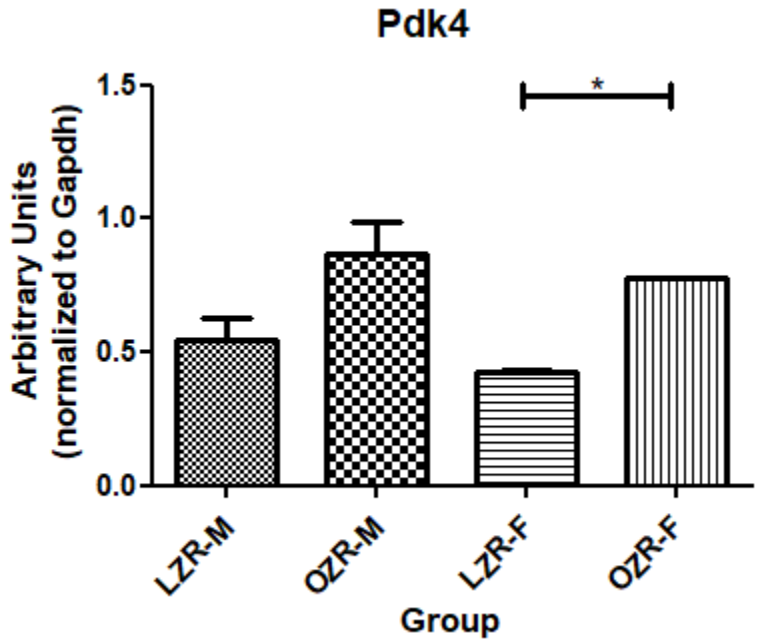

Figure 10. A: Gene expression from transcriptome. B: Gene expression from qPCR. C: Protein expression. D: Protein expression quantification. Protein level was normalized to α-actin. * indicates statistically significant ($p<0.05$).

Figure 11: Roles of sex (A) and obesity (B) in NPPA and NPPB gene expression levels between rat and human LVH.

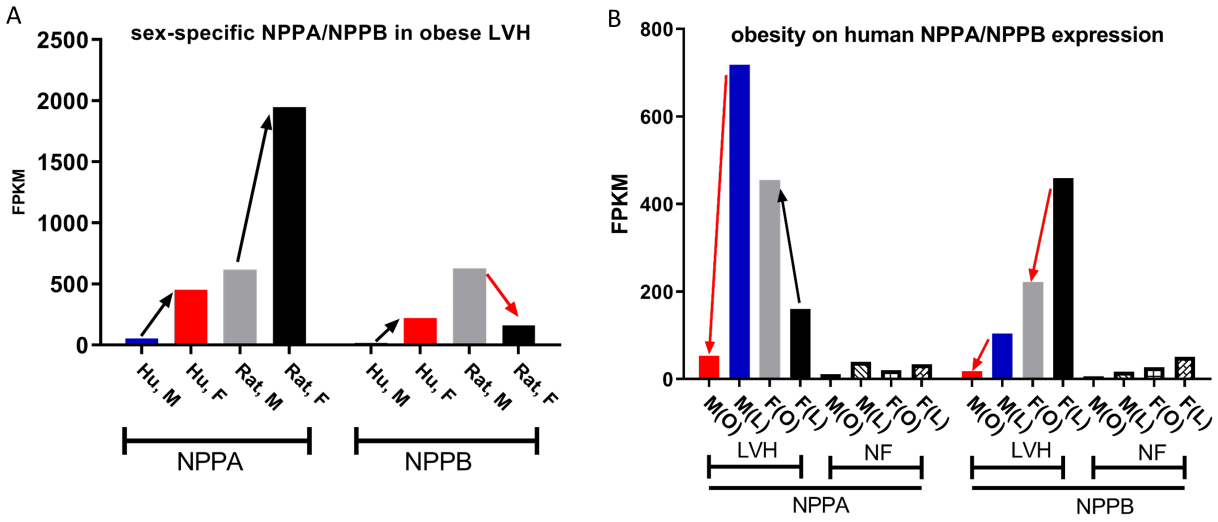

Figure 11. Black arrow: increase in paired group comparison. Red arrow: decrease in paired group comparison. NF: non-failed, non-LVH control.

Tables

Table 1: Characteristics of OZR and echocardiogram results

	Male (14-17wk) (n=4)		*Female (14-17wk)(n=4)*	
	Lean	*Obese*	*Lean*	*Obese*
Body weight(g)	350±82	607±57*	273±15	575±24*
Heart weight(g)	1.16±0.06	1.75±0.15*	0.85±0.07	1.55±0.06*
HR (bpm)	417±36	371±11	384±18	374±6
LV mass (mg)[&]	786±39	1043±96*	443±8	705±33*
IVS;d (mm)	1.79±0.21	2.05±0.04	1.72±0.04	2.02±0.12*
LVID;d (mm)	5.94±1.04	7.84±0.1*	5.38±0.13	6.95±0.15
LVPW;d (mm)#	1.75±0.15	2.31±0.35*	1.29±0.11	1.76±0.11*
EF (%)	83.16±7.25	80.10±12.13	89.92±6.90	86.90±12.42
FS (%)	53.96±8.08	51.67±12.25	64.08±13.12	60.81±15.08

*: $p<0.05$ compared to sex-matched lean control group

#: n=6-8 as more than one area was measured.

&: body-size corrected.

Table 2: Resting heart rate, ST elevation, and heart rate variability from ECG

	Male		Female	
	Lean	Obese	Lean	Obese
HR (bpm)	394±16	310±17*	228±16	198±19
STe(mV)	0.092±0.008	0.140±0.025*	0.10±0.12	0.079±0.057
nLF	0.621±0.169	0.205±0.082*	0.589±0.009	0.350±0.059*
nHF	0.379±0.169	0.795±0.082*	0.414±0.009	0.650±0.059*
LF/HF	1.951±1.062	0.267±0.129#	1.419±0.052	0.545±0.136*

*: $p<0.05$ (n=3) compared to sex-matched lean control group. #: $p=0.0526$

References

(1) Abel ED, Litwin SE, and Sweeney G. Cardiac remodeling in obesity. *Physiol Rev* 88: 389-419, 2008.

(2) Anders S, and Huber W. Differential expression analysis for sequence count data. *Genome Biol* 11: R106, 2010.

(3) Avelar E, Cloward TV, Walker JM, Farney RJ, Strong M, Pendleton RC, Segerson N, Adams TD, Gress RE, Hunt SC, and Litwin SE. Left ventricular hypertrophy in severe obesity: interactions among blood pressure, nocturnal hypoxemia, and body mass. *Hypertension* 49: 34-39, 2007.

(4) Basoor A, Cotant J, Patel K, Randhawa G, Todorov M, Halabi A, Choksi N, Shafiq A, Stein P, and DeGregorio M. Obesity and ST Elevation Myocardial Infarction in Young. *CHEST* 140: 984A, 2011.

(5) Battistoni A, Rubattu S, and Volpe M. Circulating biomarkers with preventive, diagnostic and prognostic implications in cardiovascular diseases. *Int J Cardiol* 157: 160-168, 2012.

(6) Benichou T, Pereira B, Mermillod M, Tauveron I, Pfabigan D, Maqdasy S, and Dutheil F. Heart rate variability in type 2 diabetes mellitus: A systematic review and meta-analysis. *PLoS One* 13: e0195166, 2018.

(7) Bharati S, and Lev M. Cardiac conduction system involvement in sudden death of obese young people. *Am Heart J* 129: 273-281, 1995.

(8) Bick AG, Flannick J, Ito K, Cheng S, Vasan RS, Parfenov MG, Herman DS, DePalma SR, Gupta N, Gabriel SB, Funke BH, Rehm HL, Benjamin EJ, Aragam J, Taylor HA, Jr., Fox ER, Newton-Cheh C, Kathiresan S, O'Donnell CJ, Wilson JG, Altshuler DM, Hirschhorn JN,

Seidman JG, and Seidman C. Burden of rare sarcomere gene variants in the Framingham and Jackson Heart Study cohorts. *Am J Hum Genet* 91: 513-519, 2012.

(9) Bignolais O, Quang KL, Naud P, El Harchi A, Briec F, Piron J, Bourge A, Leoni AL, Charpentier F, and Demolombe S. Early ion-channel remodeling and arrhythmias precede hypertrophy in a mouse model of complete atrioventricular block. *J Mol Cell Cardiol* 51: 713-721, 2011.

(10) Bisping E, Wakula P, Poteser M, and Heinzel FR. Targeting cardiac hypertrophy: toward a causal heart failure therapy. *J Cardiovasc Pharmacol* 64: 293-305, 2014.

(11) Burr RL. Interpretation of normalized spectral heart rate variability indices in sleep research: a critical review. *Sleep* 30: 913-919, 2007.

(12) Casale PN, Devereux RB, Kligfield P, Eisenberg RR, Miller DH, Chaudhary BS, and Phillips MC. Electrocardiographic detection of left ventricular hypertrophy: Development and prospective validation of improved criteria. 6: 572-580, 1985.

(13) Chadwick J, and Mann W. *Medical Works of Hippocrates*. Oxford: Black-well, 1950.

(14) Chua SC, Jr., White DW, Wu-Peng XS, Liu SM, Okada N, Kershaw EE, Chung WK, Power-Kehoe L, Chua M, Tartaglia LA, and Leibel RL. Phenotype of fatty due to Gln269Pro mutation in the leptin receptor (Lepr). *Diabetes* 45: 1141-1143, 1996.

(15) Cooper RS, Simmons BE, Castaner A, Santhanam V, Ghali J, and Mar M. Left ventricular hypertrophy is associated with worse survival independent of ventricular function and number of coronary arteries severely narrowed. *Am J Cardiol* 65: 441-445, 1990.

(16) Counihan PJ, Fei L, Bashir Y, Farrell TG, Haywood GA, and McKenna WJ. Assessment of heart rate variability in hypertrophic cardiomyopathy. Association with clinical and prognostic features. *Circulation* 88: 1682-1690, 1993.

(17) Courand P-Y, Grandjean A, Charles P, Paget V, Khettab F, Bricca G, Boussel L, Lantelme P, and Harbaoui B. R Wave in aVL Lead Is a Robust Index of Left Ventricular Hypertrophy: A Cardiac MRI Study. *American Journal of Hypertension* 28: 1038-1048, 2015.

(18) Das SR, Alexander KP, Chen AY, Powell-Wiley TM, Diercks DB, Peterson ED, Roe MT, and de Lemos JA. Impact of Body Weight and Extreme Obesity on the Presentation, Treatment, and In-Hospital Outcomes of 50,149 Patients With ST-Segment Elevation Myocardial Infarction: Results From the NCDR (National Cardiovascular Data Registry). *Journal of the American College of Cardiology* 58: 2642-2650, 2011.

(19) Duflou J, Virmani R, Rabin I, Burke A, Farb A, and Smialek J. Sudden death as a result of heart disease in morbid obesity. *Am Heart J* 130: 306-313, 1995.

(20) Dwyer JP, Ritchie ME, Smyth GK, Harrap SB, Delbridge L, Domenighetti AA, and Di Nicolantonio R. Myocardial gene expression associated with genetic cardiac hypertrophy in the absence of hypertension. *Hypertens Res* 31: 941-955, 2008.

(21) Electrophysiology TFotESoCtNASoP. Heart Rate Variability. *Standards of Measurement, Physiological Interpretation, and Clinical Use* 93: 1043-1065, 1996.

(22) Emdin M, Passino C, Prontera C, Fontana M, Poletti R, Gabutti A, Mammini C, Giannoni A, Zyw L, Zucchelli G, and Clerico A. Comparison of brain natriuretic peptide (BNP) and amino-terminal ProBNP for early diagnosis of heart failure. *Clin Chem* 53: 1289-1297, 2007.

(23) England J, and Loughna S. Heavy and light roles: myosin in the morphogenesis of the heart. *Cell Mol Life Sci* 70: 1221-1239, 2013.

(24) Foppa M, Duncan BB, and Rohde LE. Echocardiography-based left ventricular mass estimation. How should we define hypertrophy? *Cardiovasc Ultrasound* 3: 17, 2005.

(25) Frey N, Katus HA, Olson EN, and Hill JA. Hypertrophy of the heart: a new therapeutic target? *Circulation* 109: 1580-1589, 2004.

(26) Friddle CJ, Koga T, Rubin EM, and Bristow J. Expression profiling reveals distinct sets of genes altered during induction and regression of cardiac hypertrophy. *Proc Natl Acad Sci U S A* 97: 6745-6750, 2000.

(27) Gardner DG. Natriuretic peptides: markers or modulators of cardiac hypertrophy? *Trends Endocrinol Metab* 14: 411-416, 2003.

(28) Guimaraes PS, Huber DA, Campagnole-Santos MJ, and Schreihofer AM. Development of attenuated baroreflexes in obese Zucker rats coincides with impaired activation of nucleus tractus solitarius. *Am J Physiol Regul Integr Comp Physiol* 306: R681-692, 2014.

(29) Gurm HS, and Topol EJ. The ECG in acute coronary syndromes: new tricks from an old dog. *Heart* 91: 851-853, 2005.

(30) Hailstones D, Barton P, Chan-Thomas P, Sasse S, Sutherland C, Hardeman E, and Gunning P. Differential regulation of the atrial isoforms of the myosin light chains during striated muscle development. *J Biol Chem* 267: 23295-23300, 1992.

(31) Heckbert SR, Post W, Pearson GD, Arnett DK, Gomes AS, Jerosch-Herold M, Hundley WG, Lima JA, and Bluemke DA. Traditional cardiovascular risk factors in relation to left ventricular mass, volume, and systolic function by cardiac magnetic resonance imaging: the Multiethnic Study of Atherosclerosis. *J Am Coll Cardiol* 48: 2285-2292, 2006.

(32) Hua R, MacLeod SL, Polina I, Moghtadaei M, Jansen HJ, Bogachev O, O'Blenes SB, Sapp JL, Legare J-F, and Rose RA. Effects of Wild-Type and Mutant Forms of Atrial Natriuretic Peptide on Atrial Electrophysiology and Arrhythmogenesis. *Circ Arrhythm Electrophysiol* 8: 1240-1254, 2015.

(33) Huber DA, and Schreihofer AM. Attenuated baroreflex control of sympathetic nerve activity in obese Zucker rats by central mechanisms. *J Physiol* 588: 1515-1525, 2010.

(34) Hubert HB, Feinleib M, McNamara PM, and Castelli WP. Obesity as an independent risk factor for cardiovascular disease: a 26-year follow-up of participants in the Framingham Heart Study. *Circulation* 67: 968-977, 1983.

(35) Istenes I, Korei AE, Putz Z, Nemeth N, Martos T, Keresztes K, Kempler MS, Erzsebet VO, Vargha P, and Kempler P. Heart rate variability is severely impaired among type 2 diabetic patients with hypertension. *Diabetes Metab Res Rev* 30: 305-312, 2014.

(36) Jujic A, Leosdottir M, Ostling G, Gudmundsson P, Nilsson PM, Melander O, and Magnusson M. A genetic variant of the atrial natriuretic peptide gene is associated with left ventricular hypertrophy in a non-diabetic population--the Malmo preventive project study. *BMC Med Genet* 14: 64, 2013.

(37) Kenchaiah S, Evans JC, Levy D, Wilson PWF, Benjamin EJ, Larson MG, Kannel WB, and Vasan RS. Obesity and the Risk of Heart Failure. *New England Journal of Medicine* 347: 305-313, 2002.

(38) Kerkela R, Ulvila J, and Magga J. Natriuretic Peptides in the Regulation of Cardiovascular Physiology and Metabolic Events. *J Am Heart Assoc* 4: e002423, 2015.

(39) Kim D, Pertea G, Trapnell C, Pimentel H, Kelley R, and Salzberg SL. TopHat2: accurate alignment of transcriptomes in the presence of insertions, deletions and gene fusions. *Genome Biol* 14: R36, 2013.

(40) Kindel TL, Foster TOM, Harmann L, and Strande J. Sleeve Gastrectomy in Obese Zucker Rats Restores Cardiac Function and Geometry Toward a Lean Phenotype Independent of Weight Loss. *J Card Fail* 25: 372-379, 2019.

(41) Kleiger RE, Miller JP, Bigger JT, Jr., and Moss AJ. Decreased heart rate variability and its association with increased mortality after acute myocardial infarction. *Am J Cardiol* 59: 256-262, 1987.

(42) La Rovere MT, Pinna GD, Maestri R, Mortara A, Capomolla S, Febo O, Ferrari R, Franchini M, Gnemmi M, Opasich C, Riccardi PG, Traversi E, and Cobelli F. Short-term heart rate variability strongly predicts sudden cardiac death in chronic heart failure patients. *Circulation* 107: 565-570, 2003.

(43) Lee I-K. The Role of Pyruvate Dehydrogenase Kinase in Diabetes and Obesity. *Diabetes Metab J* 38: 181-186, 2014.

(44) Lim DS, Roberts R, and Marian AJ. Expression profiling of cardiac genes in human hypertrophic cardiomyopathy: insight into the pathogenesis of phenotypes. *J Am Coll Cardiol* 38: 1175-1180, 2001.

(45) Lin Y-C, Huang J, Kan H, Castranova V, Frisbee JC, and Yu H-G. Defective calcium inactivation causes long QT in obese insulin-resistant rat. *Am J Physiol Heart Circ Physiol* 302: H1013-H1022, 2012.

(46) Marfella R, Di Filippo C, Portoghese M, Barbieri M, Ferraraccio F, Siniscalchi M, Cacciapuoti F, Rossi F, D'Amico M, and Paolisso G. Myocardial lipid accumulation in patients with pressure-overloaded heart and metabolic syndrome. *Journal of Lipid Research* 50: 2314-2323, 2009.

(47) Maron BJ, and Maron MS. Hypertrophic cardiomyopathy. *Lancet* 381: 242-255, 2013.

(48) Maron MS. Clinical utility of cardiovascular magnetic resonance in hypertrophic cardiomyopathy. *J Cardiovasc Magn Reson* 14: 13, 2012.

(49) Maron MS, Lesser JR, and Maron BJ. Management implications of massive left ventricular hypertrophy in hypertrophic cardiomyopathy significantly underestimated by echocardiography but identified by cardiovascular magnetic resonance. *Am J Cardiol* 105: 1842-1843, 2010.

(50) Marsh SA, Powell PC, Agarwal A, Dell'Italia LJ, and Chatham JC. Cardiovascular dysfunction in Zucker obese and Zucker diabetic fatty rats: role of hydronephrosis. 293: H292-H298, 2007.

(51) Marsh SA, Powell PC, Agarwal A, Dell'Italia LJ, and Chatham JC. Cardiovascular dysfunction in Zucker obese and Zucker diabetic fatty rats: role of hydronephrosis. *Am J Physiol Heart Circ Physiol* 293: H292-298, 2007.

(52) Moghtadaei M, Polina I, and Rose RA. Electrophysiological effects of natriuretic peptides in the heart are mediated by multiple receptor subtypes. *Prog Biophys Mol Biol* 120: 37-49, 2016.

(53) Mori T, Chen YF, Feng JA, Hayashi T, Oparil S, and Perry GJ. Volume overload results in exaggerated cardiac hypertrophy in the atrial natriuretic peptide knockout mouse. *Cardiovasc Res* 61: 771-779, 2004.

(54) Mukoyama M, Nakao K, Hosoda K, Suga S, Saito Y, Ogawa Y, Shirakami G, Jougasaki M, Obata K, Yasue H, and et al. Brain natriuretic peptide as a novel cardiac hormone in humans. Evidence for an exquisite dual natriuretic peptide system, atrial natriuretic peptide and brain natriuretic peptide. *J Clin Invest* 87: 1402-1412, 1991.

(55) Nepper-Christensen L, Lønborg J, Ahtarovski KA, Høfsten DE, Kyhl K, Ghotbi AA, Schoos MM, Göransson C, Bertelsen L, Køber L, Helqvist S, Pedersen F, Saünamaki K, Jørgensen E, Kelbæk H, Holmvang L, Vejlstrup N, and Engstrøm T. Left Ventricular Hypertrophy Is Associated With Increased Infarct Size and Decreased Myocardial Salvage in

Patients With ST-Segment Elevation Myocardial Infarction Undergoing Primary Percutaneous Coronary Intervention. *Journal of the American Heart Association* 6: e004823, 2017.

(56) Newman MS, Nguyen T, Watson MJ, Hull RW, and Yu HG. Transcriptome profiling reveals novel BMI- and sex-specific gene expression signatures for human cardiac hypertrophy. *Physiol Genomics* 49: 355-367, 2017.

(57) Nolan J, Batin PD, Andrews R, Lindsay SJ, Brooksby P, Mullen M, Baig W, Flapan AD, Cowley A, Prescott RJ, Neilson JM, and Fox KA. Prospective study of heart rate variability and mortality in chronic heart failure: results of the United Kingdom heart failure evaluation and assessment of risk trial (UK-heart). *Circulation* 98: 1510-1516, 1998.

(58) Perego L, Pizzocri P, Corradi D, Maisano F, Paganelli M, Fiorina P, Barbieri M, Morabito A, Paolisso G, Folli F, and Pontiroli AE. Circulating leptin correlates with left ventricular mass in morbid (grade III) obesity before and after weight loss induced by bariatric surgery: a potential role for leptin in mediating human left ventricular hypertrophy. *J Clin Endocrinol Metab* 90: 4087-4093, 2005.

(59) Perrin MJ, and Gollob MH. The role of atrial natriuretic peptide in modulating cardiac electrophysiology. *Heart Rhythm* 9: 610-615, 2012.

(60) Phillips MS, Liu Q, Hammond HA, Dugan V, Hey PJ, Caskey CJ, and Hess JF. Leptin receptor missense mutation in the fatty Zucker rat. *Nat Genet* 13: 18-19, 1996.

(61) Potter LR, Yoder AR, Flora DR, Antos LK, and Dickey DM. Natriuretic peptides: their structures, receptors, physiologic functions and therapeutic applications. *Handb Exp Pharmacol* 341-366, 2009.

(62) Ren J, Walsh MF, Jefferson L, Natavio M, Ilg KJ, Sowers JR, and Brown RA. Basal and ethanol-induced cardiac contractile response in lean and obese Zucker rat hearts. *J Biomed Sci* 7: 390-400, 2000.

(63) Rennie KL, Hemingway H, Kumari M, Brunner E, Malik M, and Marmot M. Effects of moderate and vigorous physical activity on heart rate variability in a British study of civil servants. *Am J Epidemiol* 158: 135-143, 2003.

(64) Roden DM, Balser JR, George AL, Jr., and Anderson ME. Cardiac ion channels. *Annu Rev Physiol* 64: 431-475, 2002.

(65) RStudio-Team. *RStudio: Integrated Development for R. RStudio, Inc.* Boston, MA: 2015.

(66) Rubattu S, Bigatti G, Evangelista A, Lanzani C, Stanzione R, Zagato L, Manunta P, Marchitti S, Venturelli V, Bianchi G, Volpe M, and Stella P. Association of atrial natriuretic peptide and type a natriuretic peptide receptor gene polymorphisms with left ventricular mass in human essential hypertension. *J Am Coll Cardiol* 48: 499-505, 2006.

(67) Santolini M, Romay MC, Yukhtman CL, Rau CD, Ren S, Saucerman JJ, Wang JJ, Weiss JN, Wang Y, Lusis AJ, and Karma A. A personalized, multiomics approach identifies genes involved in cardiac hypertrophy and heart failure. *NPJ Syst Biol Appl* 4: 12, 2018.

(68) Semsarian C, Ingles J, Maron MS, and Maron BJ. New perspectives on the prevalence of hypertrophic cardiomyopathy. *J Am Coll Cardiol* 65: 1249-1254, 2015.

(69) Sergeeva IA, and Christoffels VM. Regulation of expression of atrial and brain natriuretic peptide, biomarkers for heart development and disease. *Biochim Biophys Acta* 1832: 2403-2413, 2013.

(70) Stuckey MI, Tulppo MP, Kiviniemi AM, and Petrella RJ. Heart rate variability and the metabolic syndrome: a systematic review of the literature. *Diabetes Metab Res Rev* 30: 784-793, 2014.

(71) Tarazona S, Garcia-Alcalde F, Dopazo J, Ferrer A, and Conesa A. Differential expression in RNA-seq: a matter of depth. *Genome Res* 21: 2213-2223, 2011.

(72) Tarvainen MP, Niskanen JP, Lipponen JA, Ranta-Aho PO, and Karjalainen PA. Kubios HRV--heart rate variability analysis software. *Comput Methods Programs Biomed* 113: 210-220, 2014.

(73) Tarvainen MP, Ranta-Aho PO, and Karjalainen PA. An advanced detrending method with application to HRV analysis. *IEEE Trans Biomed Eng* 49: 172-175, 2002.

(74) Trapnell C, Williams BA, Pertea G, Mortazavi A, Kwan G, van Baren MJ, Salzberg SL, Wold BJ, and Pachter L. Transcript assembly and quantification by RNA-Seq reveals unannotated transcripts and isoform switching during cell differentiation. *Nat Biotech* 28: 511-515, 2010.

(75) Tsuji H, Larson MG, Venditti FJ, Jr., Manders ES, Evans JC, Feldman CL, and Levy D. Impact of reduced heart rate variability on risk for cardiac events. The Framingham Heart Study. *Circulation* 94: 2850-2855, 1996.

(76) Vest AR, Heneghan HM, Agarwal S, Schauer PR, and Young JB. Bariatric surgery and cardiovascular outcomes: a systematic review. *Heart* 98: 1763-1777, 2012.

(77) Wang D, Gladysheva IP, Fan T-HM, Sullivan R, Houng AK, and Reed GL. Atrial natriuretic peptide affects cardiac remodeling, function, heart failure, and survival in a mouse model of dilated cardiomyopathy. *Hypertension* 63: 514-519, 2014.

(78) Wang K, Asinger RW, and Marriott HJL. ST-Segment Elevation in Conditions Other Than Acute Myocardial Infarction. 349: 2128-2135, 2003.

(79) Wong CY, O'Moore-Sullivan T, Leano R, Byrne N, Beller E, and Marwick TH. Alterations of left ventricular myocardial characteristics associated with obesity. *Circulation* 110: 3081-3087, 2004.

(80) Yates A, Akanni W, Amode MR, Barrell D, Billis K, Carvalho-Silva D, Cummins C, Clapham P, Fitzgerald S, Gil L, Giron CG, Gordon L, Hourlier T, Hunt SE, Janacek SH, Johnson N, Juettemann T, Keenan S, Lavidas I, Martin FJ, Maurel T, McLaren W, Murphy DN, Nag R, Nuhn M, Parker A, Patricio M, Pignatelli M, Rahtz M, Riat HS, Sheppard D, Taylor K, Thormann A, Vullo A, Wilder SP, Zadissa A, Birney E, Harrow J, Muffato M, Perry E, Ruffier M, Spudich G, Trevanion SJ, Cunningham F, Aken BL, Zerbino DR, and Flicek P. Ensembl 2016. *Nucleic Acids Res* 44: D710-716, 2016.

(81) Zhou YT, Grayburn P, Karim A, Shimabukuro M, Higa M, Baetens D, Orci L, and Unger RH. Lipotoxic heart disease in obese rats: implications for human obesity. *Proc Natl Acad Sci U S A* 97: 1784-1789, 2000.

Supplemental Figures

Figure S1: Principle component analysis (PCA) in female (left) and male rats showing that the groups of obese versus lean rats in both sexes are coherent.

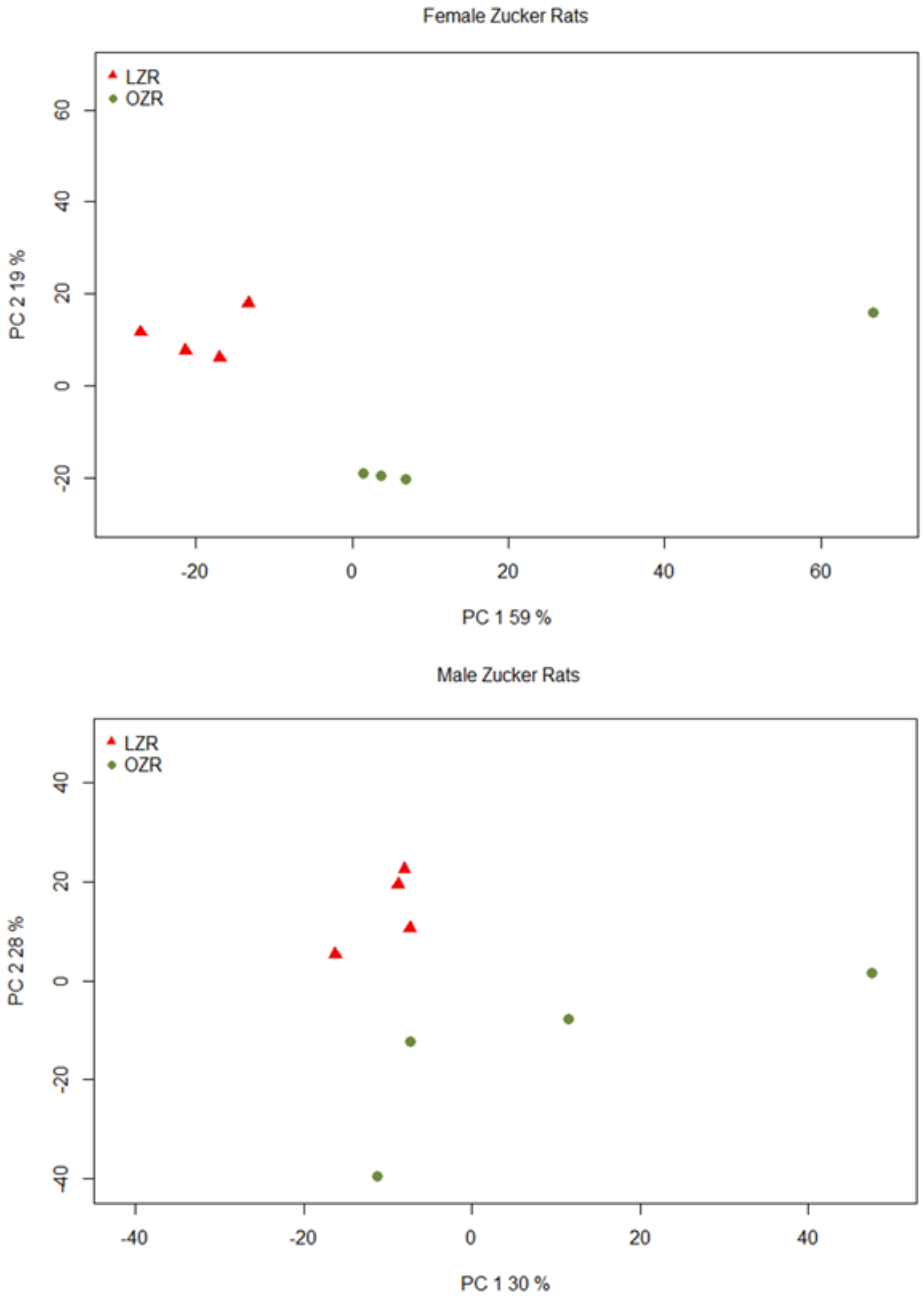

Figure S1. PCA plots displaying clustering of individual samples. Red triangles represent LZR and green circles are obese; females are displayed in the left graph and males are in the right graph.

Figure S2: Differential expression profiles between obese and lean animals (volcano plots)

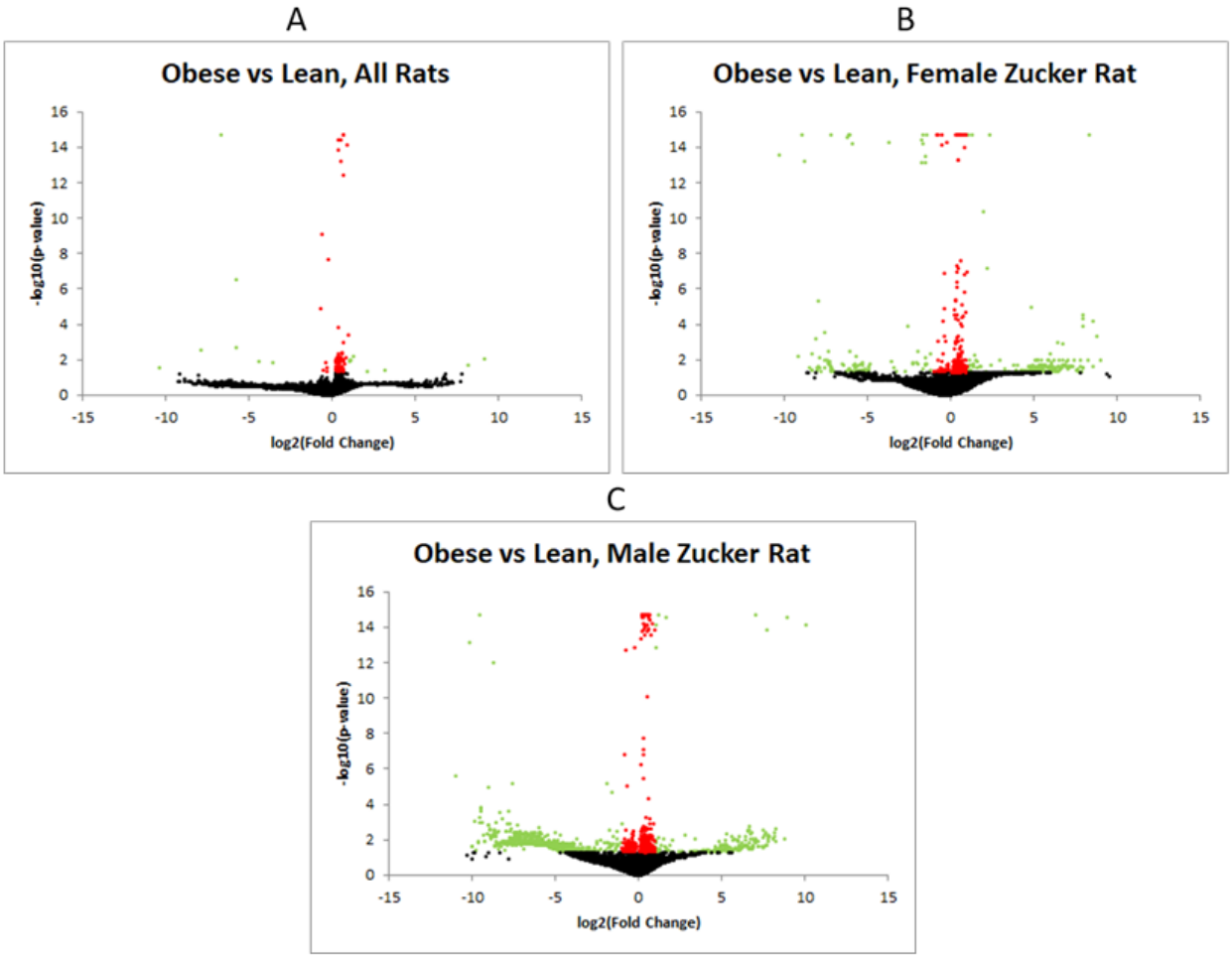

Figure S2. A: All samples analyzed without regard to sex. B: Obese versus lean females. C: Obese versus lean males. Black dots represent genes with p-value < 0.05. Red dots represent genes with p-value < 0.05 but less than a two-fold change in expression. Green dots represent genes with p-value < 0.05 and expression level greater than two-fold.

Figure S3: Heatmaps of differentially expressed genes in OZR

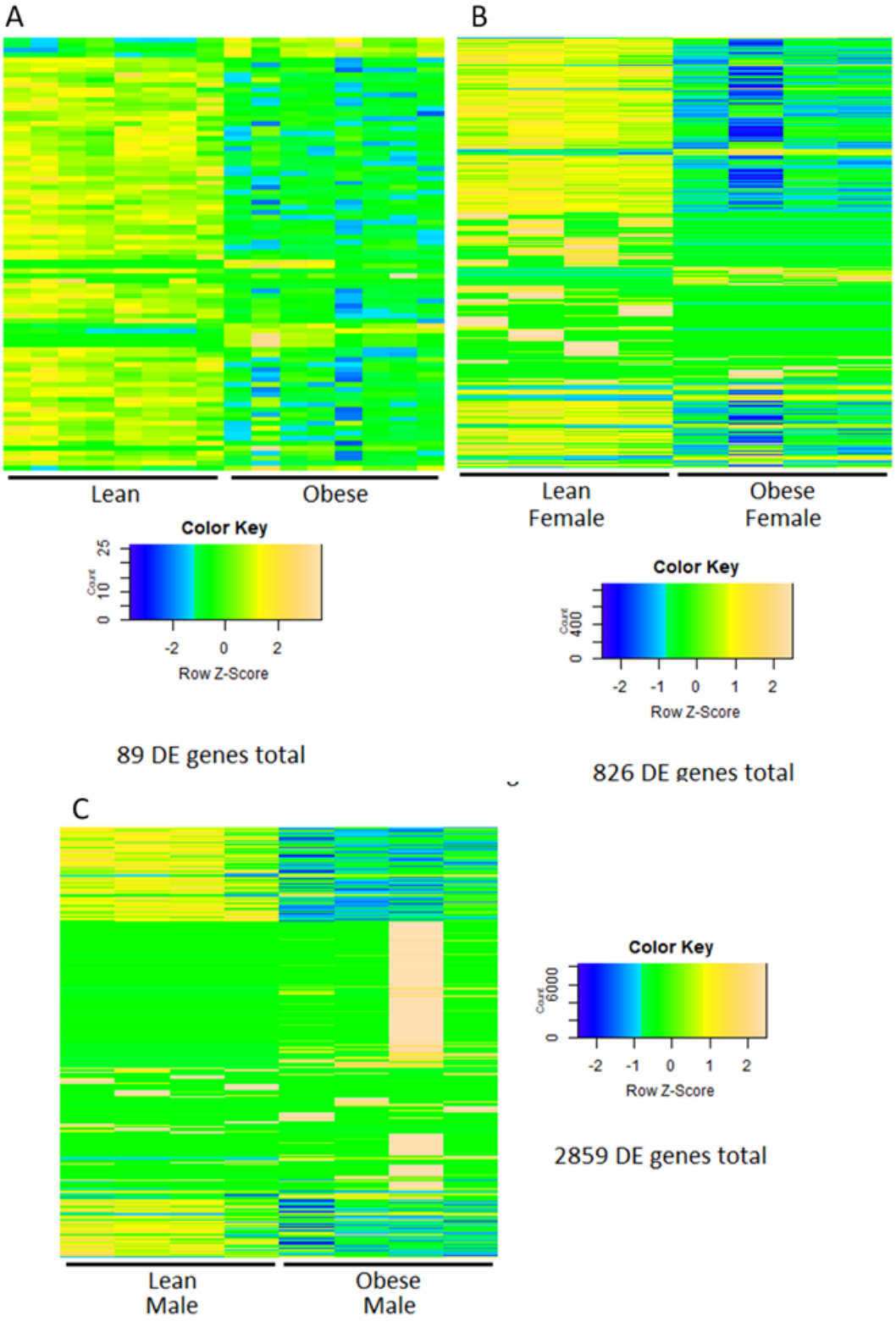

Figure S3. Each column represents one animal. Transcriptome data were analyzed for differential expression in obese versus lean animals for A: all samples (regardless of sex), B: females only, and C: males only. Heatmaps were generated using the gplot function in R.

Supplemental Tables

Supplemental Table 1. Primers used in qPCR.

Gene	Strand	Sequence
NPPA	F	GCAAACATCAGATCGTGCCC
	R	GGTCTAGCAGGTTCTTGAAATCC
NPPB	F	AGCTCTCAAAGGACCAAGGC
	R	CGATCCGGTCTATCTTCTGCC
HIST1H2AC	F	ACACCTTACCTTTTCCACTTCC
	R	GCGTCCAGACATCGTTATGC
GSTT1	F	TCCAGATGCATACTGTGGAGC
	R	TGGCCACACTCTCACACAAGG
PDK4	F	TGGTGAAGAGCTGGTACATCC
	R	ATCCCTTGTGCCATCGTAGG
MYL7	F	CTCAATGTTCGAGCAAGCCC
	R	GACACTTACCCTCCCGAGC
HBB	F	CTGGGCAGGCTGCTGG
	R	TCAGATGAGCAAAGGTGCCC
GAPDH	F	CAACTCCCTCAAGATTGTCAGCAA
	R	GGCATGGACTGTGGTCATGA

Supplemental Table 2. Significant Differentially-Expressed Genes Per Sex

GeneName	log2FC Female	p-value Female	log2FC Male	p-value Male
AABR06001092.3	-5.730464004	0.006867631	-5.587444214	0.017538338
AABR06002048.1	5.474802166	0.046768716	-5.899857199	0.020329196
AABR06003762.1	5.64791736	0.021892925	-6.049120464	0.020924976
AABR06008694.1	6.612430939	0.029549546	-8.620401091	0.005975624
AABR06009495.2	6.641521781	0.026806303	6.739967734	0.032850468
AABR06009537.6	-7.593939062	0.030485885	7.054664058	0.014314151
AABR06022532.1	5.425902591	0.04852144	-4.676637294	0.044207941
AABR06024198.1	6.630507627	0.027811611	6.834896348	0.030537616
AABR06024761.1	6.267520439	0.041113763	-6.497590744	0.014741877
AABR06025560.2	4.921446692	0.03784446	-6.584814784	0.015513413
AABR06027295.1	7.94417136	0.000132794	-7.596415435	0.012709633

AABR06027333.1	4.885063042	0.041975951	-7.725504514	0.018014809
AABR06028157.1	7.606891073	0.043823061	-8.620401091	0.005975624
AABR06028909.1	5.569160597	0.045447886	-6.724777073	0.016953624
AABR06030345.1	4.999134344	0.044856331	-5.21384995	0.026995547
AABR06030862.1	2.127493539	0.046006385	4.906853561	0.028547391
AABR06031450.1	-5.621704021	0.039238767	-6.242374048	0.016689447
AABR06031580.1	5.402081585	0.049376162	-4.845748232	0.03894374
AABR06031627.1	5.437967602	0.048072641	-5.761342842	0.00989319
AABR06042542.1	6.268881516	0.041184128	6.473725938	0.021827543
AABR06043079.1	4.771726188	0.037246584	-7.48026874	0.006872807
AABR06045328.2	-9.157541849	0.006901706	-10.97271827	2.36148E-06
AABR06045400.1	-5.694710338	0.025507481	-4.712676338	0.016914267
AABR06046610.1	5.404688557	0.049289009	-4.905580062	0.035350768
AABR06047190.1	-	0.024503013	-	0.01103747

	7.221099856		7.590851117	
AABR06047625.1	6.344460351	0.044357662	-6.724777073	0.016953624
AABR06050424.1	6.202888777	0.038097669	-8.160302291	0.012895458
AABR06052098.1	6.123638752	0.037293865	-9.756404167	0.04203545
AABR06052644.1	5.485454457	0.021961767	4.144056596	0.04674109
AABR06054455.1	-7.205285768	0.03794693	-6.604668142	0.015769722
AABR06055554.1	0.34234201	0.023637241	0.192215961	0.044637305
AABR06055804.1	0.360817095	0.044907147	0.278251212	0.044665764
AABR06058815.1	-8.134764207	0.000605044	-7.691897758	0.002479804
AABR06059337.1	-7.100043994	0.043508355	6.183120784	0.028000384
AABR06059957.1	7.144611887	0.025697511	-8.432012537	0.021791267
AABR06060284.1	-5.745410059	0.017610357	-6.747828475	0.018139359
AABR06062642.1	5.598698447	0.045957994	-8.547480448	0.012940666
AABR06065586.1	6.971913533	0.012116814	-	0.012945739

			8.157589926	
AABR06065718.1	5.61563547	0.036360555	-5.040411106	0.027845096
AABR06066181.1	0.211521378	0.033099913	0.163550338	0.042769867
AABR06066677.1	-7.409937527	0.010771029	8.757888266	0.008370517
AABR06067381.1	5.417373268	0.048832775	-6.466272791	0.014651542
AABR06068951.1	6.389230195	0.044904553	-7.812441519	0.01483145
AABR06072704.1	6.176198847	0.037337944	6.101534315	0.034619997
AABR06072709.2	7.613910522	0.033687553	7.790094159	0.005310569
AABR06074433.1	5.964886462	0.004543887	-7.079067219	0.021408484
AABR06080098.1	7.548375195	0.037056911	-10.0337192	0.023031626
AABR06081787.1	7.157602788	0.023438023	-8.615733531	0.006343379
AABR06082987.1	6.071939834	0.022714779	6.210594527	0.025812336
AABR06086439.1	6.284162273	0.041952119	-9.569094396	0.001149496
AABR06086499.1	5.624067943	0.025697759	-6.880029517	0.016140955
AABR06090020.1	6.238806385	0.039655161	-	0.017698716

			5.538778581	
AABR06091097.2	-7.167437295	0.033067049	-6.542939897	0.015052123
AABR06094518.1	6.257829499	0.040614306	-6.37649517	0.014842829
AABR06095711.1	6.165015485	0.037148165	-8.629781936	0.005308213
AABR06097617.1	7.54269473	0.036424528	-7.02241795	0.015220933
AABR06098671.1	6.572853403	0.033570852	-7.792798317	0.013885729
AABR06099363.1	6.257829499	0.040614306	-6.637953465	0.016207932
AABR06104230.1	5.410333607	0.049087063	-5.108034597	0.014642567
AABR06108042.1	-7.263823891	0.019223496	-6.603650355	0.015756253
Abca12	3.459935696	0.045383266	-6.583349949	0.012305007
Acadl	-0.607275514	0.045428879	-0.137793339	0.01684359
Acadsb	0.890668799	0.010911172	0.610398798	0.011814675
Acot2	-0.58120987	6.99441E-15	-0.504184284	0.015381101
Acsf2	0.911905096	0	1.16347644	0

Acss1	0.763344511	0	0.602589679	4.40688E-05
Acy1	0.463633853	0.049980363	0.587055716	0.033199143
Adk	0.255682302	0.029114696	0.219784555	0.04166912
Agxt2	2.900470908	0.049948297	-5.904998099	0.0147047
Ahsa1	0.317805903	0.045691948	0.367810994	0.017583951
AI314180	0.322588664	0.045671081	0.262099643	0.041062529
Akt2	0.364876397	0.045299693	0.33098406	0.034807733
Aldh6a1	0.291433591	0.020504617	0.367517539	0.02018224
Alkbh6	5.021755859	0.037088315	4.378209885	0.049806205
Alkbh7	0.685059925	0.043948886	0.726260108	0.021886513
Angptl4	-2.762245514	0.044821936	-1.621592354	0.043044403
Ap1s2	0.575564747	0.04320077	0.421136111	0.022738184
Aqp1	0.84779176	9.99201E-15	0.617937721	0.007820683
Araf	0.444347287	0.046882239	0.488105854	0.015403714
Armc2	0.708916431	0.046359758	0.858175176	0.036384405
Art3	0.290284023	0.022083772	1.072787005	1.52989E-13
Asb11	0.607055833	2.7531E-08	0.629178896	0.020466789
Asb12	0.518211405	0.025290917	0.418729307	0.022169072
Asb15	1.084577028	0.036407893	0.683651026	0.045816184
Ascl1	4.352057597	0.046318649	-7.054482108	0.004652836

Atad1	0.540673758	0.010307023	0.461574235	0.022269345
Atp1b4	-5.325617057	0.040634128	-3.50164309	0.045642034
Atp2a2	0.430244727	5.44872E-05	0.578136476	0.020096166
Atp5a1	0.192687016	0.020807169	0.281540223	0
Atp5b	0.226766549	0.02560679	0.233284958	1.9984E-15
Atp5c1	0.305654859	0.025697696	0.322398406	0.024072964
Atp5g1	0.335923395	0.049960102	0.351669153	0.009577905
Atp5hl1	4.673080873	0.044926404	-7.521594786	0.016802928
AY172581.2	-0.567404086	0	-0.862898681	1.47148E-07
Bdh1	1.288249054	0	0.869124916	0.001274565
Bgn	-0.443574479	6.35951E-05	-0.328716063	0.017853567
Btbd1	0.150384366	0.049941279	0.206918527	0.021789401
Car7	-5.079569134	0.03958806	-4.973620776	0.014694218
Ccdc47	0.373580226	0.025874844	0.273695476	0.038963574
Ccni	0.196308539	0.021827199	0.161339802	0.043513846
Cct2	0.386163662	0.000938688	0.310511156	0.02105802
Cct7	0.357514942	0.044513607	0.234008547	0.048434217
Cct8	0.238013998	0.02248408	0.274560916	0.02695599

Cd40lg	4.844293419	0.044485478	4.446372587	0.043451139
Cdh5	0.859440965	1.97549E-05	0.264170594	0.044545653
Cdkn1b	0.527213781	0.019219126	0.346736296	0.047470007
Cdrt4	6.031707691	0.014068845	-6.662422172	0.012687202
Chchd3	0.375916331	0.038491516	0.485882399	0.010444244
Cldn6	5.428940032	0.032789751	-7.080481776	0.004976843
Cmbl	0.293924191	0.025443429	0.478210835	0.032304264
Cmya5	0.599965504	0.022969986	0.382578413	0.044684262
Cnpy1	-3.701346758	4.996E-15	-2.085963564	0.043290677
Cog6	1.010510381	0.049082095	0.95711025	0.028081709
Coq10a	0.700806087	0.039580092	0.6523307	0.000652482
Corin	0.636234278	0.020801064	0.648546707	0.021778514
Cox7c	0.531007141	0.022827842	0.397048926	0.034978937
Cox8b	0.646584078	0.044211433	0.49960678	0.033445553
Cpe	0.199099236	0.021580116	0.431308743	0.006734814
Crip3	4.501527016	0.046122986	-6.27141985	0.014287448
Ctnnal1	0.537455804	0.023560928	0.543498667	0.036115532
Ctsc	0.287475747	0.03884358	0.554831424	0.002319039
Cxcr7	0.499272399	0.016356332	0.429882573	0.045035387
Cyb5a	0.601692173	0.029027781	0.601826102	0.009020331

Dazap2	0.154060009	0.022751422	0.186642237	0.038636295
Dbt	0.575277014	0.028058767	0.561446863	1.39888E-14
Dcaf11	0.275451382	0.048440423	0.307994112	8.57317E-08
Ddx17	0.501210902	0.043938017	0.323964102	0.036532778
Ddx5	0.268576837	0.04375523	0.249992452	0.02984819
Decr1	-0.652163543	0.027509875	-0.5187071	0.014851021
Defb19	6.703738406	0.001312885	6.747663372	0.008733623
Dhrs7c	0.515875476	0.048739116	0.587829231	0.031375558
Dmrtc1c1	5.388778039	0.020900257	-6.242374048	0.016689447
Dnajb9	0.635788109	0.015122747	0.571528072	0.005376241
Dnajc21	0.327115997	0.049947392	0.339162937	0.043396026
Eef2	0.18197047	0.044097174	0.195351092	0.002458975
Eif2s3y	0.258550834	0.025319813	0.152370094	0.048715015
Eif4a2	0.280357602	5.13946E-05	0.228207161	0.026698777
Eif4g2	0.357566676	0.028476509	0.167969528	0.048776968
Errfi1	1.047374125	0.048916665	1.501277055	0.009129899
Esd	0.34672104	0.024354071	0.444086828	0.009875889
Etfa	0.088128009	0.04994981	0.093316917	0.009267487
Etfdh	0.179875567	0.014792225	0.169547658	0.021716521
Fbp2	2.184454511	6.51504E-08	-1.336645279	0.00848916

Fhl1	-0.169828044	0.031326568	-0.859618505	0.008266534
Fndc5	0.687941377	0.003705992	0.561655702	0.022023328
Fyco1	0.546744855	0.020474957	0.482205858	0.037543966
G0s2	-0.767032586	0.042781289	-0.334380674	0.042298642
Gbas	0.443293473	0.000452828	0.359960788	0.008130815
Gbp1	-0.559215606	0.013353771	-0.308920826	0.04123228
Ghitm	0.418202297	0	0.312865784	0.006634025
Ghr	0.500716695	0.020634013	0.371526065	0.035498162
Gja1	0.734775814	0	0.63683554	1.9984E-15
Glud1	0.237804532	0.022793058	0.170494083	0.044330289
Gmps	0.373609811	0.023583596	0.328009742	0.002981603
Gnb3	0.631796953	0.031813391	0.535669487	0.017021638
Gnpat	0.405501911	0.048741215	0.408989621	0.022544858
Got1	0.193117007	0.046556087	0.213334232	0.021815551
Gpd1	-0.693296476	0.045779873	-0.60646849	0.018061497
Gramd3	0.386905724	0.015547556	0.528983479	0.009995589
Gstz1	0.904332157	0.031692461	0.973211633	0.012731107
H1f0	0.363319967	0.045481856	0.243498786	0.044077889
Hba1	-	5.9952E-15	-	0.026882394

	1.647942938		0.600036835	
Hba2	-1.741094957	3.9968E-15	-0.643087765	0.021083096
Helt	-5.36513805	0.020991311	-7.449490192	0.017796224
Hibadh	0.159283107	0.01226501	0.221075202	0.002311097
Higd1a	0.624835392	0.02141784	0.487003321	0.031342491
Hist1h2an	5.864474687	0.025573167	7.209439129	0.022926782
Hk2	1.33009822	0.023686687	0.92024078	0.00988869
Hnrnpa2b1	0.202225554	2.7491E-05	0.169472424	0.031424014
Hnrnph1	0.231889251	0.048935285	0.204406336	0.04417692
Hnrnpu	0.197748288	0.021401164	0.229043924	0.045871693
Hsp90ab1	0.256396299	0.043298454	0.409652815	0.036188435
Hsp90b1	0.403250982	4.996E-14	0.646557788	0.008653939
Hspa5	0.575206625	0	0.672649519	3.9968E-15
Hspa9	0.383406673	0.022723811	0.405433998	0.012355414
Hspd1	0.296398909	0.02366013	0.319764537	0.002528457
Hsph1	0.667322164	0.011084534	0.458800505	0.041292638
Hyou1	0.43884038	0.042917088	0.578139493	0.020104822
Ift81	0.496921735	0.046693081	0.611991751	0.021793987
Igfbp1	4.876591993	0.022645134	3.435201662	0.043325498
Igfbp3	0.488950937	0.02475388	1.221064305	0.007897261
Jak1	0.54779747	0.023598722	0.283372052	0.043344227

Jam2	0.519705325	0.024190673	0.330714399	0.048432169
Klhl13	0.876381078	0.022533084	0.737878985	0.04048652
Klhl23	0.653898816	0.021900883	0.560113954	0.044188559
Kpna2	0.302032745	5.02835E-06	0.496528075	0.012669943
Lamp2	0.370940598	0.028197874	0.321798796	0.02183601
Lbh	0.448217973	0.031293342	0.357983796	0.036397665
Limd1	0.572987846	0.045310275	0.421221826	0.039165117
Lipa	-0.747590807	0	-0.401158294	0.01976415
Lmod3	0.380277732	0.022340004	0.545633588	0.021276959
LOC100134871	-1.527582317	3.39728E-14	-0.719200354	0.044271973
LOC100361144	0.446578986	0.035059134	0.251863873	0.043349505
LOC100909678	4.285349624	0.045514903	-4.719098969	0.043554887
LOC100909892	0.343172566	0.037213383	0.263903409	0.040023567
LOC100910554	-6.487970228	0.02155601	5.999675928	0.03604115
LOC100911372	0.511294219	0.023801793	0.351489109	0.043467771
LOC102551744	-5.879498791	0.021013954	-6.529870966	0.0149407
LOC257643	3.79915731	0.049956973	-7.385770149	0.003845906

LOC680913	5.139484174	0.033896942	-6.20223866	0.017623722
LOC686066	7.922826547	4.84603E-05	-3.232189001	0.044311173
LOC688924	5.508452434	0.021488548	-6.247875493	0.021049443
LOC690096	6.671551504	0.023709355	-8.929140371	0.005623601
Lpl	0.621404397	0.012641857	0.449218712	0
Lppr4	4.840325657	1.12681E-05	4.559431485	0.040330654
Lrrc2	0.421303682	0.006401647	0.306901233	0.04404651
Lsamp	0.93932807	1.10439E-07	0.395534115	0.044526818
Lsm14a	0.278617135	0.022688379	0.188545533	0.048017797
Man1c1	0.58497033	0.037109006	0.769959253	0.020621537
Manf	0.508168431	0.022870533	0.543207913	0.026367214
Mccc1	0.489089221	0.029125498	0.458541728	0.01263405
Mdh1	0.260865848	0.048808294	0.27247243	0
Mipep	0.43569083	0.045441366	0.351585974	0.049402502
Mir106b	6.464125953	0.04273539	6.669207761	0.030672039
Mir146b	6.375938015	0.044875145	-8.42814873	0.021840097
Mir185	6.60527377	0.030260155	7.501240133	0.026355749
Mir208b	1.733044849	0.023087588	2.77161138	0.005244696
Mir215	8.261364471	0.010788094	6.17403579	0.028786807
Mir219-1	7.069402441	0.030964497	-	0.012740721

			7.885770762	
Mir291a	6.476929064	0.041980394	6.668336976	0.030633138
Mir34b	6.442459895	0.043778416	-9.493619944	0.000152867
Mir3558	5.993562764	0.045828521	6.19714448	0.026840829
Mir3565	5.993562764	0.045828521	6.001284771	0.036077594
Mir3574	6.002450732	0.045012008	6.147908798	0.031084988
Mir6329	7.321269164	0.022741912	-6.801412021	0.016781534
Mirlet7c-1	7.11402254	0.026788678	-6.556130256	0.015181646
Mlf1	0.442539355	0.020875663	0.746257924	0.006799298
MORF4L1	0.269771631	0.001026021	0.360598336	0.021356446
Morf4l2	0.298507711	0.015985569	0.23363319	0.047139379
Mpc1	0.535685147	0	0.406339995	0.012515641
Mt-atp6	-0.322655684	0.000857489	-0.351029683	0.005498356
Mt-co3	-0.309782854	0.036781245	-0.376647377	0.009044942
Mut	0.763244933	0.022715737	0.555791405	0.010471082
Mybphl	-7.242669913	0	-5.283511114	0.017017428
Myh6	0.484722371	0	0.849185942	0.006508847

Myl1	-2.066218174	0.01541496	-1.714350843	0.02391371
Myl4	-6.180362206	0	-1.738837883	0.017899892
Myl7	-5.894727421	5.9952E-15	-5.062004985	0.034563751
Mylk3	0.364253423	0.040744886	0.61881681	0.013239686
Myoz2	0.477453054	0.032560618	0.389574779	0.00606133
Naa20	0.353671584	0.048926165	0.316937715	0.044198825
Nap1l4	0.276249662	0.033596126	0.167673247	0.039029575
ND3	-0.541489246	0.035012667	-0.333495057	0.014649944
Nde1	0.761744761	3.48818E-05	0.529236216	0.021653924
Ndufa5	0.358119294	0.037786127	0.361412897	0.014493893
Ndufs2	0.320122194	0.036685242	0.158936416	6.10063E-07
Nhp2l1	0.418574103	0.025257259	0.265651562	0.043265386
Nnt	0.38728641	0.02776274	0.40994615	0.00059453
Nppa	-3.587057807	0.012316634	-3.489060407	0.032429637
Nqo2	0.421595158	0.007587719	0.323755669	0.007605026
Nrd1	0.286643287	0.022615264	0.238406886	0.044404817
Nudt4	0.444316208	5.4956E-14	0.514099741	0.0068294
Ogn	-	7.50511E-14	0.622915144	0.039415497

	1.517044589			
ORF1	6.947558389	0.023160009	-7.066652498	0.014681191
Oxct1	0.859356796	0	0.522432963	0
Oxr1	0.338849137	0.037049793	0.343603787	0.020950045
Oxt	4.781612056	0.037103387	-7.765527447	0.003316296
P4hb	0.353801096	7.99805E-07	0.435828318	0.018487266
Pabpc4	0.184400659	0.023130308	0.309675586	0.011851011
Paip2	0.147105462	0.046469447	0.279511843	0.031960318
Pcbp2	0.409162586	0.03835754	0.232195112	0.032978935
Pcca	0.438856185	0.004480733	0.305408389	0.021879486
Pcmt1	0.320113105	0.042688464	0.222062654	0.021684379
Pcmtd1	0.651640312	0.038305947	0.430851599	0.034487043
Pcnp	0.311853604	0.042918382	0.250522661	0.032984969
Pdia3	0.270490103	0.001245801	0.382375449	0.010957247
Pdia6	0.306357319	0.047800947	0.42094529	0.021742818
Pdk1	0.401996033	0.033524546	0.300200469	0.007800279
Pdp2	0.795951197	0.040646033	0.760647675	0.046460252
Perm1	0.433966853	0.023660323	0.563449527	0.012307557
Pfkfb2	1.343677476	0.025134986	1.051009502	0.028162362
Pfkm	0.374332624	5.16527E-08	0.311904931	0.010215595
Pfn3	4.797619167	0.037086676	-	0.015561318

			8.066475888	
Pink1	0.303467083	1.9984E-15	0.353786174	0
Pla2g12a	0.429167334	0.046783241	0.497362911	0.019218194
Pla2g1b	5.394230948	0.049637094	-6.033111504	0.021139342
Pla2g5	0.531964139	0.012158376	0.418484755	0.00302196
Pln	0.611885545	0	0.487171083	0
Ppap2b	0.369534507	0.02452327	0.212369891	0.045522686
Ppm1k	1.04256048	0.024098594	0.800913001	0.021906365
Prdx3	0.172331767	0.024719934	0.216779735	0.021343972
Prkab1	0.437144562	0.020731848	0.647356177	0.015332496
Prkag2	-0.741484668	0.038194487	-0.548375621	0.016227733
Prkar1a	0.354324266	0.047191068	0.364608273	0.031162539
Prodh	0.670490676	0.040112361	1.047710129	7.99361E-15
Pygm	0.177098891	0.04679001	0.307668088	0.027693398
Rab1	0.311944494	0.04335158	0.175881975	0.043402545
Rab1b	0.267434992	0.042236772	0.274824774	0.025815033
Rab2a	0.193801686	0.020703123	0.296478933	0.012287851
Rabggtb	0.374152168	0.024417697	0.301979266	0.047154418
Rangrf	0.442322126	0.037094256	0.510070576	0.032934084
Rcan1	-0.42039856	0.000489459	-1.320637808	0.003622015

Rcan2	0.166987093	0.039926419	0.344161112	0.006382592
Reep5	0.363332992	0.023827933	0.319514914	0.020343535
RGD1311933	8.360321364	0	7.683618454	1.39888E-14
RGD1359290	6.280055689	0.036709687	-6.54281647	0.010808496
RGD1562055	5.388757506	0.021510049	-7.161374236	0.012051296
RGD1562977	6.39601092	0.04487618	-8.990813971	0.002255316
RGD1564827	-2.29110917	0.018501671	-3.70354597	0.008954433
Rgs5	0.815605773	1.61128E-07	-0.262803809	0.041313901
Rhox4g	4.768200089	0.024449831	-6.784021813	0.016881253
Rilpl1	0.293857942	0.023018377	0.607469596	2.9976E-15
Rn50_1_1348.1	5.913640424	0.022710316	-5.542297373	0.01615152
Rn50_13_0855.2	5.476329943	0.046717937	-8.751788286	0.004494618
Rn50_X_0554.2	7.028341431	0.011078713	-7.02241795	0.015220933
Rn50_X_0648.2	5.573718404	0.045486901	-6.623984792	0.016026185
Rn50_X_0691.3	5.242856628	0.043068807	-5.497035502	0.016992814

Rn50_X_0749.4	3.791794496	0.049947288	-5.70081855	0.01923353
Rn5s	6.002450732	0.045012008	-7.190719821	0.007305141
Rpn1	0.34064496	0.023902986	0.354985577	0.031364484
Rps25-ps2	7.418557907	0.010404298	-7.235210277	0.0085834
Rragd	0.579680961	0.025698149	0.395609451	0.048330715
RT1-O1	4.825195624	0.03770872	-4.264155894	0.048020153
Sat2	0.77246277	0.025685517	0.742306141	0.018788701
Sctr	2.956339816	0.010797109	3.376015416	0.009691025
Sdha	0.35019745	0.039134469	0.304294586	0.013006413
Sdhd	0.221620844	0.040137032	0.230100248	0
Sdr39u1	0.421524854	0.045464425	0.467998642	0.034635779
Serinc1	0.27693989	0.026747424	0.244276175	0.007837025
Set	0.353025993	0.043537938	0.254170122	0.049427633
Sh3bp5	0.497247391	0.032909297	0.39812856	0.00753254
Sh3glb1	0.206964735	0.033614384	0.347115403	0.005565973
Slc25a12	0.47972219	0.048245551	0.358647876	0.041323487
Slc25a48	-5.193900842	0.033309101	-6.692227933	0.018040929
Slc2a4	0.654282011	0.000134543	0.726193595	0.005782333
Slc41a3	0.630547009	0.024876889	0.518380514	0.04542402

Slc4a1ap	0.519567558	0.041338813	0.483934951	0.049798653
Slc4a3	0.33876168	0.048698851	0.548709379	0.014402994
Slc6a8	0.626661284	0.024755298	0.364755932	0.04957447
Sln	-6.249252612	2.9976E-15	-4.011773682	0.017158246
Spink8	0.386421654	0.025694247	0.265747102	0.043299275
Spop	0.402770866	6.72427E-08	0.238048871	0.034654498
Spp2	4.671133308	0.025519088	-5.862048085	0.019812403
Spryd7	0.184628386	0.029054706	0.594132823	0.016066519
Srsf5	0.267118927	0.048027235	0.3463088	0.024224051
Sspn	0.439932453	0.045421261	0.42167133	0.043764684
Stip1	0.506683269	0.028194993	0.39469689	0.009583563
Stx4	0.439790665	0.028729016	0.422336005	0.013082737
Suclg2	0.255190729	0.023472475	0.272232127	0.021658218
Sypl1	0.442189035	0.025134988	0.355162059	0.031693223
Tasp1	0.606585577	0.044612875	0.473013139	0.034715117
Tcp1	0.29262856	0.016166257	0.33729851	0.02972758
Tcp11l2	0.63296282	4.29345E-05	0.554766865	1.29896E-14
Tex13b	4.933024755	0.047183382	-4.599443036	0.018129662
Tex26	-6.079186686	0.035908667	-6.253715727	0.015393157

Tex37	4.20211932	0.048465795	-5.955943617	0.021165841
Tfpi	0.57414975	0.024658757	0.595962395	0.006691825
Tmed10	0.193621479	0.044902391	0.22526948	0.040122885
Tmed2	0.367457129	0	0.384159887	0.018175829
Tmem182	0.269216724	0.044261483	0.194705949	0.046737539
Tmem261	0.439418432	0.048301147	0.396610755	0.043369518
Tmem262	4.897158934	0.041542947	4.857810664	0.049180656
Tmem38a	0.404869712	0.029018463	0.429458054	0.008415459
Tmem59	0.257934708	0.03835183	0.253998399	0.0437482
Tmod4	1.416557914	0.005591951	1.047646179	0.011330011
Tnni3k	0.30914724	0.04115943	0.415083184	0.00253396
Tpp1	0.375004846	0.049396333	0.415871286	0.038192909
Trav7d-5	5.454847753	0.047454887	5.449836507	0.04968536
Trim35	0.322030152	0.048002951	0.339185352	0.049867665
Trim54	-0.585604296	0.047417392	0.346719167	0.045384247
Trim63	0.414119694	0.044891724	0.460606744	0.01331858
Trim72	0.218160248	0.045660042	0.292551644	0.03189256
Tspan3	0.279582296	0.029474992	0.215675049	0.032321022
Ttc7b	0.399996563	0.046013492	0.303823738	0.047123805
Tuba8	0.651823455	8.23755E-06	0.526405928	0.011618731
Txlnb	0.334853654	0.024594464	0.425780453	0.002389614

Txn2	0.788925347	1.51281E-06	0.936578764	1.4988E-14
Ube2b	0.235490055	0.012824273	0.241000663	0.021381362
Ucp2	0.559836801	0.023534574	-0.622780018	0.010528044
Ugp2	0.229337073	0.01056207	0.586374642	0
Uqcrc2	0.301896919	3.99812E-06	0.256027418	0.007314627
Uqcrfs1	0.205493555	0.041204366	0.119762276	0.044525471
Vdac2	0.180692074	0.023427809	0.294830726	2.9976E-15
Vdac3	0.180565705	0.044786409	0.288191871	5.9952E-15
Vegfa	0.571307806	0.004749552	0.403157109	0.027571594
Vopp1	0.399416721	0.014177199	0.366496352	0.03517043
Wfdc1	0.604375385	0.001768803	0.788228807	5.9952E-15
Ywhae	0.105603012	0.047735897	0.151129557	0.022615446
Zdhhc11	3.916044848	0.041978058	3.989250623	0.042731048

CHAPTER 4

A Methodological Approach to Reducing Rat Nppa Using Targeted siRNA

Mackenzie S. Newman

Department of Physiology and Pharmacology, West Virginia University, Morgantown, WV, USA

Abstract

Nppa is a gene that encodes for Anp, a hormone that causes diuresis and decreased blood volume. Despite the known beneficial roles in LVH and HF in reducing blood pressure and cardiac fibrosis, elevated levels of circulating Anp, have been shown to modulate electrical properties in cardiac tissue and cell preparations in many species, including dogs, rabbits, rodents, and humans, which may contribute to later development of arrhythmias and HF. Previous research has shown that complete knockout of Nppa or its primary receptor is embryonic lethal in rodents, but reducing the expression of the gene postnatally has not been explored. This study aims to validate whether rat Nppa can be knocked down using targeted siRNA duplexes in a rat cardiomyocyte cell line as a proof-of-concept for further application. The efficacy of three siRNA sequences targeted at Nppa were evaluated for their efficacy at reducing Anp secreted into cell culture media. All three Nppa siRNA significantly decreased Anp levels for three days post-treatment. siRNA sequence 1 decreased Anp levels to the greatest extent when comparing all three targeted siRNA, while siRNA 2 and 3 were not statistically different over multiple days. Day 2 Nppa levels were confirmed to be decreased in the siRNA-treated groups and positive control group via RT-qPCR. These results show that rat Nppa can be targeted using any of the three siRNA duplex sequences detailed herein. This study provides a tool for specific targeting of expression of this gene that can be used in further studies to determine the effects of reducing Anp in LVH and HF models.

Introduction

Previously, Nppa gene expression has been demonstrated to be increased in both male and female OZR and obese humans. Its peptide product, Anp, followed the same pattern when analyzed via Western blot. Nppa is a gene expressed exclusively within cardiac tissue (15), thus the sole origin of Anp in circulation is the heart. As Nppa is part of the calcineurin-NFAT genetic program that is active primarily during fetal development with expression reduced over time (9, 16). In pathological LVH, this genetic program becomes re-activated and Nppa levels rise in order to compensate for cardiac overload by decreasing blood volume by action at the kidney and therefore reducing blood pressure. Anp is secreted from cardiomyocytes in response to cardiac damage as a means of controlling fluid volume: it primarily acts to induce sodium secretion in the kidney. It is considered to be a physiological antagonist to the action of angiotensin (3, 4, 6, 7, 12).

Despite the beneficial effects of Anp in many cardiovascular diseases, research has shown that exposure of cardiac tissues and cells to high concentrations of Anp can alter heart rate (HR), effective refractory period (ERP), and action potential duration (APD) from mice, rats, dogs, rabbits, guinea pigs, and humans (1, 2, 8, 10, 14). Humans possessing a frameshift mutation that causes Anp to have an extended C-terminus and increased persistence in the blood exhibited atrial fibrillation, as well as mice with the gene knocked-in (5). Thus, the potential for elevated Anp to have a detrimental effect in situations of LVH cannot be ruled out. Deletion of Nppa or its cognate receptor gene, NPR1, has been shown to be cardiac-lethal in animal models (5, 11). To circumvent this issue, in this study, I sought to reduce, but not totally ablate, Nppa (and ultimately Anp), in an immortalized rat cardiomyocyte cell line via use of an siRNA approach.

Materials and Methods

Cell culture and siRNA transfection

H9c2 cells, an immortalized rat cardiomyocyte cell line, were purchased from ATCC and routinely cultured in standard high glucose DMEM supplemented with 1X penicillin/streptomycin and 10% fetal bovine serum. After cells reached 70-80% confluence in six-well plates, they were treated with 75 pmol siRNA for 1, 2, or 3 days. Control cells at day 0 were not treated with siRNA. Transfection was carried out using 7.5 µL Lipofectamine 3000. Rat Nppa siRNA duplexes were purchased from ABM (product i564970) and are listed in Table 1. Day 0 samples were taken from media that was already in the wells. Following this, all media was replaced and siRNA/Lipofectamine was added. Day 0 wells were used for day 1 samples. All wells were exposed to siRNA at the same time but no individual well was re-used beyond day 0, e.g. samples for day 1 were not re-sampled for days 2 or 3. Anti-Gapdh siRNA in Lipofectamine (positive control, known for effectively knocking down a known gene but not sharing sequence homology with Nppa), a scrambled siRNA (also referred to as "Negative Control siRNA") construct, and Lipofectamine without siRNA were used as controls. Cell culture supernatant or cell pellets in RNALater were immediately frozen at -80 °C for further use.

ELISA

ANP Competitive ELISA Kits (Thermo Fisher #EIAANP) were used for all ELISA experiments following the manufacturer's instructions. Briefly, wells in pre-coated 96-well plates were incubated with standards or samples. Next, assay buffer, Anp conjugate, and Anp antibody were added sequentially (Anp antibody was not added to non-specific binding wells). Plates were then sealed and incubated with shaking for one hour at room temperature. Then, after four

washes with wash buffer, TMB substrate was added to the wells and incubated for 30 minutes at room temperature. Stop solution was then added and readings were taken immediately at 450 nm on a plate reader. Data were fit to a four parameter logistic curve (by the manufacturer's suggestion) using Softmax Pro software. All ELISA samples consisted of three technical replicates and three biological replicates. Information about intra- and interassay coefficients of variation, detection limit, and cross-reactivity are available via the product manual.

RT-qPCR

RNA was extracted from cell pellets using an RNA Fibrous Tissue Miniprep Kit (Qiagen) according to the manufacturer's instructions and as previously described (13). RT-qPCR for Nppa was only performed on Day 2 samples.

Statistics

ELISA data were analyzed using 1-way ANOVA with Tukey's test for multiple comparisons. RT-qPCR data were analyzed using the ddCt method.

Results

In order to address whether expression of Nppa could be knocked down using siRNA, three different siRNA duplexes were designed against rat Nppa (Table 1). These sequences were run through the Thermo Fisher BLOCK-iT platform and verified via NIH blastn to be suitable for testing due to low homology with other known rat gene sequences. Using lipofectamine, a standard transfection vehicle, each sequence was tested in H9c2 (rat immortalized cardiomyocyte cells) in comparison with a Gapdh siRNA (a positive control with known anti-proliferative effects on cells), scrambled Nppa siRNA (negative control), and vehicle with no siRNA. Media was sampled from wells after zero days (baseline), one, two, or three days. Because removing

media from wells might have an effect on cell proliferation, each well was only sampled at one time point. For each individual treatment, three wells were sampled in triplicate.

Figure 1 displays the time-course trend for all of the data. Overall, levels of Anp in culture media decreased in the three siRNA-treated groups compared to all of the controls. The positive control Gapdh siRNA resulted in reduced levels of Anp compared to the two negative control groups, but this reduction was not to the same degree as the targeted siRNA. Figure 2 shows baseline data (i.e. no siRNA treatment). There was a statistically significant different between the "no treatment" and "Nppa siRNA 3" groups, but this may have been due to outliers. No other comparisons were significant. Figure 3 shows day one exposure data. All group comparisons resulted in significance ($p < 0.05$) with the exception of the siRNA 2 versus siRNA 3. For days two and three (Figures 4 and 5), the same trends resulted: all comparisons were statistically significant ($p < 0.05$) except for scrambled siRNA versus lipofectamine only (no treatment), siRNA 1 versus siRNA 2, and siRNA 2 versus siRNA 3.

Figure 6 shows quantification of RT-qPCR for Nppa and Gapdh (normalized to β-actin) in cells from day 2 in order to verify the effect of these siRNA on transcript expression instead of Anp peptide production from ELISA. These data show that the anti-Nppa siRNA and Gapdh siRNA reduced Nppa transcript levels compared to controls (A, top panel) but only Gapdh siRNA reduced Gapdh transcript levels (A, bottom panel). Figure 6B confirms singular end products from RT-qPCR. Overall, these results show that the Nppa siRNA are effective at reducing Anp compared to the controls, but Nppa siRNA 1 has a slightly greater effect.

Discussion

In this study, the potential to reduce Anp secretion was investigated using siRNA constructs targeted toward Nppa. Given that Nppa and Anp are exclusively produced in the heart,

the risk of these constructs producing side effects due to off-target binding in other tissues is minimal. Despite the potential for siRNA constructs to have off-target effects, none of them showed significant homology to other mRNA via BLAST (siRNA 1 and 2 had 66% homology to the next non-Nppa gene and siRNA 3 had 71%). All three sequences did reduce Anp levels in culture media, but siRNA 1 appeared to have a slightly greater effect overall. Reducing circulating Anp levels via siRNA knockdown may have effects in other tissues in an animal model, primarily in the kidney, by increasing volume retention and decreasing diuresis, but this depends on the degree to which Anp is knocked down: if Anp receptors are super-saturated, reducing the amount of circulating hormone may not have a measurable effect.

As the ELISA assay only looks at secreted Anp and does not include intracellular stores, I attempted several western blots to verify a reduction in cellular Anp levels. Unfortunately, given the weak signal produced, these all required too much contrast adjustment above the background threshold to be usable for any kind of analysis. The weakness in signal is may be due to low concentrations of Anp in cells and is compounded by the lower sensitivity of Western blots compared to ELISA. In retrospect, the cells that I used for Western blots would have been much better used for RT-qPCR. In future studies, it might be advisable to perform and repeat more RT-qPCR.

siRNA-based therapeutics are a newer technology with currently only limited use in approved pharmaceuticals. For laboratory research, their major use is for targeting individual genes without the need to modify the endogenous genome. Chemical modifications, such as replacing the phosphate backbone with thiophosphate or cholesterylation increase half-life and cellular uptake of an siRNA, respectively. Ideally, moving forward, I would like to package the

siRNA 1 sequence into a modified siRNA construct and test it in OZR during the course of LVH development in order to gauge whether elevated Anp is necessary, beneficial, or detrimental.

In addition to using siRNAs, there are many other methods one could use to reduce the effect of circulating Anp. Small molecular agonists and antagonists of the Anp receptor, NPRA, have been researched in the past. However, due to the high homology between Anp and BNP, these drugs typically have affinities for both NPRA and NPRB, the cognate receptor for BNP. Another potential route to reduce the effect of Anp is direct administration of antibodies, but these have not been explored in obesity-related LVH models. An alternative way to modulate Nppa expression is through altering transcription of the gene Nppa antisense-1 (Nppa-AS1), an alternatively-spliced gene that runs concurrently with and beyond the length of Nppa. Its product is a long non-coding RNA whose role in disease is not understood. Induction of this gene, perhaps through siRNA or microRNA stabilization, is another avenue worth investigating.

Overall, the preliminary studies here show that knock-down of rat Nppa is achievable using the siRNA sequences presented. Future studies in whole animals are necessary to validate the safety and toxicity of reducing, while not completely ablating, Anp levels using the siRNA approach. Despite Anp being an important adaptive hormone against hypertrophic development, understanding the point in the development of LVH that circulating Anp levels are putting the individual at a higher risk of HF is critical. Application of the approach presented here in OZR would help address this significant issue.

References

(1) Beaulieu P, Cardinal R, De LA, Lambert C. Direct chronotropic effects of atrial and C-type natriuretic peptides in anaesthetized dogs. Br J Pharmacol 1996 Aug;118(7):1790-6.

(2) Beaulieu P, Cardinal R, Page P, Francoeur F, Tremblay J, Lambert C. Positive chronotropic and inotropic effects of C-type natriuretic peptide in dogs. Am J Physiol 1997 Oct;273(4):H1933-H1940.

(3) Deschepper CF, Masciotra S, Zahabi A, Boutin-Ganache I, Picard S, Reudelhuber TL. Functional alterations of the Nppa promoter are linked to cardiac ventricular hypertrophy in WKY/WKHA rat crosses. Circ Res 2001 Feb 2;88(2):223-8.

(4) Dries DL. Natriuretic peptides and the genomics of left-ventricular hypertrophy. Heart Fail Clin 2010 Jan;6(1):55-64.

(5) Galimberti ES, Kannankeril P, Kor K, Muhammad R, Blair M, Darbar D. Abstract 19074: NPPA Overexpression in Mice Increases Susceptibility to Atrial Fibrillation. Circulation 2012 Nov 20;126(Suppl 21):A19074.

(6) Grabowski K, Riemenschneider M, Schulte L, Witten A, Schulz A, Stoll M, et al. Fetal-adult cardiac transcriptome analysis in rats with contrasting left ventricular mass reveals new candidates for cardiac hypertrophy. PLoS One 2015;10(2):e0116807.

(7) Houweling AC, van Borren MM, Moorman AF, Christoffels VM. Expression and regulation of the atrial natriuretic factor encoding gene Nppa during development and disease. Cardiovasc Res 2005 Sep 1;67(4):583-93.

(8) Kecskemeti V, Pacher P, Pankucsi C, Nanasi P. Comparative study of cardiac electrophysiological effects of atrial natriuretic peptide. Mol Cell Biochem 1996 Jul;160-161:53-9.

(9) Maillet M, van Berlo JH, Molkentin JD. Molecular basis of physiological heart growth: fundamental concepts and new players. Nat Rev Mol Cell Biol 2013 Jan;14(1):38-48.

(10) Moghtadaei M, Polina I, Rose RA. Electrophysiological effects of natriuretic peptides in the heart are mediated by multiple receptor subtypes. Prog Biophys Mol Biol 2016 Jan;120(1-3):37-49.

(11) Mori T, Chen YF, Feng JA, Hayashi T, Oparil S, Perry GJ. Volume overload results in exaggerated cardiac hypertrophy in the atrial natriuretic peptide knockout mouse. Cardiovasc Res 2004 Mar 1;61(4):771-9.

(12) Newman MS, Nguyen T, Watson MJ, Hull RW, Yu HG. Transcriptome profiling reveals novel BMI- and sex-specific gene expression signatures for human cardiac hypertrophy. Physiol Genomics 2017 Jul 1;49(7):355-67.

(13) Newman M, Infanto AM, Watson MJ, Hull RW, Yu HG. Abstract 140: BMI- and Gender-specific Increase of MAP2K3/p38 Activity in Human Cardiac Hypertrophy. Circulation Research 2017 Feb 23;119(Suppl 1):A140.

(14) Stambler BS, Guo GB. Atrial natriuretic peptide has dose-dependent, autonomically mediated effects on atrial refractoriness and repolarization in anesthetized dogs. J Cardiovasc Electrophysiol 2005 Dec;16(12):1341-7.

(15) Uhlen M, Fagerberg L, Hallstrom BM, Lindskog C, Oksvold P, Mardinoglu A, et al. Proteomics. Tissue-based map of the human proteome. Science 2015 Jan 23;347(6220):1260419.

(16) Wilkins BJ, Dai YS, Bueno OF, Parsons SA, Xu J, Plank DM, et al. Calcineurin/NFAT coupling participates in pathological, but not physiological, cardiac hypertrophy. Circ Res 2004 Jan 9;94(1):110-8.

Figures

Figure 1: Time-course data from Anp ELISA from days 0 through 4.

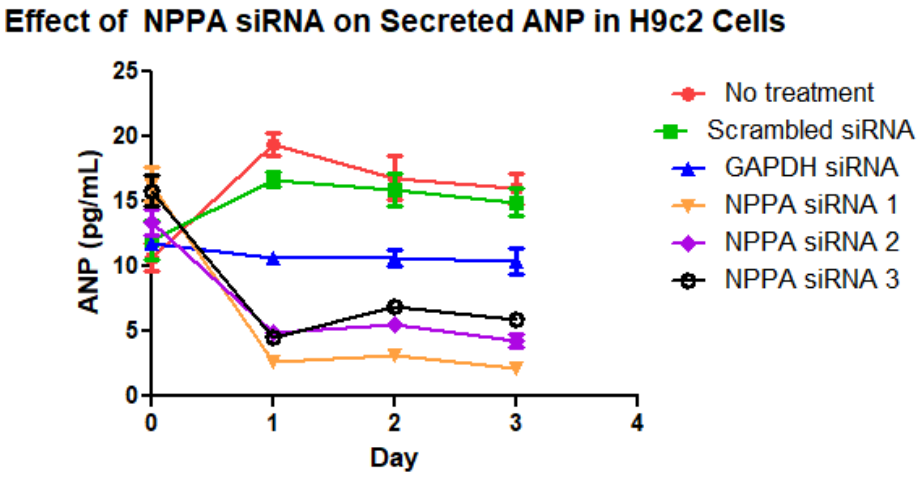

Figure 1. Time-course data from Anp ELISA from days 0 through 4. Data points on each day are discrete (i.e. media was not sampled from the same wells on multiple days), but data points are connected in this plot to delineate the groups. Data are displayed as means +/- standard deviation from three individual wells, with three technical replicates per well.

Figure 2: Day 0 quantification of Anp via ELISA

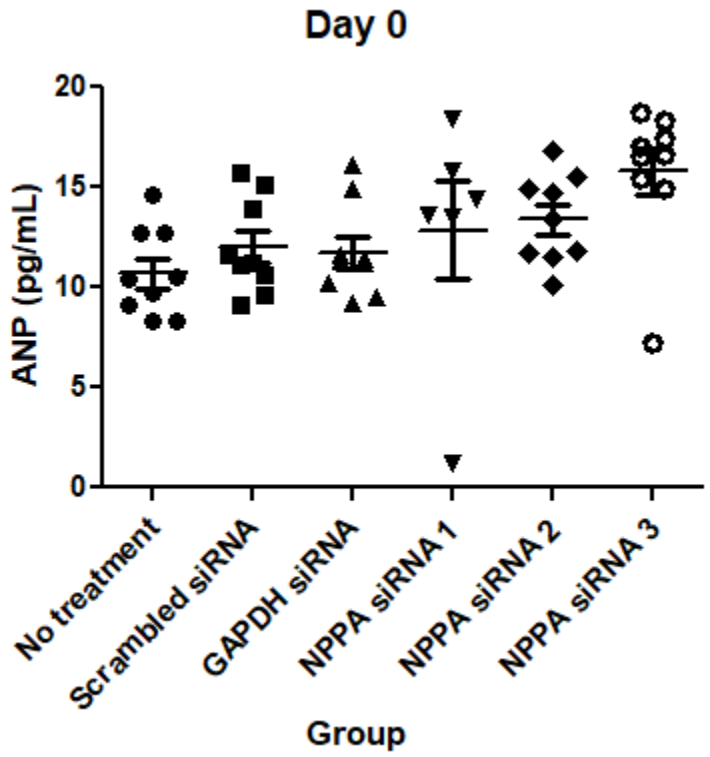

Figure 2. Day 0 quantification of Anp via ELISA. All pairwise comparisons were not statistically significant ($p < 0.05$) except for siRNA 2 versus siRNA 3. Bars represent mean +/- standard deviation for three separate wells, each with three technical replicates. Each symbol represents a signal replicate.

Figure 3: Day 1 quantification of Anp via ELISA

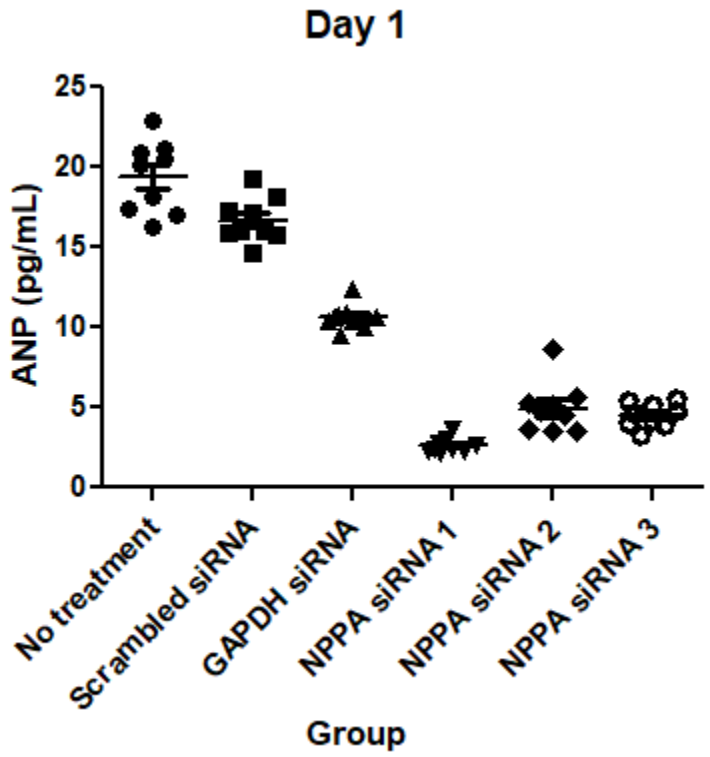

Figure 3. Day 1 quantification of Anp via ELISA. All pairwise comparisons were statistically significant ($p < 0.05$) except for siRNA 2 versus siRNA 3. Bars represent mean +/- standard deviation for three separate wells, each with three technical replicates. Each symbol represents a signal replicate.

Figure 4: Day 2 quantification of Anp via ELISA

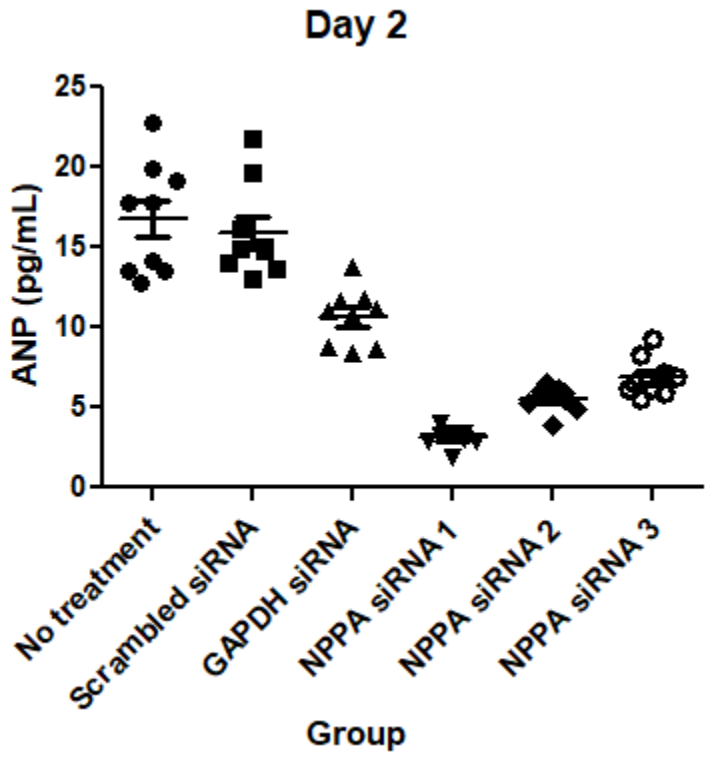

Figure 4. Day 2 quantification of Anp via ELISA. All pairwise comparisons were statistically significant ($p < 0.05$) except for scrambled siRNA versus lipofectamine only (no treatment), siRNA 1 versus siRNA 2, and siRNA 2 versus siRNA 3. Bars represent mean +/- standard deviation for three separate wells, each with three technical replicates. Each symbol represents a signal replicate.

Figure 5: Day 3 quantification of Anp via ELISA

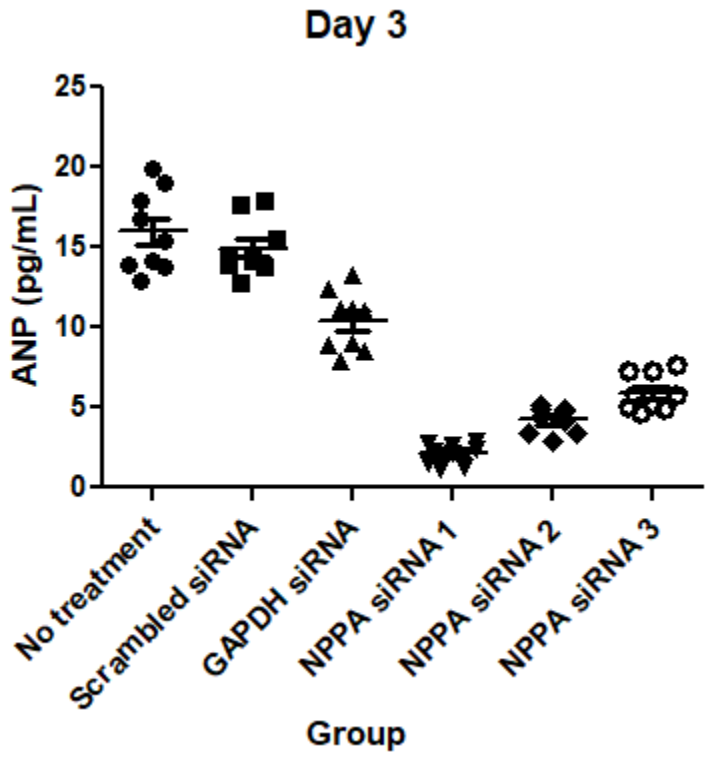

Figure 5. Day 3 quantification of Anp via ELISA. All pairwise comparisons were statistically significant ($p < 0.05$) except for scrambled siRNA versus lipofectamine only (no treatment), siRNA 1 versus siRNA 2, and siRNA 2 versus siRNA 3. Bars represent mean +/- standard deviation for three separate wells, each with three technical replicates. Each symbol represents a signal replicate.

Figure 6: Representative RT-qPCR data for Nppa and Gapdh for day 2.

A.

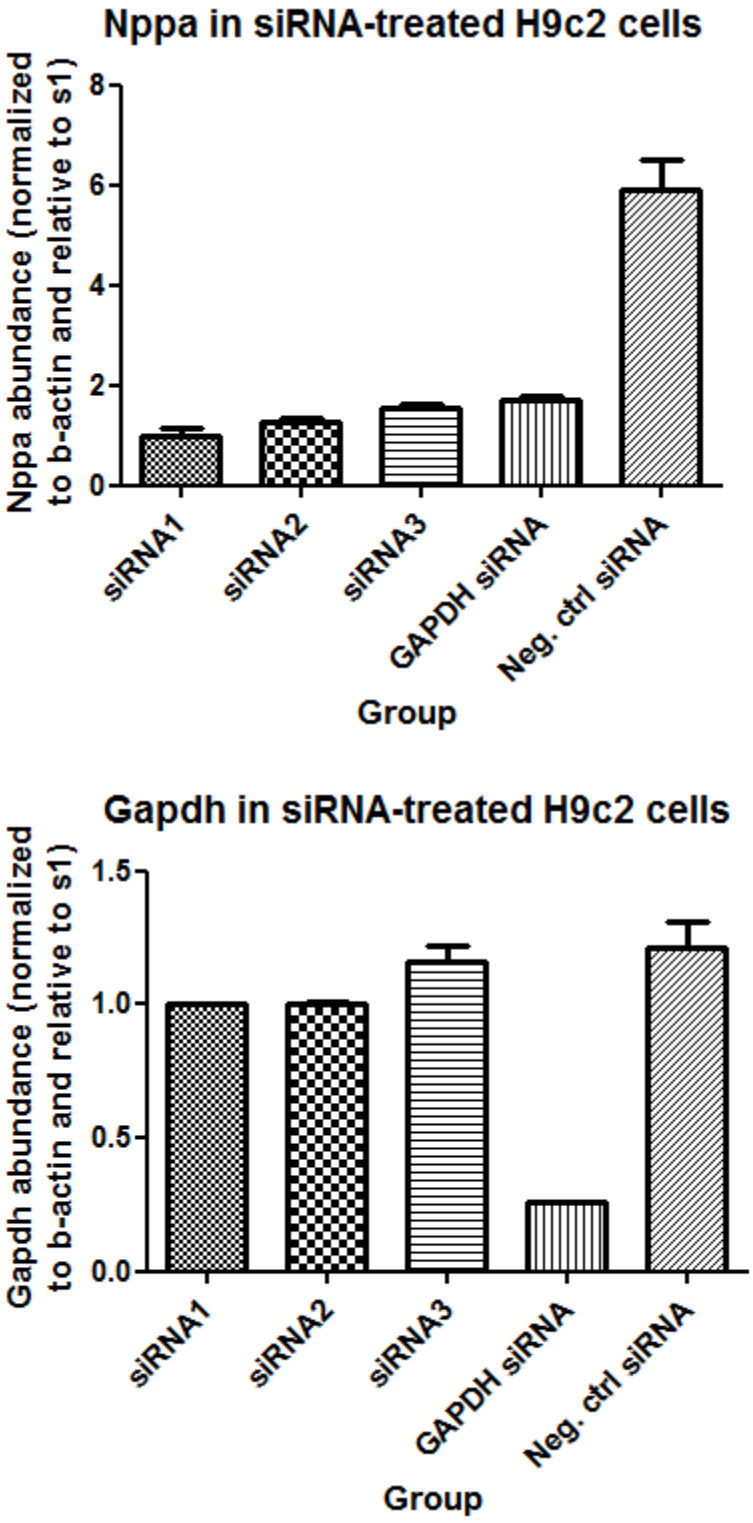

B.

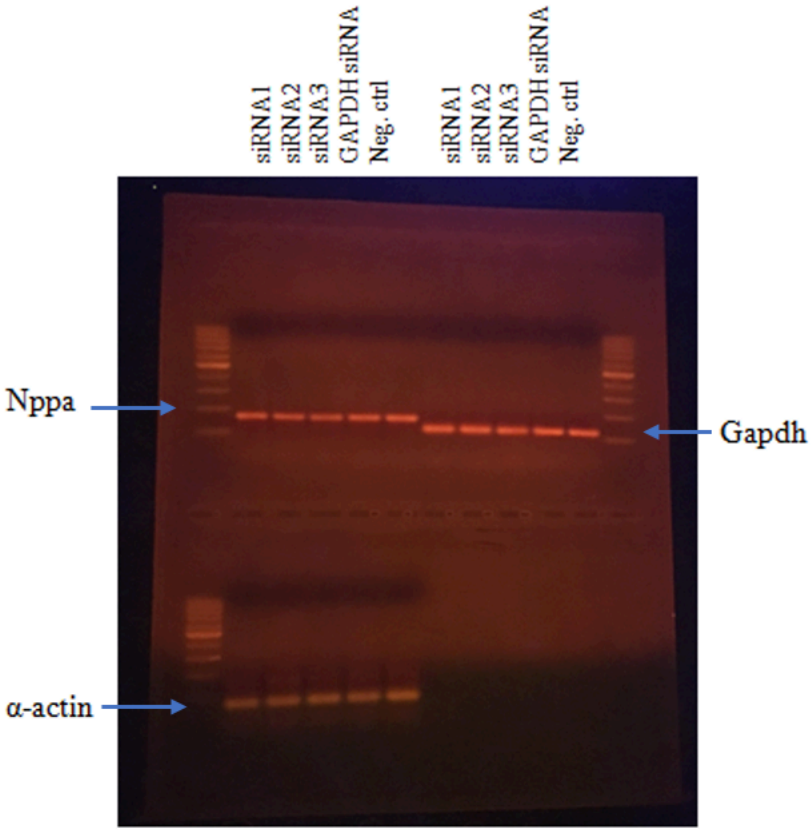

Figure 6. A: RT-qPCR quantification of Day 2 Nppa and Gapdh levels, normalized to β-actin and displayed as relative to siRNA 1. B: Gel displaying singular end products for RT-qPCR.

Tables

Table 1. Nppa siRNA Duplex Sequences

	Sequence
siRNA 1	GGAGAAGAUGCCGGUAGAATT UUCUACCCGCAUCUUCUCCTT
siRNA 2	CCGAUAGAUCUGCCCUCUUTT AAGAGGGCAGAUCUAUCGGTT
siRNA 3	GACUAGGCUGCAACAGCUUTT AAGCUGUUGCAGCCUAGUCTT

CHAPTER 5

Discussion

In Chapters 1 and 2, I aimed to describe the effects of sex and obesity on the transcriptome of LVH in both humans and Zucker rats in order to investigate the use of Zucker rats as translational model. Given the difficulty of studying LVH in humans due to the scarcity of live tissue, particularly from healthy controls, there is a major need for research models of LVH. LVH is considered to be irreversible, but once it has progressed into HF, quality of life is significantly decreased and risk of death is majorly increased. Obesity is one of the most common comorbidities of both LVH and HF. Given these facts, early detection of LVH is pivotal in preventing the transition to HF. The results of these studies reveal a litany of potential gene targets that may serve as biomarkers or pharmaceutical targets for the detection or treatment, respectively, of LVH.

When comparing the overall transcriptomes of our human and rat samples, I identified a set of 45 genes that were differentially expressed during LVH in both species and in the same direction (i.e. upregulated in male or female humans and rats or downregulated in male or female humans and rats) and other genes with sex- or species-specific expression (Chapter 3, Supplemental Table 2). Because these genes are differentially expressed in a consistent direction for one or both sexes, they warrant examination into their potential roles in LVH. Data from my human studies provided a "gene signature" of nine genes, validated at both the RNA transcriptome and protein level, which may indicate the presence of LVH. Using that same signature as a starting point for my rat studies, I was able to validate five of those genes as potentially being translationally relevant. They are discussed below.

Summary of Validated Genes

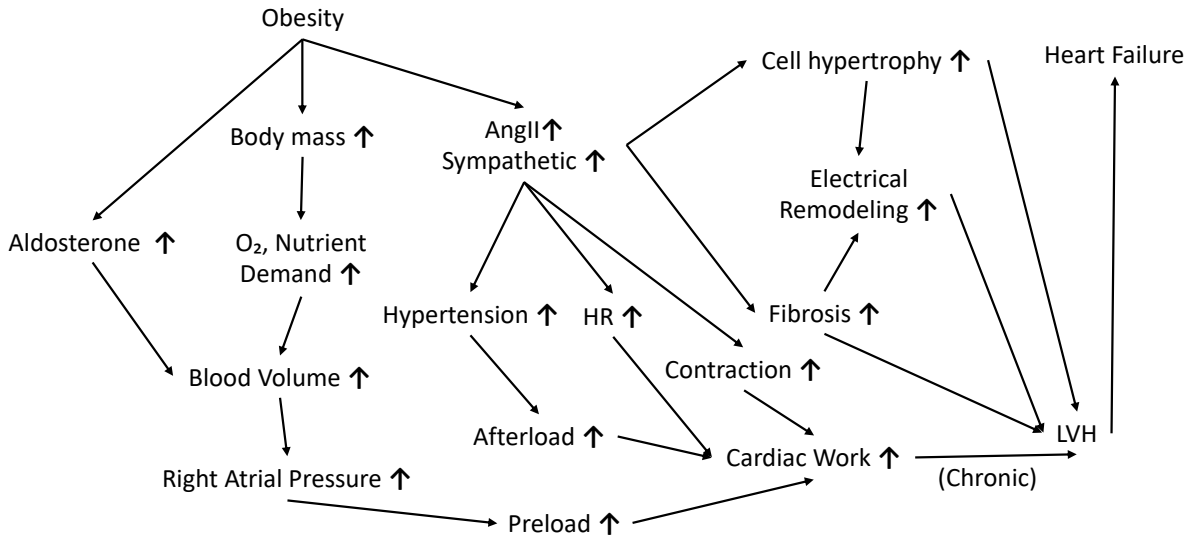

This model summarizes the main pathways that cause the development of LVH (and finally HF) as a result of obesity. Obesity, an increase in body mass, brings heightened demand for oxygen and nutrients to new tissue. Proteins such as HBB, an oxygen carrier, may play a role here. Obesity also means greater bioavailability of fat, therefore, a protein such as PDK4 may play a role in helping to utilize this energy source. A larger body mass means a larger blood volume is necessary. This is facilitated by a number of factors: 1, obesity directly causes increases in aldosterone which causes fluid retention; 2, obesity causes increases in circulating angiotensin II to increase, which causes further increases in aldosterone levels. The resultant elevation in blood volume raises right atrial pressure, which is reflected as a larger preload in the heart. Under normal conditions, under the Frank-Starling mechanism, this would cause increased cardiac output. Another branch of this mechanism is the rise in angiotensin II and catecholamines from obesity. This causes hypertension and therefore increased afterload, increases in contractility (facilitated by proteins such as MYL7), and increases in heart rate.

These factors all contribute to increased cardiac work. Chronically, these factors cause the Frank-Starling mechanism to fail and cardiac output decreases despite right atrial pressure. Circulating angiotensin II and catecholamines also contribute directly to cellular hypertrophy and fibrosis, which together lead to electrical remodeling of the ventricle and independently to promote LVH. Hormones like ANP and BNP are released from the heart as "rescue" signals, to antagonize hypertension and reduce blood volume, but in the end, all of these compensatory mechanisms ultimately cause reductions in cardiac output that cannot be sustained, thus resulting in HF.

NPPA and NPPB

I found NPPA to be the gene with the largest fold increase during LVH and obesity in both humans and OZR, with NPPB as the second-highest. Activity of NPPA in the ventricles is high during fetal development but later subsides under normal physiological conditions, while NPPB follows a similar trajectory but does not decrease to as large of an extent postnatally. ANP, the final peptide product encoded by NPPA, and BNP, the final peptide product encoded by NPPB, are circulating hormones that are primarily produced and secreted by the atria in adults, but are also produced and secreted from the ventricles in LVH (24, 38). My findings are, thus, consistent with previous findings.

My research revealed several fold changes in NPPA and ANP expression to super-physiological levels in both sexes with the presence of obesity. As discussed in the introduction, elevated ANP has been shown to decrease heart rate in rats and dogs but increase it in humans (1, 2, 26), increase the effective refractive period in dogs but decrease it in humans (26), and decrease action potential duration in human, dog, rabbit, and guinea pig cardiac preparations (26). In one family possessing a frameshift mutation in NPPA that produces an extended C-

terminal, degradation-resistant ANP, all mutation carriers had atrial fibrillation (9). Although deletion of NPPA or its cognate receptor in mice produces early cardiac hypertrophy and ultimately death via HF (28, 32), elevated ANP may be a contributing factor in LVH as a precursor to HF.

In order to study the role of ANP further, a conditional knock-down, or an siRNA-mediated knock-down of NPPA/ANP during the progression of LVH would be worth investigating. There is currently no research into the balance between NPR1 and NPR2 receptor saturation by ANP and activity of the clearance receptor NPR3; it is unknown whether ANP clearance is increased via NPR3 upon NPR1 and NPR2 saturation or if translation of the signaling receptors is upregulated instead. In a model such as OZR, where LVH presents before hypertension (unlike other transgenic obese rodent models), the role of supra-physiological ANP activity, specifically in cardiac disturbances, may be better elucidated.

HBB

HBB is a gene that encodes for the protein precursor of hemoglobin subunit beta (HBB). It functions in coordination with hemoglobin subunit alpha, HBA1, to form an active hemoglobin complex (9). In my human studies, we found significant increases in HBA1 and HBB in both males and females via transcriptome analysis, but protein levels for each were increased only in females (30). In our rat studies, HBB was significantly increased in females only in transcriptome analysis, but both obese males and females showed increased protein levels. Measurable HBA1 protein levels were difficult to detect via Western blot but were not significantly different when quantified; this is likely due to fatty contamination of samples. HBB has not been previously implicated directly in population-wide hypertrophic conditions. Research into HBB with regard to cardiovascular disorders has largely focused on its role in

sickle cell disease (16) and beta-thalassemia (3), but these diseases are associated with patient-specific gene polymorphisms and mutations (3, 16). One study of post-mortem hearts described increased levels of HBA1 and HBB mRNA associated with sudden cardiac death, but no direct mechanism was suggested (41). Increases in levels of HBA1 and HBB may occur in response to reactive oxygen species (19), which are elevated in the development of LVH and HF (37). The mechanism underlying HBB upregulation is not currently understood, though it may serve as an oxygen reserve or buffer to protect against hypoxic insult, and as a site to sequester reactive oxygen species. Unfortunately, HBB may not be a useful circulating biomarker as it is also always present in circulating erythrocytes, and elevated urinary poryphyrins (such as heme, produced by the breakdown of HBB) are common markers of liver dysfunction; however, LVH has been found in 12-30% of patients with cirrhosis (7, 31). Ventricular HBB levels may be indicative of underlying LVH, but the risk of cardiac biopsy may outweigh its ultimate prognostic outcome compared to established biomarkers like pro-NT BNP.

PDK4

PDK4 is a gene that encodes for the protein precursor of pyruvate dehydrogenase kinase-4 (PDK4). This mitochondrial enzyme is expressed in low-to-moderate amounts in many tissues, but cardiac and skeletal muscles have the greatest enrichment (45). Our studies found PDK4 to be significantly upregulated in LVH-presenting males and females via transcriptome analysis, but the protein was significantly increased only in males (30). In rats, expression was increased in both sexes in transcriptome analysis, but increases in protein were only significant in males. Despite these conflicting protein expression results, PDK4 has previously been positively associated with cardiac hypertrophy and HF (12, 27, 47), though some studies show a negative association (33, 39, 43). Induction of PDK4 activity decreases glucose utilization and increases

fat catabolism. PDK4 inhibits pyruvate dehydrogenase complexes, which are responsible for converting pyruvate (derived from glucose metabolism) to acetate (as acetyl-CoA) and carbon dioxide. Acetyl-CoA from this process is normally then used as a substrate for cellular respiration. Increased PDK4 activity decreases acetyl-CoA production from glucose which is counterbalanced by increases in fat metabolism to produce acetyl-CoA. Elevated concentrations of PDK4 in obesity may be simply due to the increased bioavailability of fats. Insulin insensitivity, a common comorbidity with obesity, has been linked to overexpression of PDK4 (44); this is likely due to decreased activation of PI3K, leading to reduced inhibition of the PDK4 promoter (18). PDK4 inhibitors have been explored with regard to treatment of cancers, diabetes, and acute cardiac ischemia (34), but have not been used to treat cardiac hypertrophy. Given the crucial role of PDK4 in regulating energy metabolism and the metabolic disturbances that are associated with obesity, and the widespread presence of PDK4 in skeletal muscle, inhibition of PDK4 may not be a suitable treatment for hypertrophy. PDK4 mRNA and protein enrichment in the heart may make it a useful local biomarker. Circulating PDK4 mRNA and protein levels have not been reported in the literature.

MYL7

MYL7 is a gene that encodes for the protein precursor of myosin light chain-7 (MYL7). Like NPPA, it is involved in cardiac development, but its expression is restricted to the atria in healthy adults (8, 40). Nonetheless, the presence of MYL7 in the ventricles has been reported in cardiac hypertrophy previously, but was not examined with regard to sex or obesity prior to my study (17, 21, 30). The main function of MYL7 is to facilitate contractility; its upregulation in hypertrophy is attributed to the increased force demand from heart muscle (8). The functional differences between these and MYL7 is unknown. MYL7 may be a putative biomarker of

hypertrophy due to being uniquely expressed within cardiac tissue, but whether it can be detected in blood is unknown. Due to its critical role in muscle contraction and sequence homology (36) with other, more ubiquitous myosin light chains (including MYL2, MYL5, MYL10, and MYL12), direct, specific targeting to increase the activity MYL7 by pharmaceutical intervention may be difficult. However, inhibition of myosin light chain kinase, which directly modulates the activity of MYL7 via reduced phosphorylation, has been explored as a treatment for cardiovascular conditions such as atherosclerosis (4) and heart ischemia/reperfusion injury (22) in rabbits and mice, respectively. These treatments have not been tested in humans.

Remainder of the Transcriptome

My studies uncovered a variety of ventricular genes that are shared in LVH by obese humans and Zucker rats. We validated a select group of them in humans and then examined these in our rat model. Not surprisingly, there are additional putative gene candidates within the dataset that may also be translationally relevant, but they are not within the scope of the present research. Both my human and rat data sets are limited by small sample size and age variability between samples. Beyond this, the human heart samples lacked full disclosure of pathology data, therefore we are not aware of any comorbidities or medications the patients were taking. Future studies would ideally rectify these issues (age-paired samples, number of samples, underlying conditions) and include functional human cardiac data for cross-comparison with the Zucker rat model. Given that LVH develops slowly over time, more research is warranted into transcriptomic and proteomic changes during the course of development, particularly with regard to specific isoforms of proteins that vary between atrial and ventricular expression. Our current transcriptome dataset does not differentiate between alternatively-spliced forms of genes. Alternate splicing is known to vary with age and can affect downstream protein structure and

function (42). Other future studies might include identification of various species of RNA, such as long non-coding RNA (20) and microRNAs (6, 13, 25, 35, 46), whose roles in the development of LVH are poorly understood. HF is not necessarily a death sentence but identifying and understanding what leads to it will save millions of lives in the future by allowing timely treatment.

Future Directions

Ideally, in order to continue to validate OZR as a model of human LVH, I would add more groups of animals: 1) LZR fed ad libitum, 2) OZR fed ad libitum, 3) LZR on a restricted diet, 4) OZR fed a restricted diet. Grouping the animals like this would allow for the results to be parsed better for the effect of obesity on LVH development. The LZR fed *ad libitum* and LZR fed a calorie-restricted diet should not show many transcriptomic changes and would serve as controls. The OZR with calorie restrictions will provide the most significant data in terms of overall LV expression: OZR with a restricted diet neither develop obesity nor LVH. Comparing these rats' transcriptomes to lean rats will reveal what genes are differentially-expressed as a product of deficient Ob-Rb signaling in the obese animals. Comparing the calorie-restricted obese animals to the ones fed *ad libitum* will reveal which genes are differentially-expressed as a function of obesity. Leptin has effects on heart rate and parameters such as contractility but its direct role in LVH is poorly understood (10, 23). Adipose tissue, which directly secretes leptin, is known to be directly adjacent to cardiac tissue in obesity, therefore local levels of leptin are elevated above circulating concentrations. Comparing the calorie-restricted obese animals to the ones fed *ad libitum* will also help differentiate the effects of local leptin in the absence of Ob-Rb on the cardiac transcriptome in obesity-related LVH. If there are no differences between the OZR fed a calorie-restricted diet and lean controls, then the implications about what the presence

of the OZR mutation does genomically and proteomically would be massive. However, the likelihood of there being zero differences between the two populations is minimal, as leptin signaling affects myriad second messenger and transcriptional pathways that have differential effects on the final proteome.

Similarly, with these groups, I would like to isolate LV RNA at different time points over the course of typical LVH development in the untreated obese group with free food access—i.e., before (e.g. week 8-10), during (e.g. week 11-14), and after pronounced LVH presentation (e.g. week 17-19). Genes and proteins involved in the development of LVH may not be present in the final presentation of LVH, and these may serve as useful mechanistic or stage-specific markers of LVH, whether for drug targeting or diagnosis. Adding groups such as Zucker diabetic fatty rats, a strain of OZR that develops diabetes, to these experiments would also allow for the effects of diabetes to be distinguished from obesity alone.

I would propose that the same experiments performed in Zucker rats herein should be performed in *ob*/*ob* and *db*/*db* mice. As discussed previously, these mice are similar to OZR with regard to dysfunctional leptin signaling at the level of the receptor (*db*/*db*) and leptin itself (*ob*/*ob*). These species develop many common pathological conditions to OZR despite not sharing the exact genetic mutation, but not all are the same or to the same degree, such as diabetes and hypertension. Moving into mice and comparing transcriptomic profiles would reveal differentially expressed genes that are shared between humans, rats, and mice, therefore further validating the translatability of the gene in the model and reducing the risk that a gene has different roles between species, e.g. a gene that is upregulated in mice but downregulated in humans and rats would be a bad target due to its role in LVH being inconsistent.

Another potential avenue for continuing this research would be to induce the mutation found in OZR Ob-Rb protein, Gln269Pro, in another common rat strain, such as Wister-Kyoto rats. This would serve as a secondary confirmation for the role of the functional leptin receptor, Ob-Rb, as a contributor to obesity-related LVH. The same groups in the previous paragraph would be useful, again, to look at the developmental profile of LVH with or without obesity. The same mutation could be introduced to a common mouse strain, as well, such as BALB/c. Unlike *ob*/*ob* and *db*/*db* mice, having the exact mutation would allow for stricter control in cross-species analysis for the role of LepR in the development of LVH and obesity. Whereas OZR, *ob*/*ob* mice, and *db*/*db* mice, all are considered to have monogenically-derived obesity, Wister-Kyoto rats and TALLYHO mice have a polygenic background that better represents genetic variability like the general human population.

In order to further confirm the role of the leptin receptor in the development of LVH, complete or partial ablation of the gene LepR within specific tissues or cell types might be considered. Numerous cell type-specific knockouts have been made, such as in endothelial cells (14), hepatocytes (15), neurons (5), astrocytes (29), and cardiomyocytes (11). Notably, the cardiomyocyte LepR knockout mice, which had a tamoxifen-inducible deletion, suffered from cardiac enlargement and eventual HF within ten days of induction (11). This evidence alone implies that LepR is critical in early development of cardiac tissue. Given that only one of the six LepR isoforms is considered dysfunctional in OZR (Ob-Rb) and they do not die of HF at such a young age, then the other isoforms might be playing a critical role in development. As discussed in Chapter 1, many leptin receptor isoforms have leptin binding capacity and therefore may serve to buffer circulating leptin levels or import leptin into cells, for example. The contributions of these other leptin receptors to cell signaling are considered to be minimal or absent, yet their

roles have not been completely elucidated. Further mutating LepR to render the other isoforms inactive may be a useful way to look at their role in the development of LVH and ultimately HF.

Summary

In the studies presented here, I sought to validate novel biomarkers of LVH in humans as they pertained to HF and then define a model to further explore these genes and proteins. My human studies resulted in the generation of thousands of transcriptomic changes that have not been previously identified, particularly with respect to sex and obesity status. The genes and proteins that I validated for humans serve as a template signature that can be verified clinically, and the process described in those studies serves as a rapid pipeline to qualify genes for further investigation in humans. The goal of my rat studies was to show that there were genes and proteins shared across species in an obesity- and sex-specific manner. Genes that are differentially expressed in each species are viable tools for research into the mechanistic underpinnings of LVH. The role of sex, in particular, has not been explored frequently with regard to LVH, especially in model systems. It is well-known that estrogen has cardioprotective effects, and differentiating how LVH develops between males and females is critical in the development of appropriate biomarkers and suitable pharmaceutical interventions. Overall, there are myriad more directions that this research could be taken, but most importantly, the outcomes for human health are at the forefront.

References

(1) Beaulieu P, Cardinal R, De LA, Lambert C. Direct chronotropic effects of atrial and C-type natriuretic peptides in anaesthetized dogs. Br J Pharmacol 1996 Aug;118(7):1790-6.

(2) Beaulieu P, Cardinal R, Page P, Francoeur F, Tremblay J, Lambert C. Positive chronotropic and inotropic effects of C-type natriuretic peptide in dogs. Am J Physiol 1997 Oct;273(4):H1933-H1940.

(3) Cao A, Galanello R. Beta-thalassemia. Genet Med 2010 Feb;12(2):61-76.

(4) Cheng X, Wang X, Wan Y, Zhou Q, Zhu H, Wang Y. Myosin light chain kinase inhibitor ML7 improves vascular endothelial dysfunction via tight junction regulation in a rabbit model of atherosclerosis. Mol Med Rep 2015 Sep;12(3):4109-16.

(5) Cohen P, Zhao C, Cai X, Montez JM, Rohani SC, Feinstein P, et al. Selective deletion of leptin receptor in neurons leads to obesity. J Clin Invest 2001 Oct;108(8):1113-21.

(6) Curcio A, Torella D, Iaconetti C, Pasceri E, Sabatino J, Sorrentino S, et al. MicroRNA-1 downregulation increases connexin 43 displacement and induces ventricular tachyarrhythmias in rodent hypertrophic hearts. PLoS One 2013;8(7):e70158.

(7) De MM, Chinali M, Romano C, Benincasa M, D'Addeo G, D'Agostino L, et al. Increased left ventricular mass in pre-liver transplantation cirrhotic patients. J Cardiovasc Med (Hagerstown) 2008 Feb;9(2):142-6.

(8) Doevendans PA, Bronsaer R, Lozano PR, Kubalak S, van BM. The murine atrial myosin light chain-2 gene: a member of an evolutionarily conserved family of contractile proteins. Cytogenet Cell Genet 2000;90(3-4):248-52.

(9) Galimberti ES, Kannankeril P, Kor K, Muhammad R, Blair M, Darbar D. Abstract 19074: NPPA Overexpression in Mice Increases Susceptibility to Atrial Fibrillation. Circulation 2012 Nov 20;126(Suppl 21):A19074.

(10) Hall ME, Harmancey R, Stec DE. Lean heart: Role of leptin in cardiac hypertrophy and metabolism. World J Cardiol 2015 Sep 26;7(9):511-24.

(11) Hall ME, Smith G, Hall JE, Stec DE. Cardiomyocyte-specific deletion of leptin receptors causes lethal heart failure in Cre-recombinase-mediated cardiotoxicity. Am J Physiol Regul Integr Comp Physiol 2012 Dec 15;303(12):R1241-R1250.

(12) Horiuchi M, Kobayashi K, Masuda M, Terazono H, Saheki T. Pyruvate dehydrogenase kinase 4 mRNA is increased in the hypertrophied ventricles of carnitine-deficient juvenile visceral steatosis (JVS) mice. Biofactors 1999;10(2-3):301-9.

(13) Huang Y, Tang S, Huang C, Chen J, Li J, Cai A, et al. Circulating miRNA29 family expression levels in patients with essential hypertension as potential markers for left ventricular hypertrophy. Clin Exp Hypertens 2017;39(2):119-25.

(14) Hubert A, Bochenek ML, Schutz E, Gogiraju R, Munzel T, Schafer K. Selective Deletion of Leptin Signaling in Endothelial Cells Enhances Neointima Formation and Phenocopies the Vascular Effects of Diet-Induced Obesity in Mice. Arterioscler Thromb Vasc Biol 2017 Sep;37(9):1683-97.

(15) Huynh FK, Levi J, Denroche HC, Gray SL, Voshol PJ, Neumann UH, et al. Disruption of hepatic leptin signaling protects mice from age- and diet-related glucose intolerance. Diabetes 2010 Dec;59(12):3032-40.

(16) Kato GJ, Piel FB, Reid CD, Gaston MH, Ohene-Frempong K, Krishnamurti L, et al. Sickle cell disease. Nat Rev Dis Primers 2018 Mar 15;4:18010.

(17) Kumar C, Saidapet C, Delaney P, Mendola C, Siddiqui MA. Expression of ventricular-type myosin light chain messenger RNA in spontaneously hypertensive rat atria. Circ Res 1988 Jun;62(6):1093-7.

(18) Kwon HS, Huang B, Unterman TG, Harris RA. Protein kinase B-alpha inhibits human pyruvate dehydrogenase kinase-4 gene induction by dexamethasone through inactivation of FOXO transcription factors. Diabetes 2004 Apr;53(4):899-910.

(19) Li X, Wu Z, Wang Y, Mei Q, Fu X, Han W. Characterization of adult alpha- and beta-globin elevated by hydrogen peroxide in cervical cancer cells that play a cytoprotective role against oxidative insults. PLoS One 2013;8(1):e54342.

(20) Li Y, Liang Y, Zhu Y, Zhang Y, Bei Y. Noncoding RNAs in Cardiac Hypertrophy. J Cardiovasc Transl Res 2018 Dec;11(6):439-49.

(21) Lim DS, Roberts R, Marian AJ. Expression profiling of cardiac genes in human hypertrophic cardiomyopathy: insight into the pathogenesis of phenotypes. J Am Coll Cardiol 2001 Oct;38(4):1175-80.

(22) Lin HB, Cadete VJ, Sawicka J, Wozniak M, Sawicki G. Effect of the myosin light chain kinase inhibitor ML-7 on the proteome of hearts subjected to ischemia-reperfusion injury. J Proteomics 2012 Sep 18;75(17):5386-95.

(23) Lin YC, Huang J, Hileman S, Martin KH, Hull R, Davis M, et al. Leptin decreases heart rate associated with increased ventricular repolarization via its receptor. Am J Physiol Heart Circ Physiol 2015 Nov 15;309(10):H1731-H1739.

(24) Man J, Barnett P, Christoffels VM. Structure and function of the Nppa-Nppb cluster locus during heart development and disease. Cell Mol Life Sci 2018 Apr;75(8):1435-44.

(25) Marketou ME, Parthenakis F, Vardas PE. Pathological Left Ventricular Hypertrophy and Stem Cells: Current Evidence and New Perspectives. Stem Cells Int 2016;2016:5720758.

(26) Moghtadaei M, Polina I, Rose RA. Electrophysiological effects of natriuretic peptides in the heart are mediated by multiple receptor subtypes. Prog Biophys Mol Biol 2016 Jan;120(1-3):37-49.

(27) Mori J, Alrob OA, Wagg CS, Harris RA, Lopaschuk GD, Oudit GY. ANG II causes insulin resistance and induces cardiac metabolic switch and inefficiency: a critical role of PDK4. Am J Physiol Heart Circ Physiol 2013 Apr 15;304(8):H1103-H1113.

(28) Mori T, Chen YF, Feng JA, Hayashi T, Oparil S, Perry GJ. Volume overload results in exaggerated cardiac hypertrophy in the atrial natriuretic peptide knockout mouse. Cardiovasc Res 2004 Mar 1;61(4):771-9.

(29) Naranjo V, Contreras A, Merino B, Plaza A, Lorenzo MP, Garcia-Caceres C, et al. Specific Deletion of the Astrocyte Leptin Receptor Induces Changes in Hippocampus Glutamate Metabolism, Synaptic Transmission and Plasticity. Neuroscience 2019 Nov 6.

(30) Newman MS, Nguyen T, Watson MJ, Hull RW, Yu HG. Transcriptome profiling reveals novel BMI- and sex-specific gene expression signatures for human cardiac hypertrophy. Physiol Genomics 2017 Jul 1;49(7):355-67.

(31) Ortiz-Olvera NX, Castellanos-Pallares G, Gomez-Jimenez LM, Cabrera-Munoz ML, Mendez-Navarro J, Moran-Villota S, et al. Anatomical cardiac alterations in liver cirrhosis: an autopsy study. Ann Hepatol 2011 Jul;10(3):321-6.

(32) Pandey KN. Genetic Ablation and Guanylyl Cyclase/Natriuretic Peptide Receptor-A: Impact on the Pathophysiology of Cardiovascular Dysfunction. Int J Mol Sci 2019 Aug 14;20(16).

(33) Razeghi P, Young ME, Ying J, Depre C, Uray IP, Kolesar J, et al. Downregulation of metabolic gene expression in failing human heart before and after mechanical unloading. Cardiology 2002;97(4):203-9.

(34) Roche TE, Hiromasa Y. Pyruvate dehydrogenase kinase regulatory mechanisms and inhibition in treating diabetes, heart ischemia, and cancer. Cell Mol Life Sci 2007 Apr;64(7-8):830-49.

(35) Sanchez-Ruderisch H, Queiros AM, Fliegner D, Eschen C, Kararigas G, Regitz-Zagrosek V. Sex-specific regulation of cardiac microRNAs targeting mitochondrial proteins in pressure overload. Biol Sex Differ 2019 Feb 6;10(1):8.

(36) Sayers EW, Agarwala R, Bolton EE, Brister JR, Canese K, Clark K, et al. Database resources of the National Center for Biotechnology Information. Nucleic Acids Res 2019 Jan 8;47(D1):D23-D28.

(37) Seddon M, Looi YH, Shah AM. Oxidative stress and redox signalling in cardiac hypertrophy and heart failure. Heart 2007 Aug;93(8):903-7.

(38) Sergeeva IA, Hooijkaas IB, Ruijter JM, van dM, I, de Groot NE, van de Werken HJ, et al. Identification of a regulatory domain controlling the Nppa-Nppb gene cluster during heart development and stress. Development 2016 Jun 15;143(12):2135-46.

(39) Sheeran FL, Angerosa J, Liaw NY, Cheung MM, Pepe S. Adaptations in Protein Expression and Regulated Activity of Pyruvate Dehydrogenase Multienzyme Complex in Human Systolic Heart Failure. Oxid Med Cell Longev 2019;2019:4532592.

(40) Small EM, Krieg PA. Molecular regulation of cardiac chamber-specific gene expression. Trends Cardiovasc Med 2004 Jan;14(1):13-8.

(41) Son GH, Park SH, Kim Y, Kim JY, Kim JW, Chung S, et al. Postmortem mRNA expression patterns in left ventricular myocardial tissues and their implications for forensic diagnosis of sudden cardiac death. Mol Cells 2014 Mar;37(3):241-7.

(42) Stegeman R, Weake VM. Transcriptional Signatures of Aging. J Mol Biol 2017 Aug 4;429(16):2427-37.

(43) Taegtmeyer H, Razeghi P, Young ME. Mitochondrial proteins in hypertrophy and atrophy: a transcript analysis in rat heart. Clin Exp Pharmacol Physiol 2002 Apr;29(4):346-50.

(44) Thoudam T, Ha CM, Leem J, Chanda D, Park JS, Kim HJ, et al. PDK4 Augments ER-Mitochondria Contact to Dampen Skeletal Muscle Insulin Signaling During Obesity. Diabetes 2019 Mar;68(3):571-86.

(45) Uhlen M, Fagerberg L, Hallstrom BM, Lindskog C, Oksvold P, Mardinoglu A, et al. Proteomics. Tissue-based map of the human proteome. Science 2015 Jan 23;347(6220):1260419.

(46) Wang Y, Chen S, Gao Y, Zhang S. Serum MicroRNA-27b as a Screening Biomarker for Left Ventricular Hypertrophy. Tex Heart Inst J 2017 Dec;44(6):385-9.

(47) Zhao G, Jeoung NH, Burgess SC, Rosaaen-Stowe KA, Inagaki T, Latif S, et al. Overexpression of pyruvate dehydrogenase kinase 4 in heart perturbs metabolism and exacerbates calcineurin-induced cardiomyopathy. Am J Physiol Heart Circ Physiol 2008 Feb;294(2):H936-H943.